Universidade de Aveiro Departamento de Geociências
2011

Carlos César Dias de Jesus

Vias de transporte de sedimentos finos recentes na margem continental central Portuguesa

Pathways of recent fine-grained sediment transport on the central Portuguese continental margin

Universidade de Aveiro Departamento de Geociências
2011

Carlos César Dias de Jesus

Vias de transporte de sedimentos finos recentes na margem continental central Portuguesa

Pathways of recent fine-grained sediment transport on the central Portuguese continental margin

Dissertação apresentada à Universidade de Aveiro para cumprimento dos requisitos necessários à obtenção do grau de Doutor em Geociências, realizada sob a orientação científica do Doutor Fernando Joaquim Fernandes Tavares Rocha, Professor Catedrático do Departamento de Geociências da Universidade de Aveiro, do Doutor Hendrik de Stigter, Investigador do Netherlands Institute for Sea Research (NIOZ), e da Doutora Anabela Tavares Oliveira, Técnica Superior do Instituto Hidrográfico.

Apoio financeiro da FCT e do FSE no âmbito do III Quadro Comunitário de Apoio

UNIÃO EUROPEIA
Fundo Social Europeu

QUADRO DE REFERÊNCIA ESTRATÉGICO NACIONAL
PORTUGAL 2007.2013

à minha família e *ao*s *meu*s *am*ig*o*s que estive*r*am sempre presentes

o júri

presidente

Doutor José Manuel Lopes da Silva Moreira
Professor Catedrático da Universidade de Aveiro

Doutor Fernando Joaquim Fernandes Tavares Rocha
Professor Catedrático da Universidade de Aveiro

Doutor Eduardo Anselmo Ferreira da Silva
Professor Catedrático da Universidade de Aveiro

Doutora Cristina Maria de Almeida Bernardes
Professora Associada da Universidade de Aveiro

Doutora Maria Isabel Rola Rodrigues Abrantes
Professora Adjunta da Escola Superior de Educação do Instituto Politécnico de Viseu

Doutora Anabela Tavares Campos Oliveira
Técnica Superior do Instituto Hidrográfico

Doutor Hendrik Corstiaan de Stigter
Investigador do Royal Netherlands Institute for Sea Research

Agradecimentos/ Acknowledgements

Foram muitos anos a pensar nesta tese, permitam-me que seja emotivo.

Henko de Stigter, I admire and appreciate your constant enthusiasm and positive view during all phases of this study. Among many things, I would like to thank you for the patience you had with me throughout these years. I feel fortunate to have had the opportunity to work with such a dedicated, such an intelligent and such a friendly person as you are. Thank you for everything.

Professor Doutor Fernando Rocha, obrigado pela confiança que depositou em mim ao dar-me liberdade na gestão do projecto de doutoramento. Agradeço também os ensinamentos e o gosto que me incutiu pela mineralogia.

Anabela Oliveira, obrigado pela simpatia e pelas discussões ao longo do trabalho. Agradeço também a forma acolhedora como fui sempre recebido no Instituto Hidrográfico.

Thomas Richter, thank you so much for all the things I have learned with you about geochemistry, especially about lead stable isotopes. Your contributions on Chapter 7 were essential to make it as it is.

Wim Boer thank you for the things you thought me about geochemistry and for your friendship during my stay at the NIOZ.

Paulo Miranda, eu tenho tanto a agradecer-te que nem sei por onde começar. Talvez pela amizade que sempre demonstraste ao longo destes últimos 10 anos. Ou pela ajuda fundamental no laboratório, no tratamento das amostras. Ou talvez pela ajuda prestada com “softwares”, com discussões proveitosas, ou talvez pelos inúmeros artigos enviados durante a minha estadia na Noruega e em Lisboa. Estiveste sempre presente, obrigado.

Pedro Marques, quero agradecer-te por tudo! Desde os milagres de Photoshop à paciência que sempre tiveste comigo.

Denise Terroso, obrigado pela amizade ao longo destes últimos anos e pela assistência sempre presente em qualquer problema que surgisse no laboratório (e não só!), pelos conselhos e simpatia.

Teresa Melo, obrigado pelo estímulo ao trabalho e ao querer sempre ser melhor. Lembro-me do apoio que me deste aquando da minha primeira incursão para o NIOZ na Holanda, mas a verdade é que podia encher esta página com exemplos…

Cristina Sequeira, obrigado pelas inúmeras análises de DRX que foram feitas ao longo destes últimos 6 anos e pela constante simpatia e disponibilidade.

Luís Serrano Pinto, foi muito bom partilhar gabinete contigo. Obrigado pela sempre boa disposição e bom astral…”ah, mi chama di”…

Alexandra Morgado, obrigado pela constante simpatia e pela ajuda a angariar informação SIG.

Ana Santos, muito obrigado pela constante simpatia e por toda a ajuda prestada no IH nomeadamente nas análises granulométricas e mineralógicas.

Jesus Vidinha, obrigado pelo apoio prestado na fase inicial deste trabalho.

Mário Mil-Homens, obrigado pelas frutíferas discussões sobre geoquímica e ainda pela disponibilização de informação muito relevante para este trabalho.

Hannes Wagner, although we never discussed the results of this thesis directly, the discussions we had together when working on other studies were important for the work that is here presented. For that I thank you.

Ingunn Nilssen, er det min plikt å skrive denne teksten på norsk. Det var takket være deg at jeg har lært noe om dette vanskelige språket.
Jeg vil gjerne takke deg for en slik fantastisk opplevelse i Norge, og også for din stadig til stede smil...

Agradecimentos/ Acknowledgements

Sr. João Graça, obrigado pela ajuda de campo prestada e pela simpática companhia no laboratório durante vários anos.

Queria também agradecer ao João Cascalho, à Anabela Cruces, à Carlota Cortesão e ao Philippe Quevauviller o envio de informação que me foi muito útil para a realização deste trabalho.

Aos amigos e colegas Sofia Mota Leite, Mafalda Costa, Isabel Abrantes, Manuela Inácio, Catarina Guerreiro, Sónia Rey, Mariana Rebelo, Marina Cabral Pinto, Carlos Miraldo, Clara Sena, Barrosinho, Teresa Amaro, Raquel Agra, Sofia Almeida, Virgínia Martins, Eduardo Ferraz, Carina Santos o meu muito obrigado pelas discussões sobre trabalho, pelas discussões sobre outras coisas que não trabalho, pela simpatia, pela companhia, pelos tempos passados juntos.

Ao Instituto Hidrográfico, na pessoa do seu director e da Doutora Aurora Rodrigues, pela cedência das condições de laboratório e de espaço, imprescindível à execução da tese.

À FCT pela atribuição da bolsa de doutoramento que me possibilitou a execução da tese e, por isso também, de vivências que não vou esquecer! Reconheço também a importante contribuição dos projectos europeus EUROSTRATAFORM e HERMES e do projecto interno do Instituto Hidrográfico, SEPLAT, para a obtenção das amostras estudadas na presente tese.

palavras-chave

Plataforma continental, Canhão Submarino de Setúbal, Lisboa, Nazaré e Cascais, transporte sedimentar, minerais de argila, metais traço, isótopos estáveis de chumbo.

resumo

Com o intuito de estudar as principais vias de transporte de sedimentos finos recentes na zona central da margem continental Oeste Portuguesa, parâmetros geoquímicos, mineralógicos e granulométricos foram analisados em sedimentos superficiais e em matéria particulada colhida em armadilhas de sedimentos e integrados com observações da hidrodinâmica de fundo. Os parâmetros geoquímicos foram também estudados na coluna de sedimentos depositada nos últimos 150 anos e em sedimentos pré-industriais. Os referidos parâmetros determinados foram: concentrações elementares, isótopos estáveis de Pb, teores em materiais litogénicos, carbonato de cálcio e carbono orgânico. Os canhões de Lisboa-Setúbal e Cascais tiveram especial destaque no presente estudo dado que, até à data, encontram-se menos estudados que o Canhão da Nazaré. Os resultados mostram que a distribuição de sedimentos na zona central da margem ocidental Portuguesa é particionada pelos canhões e que a exportação de sedimentos da plataforma para zonas mais profundas da margem é restringida pelas correntes do talude, excepto onde os canhões funcionam como corredores para o transporte de sedimentos. Enquanto no Canhão de Lisboa-Setúbal, e provavelmente no Canhão de Cascais, o transporte de sedimentos até à zona inferior é limitada, provavelmente apenas despoletado por eventos de elevada energia, no Canhão da Nazaré o transporte ao longo do todo o canhão parece eficiente. As zonas superiores dos canhões de Lisboa-Setúbal e Cascais presentemente actuam como armadilhas de sedimentos finos, aprisionando partículas em suspensão provenientes da plataforma adjacente. A introdução directa de sedimentos provenientes das plumas dos rios Tejo e Sado nas zonas superiores dos canhões parece limitada, contudo a resuspensão dos sedimentos do prodelta do Tejo como resultado de ondas de tempestade e ondas de maré interna permite o transporte de sedimentos para os canhões adjacentes. Na plataforma de Lisboa-Setúbal-Sines foram identificadas as assinaturas geoquímicas e mineralógicas de diferentes fontes de sedimentos finos (e.g. estuários do Tejo e Sado, arribas costeiras, lagoas de St. André e Melides). As concentrações elementares pré-industriais são muito semelhantes nos canhões da Nazaré e Lisboa-Setúbal, mas variados graus de enriquecimento antrópico de metais traço estão presentes nos sedimentos recentes. A mais acentuada influência antrópica na última área referida é consistente com a sua proximidade a áreas densamente povoadas e industrializadas e com *input* de sedimentos originários dos rios Tejo e Sado, potenciais transportadores de partículas poluentes. A dispersão de Pb atmosférico parece também significativa sendo que toda a zona da plataforma continental adjacente aos canhões de Lisboa-Setúbal e Cascais apresenta-se enriquecida. A principal fonte de Pb antrópico identificada através de isótopos estáveis de Pb é consistente com a assinatura das cinzas de incineradoras. No Canhão de Lisboa a imersão de dragados contaminados parece ser também uma potencial importante fonte de metais traço antropogénicos.

keywords

Continental shelf, Setúbal, Lisbon, Nazaré, Cascais submarine canyons, pathways of sediment transport, clay minerals, trace metals, stable lead isotopes.

abstract

In order to study the main pathways of recent fine sediment transport in the central area of the west Portuguese continental margin between the Nazaré Canyon and Cape Sines, geochemical, mineralogical and grain size parameters were analysed in surface sediments and sediment trap particulate material. This data was integrated with observations on near-bottom hydrodynamics and sediment dispersal. The sediment column deposited over the last 150 yrs and pre-industrial sediments were studied for the geochemical parameters. The determined geochemical parameters include elemental concentrations, stable Pb isotopes, contents of lithogenic material, calcium carbonate and organic carbon. The Lisbon-Setúbal and Cascais canyons received special attention in this study as these structures have had much less attention than the Nazaré Canyon. The results show that sediment distribution on the central Portuguese margin is partitioned by submarine canyons and export of shelf sediments towards the deeper continental margin is restricted by slope currents, except where canyons provide corridors for down-slope transport. While in the Lisbon-Setúbal Canyon, and probably in the Cascais Canyon, down-canyon transport of sediments to the lower canyon is limited, conceivably only triggered by high energy events, in the Nazaré Canyon down-canyon sediment transport seems efficient. The upper reaches of the Lisbon-Setúbal and Cascais canyons presently act as traps for fine-grained sediments entrained in suspension from the adjacent shelf. Direct sediment input from the Tagus and Sado river plumes into the upper canyons seems limited. However, resuspension of sediments from the Tagus prodelta as a result of storm waves and internal tidal waves seems enough for an efficient transport of sediments into the upper Lisbon and Cascais canyons. In the Lisbon-Setúbal-Sines continental shelf geochemical and mineralogical signatures from various fine sediment sources were identified (e.g. Tagus and Sado estuaries, sea-cliffs, St. André and Melides lagoons). The contribution of trace metals from anthropogenic sources was assessed by comparing present-day and average elemental concentrations for the industrial period with pre-industrial baseline values. Baseline elemental concentrations are very similar for the Nazaré and Lisbon-Setúbal canyons, but varying degrees of anthropogenic trace metal enrichments are recorded in more recent sediments. Enhanced anthropogenic influence in the latter area is consistent with its proximity to heavily populated and industrialized areas and with sediment input originated from the Tagus and Sado rivers, potential major carriers of pollutant particles (Pb, Zn and Cu). Atmospheric dispersal of Pb seems important as well in the Lisbon-Setúbal-Sines margin and virtually all the studied continental shelf adjacent to the Lisbon-Setúbal and Cascais canyons shows enrichment of Pb. The main source of anthropogenic Pb identified through Pb stable isotope signatures seems to be incinerator fly ashes. Discharge of dredged contaminated sediments in the Lisbon Canyon appears also as a potentially important source of anthropogenic trace metals.

Index

List of figures

List of tables

Structure of the thesis

The thesis here presented is organised in four parts and eight chapters.

Part I (Introduction, Regional Setting and Materials and Methods) – Includes three introductory chapters which provide scientific and regional backgrounds, and describe the materials and methods used.

Chapter 1 presents a state-of-art about the recent developments on the knowledge of continental margins and the special focus of EU-Projects on submarine canyons and their roles in transferring particulate matter to the deep sea. The objectives of the present thesis are also presented.

Chapter 2 is intended to be a characterisation of the submarine canyons from the western Portuguese margin. The surrounding areas of the Lisbon-Setúbal and Cascais canyons (adjacent continental margin, beaches, and river basins) are also described in terms of geomorphology, geology, oceanography and climate.

In *Chapter 3* the materials (core, trap and grab sediment samples) and methods (geochemistry, mineralogy and grain size of sediments; mass deposition fluxes, sediment accumulation rates and near-bed hydrodynamic data) used for the present study are presented.

Part II (Continental shelf and upper slope) – Results about the continental shelf are presented and discussed in two chapters.

Chapter 4 is focused on mineralogical parameters determined in surface sediments from the shelf/upper slope and its discussion deals mainly with using these parameters to identify the main sources of fine-grained sediments and to gain insight in prevailing dispersal processes acting on the shelf.

Chapter 5 presents elemental contents of surface sediments from the shelf/upper slope and its discussion is focused on trace metal dispersal in surface sediment and its relationships with pathways of recent sediment transport in the shelf.

Part III (Submarine canyons and open slope) – Results about submarine canyons and open slopes of the central Portuguese margin are presented and discussed in two chapters.

In *Chapter 6* near-bottom hydrodynamic data and sedimentological data (general composition, grain size, C_{org}/N ratios and mineralogy) from surface and sediment trap

material collected throughout the canyon are integrated in order to understand the recent sedimentary dynamics of the Lisbon-Setúbal Canyon system. Data from the Nazaré and Cascais canyons and from the open slope areas of Mondego, Estremadura and Sines are also presented in order to obtain an overview about the pathways of recent fine-grained sediment transport on the central Portuguese margin, with especial focus on the Lisbon-Setúbal Canyon.

Chapter 7 presents geochemical data from surface and sediment trap material so as to determine anthropogenic inputs of trace metals. The knowledge of specific signatures and its dispersion will give insight into sedimentary processes operating on the central Portuguese margin, again with especial focus on the Lisbon-Setúbal Canyon.

Part IV (Data integration and conclusions) – In this part, composed of one chapter, data from the Lisbon-Setúbal-Sines continental shelf and Lisbon-Setúbal and Cascais submarine canyons are integrated, the main conclusions from the thesis are summarised and proposals for future investigations are indicated.

Chapter 8 is intended to integrate data from the four last chapters so as to build a model for the main pathways of fine-grained sediments in the Lisbon-Setúbal Canyon and adjacent shelf area.

Part I
Introduction, Regional setting, Materials and methods

1. INTRODUCTION

1.1. Continental margins: main sedimentary processes

Continental margins form relatively narrow transition zones between continental land masses and deep-ocean basins. They are the main regions of input and transfer of particulate matter to the oceans and, as such, they represent important zones of particulate matter flux.

The continental margin is made up of the shallow, relatively flat continental shelf, bordered by an inclined continental slope, at the base of which there is often a wedge shaped accumulation of sediments, the continental rise. The continental shelf, which depending on the geological setting may span from few to hundred kilometres wide, can roughly be subdivided in three other areas: inner shelf (10 - 50 m WD), middle shelf (50 - 100 m WD) and outer shelf (100 - 200 m WD).

1.1.1. Continental shelves

The continental shelf is generally an area where material derived from the continent is initially deposited, although it commonly only represents a temporary resting place for sediments. On the shelf there are two main directions of transport of particulate matter: along-shelf and across-shelf transport. The magnitude of along-shelf particulate transport is usually much greater than that of across-shelf transport. Across-shelf transport can be important near capes and canyons, diverting flows across the shelf more effectively than other physical mechanisms.

Particulate transport in both the along-shelf and across-shelf dimension is driven almost entirely by water motions. The surf zone (traditionally not included in the continental shelf) is the area where the highest volumes of sediment move alongshore. The dominant mechanism envisaged in alongshore transport in the surf zone is movement of sediment by longshore-directed currents generated by oblique waves. Since most wave energy dissipation takes place in the surf zone, this is a zone where both suspended load and bedload longshore transport takes place.

Comparably lower but still considerable volumes of sediment move alongshore on the shelf immediately seaward of the surf zone. Sediment transport in the inner shelf and further offshore is primarily wind-driven (Savidge & Bane Jr., 2001) and highly dependent

on sediment availability, topography and geology. Additionally, tidal currents have been identified as responsible for significant longshore transport of sediments.

The flow regimes of continental shelves vary appreciably as water depth changes from shore to shelfbreak. Not only do flow velocities change across the shelf, but so do the relative importance of various types of flows. The mechanisms that contribute most to across-shelf particulate transport are: 1) wind-driven upwelling and downwelling flows; 2) internal waves; 3) wave-orbital flows; 4) infragravity oscillations; 5) buoyant plumes (positive and negative); and 6) surf zone (wave driven) processes. Most of the above driving processes are bidirectional and therefore capable of reversing direction of transport. A review on the processes affecting transport of particles across continental shelves can be consulted, for example, in Nittrouer & Wright (1994).

1.1.2. Continental slope and rise

Once on the slope, material exported from the shelf is subject to further transport under influence of a variety of across-slope, along-slope and hemipelagic processes (Figure 1.1). Continental margin systems are likely to include all three components, albeit in differing proportions in space and time. It is important not only to recognize the interaction of these processes, but also to appreciate their variation in magnitude, and their frequency (Evans *et al.*, 1998).

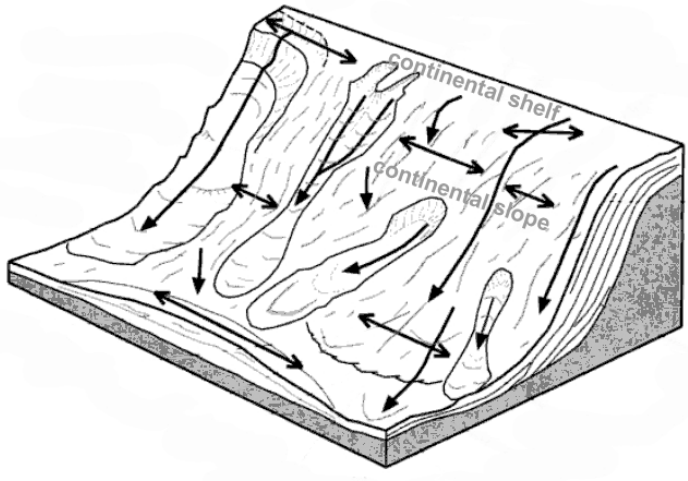

Figure 1.1. Schematic model of the continental margin depicting the main processes described in the text. The arrows indicate the directions of sediment movement.

On short time scale, across-slope sediment transport is often dominated by bidirectional tidal currents, moving sediment both in upslope and downslope direction. Internal tides are an efficient driver of sediment transport, especially in the deep and narrow upper reaches of canyons where tidal currents are focused. On longer time scales, however, across slope transport is predominantly in downslope direction, driven by gravitational forces that continuously or episodically move sediment downslope over the sea floor into deeper water. They range in scale from minor creep to major translational slides, and may take place on a range of timescales. Sediment creep is a semi-continuous process caused by load-induced stress, whereas discrete debris flows, slumps and slides may occur episodically, in between long periods of relative quiescence. Mass wasting events may last from minutes to hours. Turbidity currents are another type of frequent downslope event and they are sediment-laden water moving down a slope through water. The current moves because it has a higher density (and turbidity) than the fluid through which it flows. Turbidity currents may flow for hours (high-density flows) up to days (low-density). During any single downslope event these various processes may operate together or in temporal sequence, slumps often disintegrating into debris flows and then into turbidity currents. Continental margins subject to frequent downslope activity are commonly characterised by slope aprons and submarine fans (Stow, 1986).

Bottom-current activity greatly influences both sediment accumulation and erosion on continental slopes. The effects of along-slope currents (contour-following, deep, geostrophic currents) are particularly marked on slopes and basin plains within and adjacent to continental margins, where a variable sea-floor bathymetry may locally intensify and focus current activity. Sediment drifts and associated bedforms are the characteristic depositional product of along-slope bottom currents, and commonly accumulate where there is a change in the gradient of the seabed, such as at the base of continental slopes. Where particularly strong, bottom currents may cause erosion of the seabed and the formation of channels, moats and furrows (Evans *et al.*, 1998).

Hemipelagic sedimentation includes the settling of pelagic as well as land-derived material. Although commonly represented as a vertical flux, the settling velocity of the very fine-grained bulk of hemipelagic sediment is usually far less than the velocity of prevailing horizontal currents, and the resulting flux is therefore nearer to horizontal than to vertical. Hemipelagites, formed by hemipelagic sedimentation, are poorly sorted, predominantly fine-grained sediments, with variable composition according to the contribution from pelagic and terrestrial sources. They are commonly devoid of primary

sedimentary structures other than lamination, although lamination is usually thoroughly reworked by bioturbation. Their study is important because hemipelagic sedimentation is the primary "background" process on margins.

The various processes operating in the continental shelf and slope need to be integrated to produce a model of margin development. The characteristics, sources and fate of particulate matter in the sea are of great interest for other reasons than those related to sedimentology only. Two examples would be the dispersion of contaminants (Puig *et al.*, 1999) and the nourishment of benthic ecosystems (Pfannkuche, 1993; Cartes *et al.*, 2002). A holistic approach is therefore needed in order to understand the complex environments found on the continental margins.

1.2. Continental margins and submarine canyons: the state of art

In the past decades, several major multidisciplinary studies have been conducted all over the world to examine the processes and extent of exchange between the continental shelf, slope and deep sea.

A holistic approach is necessary in these complex dynamic settings moulded by the interplay of biology, physics, geochemistry and sedimentology.

The first great multidisciplinary effort was conducted in the Mid-Atlantic Bight on the eastern US continental shelf and slope during the SEEP-I (1983-1984) and SEEP-II (1988-1989) projects (Biscaye *et al.*, 1988, 1994). The overall SEEP working hypothesis was that a large part of the organic particulate matter that is formed on or introduced to the shelf and not consumed there is not deposited and buried on the shelf but transported further seaward, to the adjacent slope and open ocean. The results of the project SEEP-II led to reject that hypothesis. The experiment revealed that only a small proportion (<< 5 %) of this organic matter was exported to the adjacent slope (Biscaye *et al.*, 1994), and much of the exported organic matter may have initially been deposited on the shelf or shelf break and resuspended and transported down-slope thousands of years later (Anderson *et al.*, 1994). Most of the biogenic particulate matter is recycled on the shelf and only the most refractory (particulate) organic matter is likely to be exported (Bacon *et al.*, 1994).

De Haas *et al.* (2002) reviewed several studies on continental shelves of the world and concluded that large areas of the world shelves do not show any accumulation of organic matter under present-day conditions. Only locally, where hydrological and

sedimentological conditions are favourable for organic matter accumulation, considerable amounts of organic carbon are buried, mainly where rivers introduce large amounts of fine-grained sediments and organic matter on the shelf, for example the Amazon River. For most continental shelves, de Haas *et al.* (2002) depicted the following scenario: once the fine-grained sediments associated with the organic carbon reach the shelf, a continuum of bioturbation and cycles of erosion, transport and redeposition takes place under the influence of tidal and large scale shelf currents and storm induced waves and currents. After several cycles of successive exposition to oxic and anoxic conditions, most of the organic matter is mineralised; the sediments with the more refractory remainder of the organic matter reach their final destination and become buried.

It is important to bear in mind that the SEEP experiments focused on the processes taking place across the open slopes, largely avoiding submarine canyons.

Partly concurrent with the SEEP effort, the interdisciplinary ECOMARGE project (1986-1988) (Monaco *et al.*, 1990a) based in the Gulf of Lions did recognise the importance of canyons in the shelf-slope exchange. It was noted that export of material preferentially occurred down the canyon systems, notably the Lacaze-Duthiers Canyon (Monaco *et al.*, 1990b). The project ECOFER (1989-1991) (based on the Cap Ferret Canyon) also showed preferential focusing of particulate matter in a submarine canyon incising the slope of the southeastern Bay of Biscay (Monaco *et al.*, 1999a).

SEEP-I & II, ECOMARGE and subsequent multidisciplinary projects like KEEP (1989-1994), OMEX I (1993-1996) II (1997-2000), or FRUELA (1995-1996), concluded that organic particle flux to the slope is mainly supplied by lateral transport from the shelf and upper slope rather than by pelagic settling. Other authors reached the same conclusion from the deficit found between the vertical flux of organic matter and the energy and material requirements of the benthos (e.g. Thomsen, 1999; Druffel & Robinson, 1999). In other words, the concept of a "biological pump" dominated by vertical processes, as conceived in open oceans, seems not applicable to ocean margin settings, where resuspension and lateral advection are major drivers of particle transport.

Another key finding of these projects was the importance of the along-shelf and along-slope transport driven by the general circulation, as opposed to processes that transport material offshore, which tend to be less common and focused in specific areas (Monaco *et al.*, 1999b); this does not imply that offshore transport (e.g. upwelling processes) may not have major impact on particulate fluxes in specific areas of the globe.

With regards to the carbon cycle, the relatively limited export of organic particulate matter from the continental shelf to the slope and beyond found in the SEEP projects, has later been confirmed in other margins of the world. After all, the SEEP results identified a mid-slope depocentre of organic carbon, whereas the OMEX-I project, found no obvious depocentre of organic carbon in the northern Bay of Biscay margin (Wollast & Chou, 2001). However, Wollast & Chou (2001) added to that conclusion that the possible role and importance of submarine canyons for the transportation of organic carbon to the slope had not been addressed in OMEX-I. This point was explored and confirmed in OMEX-II, namely in the Nazaré Canyon (Van Weering *et al.*, 2002). High sedimentation rates (Schmidt *et al.*, 2001) and high burial efficiencies of organic carbon (Epping *et al.*, 2002) and reactive phosphorus (Van der Zee *et al.*, 2002) were encountered in the Nazaré Canyon sediments. The role of this canyon in the formation and offshore channelling of thick nepheloid layers was also highlighted (McCave & Hall, 2002).

A workshop on the role and functioning of canyons held in Sitges (Spain) in 2002 revealed that only few of the canyons across the NW Mediterranean and NE Atlantic European margin had been mapped and sampled in detail, and that transport processes and mass fluxes of particles, including organic matter, anthropogenic substances and urban waste to the deep sea and their sites of final deposition were virtually unknown (Van Weering & Weaver, 2007).

As a consequence of the above, submarine canyons dissecting the European continental margins were one of the main targets of the EC-EUROSTRATAFORM (2002-2005) and HERMES projects (2005-2009). The EUROSTRATAFORM was the first EU-project specifically looking at different submarine canyons from the European margins with the objective of understanding their role in ocean margin strata formation. This project aimed to understand sedimentary systems from source to sink. A key aim was to gain a better understanding of how sediment particles are transported from river mouths, across the shallow shelf and/or through submarine canyons, down to the deep sea. By studying different areas of the NE Atlantic and Mediterranean margins, it was possible to gain an idea on how these sedimentary systems work in different regional settings.

In April 2005 a new EU-project started with a different point of view. HERMES (Hotspots Ecosystems Research on the Margins of European Seas) was designed to gain new insights into the biodiversity, structure, functioning and dynamics of marine ecosystems along Europe's deep-ocean margin. It represented the first major attempt to investigate and understand deep-water ecosystems and their environment in an

integrated way by bringing together expertise in biodiversity, geology, sedimentology, microbiology, physical oceanography and biogeochemistry. Submarine canyons were again one of the main study areas in focus on this project. This time the goal was more ambitions since it was not only about investigating the driving forces that control ocean margin strata formation but also the ecosystems associated (Weaver *et al.*, 2004).

1.2.1. Submarine canyons: conducts for across-margin transference of particulate matter

Submarine canyons, incisions of up to hundreds of meters below the level of the surrounding continental shelves and slopes, may constitute a significant alternative to the scenario depicted by De Haas *et al.* (2002). The focusing and channelling effect of submarine depressions may allow an important fraction of the labile organic matter to reach the open ocean, bypassing the slow pathway and subsequent intense remineralisation characteristic of non-dissected, gently sloping margins. This might translate into a greater percentage of labile organic matter to fuel deep sea food webs, and also in a larger amount of carbon sequestered from exchange with the atmosphere. This rapid lateral transfer of organic matter is especially important in a semi-enclosed sea as the Mediterranean, where the high thermal stability of deep waters promotes rapid degradation of organic matter.

Submarine canyons have often been regarded as relics of glacial periods of lowered sea-level, when voluminous quantities of sediment were carried by rivers right across what are now continental shelves (Pickering *et al.*, 1989). Flooding of the continental shelves after the last glacial period decoupled continental drainage systems from depocentres on the slope, and consequently the sedimentary regime on continental slopes has shifted from a situation dominated by turbidity currents to another regime dominated by hemipelagic deposition (Nelson, 1976; Thorbjarnarson *et al.*, 1986). Sediment supply to the continental slope and the role of submarine canyons as pathways of sediments to the deep-sea floor, have both been drastically reduced. However, there is evidence that, even with the present high sea-level stand, many submarine canyons of the world's continental margins continue to channel and/or accumulate substantial quantities of sediment and therefore organic matter (e.g. Puig & Palanques, 1998a; Lewis & Barnes,

1999; Van Weering *et al.*, 2002; Xu *et al.*, 2002; Paull *et al.*, 2003; De Stigter *et al.*, 2007b).

One of the main contributions from the EUROSTRATAFORM was that at the present climatically controlled high sea-level stand, the majority of the finer grained material transported into the canyons is retained largely in the upper and middle part of the canyons (1500–3000 m water depth) and these parts of the canyons act as a temporary buffer for the storage of sediment and carbon (Van Weering & Weaver, 2007).

Modern sedimentation rates (e.g. Carpenter *et al.*, 1982; Sanchez-Cabeza *et al.*, 1999; Schmidt *et al.*, 2001, Van Weering *et al.*, 2002; Turchetto *et al.*, 2007) and downward particulate matter fluxes (e.g. Puig & Palanques, 1998a; Monaco *et al.*, 1999b; Hung *et al.*, 2003; De Stigter *et al.*, 2007b) have been found much higher in many submarine canyons than on the adjacent open slopes.

Many canyons continue to be favourable sites for the concentration of fine-grained sediments, whereas some of them are able to tap on abundant terrigenous sediment supplies, namely those that head off large rivers. In certain cases the canyon enters the river mouth, forming a continuum with the river bed, as for example the Sepik Canyon (Walsh & Nittrouer, 2003) or the Zaire Canyon (Khripounoff *et al.*, 2003).

However, proximity to a river is not a prerequisite for canyons to be active. On narrow, tectonically active margins, canyons have cut headward across the continental shelf, intercepting the sediment transported by along-shore currents (Lewis & Barnes, 1999). For example, the Nazaré Canyon (central Portuguese margin) is remote from any major stream, but as the canyon crosses the full length of the continental shelf and virtually reaches the shore, substantial amounts of material transported by the along-shelf currents are trapped in the canyon. Exports of material from the shelf to the deeper canyon is testified by thick nepheloid layers observed throughout the upper and middle canyon (McCave *et al.* 2001), and strong downward fluxes of sandy sediments and terrestrial plants debris observed at 3200 m water depth near the bottom (Martín *et al.*, 2004). In the canyon below 2700 m water depth most of the suspended sediments settle and are only transported to the lower canyon by sediment gravity flows occurring on a yearly or longer timescale (De Stigter *et al.*, 2007b).

Also for the Cap Ferret Canyon on the southern Bay of Biscay margin, Mulder *et al.* (2001) proved that turbidity currents are occurring in present times, despite the absence of a direct connection with an important fluvial sediment source.

Thus, while some canyons act as passive depocentres for the particles entering them via hemipelagic settling (Hickey *et al.*, 1986; Carson *et al.*, 1986), others are able to convey the particulate matter further to deeper water, acting as preferential conduits for matter transfer to deeper domains (Gardner, 1989; Puig & Palanques, 1998a; Hung *et al.*, 2003).

Inside canyons, particulate matter can be transported through nepheloid layers generated by tidal or residual currents (Gardner, 1989; Puig & Palanques, 1998b; Van Weering *et al.*, 2002), but also, turbidity currents, slumping from the walls, and other gravitational processes have been described in contemporary submarine canyons (May *et al.*, 1983; Ferentinos *et al.*, 1985; Xu *et al.*, 2002; De Stigter *et al.*, 2007b).

Turbidity currents flowing along the canyon axis are known to occur in present times, and are documented either indirectly (for a review cf. Nisbet and Piper, 1998), or shortly before the measuring instruments were broken down or dragged away by the violent currents (Paull *et al.*, 2003 and Khripounoff *et al.*, 2003). A successful in situ observation of contemporary turbidity currents was achieved by Xu *et al.* (2002) in the Monterey Canyon. Aside from these extraordinary events, observations in the Eel Canyon have demonstrated that sediment gravity flows of lesser magnitude but higher frequency may constitute an important agent in the effective across-margin transport of sediments in canyons receiving large amounts of sediment (Puig *et al.*, 2003, 2004).

The role of a canyon as a trap or a channel for sediments may differ according to the time-scale considered, due to redistribution processes operating on different time-scales. This is a critical point, since the net transport in these environments may be largely event-driven. Thus, observations within a small temporal window may lead to ambiguous mean fluxes, either dominated by exceptional events, or on the contrary, reflecting the "normal" conditions of relative quiescence, missing single events that may overwhelm, in terms of net fluxes, the cumulative values between events (Martín, 2005).

The modifications of water circulation associated to topographic features such as canyons have important implications for marine ecosystems. By altering the main currents, they affect biomass patterns (Masó & Duarte, 1989; Sabatés *et al.*, 1989), composition of phytoplankton assemblages (Estrada *et al.*, 1999), and distribution of fish larvae due to inshore-offshore exchange of water masses (Olivar *et al.*, 1988; Sabatés & Masó, 1990).

Unfortunately, canyons are also prone to transport and accumulate pollution (e.g. trace metals, Palanques *et al.*, 2008 and Jesus *et al.*, 2010; pesticides, Paull *et al.*, 2002; or litter, Galgani *et al.*, 1996), which further raises the need for research and protection.

The current multidisciplinary European project HERMIONE (Hotspot Ecosystem Research and Man's Impact On European Seas) envisages to give answer to questions regarding the ecology of submarine canyons, along with various other continental margin ecosystems, and also to focus on the impacts made by human activities on these ecosystems.

As a conclusion, one may notice that submarine canyons are complex systems in terms of hydrography, sedimentology, biogeochemistry and biology and great variability occurs both within individual canyon systems and between different canyons. Individual canyons have very different environmental characteristics that determine the diversity and the ecology of their fauna.

1.3. Objectives of the present study

In various EU-projects (OMEX-II, EUROSTRATAFORM and HERMES) the Nazaré Canyon on the Portuguese margin was an area of specific interest and as a consequence numerous papers dealing with this canyon have been published. On the other hand, the geographically nearby and equally huge Lisbon-Setúbal Canyon has so far received much less attention. The main goal of the present thesis is therefore *to study the pathways of recent fine-grained sediment transport on the central Portuguese continental margin with special focus on the Lisbon-Setúbal Canyon and adjacent shelf area*.

The Nazaré and Cascais canyons were also studied along with the Lisbon-Setúbal Canyon, so that a comparison can be made between canyons with different sedimentary setting and anthropogenic pressures.

The Sines, Estremadura and to some extent the Mondego open slopes were studied through cross-margin transects allowing comparison with transects in the submarine canyon systems.

The present thesis is based on comprehensive sediment sampling and collection of hydrographic data in the Lisbon-Setúbal, Nazaré and Cascais submarine canyons and adjacent open slopes. In order to achieve the above goal, the compositional variability of

sediments was assessed along the canyon axes in the three canyon systems. Short-term sedimentation from sediment traps was compared with the longer-term integrated sedimentary signal from core tops. The geochemical (elemental and isotopic) and mineralogical results were also integrated with data on processes and pathways of sediment transport (total mass fluxes through sediment traps, sediment accumulation rates through ^{210}Pb geochronology, horizontal SPM fluxes) for the Lisbon-Setúbal and Nazaré canyons. For the latter canyon, data on processes and pathways of sediment transport were previously published by De Stigter *et al.* (2007b).

Overall, the here presented data yield information on sedimentary processes presently operating within submarine canyons on timescales of days to decades and more, and specifically on sources and dispersal pathways of natural and anthropogenic trace metals affecting deep sea areas yet poorly known, such as submarine canyons.

In the next chapter a description of the central Portuguese margin will be presented focusing especially on the submarine canyons and also on the shelf and slope adjacent to the canyons. Since the Lisbon-Setúbal Canyon and the adjacent shelf and slope are the central topic of the present thesis, a more comprehensive description of these areas will be given, including a description of the adjacent hinterland areas (basin watersheds and coastal areas).

2. REGIONAL SETTING

2.1. Portuguese Atlantic margin

The Portuguese Atlantic margin is characterised by a narrow shelf and steep irregular slope, dissected by several deep canyons. Structural trends of the margin are determined by fault systems present in the Hercynian basement, by Mesozoic extensional tectonics related to the opening of the North Atlantic, and by Cenozoic compression resulting from the collision of the European and African plates (e.g. Vanney & Mougenot, 1981). The present morphology of the margin was basically established since the Miocene, when major subsidence occurred and prograding sedimentary series were deposited on the shelf and slope (e.g. Alves *et al.*, 2003). The latter were subsequently incised by canyons, which channelled large volumes of sediment towards submarine fans at the base of the slope. The main submarine canyons from north to south are: Porto, Aveiro, Nazaré, Cascais, Lisbon-Setúbal and São Vicente, which exhibit a very general northeast–southwest trend (Figure 2.1). These canyons, dividing the western Iberian margin into sub-margins with different features, are the main pathways through which shelf sediments are transported to the abyssal plains (Vanney & Mougenot, 1990). The sub-margins (shelf and slope) are here referred from north to south as (Figure 2.2):

- Aveiro margin between Espinho and Cape Mondego;
- Mondego margin between Cape Mondego and the Nazaré Canyon;
- Estremadura margin between the Nazaré Canyon and Cape Roca;
- Lisbon margin between Cape Roca and Cape Espichel;
- Setúbal margin between Cape Espichel and the Setúbal Canyon;
- Sines margin between the Setúbal Canyon and Cape Sines.

At depths over 4500 m the Aveiro and Mondego slope run out into the Iberia Abyssal Plain, and the Lisbon, Setúbal and Sines slope into the Tagus Abyssal Plain. The Estremadura spur, projecting westwards from the Estremadura margin, separates the Iberia and Tagus abyssal plains (Figure 2.1).

The Minho, Douro, Mondego, Tagus (Tejo) and Sado rivers supply sediment to the shelf, which is composed of a thick (> 1000 m) Cenozoic sediment wedge draping a Mesozoic substrate (Coppier & Mougenot, 1982). Cliff erosion and reworking of shelf

deposits are additional sources of recent sediment, next to biogenic sediment. Recent sediments are predominantly deposited on the shelf in a narrow belt along the shore and in mid-shelf mud patches. Further dispersal of fine-grained suspended sediment along and across the shelf occurs mainly in winter under the influence of southerly storms (Vitorino *et al.*, 2002b; Oliveira *et al.*, 2002). Transport of shelf sediments towards the deeper continental margin is limited by poleward flowing slope currents, in particular the flow of Mediterranean Water on the upper continental slope (Van Weering *et al.*, 2002). Submarine canyons like the Lisbon, Setúbal and Nazaré Canyon which cut deeply into the continental shelf, are likely to intercept the sediment transport along the shelf and provide corridors for transport down the continental slope.

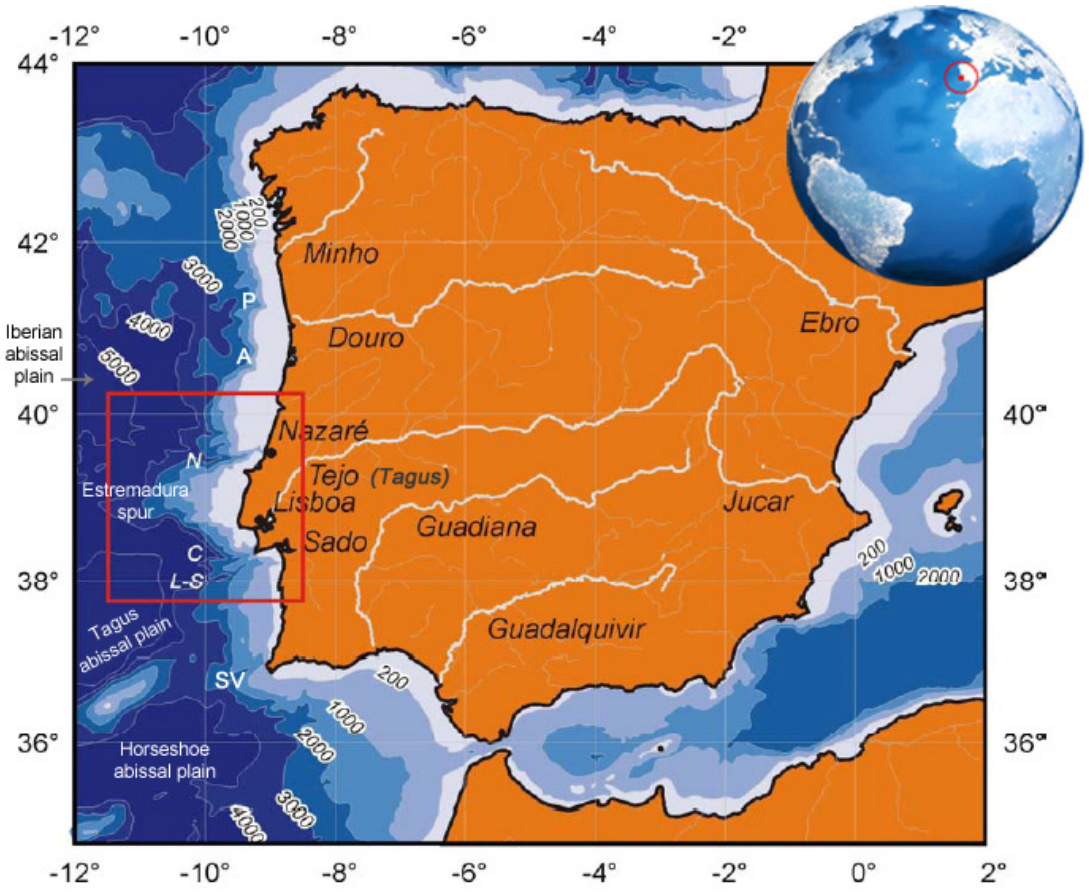

Figure 2.1. The Iberian Peninsula with major rivers and bathymetry of the adjacent continental margins and ocean basins. Inset shows location on the globe. Rectangle marks the study area. Porto, Aveiro, Nazaré, Cascais, Lisbon-Setúbal and São Vicente canyons are indicated with P, A, N, C, L-S and SV, respectively.

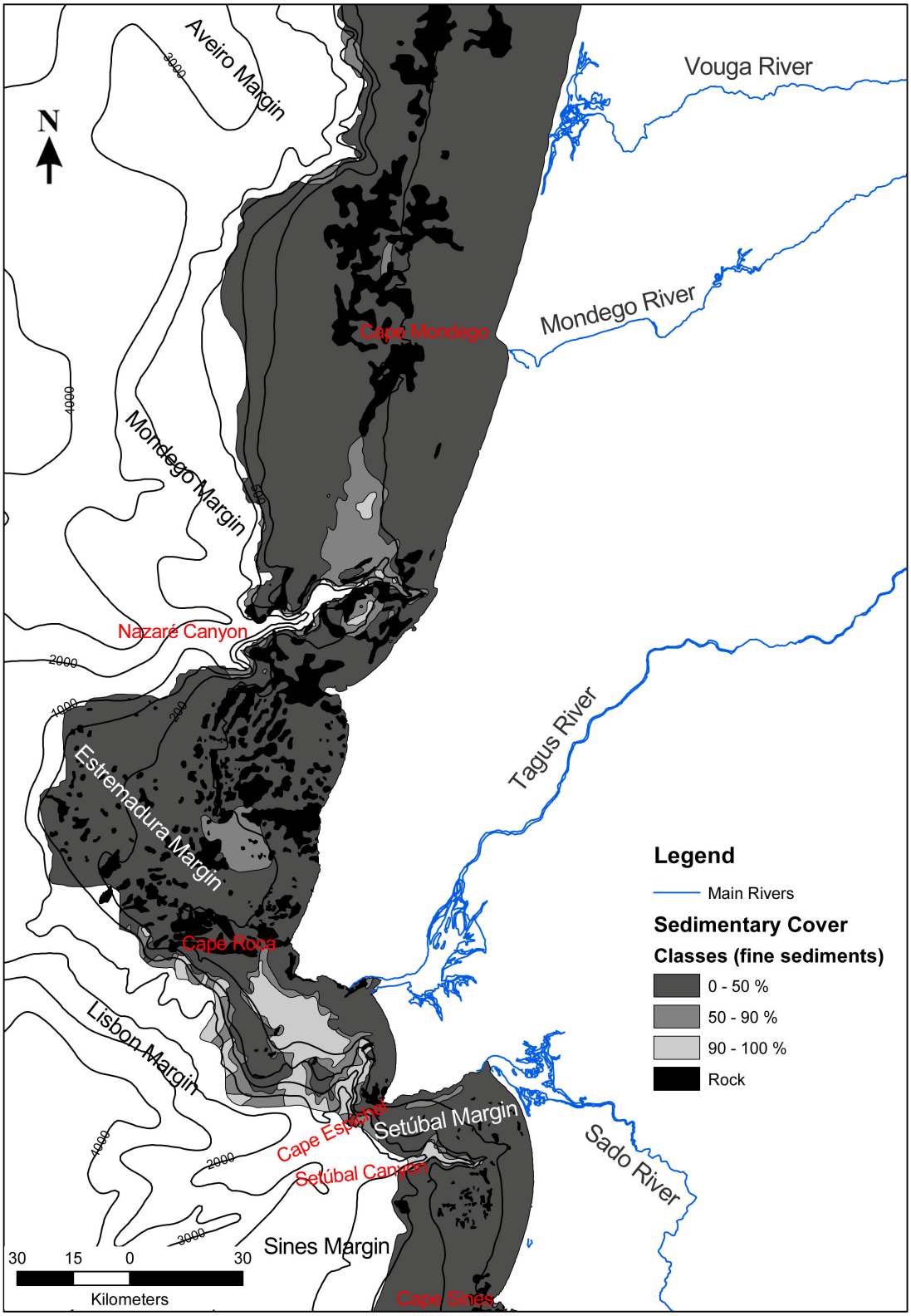

Figure 2.2. The central Portuguese margin and its sub-divisions: Aveiro, Mondego, Estremadura, Lisbon, Setúbal and Sines margin. The sedimentary cover of the shelf and upper slope is also presented, distinguishing sediment types with different contents of fine sediment. Shelf sediment cover drawn after Sedimentary Cover Map 5 from Instituto Hidrográfico (2005) for shelf between Cape Sines and Cape Roca;

from Balsinha (2008) for shelf between Cape Roca and the Nazaré Canyon and Pombo (2004) for shelf north of the Nazaré Canyon.

2.1.1. Lisbon, Setúbal and Sines margins

The continental shelf between Cape Raso and Cape Sines, in this study referred to as the Lisbon, Setúbal and Sines shelf, has a width ranging from 3 to 30 km, with the shelfbreak located around 200 m depth (Figure 2.2).

The sedimentary cover of these shelf areas was virtually unknown until the middle 1970's when the mapping of surface sediments was initiated with the SEPLAT Programme, carried out by the Instituto Hidrográfico of Portugal. Figure 2.3 showing the sedimentary cover of the study area is redrawn from the map published in 2005 by the Instituto Hidrográfico, as a result of this programme.

The close proximity to two rivers and protection of an important portion of the continental shelf from the main swell coming from the NW allowed the formation of mud patches in the shelf off the rivers. As a result of the sea-level rise since the last glaciation, paleocoast deposits can also be found in the shelf. In general, the sedimentary cover of the Iberian margin is mainly composed of late Quaternary and Holocene sediments (Dias, 1987).

River-derived sedimentary deposits

On the Lisbon and Setúbal continental shelves, sediment discharges from the Tagus and Sado estuaries have resulted in the formation of submarine protofluvial deltas in front of the river mouths. The sedimentary deposits off the Tagus River are essentially muddy (Figure 2.3). Protected against swell from the northwest, almost the entire Lisbon continental shelf is covered by a large expanse of muddy deposit.

The Tagus mud patch with an area of about 560 km^2 is the most important riverine-derived deposit of the Portuguese margin. Sediments from this deposit are composed of more than 85 % of terrigenous material whereas carbonate contents vary from 5 to 9 %, occasionally reaching values between 17 and 25 % (Jouanneau *et al.*, 1998 and Alt-Epping *et al.*, 2007). Linear sediment accumulation rates vary between 0.07 and 0.18 cm $year^{-1}$, with maximum values of 2.13 cm $year^{-1}$ (Jouanneau *et al.*, 1998).

Muddy deposits of the Sado protofluvial delta cover only a relatively small area confined to the river outlet, in accordance with the much smaller size of this river. The

sedimentary deposits covering the continental shelf adjacent to the Sado River are mainly sandy muds. Muddy sediment areas in the Setúbal shelf are restricted to the northern coast of the bay in front of Sesimbra and to the upper Setúbal Canyon (Monteiro & Moita, 1971; Moita & Quevauviller, 1986). The sedimentary cover of the Setúbal shelf is predominantly composed of terrigenous lithoclastic material, mostly quartz, whereas bulk carbonate content is mostly below 30 % (Figure 2.4).

Sandy deposits of the inner and outer shelves

Sandy deposits occur on the inner part of the Lisbon, Setúbal and Sines shelves, where the energy of littoral currents is sufficiently high to remove the finer sediment fractions. On the Sines shelf, coarse sandy deposits occurring on the outer shelf near the shelfbreak are a remnant of an old shoreline dated ~16 000 years B.P., which has not become covered by recent muddy deposits because of prevailing dynamics of the outer shelf (Dias, 1987). These deposits have carbonate contents which can exceed 50 % although contents below 30 % predominate (Figure 2.4). Local rock outcrops occur on all the three shelves but are most common on the Sines shelf (Figure 2.3).

Whereas the Lisbon and Setúbal outer shelves around 200 m WD pass abruptly into the steeply dipping slope leading down to the Tagus Abyssal Plain, the Sines shelf passes more gradually into the gently dipping slope. In this area steep slopes are only found at the intersection with the Setúbal Canyon.

2.1.2. Lisbon-Setúbal Canyon

The Lisbon-Setúbal Canyon is located on the Portuguese continental margin around 38º00'-38º30'N; 009º-010º30'W (Figure 2.5). The Lisbon-Setúbal Canyon intersects the Portuguese margin just south of Lisbon near the mouth of the Tagus and Sado rivers. It is a canyon system since it is characterised by having two upper-canyon parts: the Lisbon Canyon and the upper Setúbal Canyon. The head of Lisbon Canyon is located close to the mouth of the Tagus River, the largest river of the Iberian Peninsula. The head of Setúbal Canyon is located close to the mouth of the Sado River, a smaller river south of the Tagus. These two branches join together at around 2010 m WD. From the junction point onward the canyon, usually named Setúbal Canyon after the longest of the two branches, continues in WSW direction for another 127 km to the foot of the continental slope at 4500 m.

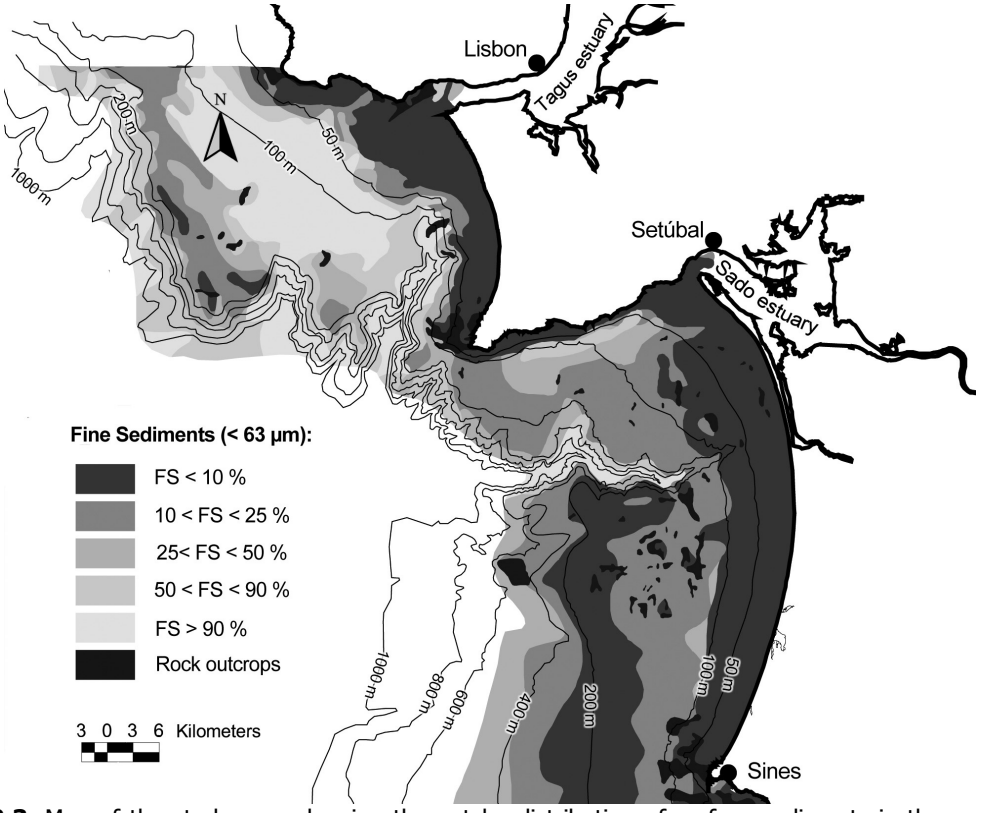

Figure 2.3. Map of the study area showing the patchy distribution of surface sediments in the continental shelf between Cape Raso and Cape Sines. Drawn according to the Instituto Hidrográfico's Sedimentary Cover Map 5 (2005).

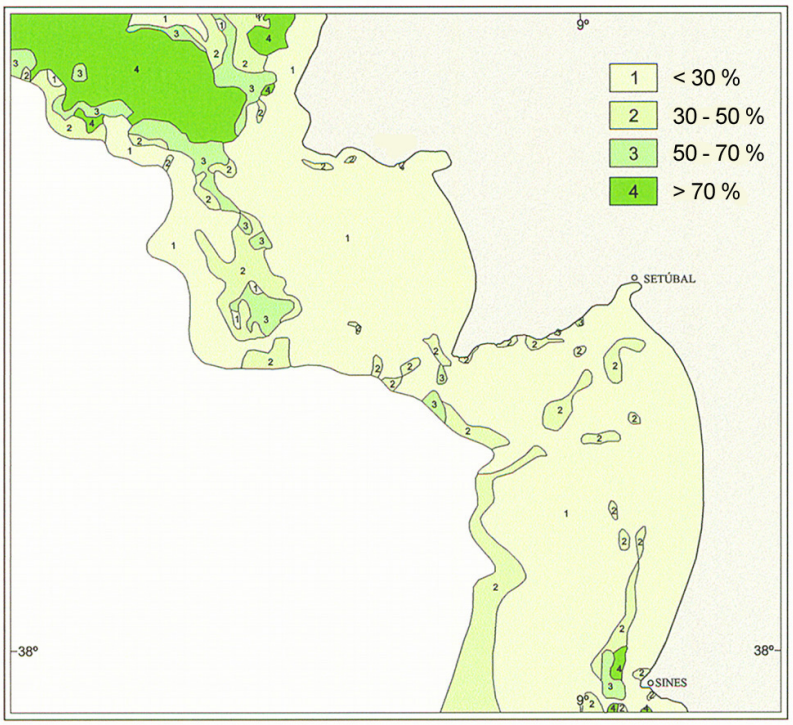

Figure 2.4. Patchy distribution of bulk carbonate contents in surface sediments from the continental shelf between Cape Raso and Cape Sines. Drawn according to the Instituto Hidrográfico's Sedimentary Cover Map 5 (2005).

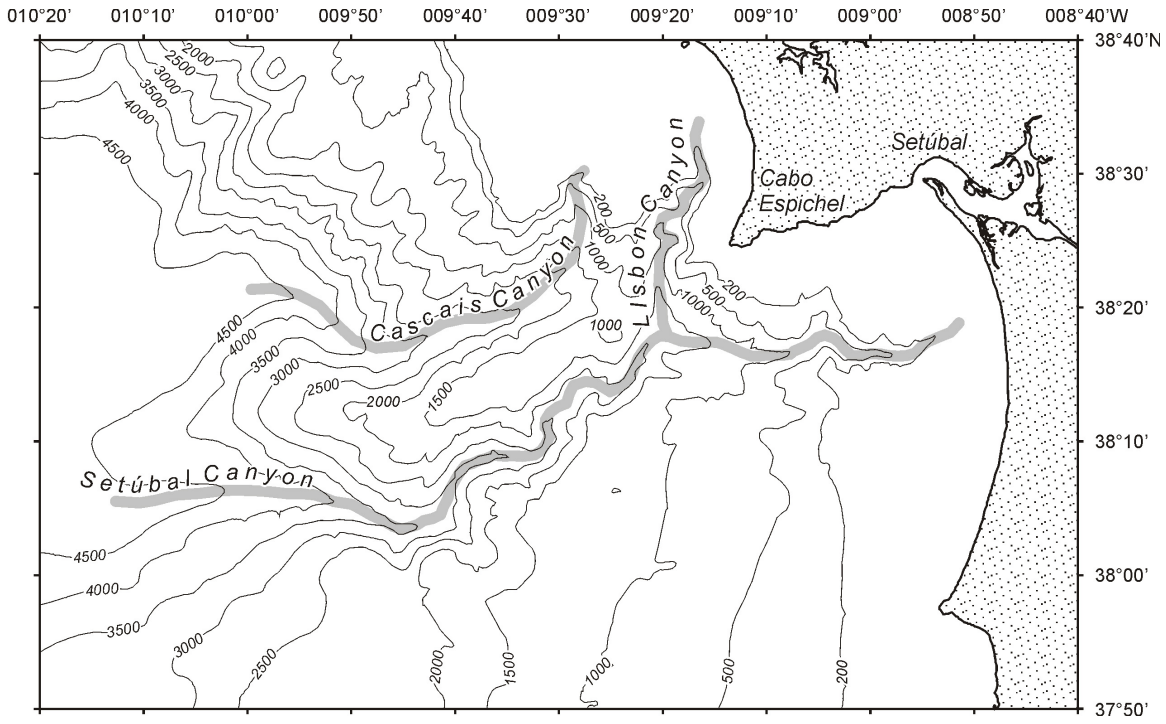

Figure 2.5. Bathymetric map of the Lisbon-Setúbal and Cascais canyons (from de Stigter *et al.*, 2004).

Upper Setúbal Canyon and Lisbon Canyon

The Lisbon-Setúbal Canyon is fed by two main canyon branches, the east–west-oriented Setúbal branch and the north–south-trending Lisbon branch (Figure 2.5). The Setúbal branch canyon head is located at 38°18'45"N, 8°52'49"W, at ~90 m WD, 20 km south-southwest of the Sado River mouth and 6 km west of the nearest coastline between Tróia and Sines. The branch cuts 45 km into the continental shelf with low sinuosity, although in its shallowest course it displays some open meanders; this section has a width of less than 8 km from edge to edge (section 9 of Figure 2.6c). Small terraces can be identified in TOBI imagery, both in its northern and southern walls (Lastras *et al.*, 2009) (Figure 2.7e).

The Lisbon branch canyon head is located at 38°33'15"N and 9°16'48"W, at ~120 m water depth, 13 km south-southwest of the Tagus River mouth, and 5 km west of the nearest coastline. It cuts 28 km into the shelf and is sinuous, with a total length of 38 km, due to a series of sharp meanders entrenched between high gullied walls (Figure 2.7c and Figure 6.2). A straight escarpment marks the western wall down slope of the major

meanders, where the canyon axis straightens (Figure 2.7c) before its almost perpendicular junction with the Setúbal branch at 38°17'38"N and 9°19'39"W around 2010 m WD.

The along-canyon profiles of the Setúbal (C–C2 in Figure 2.6c) and Lisbon (C–C1 in Figure 2.6c) branches differ substantially. The Lisbon branch displays a concave bathymetric profile that matches the profile of the Setúbal Canyon at water depths exceeding 2010 m. It is also parallel to the bathymetric profile of the lower part of the Setúbal branch, that is, between 1420 and 2010 m. However, that parallelism disappears upslope of 1420 m WD. There, the Setúbal branch displays a convex morphology with a knick point at 1040 m WD and high slope gradients in the canyon axis between 1040 and 1420 m WD (Lastras *et al.*, 2009) (Figure 2.6c).

There is a third, minor branch (C–C3 in Figures 2.6a and c), which starts at ~250 m WD and joins the middle course of the Setúbal Canyon at 2165 m WD, hanging 350 m over the canyon axis (section 8 in Figure 2.6c).

Setúbal Canyon - middle course

The middle course of the Setúbal Canyon is more than 25 km wide (from edge to edge) in some areas and 70 km long, measured from the confluence of the Lisbon and Setúbal branches at 2010 m down to the Setúbal Canyon mouth (the area where the canyon widens onto the lower portion) at 4170 m WD. Most of the middle course is characterised by a flat-bottomed canyon axis. This is most evident between 2150 and 2320 m WD, where a 500 m wide thalweg just upslope of a 110° sharp meander and a number of terraces in the northern wall can be identified, together with an over deepened pond (Lastras *et al.*, 2009) (Figure 2.7g).

Some short sections show, on the contrary, V-shaped axes, as happens in a north–south-oriented straight section at ~2600 m WD. In this part, the Setúbal Canyon is strongly incised. The external walls of meanders in the middle course show evidence of intensive gullying. The final part of the middle course, between 3700 and 4170 m WD, displays a striking variety of sedimentary processes (Lastras *et al.*, 2009). A flat-bottomed and slightly incised canyon thalweg of up to 1 km wide is bounded to the south by up to four levels of terraces, each more than 200 m wide. These terraces are swept by material coming from a 1200 m-wide notch in the southern wall and, down-slope, by a linear escarpment at the base of the southern wall. Large blocks and debris are clearly visible below this escarpment (Figure 2.7f), according to Lastras *et al.* (2009).

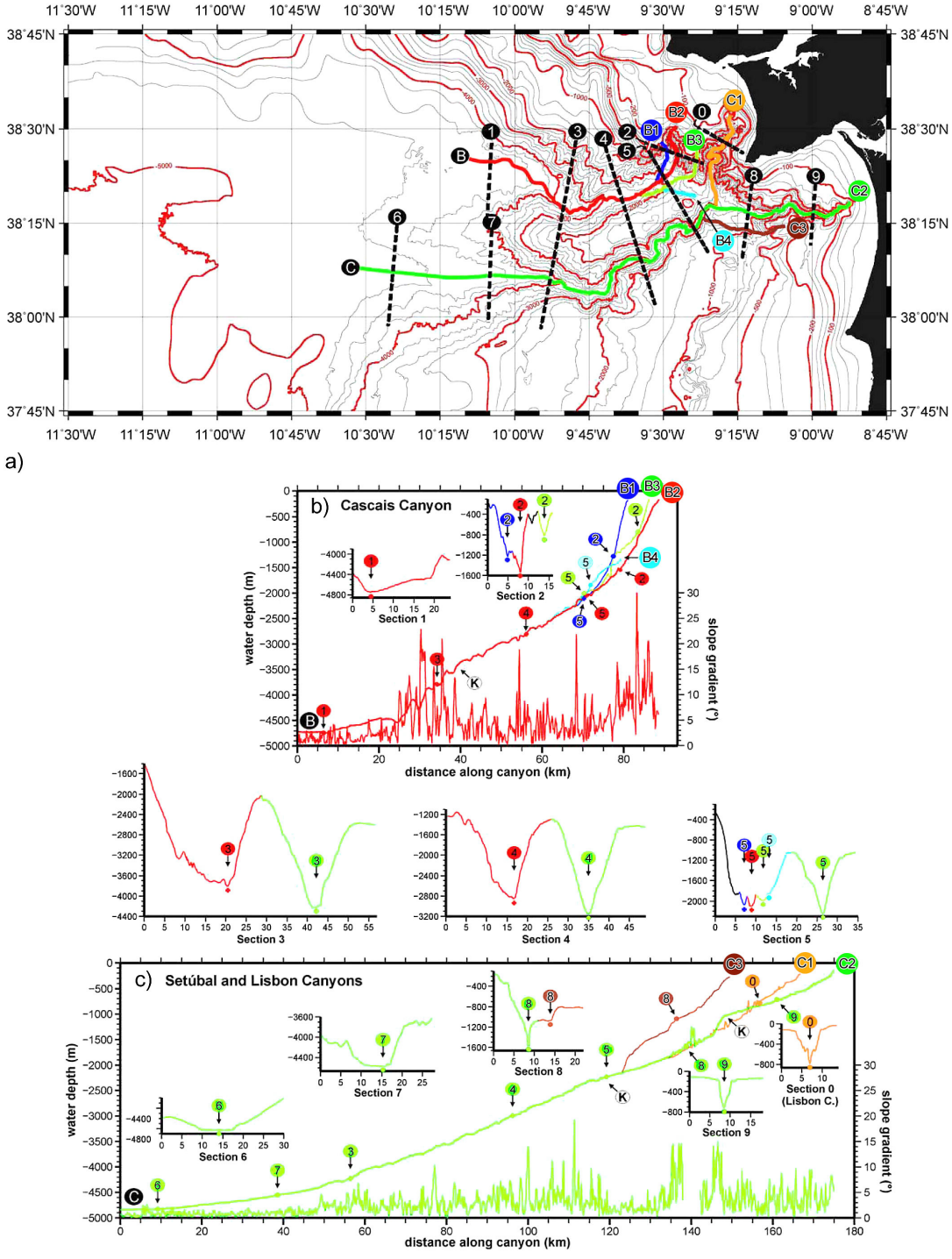

Figure 2.6. (adapted from Lastras *et al.* 2009) **a)** Bathymetric maps of the Cascais and Lisbon–Setúbal canyons. Contour map with location of bathymetric sections B–B1 (dark blue), B–B2 (red, main section), B–B3 (light green) and B–B4 (light blue) along the four main branches of the Cascais Canyon, C–C1 (orange) along the Lisbon branch of the Setúbal Canyon, and C–C2 (dark green, main section) and C–C3 (brown) along the two other branches of the Setúbal Canyon in panel c), as well as sections 1 and 2, across the Cascais Canyon in panel b), sections 6, 7, 8, 9 and 0, across the Setúbal–Lisbon Canyon in panel c), and sections 3, 4 and 5 across the two canyon systems in panel c), all of them in dashed black lines. Colour of

each section coincides with colours in b) and c).
b) and **c)** Topographic sections derived from the bathymetric maps in panel a) along the axis of (B) the four main branches of the Cascais Canyon, and (C) the Lisbon branch and the other two main branches in the Setúbal Canyon. For the main branch of each canyon system (B–B2 for the Cascais and C–C2 for the Setúbal Canyons), an along-canyon slope gradient section is also provided. Two cross-canyon sections (1 and 2 in B) for the Cascais Canyon, five (6 to 9 and 0 in C) for the Setúbal–Lisbon Canyon, whereas three more (3 to 5, drawn separately between B and C) are common for both Cascais and Lisbon-Setúbal canyons. Crossing points between longitudinal and cross sections are marked with a label that corresponds to the colour of the longitudinal section and number of the cross section.

Setúbal Lower Canyon

At 4170 m WD, the Setúbal Canyon abruptly widens and opens onto the lower part through the Setúbal Canyon mouth. The northern wall of the canyon mouth region displays pervasive signs of grooving. The first 11.5 km of the lower part, between 4170 and 4460 m WD, display a flat-bottomed, 1.9 km-wide thalweg bounded by high, steep walls (Figure 2.7f). The canyon thalweg gradually widens up to 5 km over the following 25 km, where tributaries join it from both walls. The thalweg is composed generally of high backscatter deposits in this section, with small low backscatter spots (Figure 2.7b). According to Arzola *et al.* (2008) the largest failure deposit from the Lisbon-Setúbal Canyon occurs in this area. Seismic shaking was interpreted as the likely cause of such a localised slope failure event on the northern levee. Over the following 11 km, i.e., between 46 and 57 km downslope from the canyon mouth, the thalweg has a very low slope gradient, and gains only 40 m in depth, from 4820 to 4860 m WD; beyond this point the canyon opens gradually onto the Tagus Abyssal Plain (Figure 2.2). Between 46 and 57 km, close to the southern rim, the thalweg displays evident signs of erosion, with elongated scours perpendicular to the canyon direction (Figure 2.7d). These scours tend to be orientated parallel to the canyon axis in the central parts of the thalweg. The Setúbal Canyon finally opens out onto the Tagus Abyssal Plain 57 km away from the canyon mouth, but its influence can be traced much farther away. TOBI imagery shows pervasive chevron-shaped scouring and other erosional morphologies 95 km away from the canyon mouth (Lastras *et al.*, 2009) (Figure 2.7a).

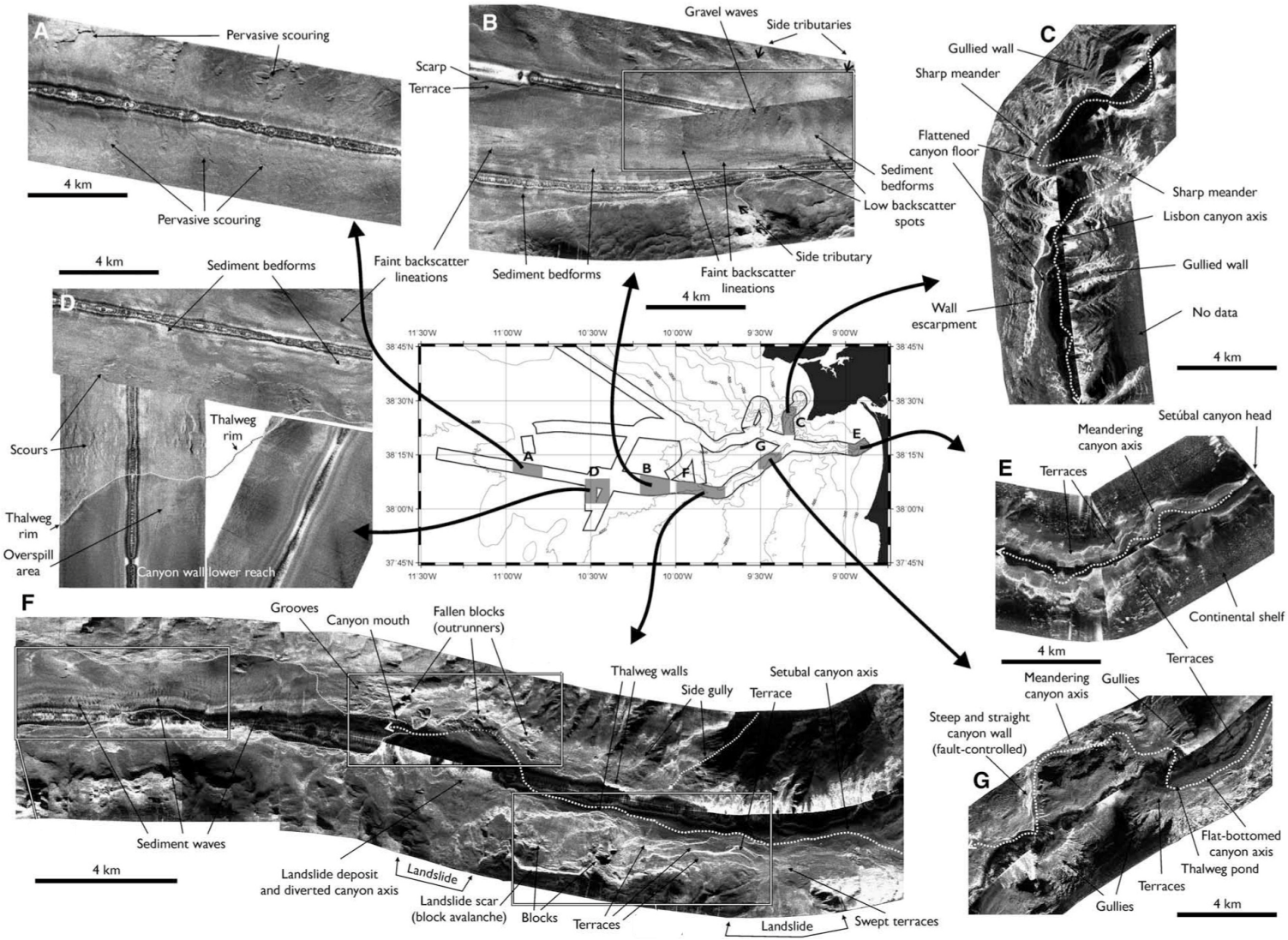

Figure 2.7. (adapted from Lastras *et al.*, 2009) TOBI side-scan sonar mosaics from the lower course + middle course (A, B, D, F and G) and upper course and head (C and E) of the Lisbon-Setúbal Canyon. Locations of A to G are provided in grey in the central map.

2.1.3. Cascais Canyon

The Cascais Canyon is incised in the shelf edge and slope northwest of the Lisbon-Setúbal Canyon (Figure 2.5), being separated from the latter by the Afonso de Albuquerque plateau (Vanney & Mougenot, 1981). Compared to the Lisbon-Setúbal and Nazaré canyons it is the shortest in length, taking almost 90 km in an open U-turn to cover a straight-line distance of 62 km between canyon head and mouth. Since it spans a depth range similar to that of the other two, it is also the steepest one, with slope gradients typically exceeding 10° (Lastras *et al.*, 2009).

The Cascais Canyon head has a very complex morphology when compared to the other central Portuguese canyons, with multiple branches and gullies slightly incised in the shelf edge (see Figure 2.6b, section 2), reflecting an initial phase in submarine canyon evolution (Twichell & Roberts, 1982; Farre *et al.*, 1983 *in* Lastras *et al.*, 2009). It displays pervasive gullying of its walls, has a 4.2 km wide V-shaped morphology and is incised up to 1350 m below the continental shelf.

The middle course of the Cascais Canyon runs from 2200 down to 4510 m WD, a distance of 43 km across the continental slope and base of slope. It is the most sinuous section of the canyon. In contrast to the upper section, which has an almost north–south mean direction of 196°, the middle section trends east–west. It has a width of up to 22 km, and is incised as much as 1800 m. Although the four axial incisions, corresponding to the four branches of the canyon, have joined to form one single axis, numerous gullies still enter the Cascais Canyon through its northern wall, whereas the southern wall is smoother and more regular. A wide canyon axis characterises the first part of the middle course, between 2200 and 3300 m WD, with slope gradients not exceeding 8° (see Figure 2.6b). In contrast, between 3300 and 4510 m WD, the Cascais Canyon thalweg is steeper, with slope gradients in places exceeding 15° and with widespread evidence of erosion, like grooving both in the thalweg and in the canyon walls, thalweg escarpments and over-deepened ponds (Lastras *et al.*, 2009).

The steep final part of the middle course of the Cascais Canyon opens at 4510 m WD into the lower-canyon. The lower part of the Cascais Canyon has a smooth, flat-bottomed and less incised valley, which in turn opens out into the Tagus Abyssal Plain (Figures 2.1 and 2.5).

2.1.4. Mondego and Estremadura margins

The Mondego margin has a shelf which varies from 65 km in width in its northern part down to 45 km close to the Nazaré Canyon. The main features of this portion of the Portuguese shelf are the mid-shelf rock outcrops in the north and a mid-shelf mud patch in the vicinity of the Nazaré Canyon. This middle shelf deposit, sub-parallel to the bathymetry, is 38 km long and 11 km wide (in average) but only 1-2 m thick. It is essentially formed by coarse silt, showing relatively high percentages of clay material (38 %) (Oliveira *et al.*, 2007). The rest of the shelf is composed of sandy sediments. In the area where rock outcrops occur, sandy sediments have gravel contents higher than 25 % (Dias, 1987). According to this same author, similar sediments can also be found half way between the Cape Mondego and the Nazaré Canyon head in a 20 km long deposit sub-parallel to the 50 m WD bathymetric line.

The Estremadura margin (also known as the Estremadura Spur) is composed of a shelf about 70 km wide at its largest extension and a slope spur projecting to the West (Figure 2.2). To the North and South the Estremadura spur has steep and irregular slopes, incised by numerous deep valleys, some of which act as tributaries to the Nazaré and Cascais canyons. In its lower part the spur separates the Iberia and Tagus abyssal plains. The Estremadura shelf is dominated by rocky outcrops, rising up next to lower lying areas which act as traps for coarse sediment. Especially between 70 and 130 m WD the terrain is very rough (Badagola *et al.*, 2006). The sediment traps are filled by coarse sand and gravely sediment (Balsinha, 2008) and normally the sediment column does not exceed 8 m (Badagola *et al.*, 2006). There is a muddy area, surrounded by rocky outcrops, just southwards from the Nazaré Canyon. The patch is 4 to 6 m thick (Pombo, 2004) and sediments have clay percentages around 28 % (Duarte, 2002). In the inner shelf, close to the canyon head, fine to very fine sandy sediments are found.

2.1.5. Nazaré Canyon

The Nazaré Canyon with an axial length of more than 200 km is among the largest canyons of the European continental margin (Figure 2.8). It is located between 39º25'N and 39º50'N, bounded eastward by the low coastal hills and cliff-coast of the Estremadura region, and sloping westward into the 5000 m deep Iberian Abyssal Plain. The most accepted theory about the canyon's tectonic setting states that the incision of the canyon

around 39º40'N is largely determined by an E-W trending transpressive faultzone affecting the Paleozoic basement and Mesozoic and Cenozoic sedimentary strata of the margin, and which forms the seaward continuation of the late Paleozoic NE-SW trending Nazaré fault on land (Vanney & Mougenot, 1990). The uplifted and deformed Estremadura promontory south of the faultzone delineates the southern boundary of the canyon. The lower-lying northern faultblock forms the broad shelf and slope north of the canyon. Another theory, however, assumes a more complex interplay between different faults forming the main valley of the canyon. According to this theory the faults that determine the canyon do not continue on land (Dinis, 2006).

According to the subdivision of the canyon used by De Stigter *et al.* (2007b) essentially following that of Vanney & Mougenot (1990), the upper part of the Nazaré Canyon is a sharp V-shaped valley that is deeply incised into the shelf and steep upper slope, and which descends from the shoreline to 2700 m depth over a length of 60 km measured along the canyon axis (Figure 2.9, sections f, g, h, i).

The main valley follows relatively straight sections of a few kilometres long, trending alternatingly in NE-SW and NW-SE direction parallel to the dominant structural trends of the shelf.

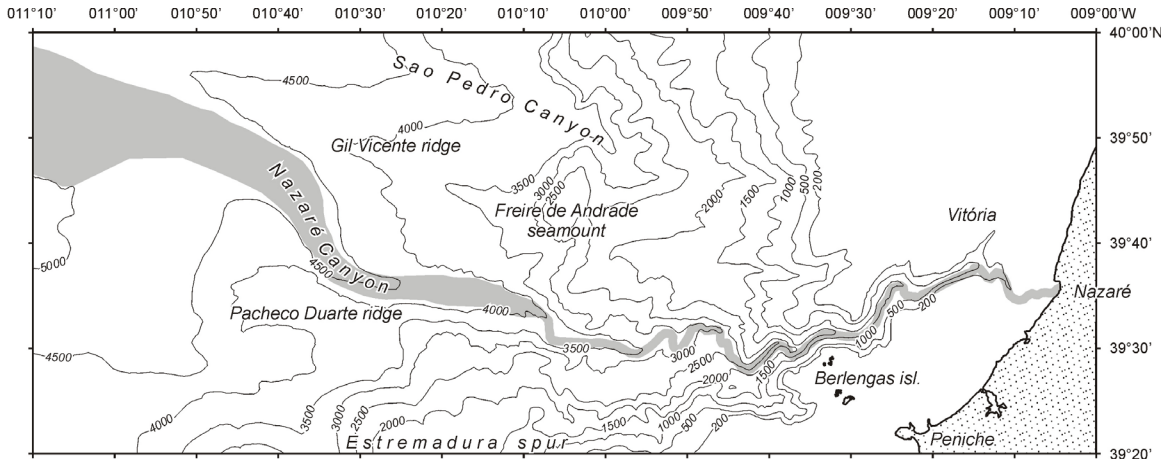

Figure 2.8. Bathymetric map of the Nazaré Canyon and adjacent open slope and shelf (from De Stigter *et al.*, 2004).

The Nazaré Canyon forms a canyon system as the upper canyon has one short side-valley branching off in NE direction from the main valley, known as the Vitória branch. In the canyon head, very fine mud covers the walls, whereas sand is present on the canyon thalweg below a drape of mud.

The middle part of the canyon is a broad meandering valley, incised into the middle slope and descending from 2700 to 4000 m depth over 50 km. The main valley has terraced slopes and a V-shaped axial channel (Figure 2.9, section d).

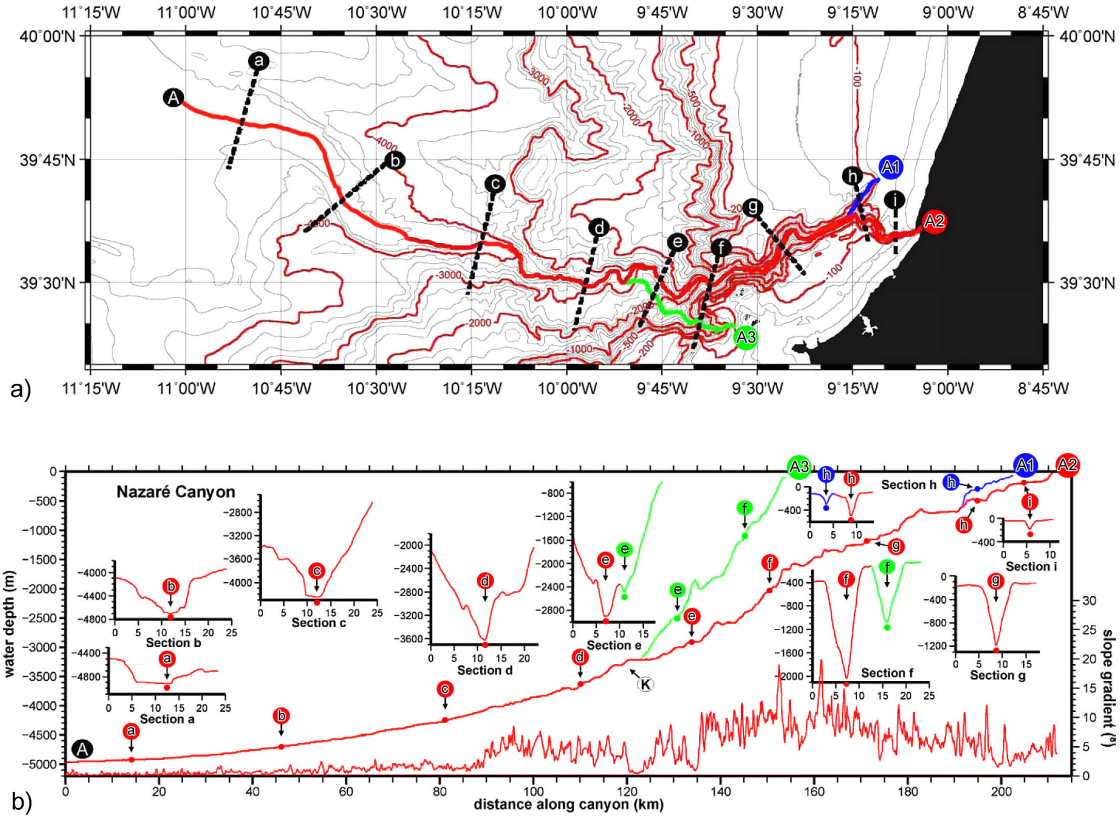

Figure 2.9. (adapted from Lastras *et al.* 2009) **a)** Bathymetric map of the Nazaré Canyon with location of longitudinal sections A–A1 (dark blue), A–A2 (red, main section) and A–A3 (light green) along the three main branches of the canyon, and cross sections a to i (dashed black lines), illustrated in panel b. Colour of each section corresponds with colours in panel b.
b) Sections along and across the three main branches of the Nazaré Canyon. For the main branch of the Nazaré Canyon system an along-canyon slope gradient is also shown. Nine cross-canyon sections (a to i in A) have been drawn for the Nazaré Canyon. Crossing points between longitudinal and across sections are marked with a label that corresponds to the colour of the longitudinal section and number of the cross section.

The lower-canyon, located on the lower continental slope, is a flat-floored valley with one or two incised axial channels, flanked to the south by the structurally defined Pacheco Duarte ridge and to the north by the up to 1 kilometre high sedimentary levee known as the Gil Vicente ridge (Figure 2.8). The lower-canyon valley descends very gently from 4000 to 5000 m depth over a length of 100 km and its flat-bottomed thalweg gradually increases in width from about 3 km to over 15 km. The ridges flanking the valley decrease in height in westward direction until they end on the abyssal plain. The construction of

the northern levee has been attributed to northward deflection of turbiditic sediments transported through the canyon by Coriolis forcing (Faugères *et al.*, 1984; Vanney & Mougenot, 1990 *in* De Stigter *et al.*, 2007b).

2.1.6. Oceanographic setting

Tides and wave climate

On the Portuguese coast, the dominant tide is semi-diurnal with a period of 12.25 hours, moving from south to north. In the Sines harbour the tidal amplitude varies from 3.4 m during spring tides to 0.7 m during neap tides (Instituto Hidrográfico, 1990).

The Portuguese coastal area is exposed to the highly energetic North Atlantic swells. According to Costa *et al.* (2001), the dominant wave directions are from NW and W (97 %), with the SW direction representing only 3 % of the observations. Waves with heights of 1-2 m and periods of 5-7 s represent almost half of the observations (49 % and 44 %, respectively). During storm events (3 % of the observations) waves are as high as 5-6 m with peak periods of 9-13 s.

Data recorded by the wave-rider buoy off Sines between 1992 and 1999 (Table 2.1) fits well to the general data for the Portuguese coast presented above. In northward direction from Sines towards Tróia there is an increasing sheltering effect of Cape Espichel which reduces the wave energy and deflects the incoming waves from the NW. In the northern part of the Tróia peninsula the waves are deflected so much as to arrive from SW directions, causing a northwards longshore drift. The same occurs on the coastal arc between Trafaria and Cape Espichel where a northwards increase of the sheltering effect is caused by Cape Roca.

In the above dataset collected between 1992 and 1999, the mean significant wave height (H_s) was 1.65 m, with a maximum of 7.69 m. The most energetic wave conditions (monthly H_s mean > 2.0 m) and the highest numbers of single records corresponding to storms (H_s > 5 m) were measured in November, December and January (Miranda, 2006).

Hydrological conditions of the Portuguese margin

The water column in the study area consists of several water masses (Fiúza *et al.*, 1998; Garcia *et al.*, 2003). At the surface, below the seasonally varying thermocline, a warm (11-15 ºC) and salty (≤ 36.0 psu) body of Eastern North Atlantic Central Water

(ENACW) can be distinguished (Figure 2.10). This water mass has a low concentration of suspended particles (~8-15 µg/l), although intermediate layers are observed with higher turbidity (Hall *et al.*, 2000).

Table 2.1. (adapted from Miranda, 2006) Summary of wave directions recorded between 1992 and 1999 by Instituto Hidrográfico's wave-rider buoy offshore Sines. Numbers represent percentage of wave incidence for different directions.

Year	N	NE	E	SE	S	SW	W	NW
1992	0.00	0.00	0.00	0.00	0.23	1.31	19.05	79.41
1993	0.16	0.00	0.00	0.00	0.37	3.78	15.02	80.67
1994	0.00	0.00	0.00	0.00	0.00	0.95	14.40	84.64
1995	0.00	0.00	0.00	0.00	0.33	2.79	25.74	71.14
1996	0.00	0.00	0.00	0.00	0.05	2.86	27.21	69.88
1997	0.08	0.00	0.00	0.00	0.08	2.63	34.77	62.43
1998	0.07	0.00	0.00	0.04	0.04	1.92	20.04	77.90
1999	0.15	0.00	0.00	0.00	0.04	0.80	16.90	82.11
Mean	0.06	0.00	0.00	0.00	0.14	2.13	21.64	76.02

Below the ENACW, between 600 and 1600 m WD, occurs the relatively warm (~10 ºC) and saline (> 36.0 psu) Mediterranean Outflow Water (MOW); a salinity maximum is centred at 1100 m depth. The MOW flows northwards along the western Iberian continental slope in a narrow vein of 100 to 150 km width, with a mean current velocity of approximately 12 cm s^{-1}. An upper core of MOW closely follows the continental slope, whereas a lower core of MOW meanders west and northwestwards (Schönfeld, 1997 and references therein).

The North Atlantic Deep Water (NADW) dominates below the MOW (between 1500 and 3000 m WD), with cooler (2-6 ºC) and less salty (~35.0 psu) properties. This water mass consists of a mix of Iceland-Scotland Overflow Water and Labrador Sea Water (Van Aken, 2000b).

The relatively thin (~200 m WD) superficial water layer flowing along the Portuguese margin is influenced by fresh water inputs from rivers and by wind stress which are variable throughout the year. Vertical movements associated with upwelling and downwelling essentially occur within this superficial water layer.

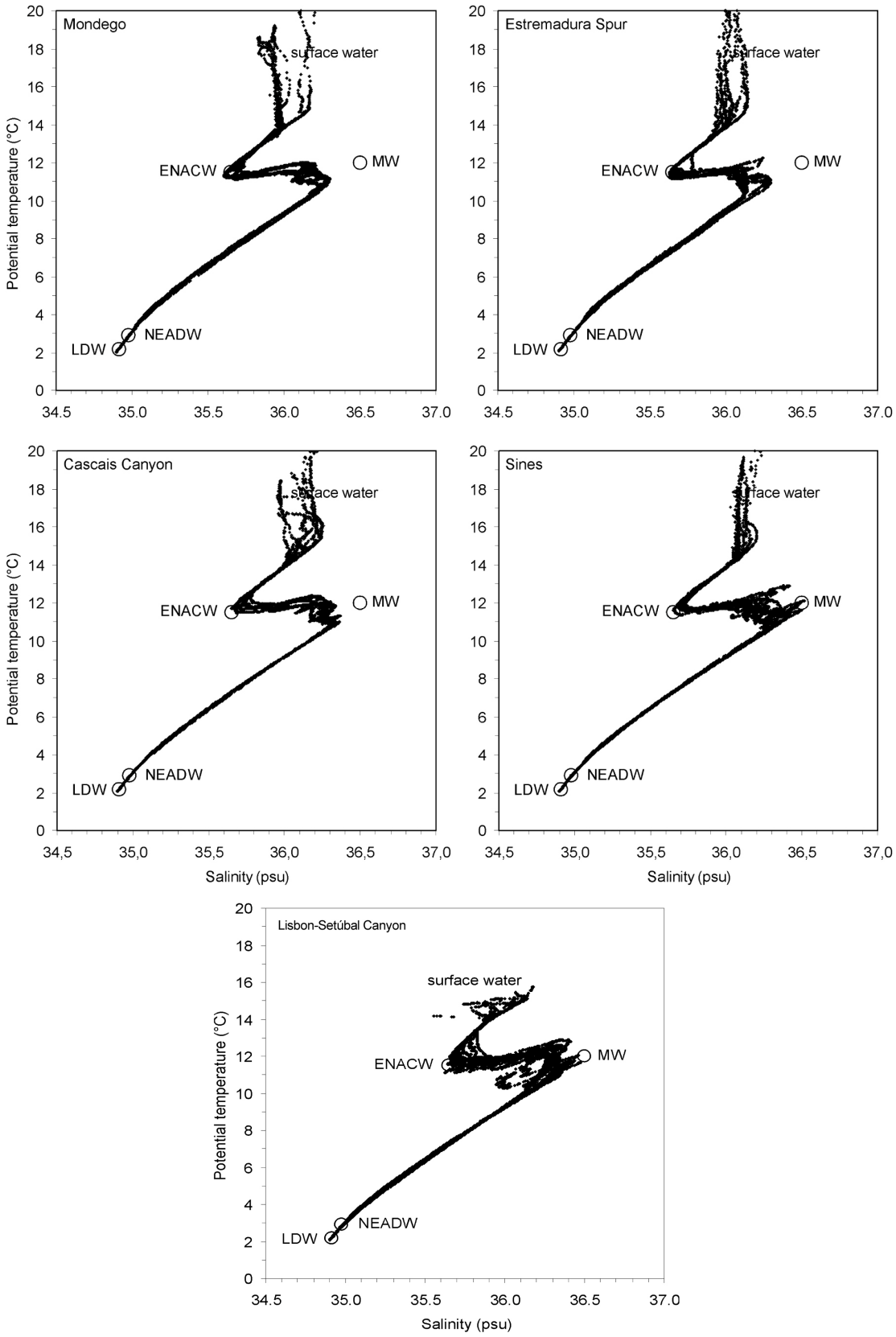

Figure 2.10. (De Stigter *et al.*, 2004 (report of cruise 225) and De Stigter *et al.*, 2007a (report of cruise 252)) Potential temperature-salinity diagrams constructed from CTD measurements along different transects. *Θ-S* values for Mediterranean Outflow Water (MOW) at Gibraltar, and North East Atlantic Deep Water (NEADW) and Lower Deep Water (LDW) at the western Iberian margin according to Van Aken (2000a).

Winters (typically December – January) are characterised by prevailing southerly winds often associated with storms, leading to downwelling and offshore Ekman transport (Vitorino *et al.*, 2002a). Under these conditions a northward flow of relatively warm water occurs over the continental shelf, which is known as the Portugal Coastal Countercurrent (PCCC). As a result of the accumulation of water in the coastal area a downward flux occurs over the shelf with bottom currents directed offshore (Vitorino *et al.*, 2002b). Intense winter storms appear capable of eroding sediments at mid-shelf depths, and in combination with an offshore-directed bottom flow this leads to offshore transport of fine-grained sediments in the form of bottom nepheloid layers (Vitorino *et al.*, 2002a, b).

During summer northerly winds prevail, leading to development of an upwelling regime, which is most active between June and September (Huthnance *et al.*, 2002). Although a southward superficial current is formed over the shelf, the northwards current over the shelf edge and upper slope continues to exist. The upwelled water is fed by the ENACW of either sub-tropical (ENACWst) or sub-polar (ENACWsp) origin, which forms the permanent thermocline at water depths below approximately 100 m. Depending on the wind strength both types of water can be upwelled. The poleward flowing ENACWst is lighter, relatively warmer and saltier than southward flowing ENACWsp and contains less nutrients. The ENACWst is formed along the Azores front during winter and then contributes to the PCCC. The ENACWsp, which flows below the sub-tropical ENACWst is formed in the eastern North Atlantic around 46ºN (Fiúza, 1984; Fiúza *et al.* 1998; Ríos *et al.*, 1992).

When seasonal coastal upwelling predominates off western Iberia, the upwelled water forms a cold and nutrient-rich band of water along the west coast (Figure 2.11a, b, c). This water is transported southwards by the Portugal Coastal Current (PCC) in a band of about 50 km wide, as documented by satellite infrared images (Figure 2.11a). The different upwelling patterns off western Iberia are largely determined by the bathymetry, the coastal morphology, and local wind conditions (northerly wind along the west coast). Filaments and plumes of cold water with high pigment concentrations are modulated by topographic features like submarine ridges and capes (Figure 2.11). Such filaments can extend as far as 200 km (e.g. off Lisbon - 39ºN, Cape Roca). Plumes are observed south of Cape Espichel and Sines (Figure 2.11b).

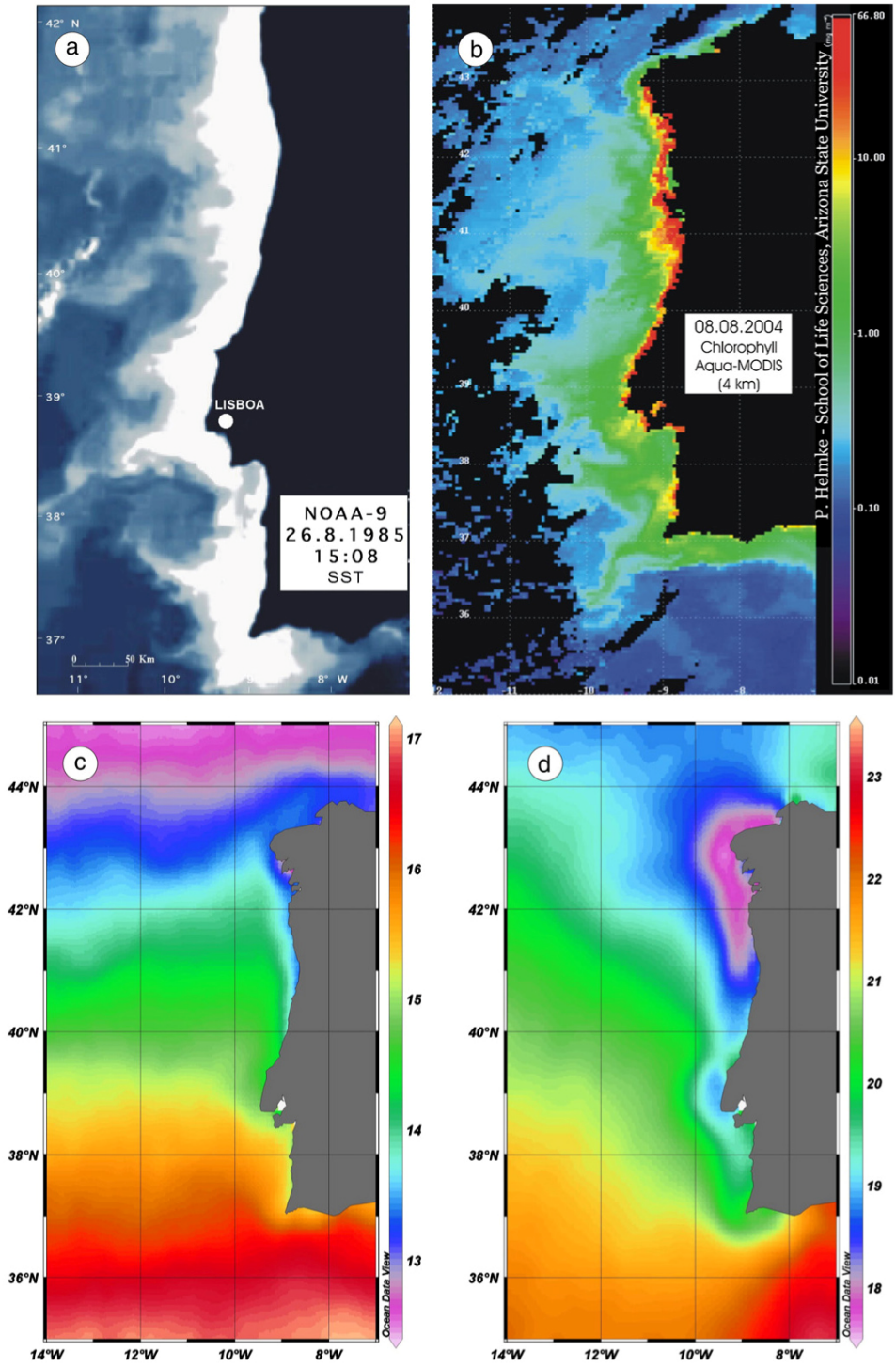

Figure 2.11. (Salgueiro *et al.*, 2008). Sea Surface Temperature and chlorophyll concentration along the Iberian margin. **a)** Satellite image, Tiros — N thermal infrared image, obtained in August 1985 (courtesy of A. Fiúza). Sea Surface Temperature (SST) values increase from white (coldest waters) to dark blue (warmest waters). **b)** SeaWiFS chlorophyll data for August 8th, 2002 (SeaWiFS Project, NASA/Goddard Space Flight Center). Mean satellite-derived SST (1985–2003) for winter (**c**) and summer (**d**). Note the different scales in c) and d).

2.2. Regional Climate

The continental Portuguese territory is located at the boundary between the subtropical anticyclone zone and the subpolar low-pressure zone (SPLZ). The subtropical anticyclone zone (high-pressure zone) is known as the Azores Anticyclone (Azores High) in the Atlantic Ocean. This high-pressure cell is neither permanent nor stationary. In summer the Azores Anticyclone shifts NW towards the Iberian Peninsula, causing ridging across France, northern Germany and the SE United Kingdom (Naya, 1984). During this period, the boundary between the Azores High and the SPLZ normally stays north of 45 ºN and so the Portuguese continental territory is under the influence of subtropical anticyclonic air masses which may affect the country for long periods (Brito, 1994). In the winter, the Azores High moves SE South of the Azores Islands and the limit between the SPLZ and Azores High may shift southward to latitudes around 30 ºN. During this period, continental Portugal, especially the northern part, is under influence of the subpolar depressions characterised by humid and cold air accompanied by abundant precipitation.

Apart from the large-scale pressure fields over the NE Atlantic, local factors such as the orography, the influence of the Atlantic Ocean and the continentality are responsible for significant lateral and temporal variation in air temperature and precipitation. For instance, the orography change along the country is responsible for the decrease of precipitation from north to south, from annual values higher than 3000 mm in the north to less than 400 mm in the south. The Tagus valley approximately marks the transition between the temperate and humid climate of the northern Portugal and the warm and dry climate of the south.

2.3. Hinterland areas adjacent to the Lisbon-Setúbal-Sines margin

2.3.1. Coastal area

The coast adjacent to the study area consists of two broad arc segments: Tróia - Sines and Trafaria - Espichel, almost homothetic in trend, shape and boundaries. The northern boundary of each segment is a major estuary (Sado and Tagus, respectively). Between the Sado Estuary and Cape Espichel the coastline is determined by the E-W trending Arrábida Mountains chain. Similarly, the rocky coastline north of the Tagus Estuary extends westwards until the Cape Raso (Figure 2.12). The southern boundaries are defined by Cape Sines and Cape Espichel, respectively. Both coastal arcs include a northern section with low lying beaches and dunes and a central and southern section with Mio-Pleistocene sea-cliffs (see Figure 2.13 for illustrations from the Tróia – Sines arc). In some places these outcrops can reach 40 m height. Sea-cliffs of these areas are mainly composed of detritic sedimentary sequences dating from the Miocene (silty-clayey sands, clays and calcareous arenites) and from Pliocene-Pleistocene (finesands to coursesands, gravels, clays and ferruginous crusts) (Quevauviller, 1988; Marques, 1999; Gomes, 1992 and Gama, 2004).

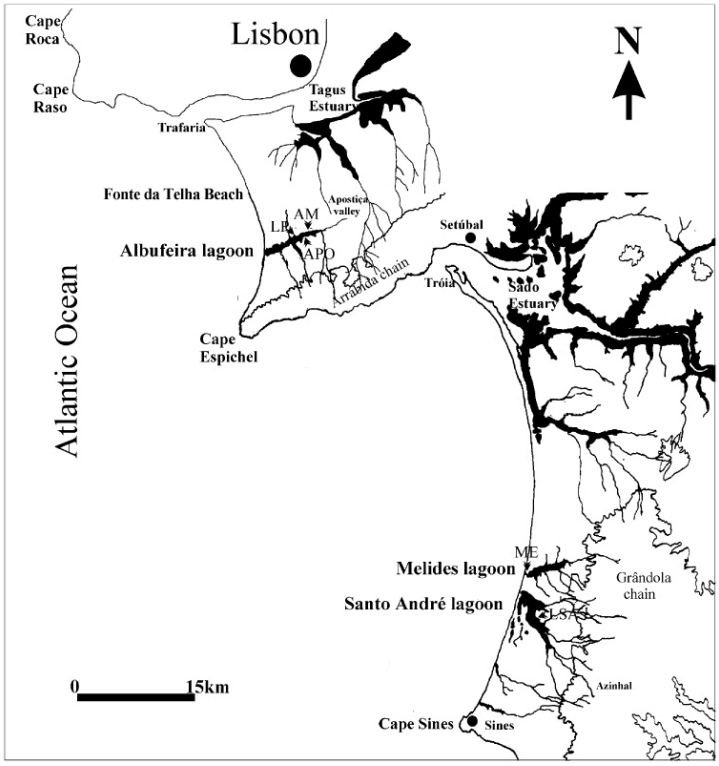

Figure 2.12. (adapted from Freitas *et al.*, 2002) Coastal zone adjacent to the study area. Areas filled in black represent marshland, tidal flats, floodplains or lagoon areas.

Both arcs have also lagoons in their southern parts: Melides, Santo André and Sancha Lagoons in the Tróia-Sines arc and Albufeira Lagoon in the Trafaria-Espichel arc

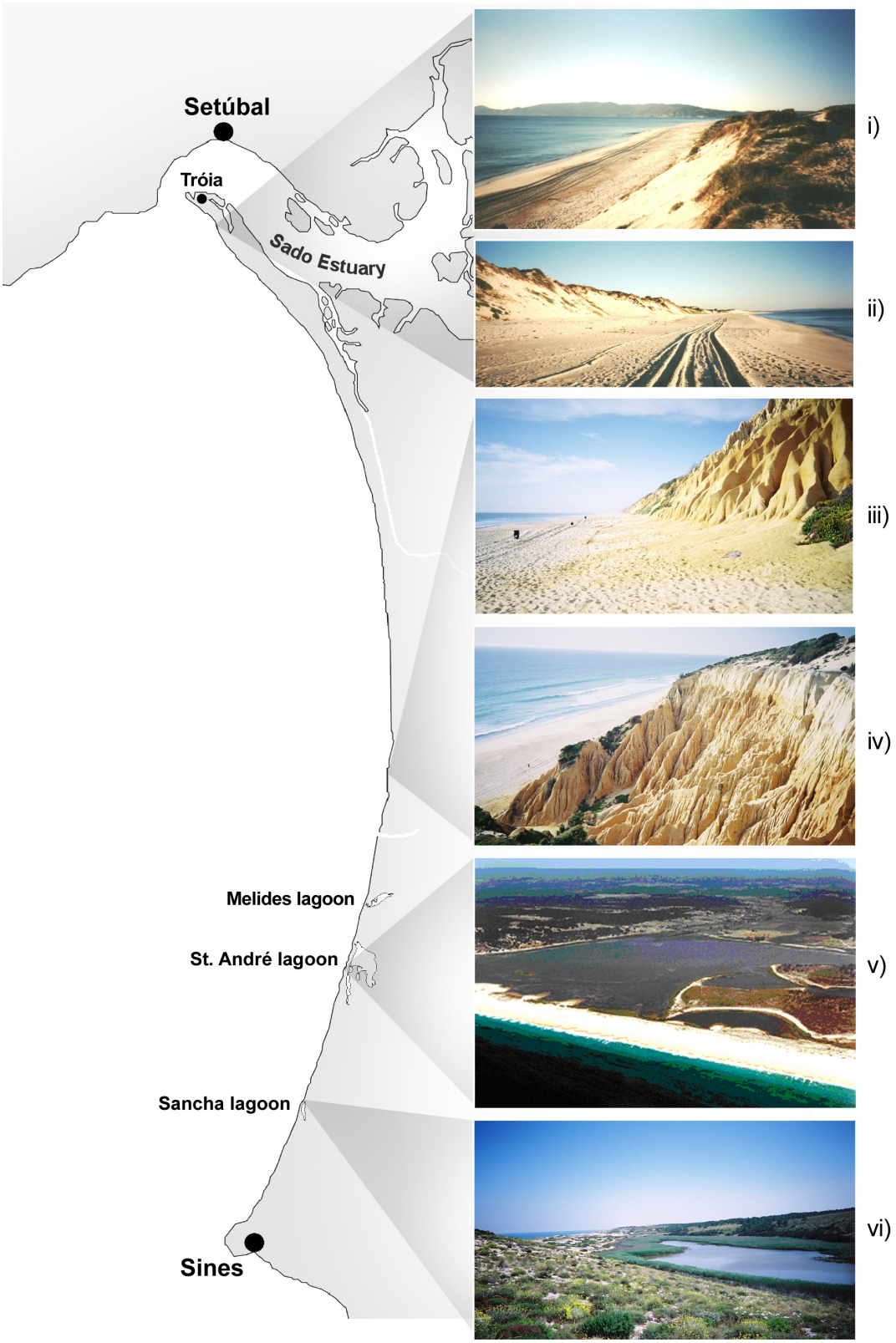

Figure 2.13. Pictures from the coastal area between Tróia and Sines. **i)** and **ii)** northward and southward views from Tróia beach, respectively; pictures taken by Jesus Vidinha; **iii)** and **iv)** Sea-cliffs at the Galé beach; pictures taken by the author; **v)** Aerial view of the Santo André Lagoon; picture was taken from the Santiago do Cacém municipality web-page (www.cm-santiagocacem.pt); **vi)** Sancha Lagoon; picture taken by the author.

(Figure 2.12 and 2.13). These lagoons have as common feature a narrow, linear and reflective sand barrier which is attached to the mainland at both ends. In the Santo André, Melides and Albufeira lagoons an ephemeral tidal inlet is artificially and regularly opened to promote water exchange, to prevent eutrophication and to drain the nearby alluvial plains which are reclaimed for agriculture and which are silting up by natural means (Freitas *et al.*, 2002).

The Tróia – Sines coastal arc is delimited to the south by Cape Sines, an outcrop of sub-volcanic rocks of Late Cretaceous age, which more inland are covered below Cenozoic sand and gravel (Figure 2.17). Seismic reflection and field sampling in the adjacent shelf indicates that the sub-volcanic massif extends seawards over an area of about 12 x 3.5 km (Inverno *et al.*, 1993). The emerged part is composed of basic and intermediate igneous rocks (gabbros, diorites and syenites) surrounded by a dense field of basic igneous dykes (Inverno *et al.*, 1993).

Between both coastal arcs stands the Arrábida coast, extending between Cape Espichel and the Sado River and defined by an E-W trending fault delimiting the uplifted Mesozoic Arrábida Mountain chain. This tectonically controlled coastal area is much higher compared to the nearby coastal arcs with an altitude of 380 m at the summit of Risco Mountain. It is dominated by calcareous rocks and beaches occur mainly as pocket beaches in small bays protected against the main swell (e.g. Portinho da Arrábida).

2.3.2. Hydrological basins

The main fluvial systems debouching on the central Portuguese margin are the Tagus (Tejo) River, draining an area of more than 80,000 km^2 and with a mean annual discharge of 16 x 10^9 m^3 y^{-1}, and the much smaller Sado River, which has an order of magnitude lower drainage area and annual discharge (Figure 2.14).

Fluvial networks have been extensively modified after the 1940s, especially by the construction of multiple dams and reservoirs for water storage, energy production and flood control, which has dramatically reduced the sediment yield to the coast (Figure 2.15). Also more sediment has been progressively retained within the drainage area due to the changes in land-use. Specifically, reforestation programs and soil conservation practices in agriculture have been growing in importance since the last quarter of the 20th century. In addition, the mining of sand and shingle from river beds and flood plains for

construction and navigation has been steadily growing throughout the 20th century, enhancing the sediment storage capacity of fluvial systems, and as a result leading to the undersaturation of the potential longshore drift and starvation of the coast.

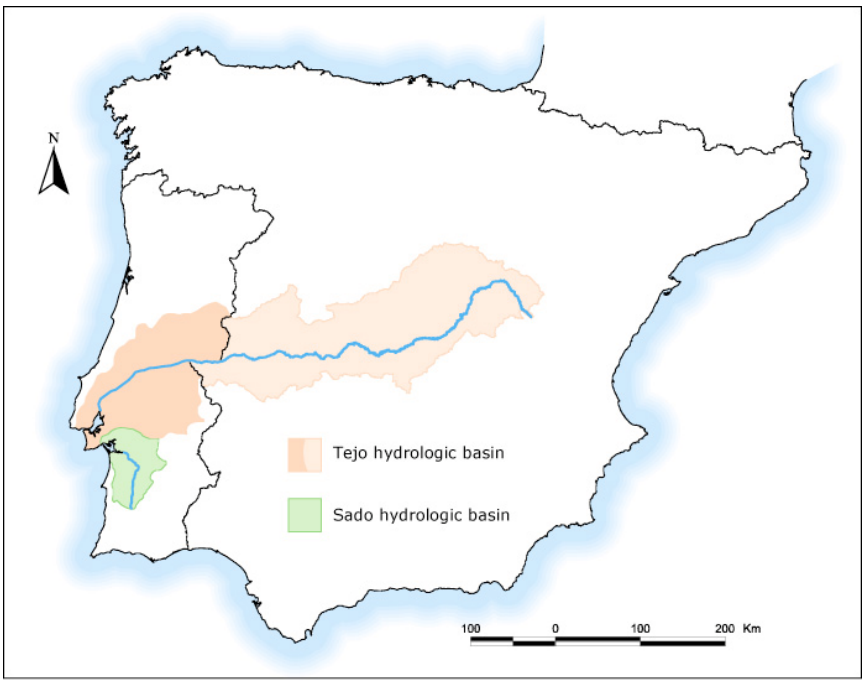

Figure 2.14. The hydrologic basins of the Tagus and Sado rivers.

Figure 2.15. (adapted from Dias, 1990) Original source areas of fluvial sediment discharge to the Portuguese margin, and present day effective source areas resulting from the construction of dams.

Furthermore, during the present high sea-level stand, estuaries tend to work as sediment traps, especially for the coarser bedload sediment, and therefore the sediment transported to the adjacent sea consists mostly of fine-grained suspended material.

In the Plan of the Tagus Hydrographic Basin (Procesl *et al.*, 1999) 2043 dams were identified in the Portuguese part of the Tagus basin. Fourteen of these are important dams with storage capacity > 10 hm^3. Presently the Tagus supplies less than 1/3 of its potential solid load to the inner estuary (Ramos & Reis, 2001). According to Procesl *et al.* (1999), under natural conditions the Tagus River has a capacity to transport 1,200,000 m^3 y^{-1} of sediment through traction and saltation. Between 1956 and 1966 the mean sediment transport capacity of the river decreased to 530,000 m^3 y^{-1} and it was estimated to be around 350,000 m^3 y^{-1} for the year 2000.

In 1999 around 800 dams were identified in the Sado Basin (Hidroprojecto *et al.*, 1999). Most of them (>700) are small dams, together representing around 9 hm^3 of water storage capacity, whereas 8 are considered to be significant ones, each with a storage capacity > 10 hm^3.

Tagus (Tejo) Basin

The Tagus River is the longest river of the Iberian Peninsula with a length of more than 1100 km and a drainage area of 80,629 km^2 covering an important part of central and western Iberia. Approximately 30 % of the drainage area is on Portuguese territory. The mean annual discharge of the Tagus is 16 x 10^9 m^3 y^{-1}, with interannual variation ranging between 3 x 10^9 and 23 x 10^9 m^3 y^{-1} (e.g. Benito *et al.*, 2003). Monthly average discharge varies from 0.03 x 10^9 to 69 x 10^9 m^3 y^{-1} (Loureiro, 1979; Loureiro & Macedo, 1986).

The Tagus drainage basin can be subdivided in four parts, each with distinctive morphological and hydrological characteristics, on the basis of different geological setting (Figure 2.16): 1) the Iberian Range (at the head); 2) the NE Cenozoic basin (upper course); 3) the Hesperian Massif (middle course); and 4) the SW Cenozoic basin (lower course).

The Tagus River head (from its source to Sacedón) is located in the Iberian Range, a NW–SE-trending Alpine chain consisting of Mesozoic sedimentary strata (Triassic feldspathic sandstones, Jurassic and Cretaceous marine carbonates and subarkosic sandstones) (Arribas & Tortosa, 2003).

The upper course (from Sacedón to Navalmoral) lies embedded in continental clastics, carbonates and tabular evaporites of Neogene age. In this segment, the northwest watershed of the drainage area is situated in the Central System, a mountainous range that consists of a large exposure of granitoids that intrude pre-Hercynian metamorphic basement.

The middle course (from Navalmoral to Abrantes) cuts low-grade metamorphic rocks (Precambrian greywacke and slates, Cambrian slates and quartzites and associated intruding granitoids) from the Central Iberian Zone in the Hesperian Massif.

The lower course of the Tagus River (from Abrantes to Lisbon) is developed on the SW Cenozoic basin which continues into the Sado drainage area (Freire, 1993). The tabular arrangement of the Tertiary detrital deposits favours the wandering course of the Tagus River, with a wide alluvial plain with meander bars and a well-developed system of Quaternary terraces. Estuarine deposits are also present near the river mouth. Head streams of tributaries at the north and south also drain Jurassic carbonate and metamorphic terranes from the Hesperian Massif, respectively, cropping out at the edges of the Neogene basin (Figure 2.16).

According to Pera & Arribas (2004), most of the sand deposited on the Tagus Estuary is derived from the erosion of Mesozoic carbonates and Tertiary to Quaternary detrital sediments at the distal margin of the drainage basin.

The average suspended sediment load discharged by the Tagus into the estuary is 4 x 10^5 t y^{-1} but may reach 1 x 10^6 t y^{-1} during years when there are several flood events (Vale & Sundby, 1987). In the Tagus Estuary, the SPM concentration is considered to be low, with values typically < 30 mg l^{-1} (Câmara *et al.*, 1986), but with a great variability in time and space, related to the discharge of the Tagus River and meteorological and tidal dynamics in the estuary. Vale (1981) recorded a maximum value of turbidity in the order of 500 mg l^{-1} in the upper estuary during spring tide. Although the tide is important for the transport of water, sediments export to the shelf, estimated at 1 – 77 x 10^6 t y^{-1}, appears largely driven by exceptional storms and river floods (Bettencourt *et al.*, 1980; Vale, 1981). According to Valente & da Silva (2009), precipitation, river discharge and winds, increase the turbid plume issuing from the Tagus Estuary, but the fortnightly cycle appears to be superimposed on the large time-scale variability.

Sado Basin and coastal lagoons

The Sado drainage basin comprises an area of approximately 7,737 km^2 (Miranda, 2007) limited to the north by the Tagus basin, to the east by the Guadiana basin and to the south by the Mira basin. To the West there are several creeks which flow directly to the sea.

The Sado River (the main watercourse of the basin) is a small river compared to the Tagus River spanning only 180 km from its origin in the Vigia Mountains (230 m high) to the point where it flows into the sea. It has an annual mean discharge of 1.2 x 10^9 m^3 y^{-1} (Cabeçadas, 1993) with pronounced seasonal variability (peak values in February / March and minima in August) and large interannual variations (e.g. Trigo *et al.*, 2004) resulting in highly variable suspended sediment loads (Vale, 1990; Vale *et al.*, 1993).

The water flow within the estuary is mainly controlled by the tide, as fresh water inflow from the Sado and a number of smaller rivers is insufficient to have a significant influence on circulation (Bettencourt & Ramos, 2003).

The geology of the Sado Basin is dominated by Paleozoic and Cenozoic deposits which occupy 49 and 47 % of the basin surface, respectively (Miranda, 2007). The remaining 4 % represent Jurassic limestones, marls, dolomites and dolomitic limestones of the Arrábida and Grandola Mountains and some outcrops of post-Hercynian intrusive rocks (Figure 2.17) of which the outcrop at Cape Sines is the most relevant to this study.

Paleozoic outcrops in the Sado Basin can be divided in two main groups: 1) low grade metamorphic sediments and 2) igneous rocks and medium to high grade metamorphic sediments. According to Pimentel (1997), the first group consists mainly of schist and greywacke which are not very resistant to weathering and thus yield mica-rich and clayey sediments. The occurrence of quartz veins associated to late periods of schist deformation is the main source of clastic quartz. The second group characterised by weathering resistant outcrops, comprises felsitic gneisses, rhyodacite porphyry, granular basic and ultrabasic rocks and granular acid and intermediate-acid rocks.

Cenozoic rocks are found throughout the basin especially in the central and coastal areas. In general, Tertiary deposits consist of clays, sands, arenites, gravels and calcareous rocks / limestones (Figure 2.17). According to Pimentel (1997), these deposits were produced by weathering of Paleozoic rocks. Quaternary deposits consist essentially of gravel beds and sands occurring in alluvial channels and terraces, dunes and beaches.

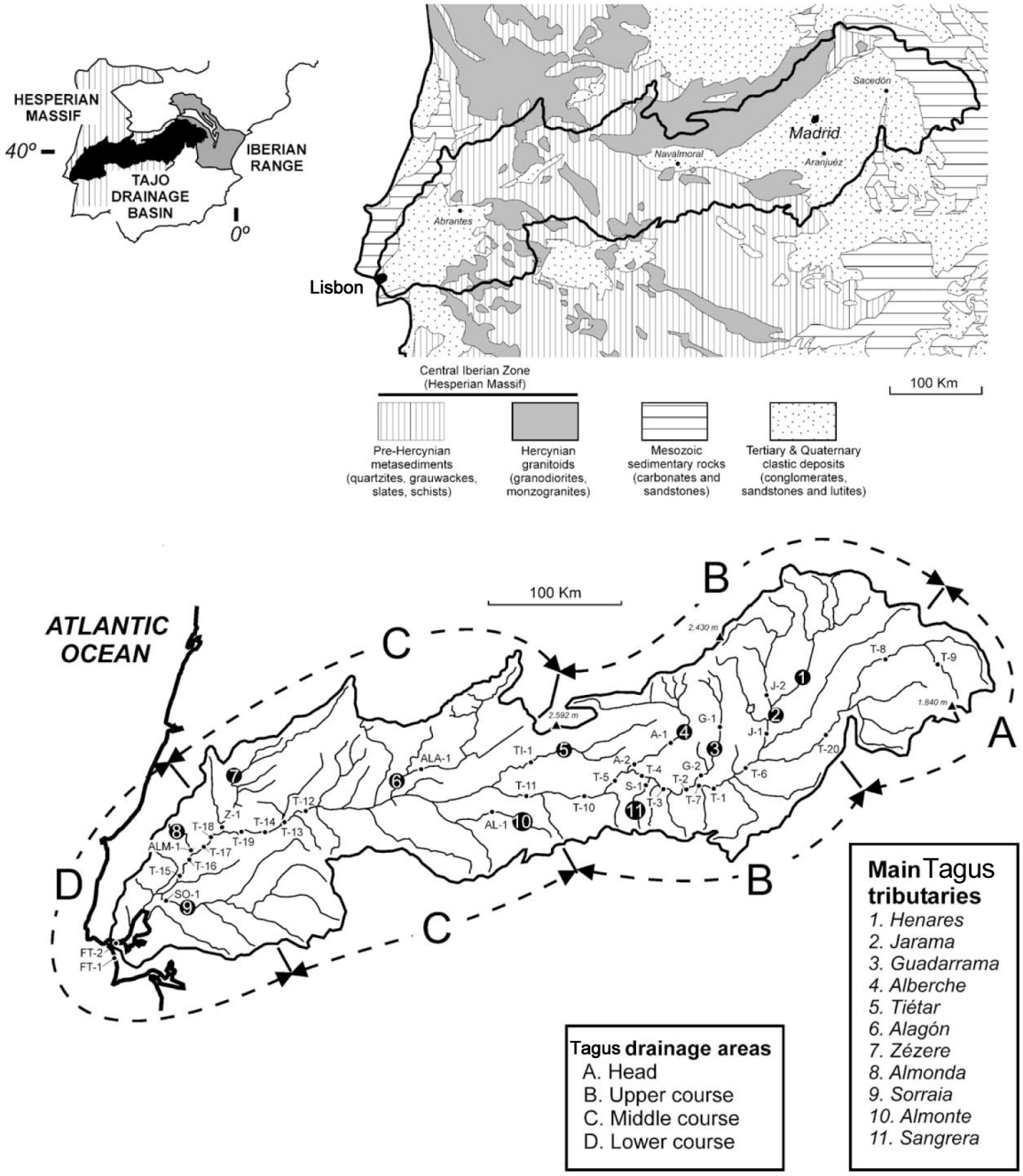

Figure 2.16. (adapted from Pera & Arribas, 2004) Generalised bedrock geology and fluvial drainage network of the Tagus River basin.

The geology of the small basins of the Melides and St. André lagoons is presented in Figure 2.18. The Melides lagoon receives the discharge of a small brook which has the same name as the lagoon. The small basin has an area of ~60 km^2 of which 38 % corresponds to Carboniferous greywackes, different types of schists and also volcanic tuffs. Holocene dune sands and alluvium and Plio-Pleistocene gravels and sands cover 25 and 23 % of the area, respectively.

The Santo André Lagoon is fed by the Cascalheira and Ponte brooks, representing a total watershed area of 157 km^2. Carboniferous greywackes, different types of schists and also volcanic tuffs comprise 27 % of the watershed area while Pliocene, Plio-Pleistocene and Holocene deposits cover 26, 13 and 12 % of the area, respectively (Figure 2.18).

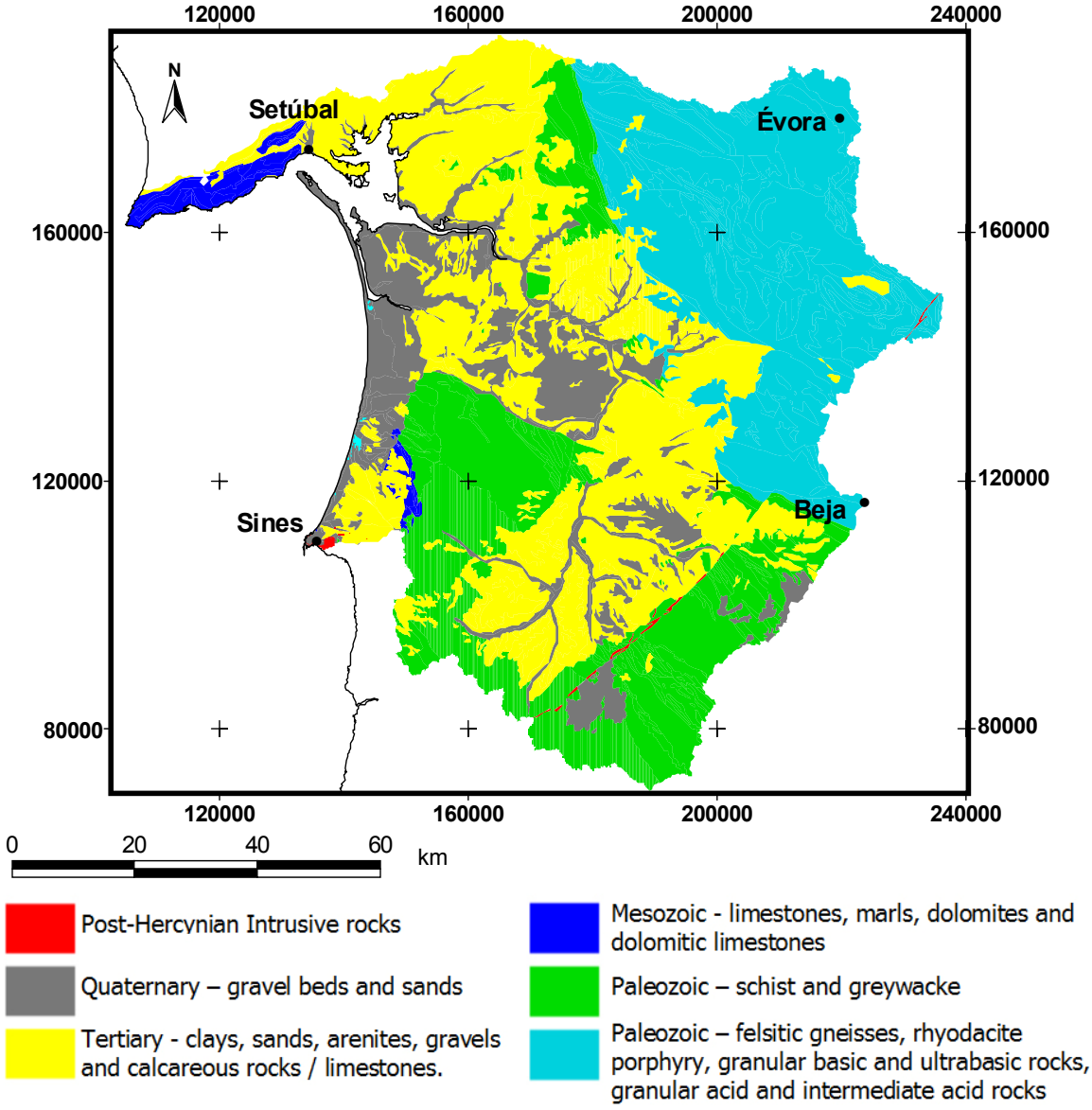

Figure 2.17. (adapted from Miranda, 2007) Generalised bedrock geology of the Sado Basin and small basins of coastal brooks (e.g. Melides Brook).

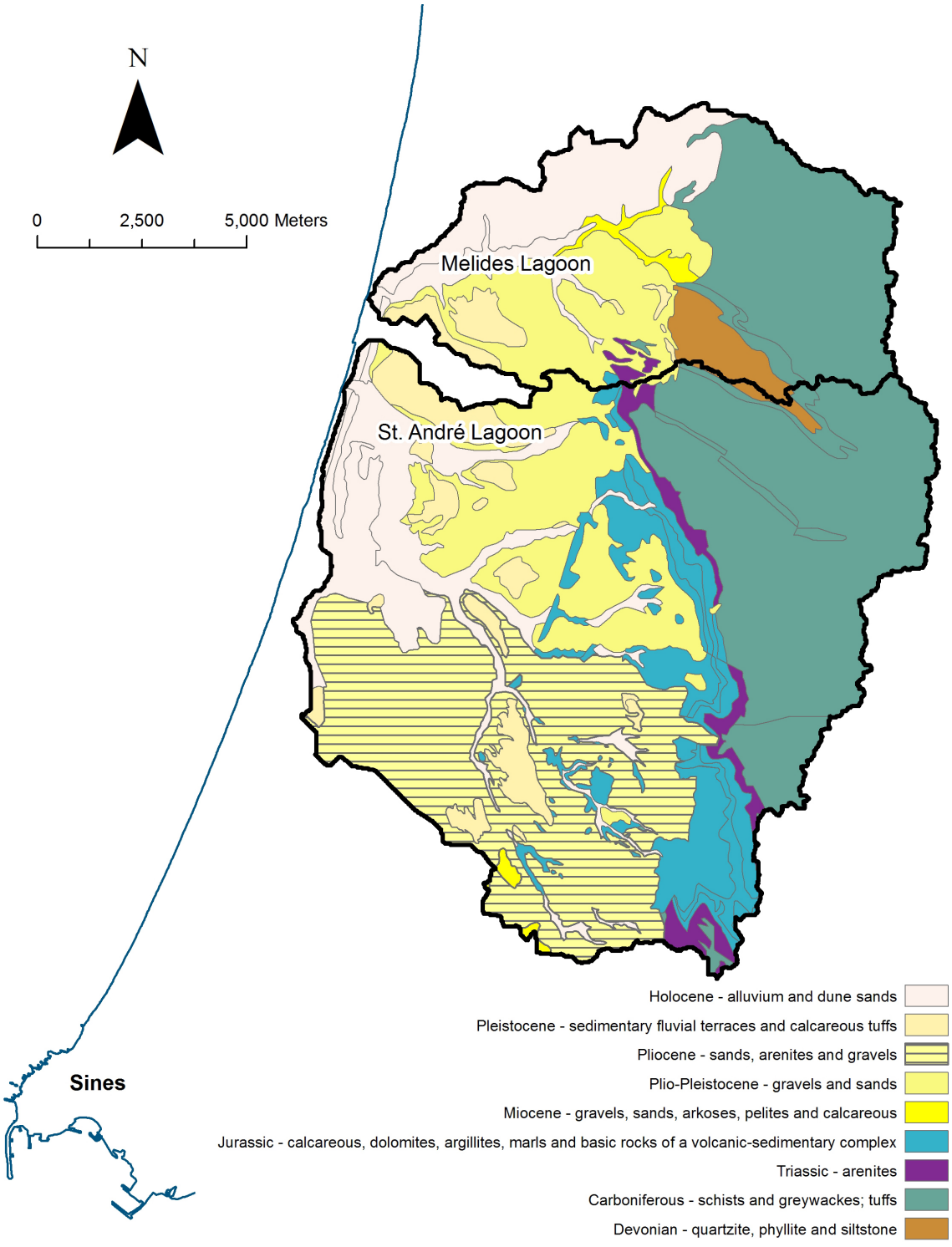

Figure 2.18. Bedrock geology of the St. André and Melides Lagoon watersheds (Data from Geologic Map of Portugal, 1: 50 000 – sheet 42C).

3. MATERIALS AND METHODS

3.1. Field sampling and sample preparation

3.1.1. Cruises and sampling gear

Surface sediment samples from the continental shelf and upper slope between the Tagus River mouth and Cape Sines were collected between 1980 and 1987 during several cruises conducted within the framework of Instituto Hidrográfico's internal project SEPLAT. Hundred and seventeen sediment samples were collected from water depths between 1 and 572 m (Figure 3.1). These samples, representing approximately the first 15 cm of the sediment column, were collected using *Shipeck*, *Van Veen* and *Smith McIntyre* grabs.

Sediment samples and other data presented from Portuguese canyons and open slopes were recovered during a series of cruises with RV "Pelagia" of the Royal Netherlands Institute for Sea Research (NIOZ), conducted in November 2002, March 2003, October 2003, April/May 2004, May 2005, August/September 2006 and May/June 2007 (cruises 64PE204, 64PE208, 64PE218, 64PE225, 64PE236, 64PE252, 64PE269, respectively). Subsequently, stations are referred to by cruise number combined with station number (e.g. 204-23). Sampling locations are shown in Figure 3.2 and positions are given in Appendix Tables A1.1 and A1.2. Location of samples from the Mondego transect are shown in Appendix A2.

Fifty box-, multi- and piston-cores were studied: 19 from the Nazaré Canyon, 16 from the Lisbon-Setúbal Canyon and 5 from the Cascais Canyon (Figure 3.2, Appendix Table A1.3). Ten more multi-cores collected in the open slope away from the canyons were also studied (open slope transects). All sediment cores were stored at 4°C for later analysis. Loss of surface sediment resulting from impact of the corer on the seabed is considered minimal since the oxidized surface sediment layer and intact arborescent foraminifera were commonly preserved in the top of the cores (Figure 3.3) (De Stigter *et al.*, 2007b).

The MUC 8+4 multiple corer developed by Oktopus GmbH was equipped with an array of eight 6-cm diameter and four 10-cm diameter polycarbonate coring tubes of 61 cm length (Figure 3.4a). One of the 10-cm diameter polycarbonate tubes was usually replaced by a PVC tube of equal diameter, used for sedimentological analysis. The

standard boxcorer developed by NIOZ is equipped with a cylindrical coring barrel of 30 cm diameter and 55 cm length (Figure 3.4b). Upon retrieval a lid closes off the top of the coring barrel, allowing recovery of relatively undisturbed cores complete with overlying water.

The NIOZ pistoncorer consists of a steel coring barrel of 6 or 12 m length with lead weight of about 1500 kg (Figure 3.4c). The coring barrel had an 11-cm diameter plastic liner, a teflon head with core catcher and adjustable piston regulating the pressure inside the liner during coring. A trip weight of 100 kg with a smaller size coring barrel was used to release the pistoncorer for a free fall at about 3 m above the bottom.

Mass deposition flux, current dynamics, temperature, salinity and turbidity in the near-bottom water layer were measured with three BOBO (BOttom BOundary) benthic landers developed by Royal NIOZ (Van Weering *et al.*, 2000) (Figure 3.4d, e).

3.1.2. BOBO landers and sediment traps

The 4 meter high tripod landers designated as BOBO were each equipped with an RDI 1200 kHz ADCP facing downward at 2 m a.b. (above bottom), SeaBird conductivity and temperature sensor at 3 m a.b., SeaPoint optical backscatter sensors attached at 1 and 3 m a.b., and a PPS4/3 sediment trap with its 0.05 m^2 opening positioned at 4 m a.b (Figure 3.4d, e).

Instruments were set to measure at 5- or 15-minute intervals. The ADCP collected current velocity and acoustic backscatter data in 5-cm vertical intervals. The data presented here always refer to a level at 100-cm interval above the bottom.

Thirteen deployments were made, 5 in the Nazaré Canyon, 7 in the Lisbon-Setúbal Canyon and 1 on the Afonso de Albuquerque Plateau ranging in depth between 343 and 4975 m and with recording periods of 2 days up to 12 months (Figure 3.2 and Appendix Table A1.2). Sediment trap sample length was between 1 and 30 days. Before deployment, sediment trap sample bottles (Figure 3.4f) were filled with filtered seawater poisoned with mercury (II) chloride (1 mg cm^{-3}) and buffered with borax (2 mg cm^{-3}).

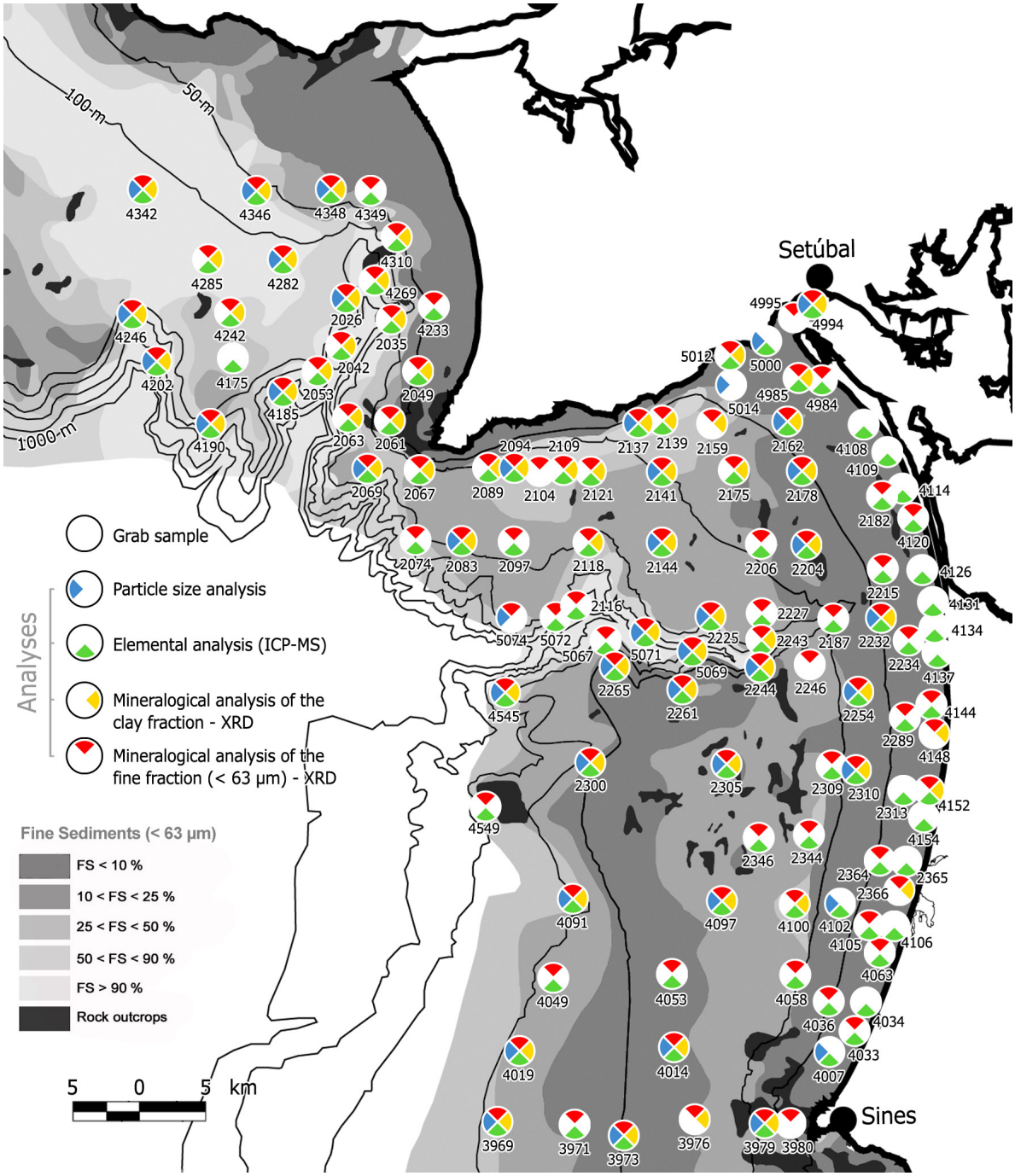

Figure 3.1. Location map of surface sediment samples collected on the continental shelf and upper slope between the Tagus River outlet and Cape Sines. Colour codes in circles represent the different analyses performed on the samples.

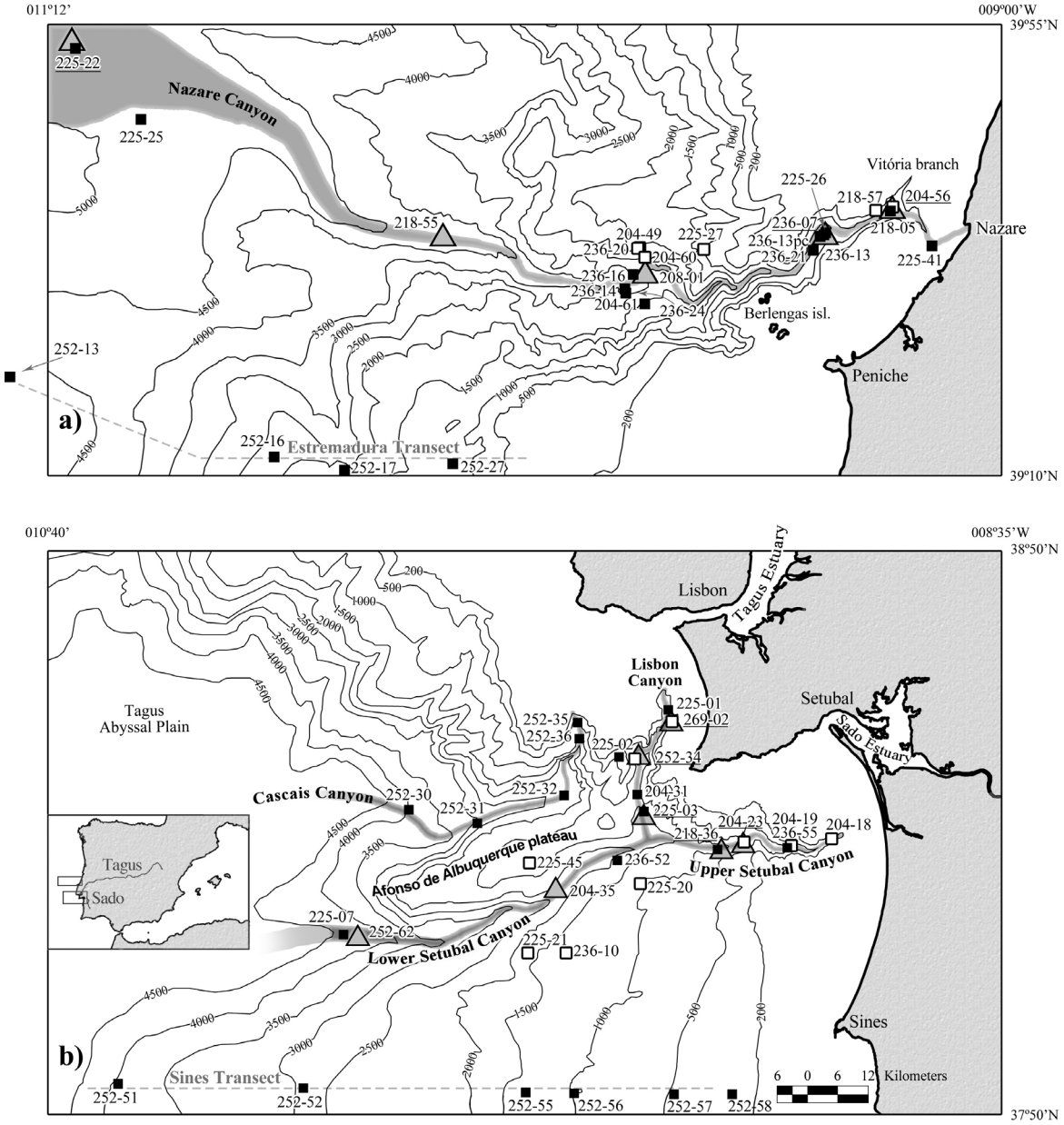

Figure 3.2. Location map and bathymetry of the Nazaré Canyon and Estremadura open slope (**a**) and Lisbon–Setúbal and Cascais canyons and Sines open slope (**b**). Canyon thalwegs are outlined in grey. Squares represent sediment cores and grey triangles represent sediment traps attached to bottom landers. Stations are referred to by cruise number combined with station number. White squares represent cores used to define the baseline used in enrichment factor calculations (Chapters 5 and 7). Inset in panel b) gives geographic context with respect to the Iberian Peninsula and the Tagus and Sado rivers.

Figure 3.3. Arborescent foraminifera on the surface of multi-core 64PE252-26, collected from 1218 m WD on the Estremadura Spur. Specimen in centre of view is about 2 cm high (De Stigter *et al.*, 2007a). Photo: Henko de Stigter.

Assessment of sediment trap efficiency

Sediment traps are the best presently available tools for studying particle composition and fluxes to the sea-floor over periods of weeks and years. These devices have been in use for several decades and have provided valuable insight into the rates, timing and mechanisms of material and energy transfer in the oceans (Asper, 1996 and references therein). However, the observation that in sub-aquatic environments, horizontal current speeds often exceed the settling velocities of suspended particles by several orders of magnitude has raised awareness to the impact that water flow relative to a sediment trap can cause on trapping efficiency (for reviews see Knauer & Asper, 1989; Gardner, 1995).

Laboratory and field experiments conducted by Gardner (1980a, b) demonstrated that above a certain critical flow speed, which depends mainly on trap geometry, the trap will underestimate the downward flux. In Gardner's calibration experiments, cylindrical traps proved to give the most reliable estimate of downward fluxes. Further, the most important factor controlling the trapping efficiency of cylindrical traps is the height/diameter ratio (aspect ratio). Under laboratory conditions cylinders with aspect ratio between 2 and 3 appeared to yield accurate measurements of vertical fluxes in flows up to 15 cm s^{-1} (Gardner, 1980b). In the field, Baker *et al.* (1988), using cylindro-conical traps, found that the magnitude and compositional characteristics of the flux collected under flow speeds < 12 cm s^{-1} were indistinguishable from those simultaneously recorded by drifting traps, used as a reference not biased by water flow. In other field experiments, Gardner *et al.* (1997) found that collecting efficiencies of cylinders of aspect ratio 3 were

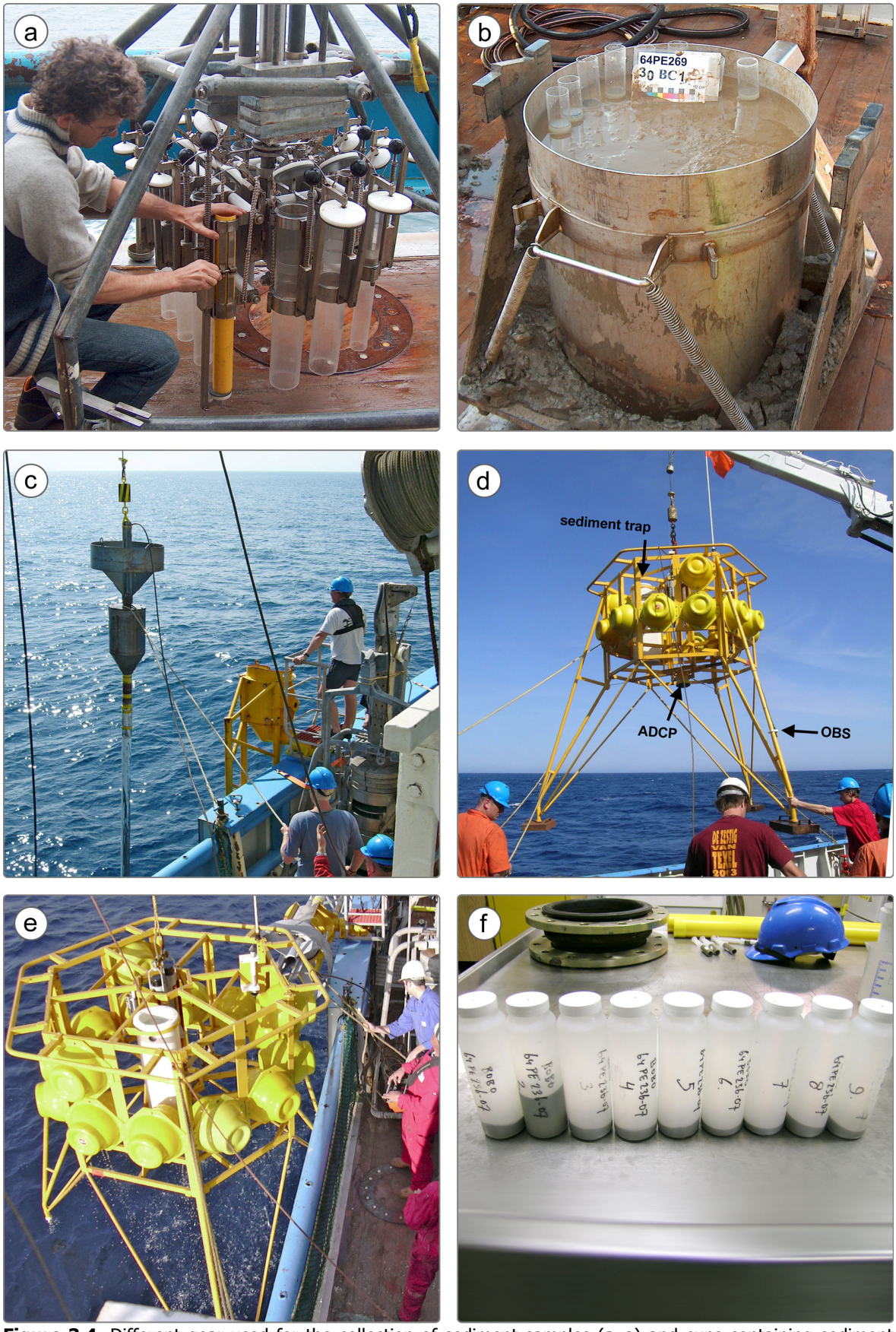

Figure 3.4. Different gear used for the collection of sediment samples (**a-e**) and cups containing sediment

trap samples of deployment 236-07 (**f**) (Photo: Henko de Stigter). Sampling gear: **a** – multiple corer (Photo: Carlo Fiori); **b** - standard boxcorer developed by NIOZ (Photo: Carlo Fiori); **c** - NIOZ pistoncorer (Photo: Tanja Kouwenhoven); **d, e** - deployment of the BOBO lander (Photos: Henko de Stigter). In panel **d**, sediment trap, downward looking ADCP and OBS sensor at 1 m a.b. are indicated by arrows.

not affected under flow speeds less than 22 cm s^{-1}. Taking into account that the traps used in this study have a higher aspect ratio (4) than those tested by Gardner *et al.* (1997), the critical current speed may be higher in our case.

Figure 3.5 illustrates the positive correlation between turbidity measured through acoustic backscatter and mass fluxes measured with a PPS4/3 sediment trap. This gives confidence in the efficiency of the sediment traps used in the present study in trapping sediments under different conditions, both for situations where resuspended materials predominate and current speed is as high as 30 cm s^{-1} (Figure 3.5a), as well as for situations where pelagic inputs predominates and current speeds are low (Figure 3.5f).

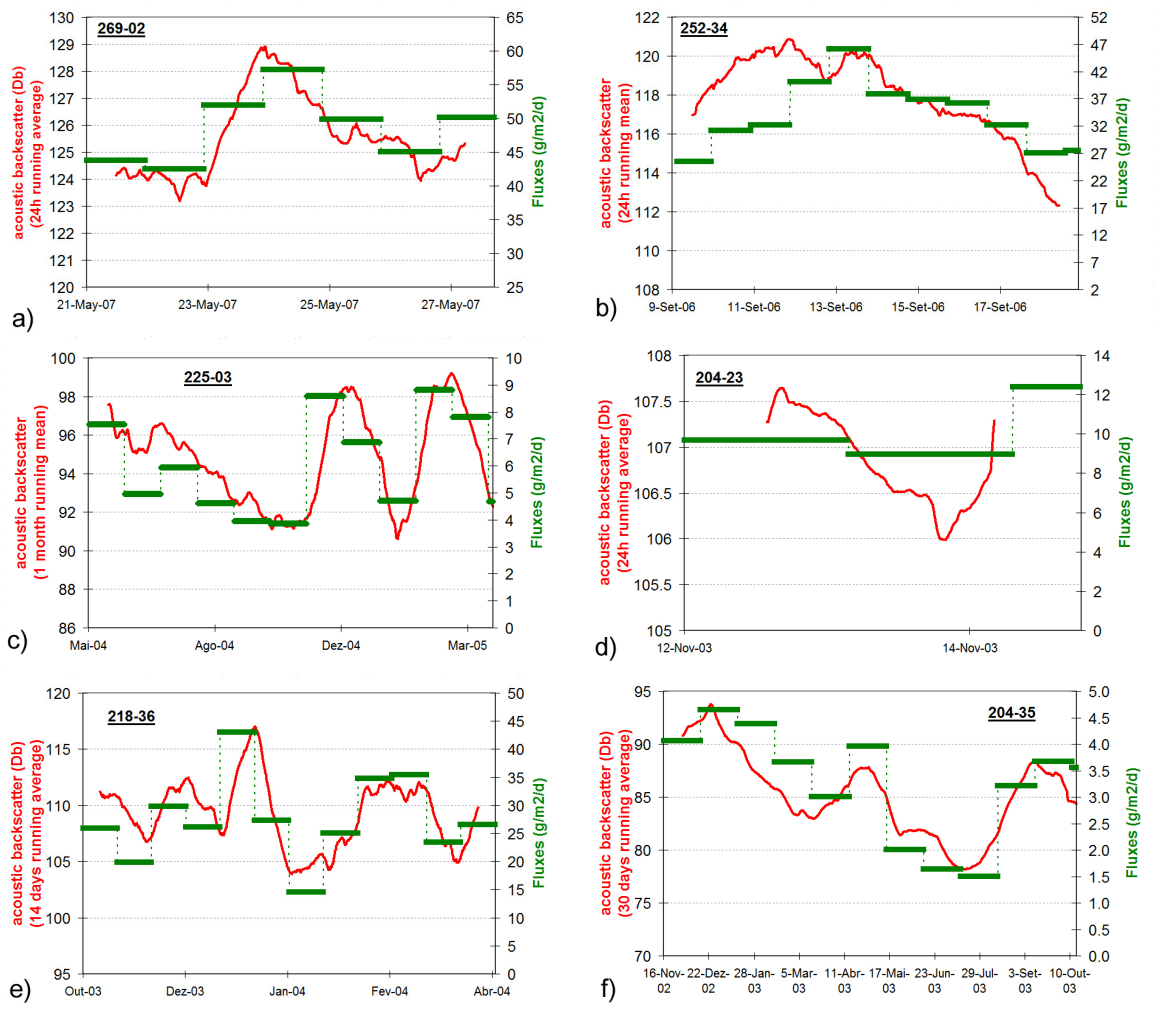

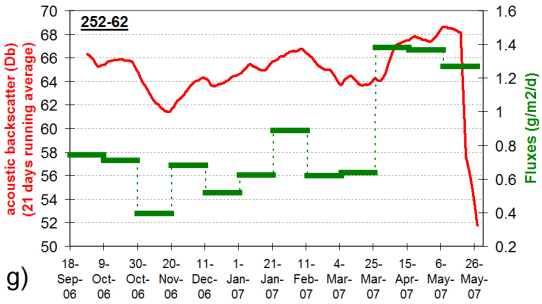

g)

Figure 3.5. Acoustic backscatter plotted against mass fluxes measured in the sediment traps. A-C - Lisbon Canyon; D, E – Upper Setúbal Canyon; F – Middle Setúbal Canyon; G – Lower Setúbal Canyon. Station number is given in upper left or right corner of each graph. Note the different scales for acoustic backscatter and flux.

3.1.3. Sample preparation in the laboratory

Grab samples

Each shelf sample was homogenised and split in two samples for different analyses: 1) mineralogical and grain size analyses and 2) elemental analysis. The first set of samples was treated with hydrogen peroxide (H_2O_2, 5 %) to remove organic material. H_2O_2 was added stepwise until no more reaction occurred. Subsequently, samples were rinsed several times with distilled water to make sure that all the organic matter was removed. These organic-matter-free samples and the second set of untreated samples were then wet-sieved through a 63 µm sieve in order to normalise all sediments collected on the continental shelf to the same grain size fraction.

Trap samples

After recovery of the lander, the sediment trap samples were sieved over a 1 mm sieve to remove swimmers (Figure 3.6a, b), and the < 1 mm fraction was subsequently split into sub-samples with either a Folsom or NOAA-type high precision splitter (Figure 3.6c). Particulate matter was extracted by centrifugation at 3500 rpm or filtration on 0.4 µm polycarbonate filters, and then freeze-dried. Compositional analyses were performed on bulk samples, but particle size was determined in samples from which the > 150 µm fraction had been removed by wet-sieving.

Core samples

In the laboratory sediment cores were split, photographed and macroscopically investigated for lithological composition and presence of sedimentary or biogenic structures. X-radiographs were made of all box- and multi cores and selected piston

cores. Sampling was done with cut-off syringes and by slicing at 0.5- or 1-cm intervals, after which samples were freeze-dried. Sediment dry bulk density was determined from volume, wet and dry weight and applying a correction for pore-water salt content.

a)

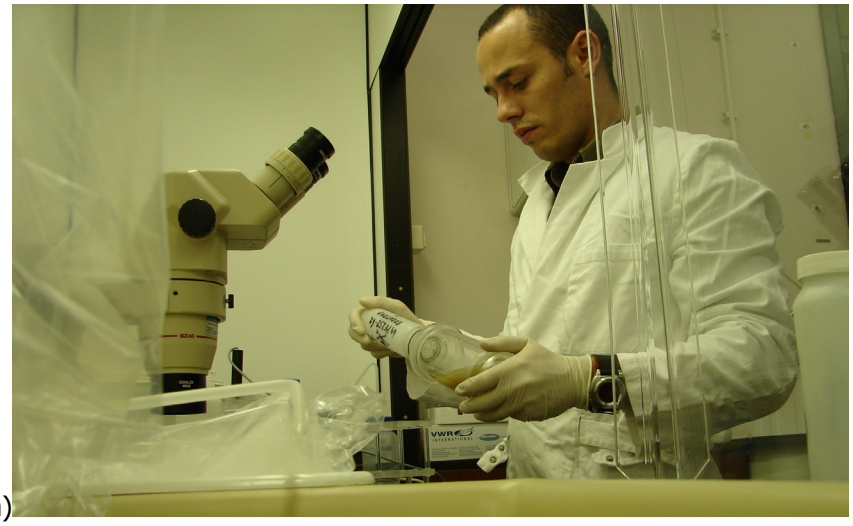

b)

c)

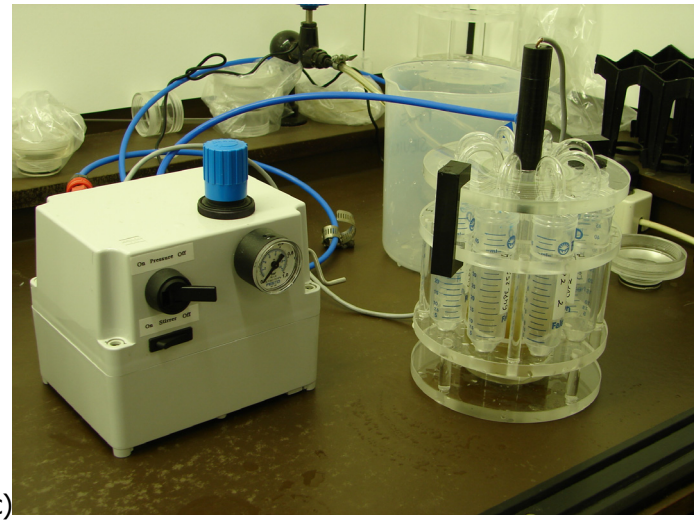

Figure 3.6. Sieving and splitting of the sediment trap samples into sub-samples with a NOAA-type high precision splitter developed at the NIOZ. **a)** Sieving of the bulk samples over a 1 mm sieve to remove swimmers. **b)** Sieved sample; swimmers over the sieve and < 1 mm samples in the bottle. **c)** NOAA-type precision splitter and the obtained eight sub-samples.

Down-core analyses for trace metals were done in several cores selected on the basis of having regular ^{210}Pb profiles. In each one of these cores three samples were analysed: a surface sample (0-5 mm, occasionally 10 mm), a mix sample was composed integrating the core interval where ^{210}Pb excess activity was still detectable (> 1 % of surface $^{210}Pb_{xs}$), and a deep sample was taken in the first centimetre below the level of detectable ^{210}Pb excess activity (Figure 3.7). Mix and deep sample represent sediment deposited

during the industrial period of the last 150 years and the pre-industrial period, respectively.

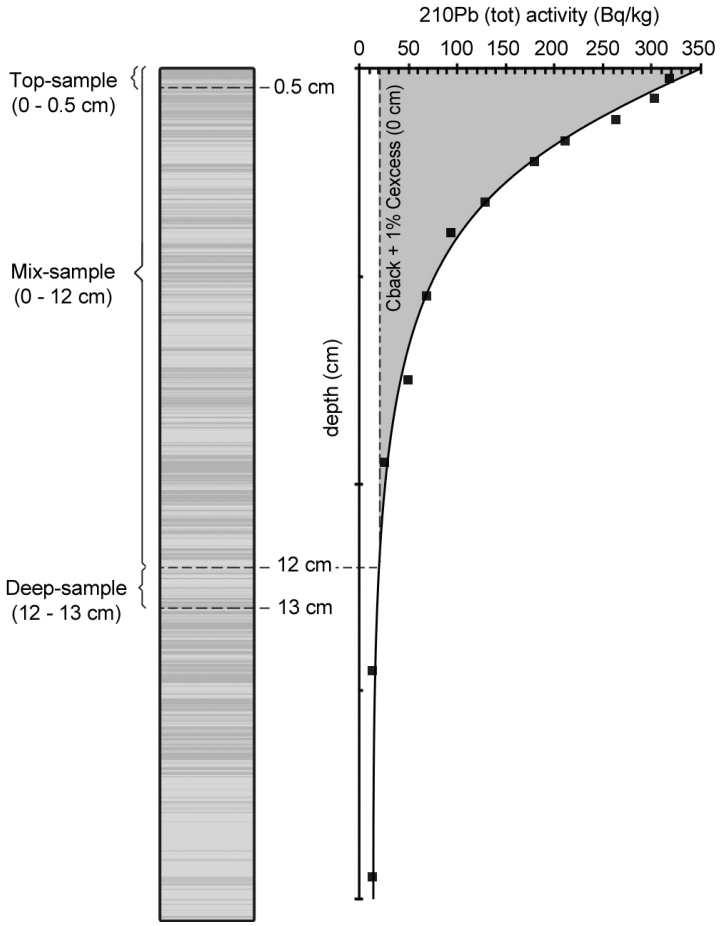

Figure 3.7. Sketch showing the selection of down-core samples based on the core's total ^{210}Pb activity profile. C_{back} is the background activity of ^{210}Pb; C_{excess} (0 cm) is the ^{210}Pb excess activity at surface.

3.2. Laboratory procedures

3.2.1. Determination of grain size spectra

Grain size spectra of fine sediments from the continental shelf/upper slope (Chapters 4 and 5) and sediment trap samples and surface sediments from submarine canyons and open slopes (Chapters 6 and 7) were determined with a laser forward-scattering particle sizer. The analyses of the first were carried at the Instituto Hidrográfico with a MALVERN MicroP 2000 while the second were done at the Royal NIOZ with a Coulter LS230. The sediment was mechanically dispersed by ultrasonication without use of a chemical dispergent. Grain size spectra are presented as volume % in logarithmic size classes, and volume is calculated from particle diameter assuming spherical particles.

3.2.2. Total organic carbon and $CaCO_3$

Freeze-dried, homogenised core and sediment trap samples were analysed for total carbon (C_{tot}), total organic carbon (C_{org}) and nitrogen on a Carlo-Erba 1500 elemental analyser following the procedure of Verardo *et al.* (1990) and modified after Lohse *et al.* (1998, 2000). For C_{org} determination, carbonates (predominantly $CaCO_3$) were removed by progressive and controlled acidification with sulphurous acid. Content of organic material in bulk sediment was calculated by multiplying C_{org} with 2.5. $CaCO_3$ content was calculated from C_{tot} and C_{org} as:

$$CaCO_3\,(\%) = (C_{tot} - C_{org}) \times (\frac{100}{12}) \qquad (1)$$

C_{org}/N ratio was also calculated and used as indicator of marine/terrestrial origin of organic matter.

3.2.3. Multi-elemental and ^{210}Pb analysis

Multi-elemental analysis with ICP-MS: shelf surface sediments

Hundred and six shelf sediment samples were analysed through ICP-MS for total concentration of Ca, Al, Fe, Mg, Ti, Mn, Zn, Cr, Pb, Ni, Cu, As, Th and U. The analysis was done in an international accredited laboratory – ACME Analytical Laboratories Ltd – ISO-

9002 Accredited Co. According to routine procedure of the laboratory, 0.25 g of sample was heated in HNO_3-HF-$HClO_4$ to fuming and then evaporated to dryness. The residue was dissolved in HCl. The diluted samples were analysed using an ICP-MS. All samples were analysed in a single run to reduce instrumental drift-effects. Several samples were repeated in the beginning and at the end of the run to assess the amount of drift.

Accuracy and precision were assessed through analysis of 8 repeats of reference material DST6 done voluntary by the laboratory. Unidentified repeats (10 % of the total number of samples, according to recommendations of Darnley *et al.*, 1995) and two samples of reference material GBW 07309A (China Centre for certified Ref. Mat.) were also included among our samples.

Accuracy calculated from the reference material DST6 was between 90 and 110 % for most elements, except for Zn which seems to have been underestimated (88 %). Accuracy calculated from the standard reference material GBW 07309A indicated underestimation of Cr (67 %), U (87 %) and Ti (82 %). However, only 2 samples were considered to calculate the latter accuracy while the former was calculated on the basis of 8 samples.

Precision was assessed through relative standard deviation (RSD) and based on replicate analyses made voluntarily by the laboratory and 12 replicate samples included in our set of samples. According to Huber (1998) *in* Ribani *et al.* (2004) values of RSD < 5 % and < 20 % are acceptable for major and minor elements, respectively. RSD values calculated through the laboratory's replicate analyses were under the above percentages for all elements except Ti, which had a precision of 9 %. RSD values calculated using the 12 included replicate samples give also percentages below the above limits for all elements except again Ti with the same accuracy of 9 %.

Multi-elemental analysis with ICP-MS: canyon and open slope sediments

The following sample preparation and analysis for the determination of multi-elemental concentration, Pb stable isotope ratios ($^{206}Pb/^{207}Pb$, $^{208}Pb/^{206}Pb$) and activity of ^{210}Pb took place at the Royal NIOZ and were carried out under clean-room conditions (class 100 laminar flow hood, clean laboratory class 100). All labware was acid-cleaned using a Milestone traceClean® device and stored in plastic bags.

A combined method was used to for the preparation of sediment samples for multi-elemental, Pb stable isotope ratios and ^{210}Pb analysis. First, 1 ml of ^{209}Po spike solution (79.8 mBq g^{-1} in 1 M ultra-grade HNO_3) was added to a teflon bomb. Subsequently, about

10 mg of freeze-dried and ground sample was added to the bomb, and digested in a microwave in a mix of 1 ml Milli-Q-Element (Millipore) high purity water (18.2 MΩ), 6 ml concentrated ultrapure HNO_3 and 0.2 ml concentrated HF (suprapur). Subsequently, 1 ml concentrated ultrapure $HClO_4$ was added as an additional digestion step and to ensure effective removal of HF during evaporation. The sample solution was evaporated to dryness, after which the residue was dissolved again with concentrated ultrapure HNO_3 and diluted with 18.2 MΩ Milli-Q to 1M HNO_3. Finally, scandium, thallium and indium (Merck, Certipur, stock solution 1000 mg L^{-1}) were added as internal standards. Elemental concentrations (Ca, Al, Fe, Mg, Mn, Zn, Cr, Pb, Ni, Cu and U) and stable isotope ratios were obtained in separate analytical runs using an Element-2 high resolution double focusing ICP-MS (Thermo Fischer Scientific, Bremen, Germany) with a teflon microflow nebulizer and a double spray chamber to obtain a stable signal. All analyses were performed in duplicate. For more information on the determination of the Pb stable isotope ratios consult Richter *et al.* (2009).

The accuracy of the overall procedure (digestion and analysis) was assessed by analysing standard reference material GBW 07309A within every batch of 10 samples. The number of batches was 30 (n = 30). The accuracy for most of the analysed elements was 90 – 110 %. Only Al had an accuracy of 85 % and Zn showed an accuracy of 113 %. Major elements (Fe, Ca, Mg) had precisions < 10 %, except Al with a precision of 12 % and trace metals < 20 %. Procedural blanks for Fe, Al, Mg, Ca and Mn generally yielded intensities corresponding to less than 1 % of the signal in sediment samples. Intensities for Pb and U were < 3 %; for Cr < 10 % and < 15 % for Ni, Zn and Cu.

^{210}Pb analysis with alpha spectrometry

For ^{210}Pb analysis, the sediment solution with ^{209}Po internal standard, prepared as described above, was again evaporated to dryness to remove HNO_3. Subsequently, the dry residue was dissolved in 5 ml of concentrated HCl (12 M) and the solution was heated, after which 50 ml of diluted HCl (0.5 M) and 5 ml of ascorbic acid (20 g / 500 ml) were added. Silver plates were then suspended in the teflon bombs with solution during 16 h at 70 ºC, to collect Po via spontaneous deposition. The activity of ^{210}Pb was measured in these plates indirectly via its granddaughter ^{210}Po, with a half-life of 138.4 days, via α-spectrometry with Canberra Passivated Implanted Planar Silicon (PIPS) detectors.

Sample preparation and analysis took place at the Royal NIOZ and were carried out under clean-room conditions (class 100 laminar flow hood, clean laboratory class 100). All labware was acid-cleaned using a Milestone traceClean® device and stored in plastic bags.

3.2.4. Mineralogy of the fine and clay fractions

Irradiation of crystalline mineral groups with X-ray produces specific patterns of X-Ray diffraction (XRD) on the crystal structural planes from which minerals can be identified, even in a mixture of minerals (Gomes, 1988). For the present study a total of 274 surface and trap samples were analysed for bulk mineralogical content and 232 samples for clay mineralogical contents, by means of XRD analysis. The majority of analyses were carried out at the Geosciences Department of the University of Aveiro, and a smaller number at the Instituto Hidrográfico in Lisbon. In both laboratories analyses were carried out using a Philips PANalytical diffractometer, with CuKα radiation, following the same analytical procedure. The main mineral phases present in the samples were identified using the database from Brindley & Brown (1980) and MacDiff software's database (Petschick, 2000) (see Figure 3.8 and 3.9). An attempt to quantify relative abundance of minerals was also done, on the basis of the percentage approach, which means that the sum of all identified phases in a sample is taken as 100 %. Since this is a relative quantification the term semi-quantification is used in the presented estimates. For semi-quantitative analysis, the peak areas from basal reflections of minerals were estimated using MacDiff software (Petschick, 2000) and afterwards weighted by empirically estimated factors (Tables 3.1 and 3.2).

Fine fraction

The term "randomly oriented specimen" will be used to refer to the analysis of bulk softly grounded sediment (< 63 µm). In this case, sample was not compressed within the XRD sample container in order to avoid preferential orientation of crystals with different habits, and thus to obtain a more realistic semi-quantification (Gomes, 1988). For randomly oriented specimens, scans were run between 0º and 60º 2θ as shown in Figure 3.8 and the main groups of minerals identified and the respective peak used for quantification are indicated in Table 3.1.

Clay fraction

After analysing the fine-fraction mineralogy, the clay fraction was separated by sedimentation in a settling column filled with distillated water according to Stoke's law, using 1 % sodium hexametaphosphate solution to avoid flocculation (e.g. Rocha, 1993).

In order to identify minerals in the clay fraction, XRD analysis is most commonly done on oriented specimens, since this type of preparation enhances the signals originating from the 001 cleavage plane. However, the bias caused by preferential orientation of crystals with different habits is not important here since most of the minerals present in this fraction are layered silicates. This procedure facilitates recognition of individual clay mineral phases (Kahle *et al.*, 2002) and increases the sensitivity of the method.

Table 3.1. Minerals / groups of minerals identified and their characteristic peaks and empirically estimated weighing factors used for semi-quantification.

Mineral / Group of minerals	Peak (Å) used for semi-quantification	Empirically estimated factors
Aragonite	3.39	1*
Calcite	3.03	1*
K-feldspars	3.24	1*
Mg-Calcite	3.00	1*
Phyllosilicates	4.47	0.2**
Plagioclase	3.18	1*
Quartz	3.34	2*

* determined by Huertos & de los Monteros (1974) *in* Gomes (1988) in a similar mixture of minerals as the one present in our samples; ** used by Rocha (1993), Oliveira (2001) and Abrantes (2005).

To prepare oriented clay mounts, a small volume of the suspension containing the < 2 μm fraction was placed on a thin glass plate and air dried. After that, three successive XRD scans were performed on the sample: a first scan on the original air dried sample, a second scan after saturating the sample with glycerol, and a third scan after heating the glycerol-saturated sample to 500 °C for 90 minutes. Differences between successive scans are illustrated in Figure 3.9a, b, c. The scans were run between 2º and 20º 2θ for the air dried aggregates and between 2º and 15º 2θ for the other two treatments.

The clay mineral analysis allowed distinction of four clay mineral groups with relatively broad peaks: illite, kaolinite, smectite and chlorite. The characteristic peak sizes

and empirically estimated weighing factors applied to peak area are indicated in Table 3.2. Through XRD analysis it was not possible to make a finer differentiation within these four clay mineral groups.

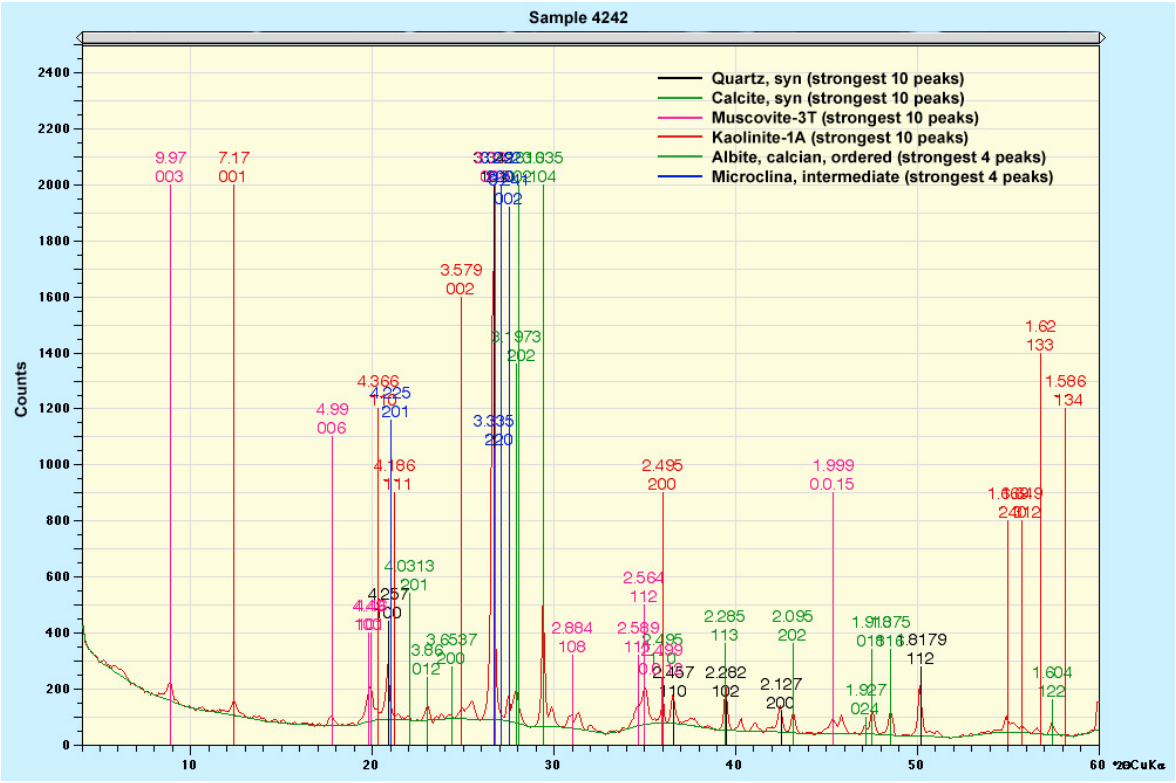

Figure 3.8. Diffractogram for sample 4242 (fine fraction) obtained through a Philips PANalytical diffractometer and identified manually with the database from Brindley & Brown (1980) and using MacDiff software database. Estimation of the peak areas was estimated using MacDiff software.

Table 3.2 List of clay mineral groups identified, their characteristic peaks and empirically estimated determined weighing factor used for semi-quantification.

Group of minerals	Peak (Å) used for semi-quantification (diffractogram used)	Empirically estimated factors
Illite	10 (in natural specimen)	0.5
Kaolinite	7 (in natural specimen after removal of the chlorite-002 peak)	1
Smectite	17 (in specimens treated with glycerol)	4
Chlorite	14 (in 500 ºC heated specimens)	0.75

Empirically estimated factors according to Rocha (1993), Oliveira *et al.* (2002) and Abrantes (2005).

The 5 Å / 10 Å peak intensity ratio of illite was considered to estimate the "octahedral character". According to Esquevin (1969), high ratio values > 0.4 correspond to Al-rich illites whereas Fe- and Mg-rich illites have values below 0.15.

a

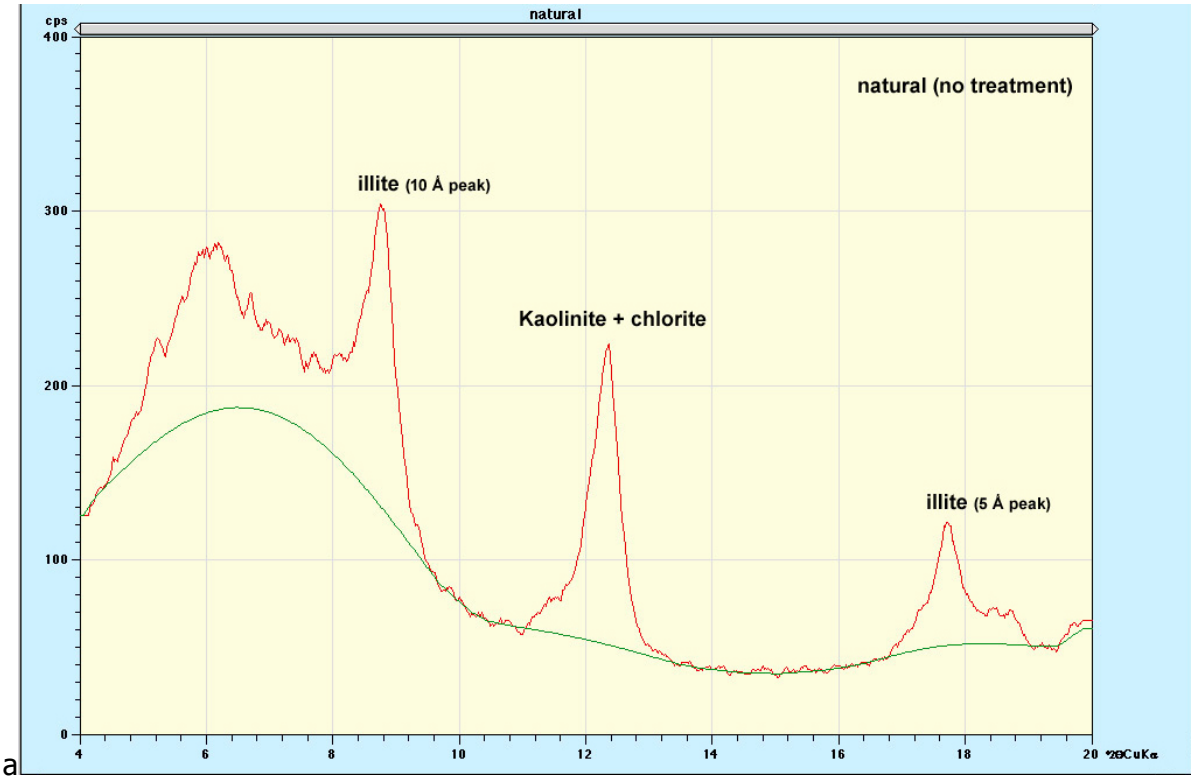

b

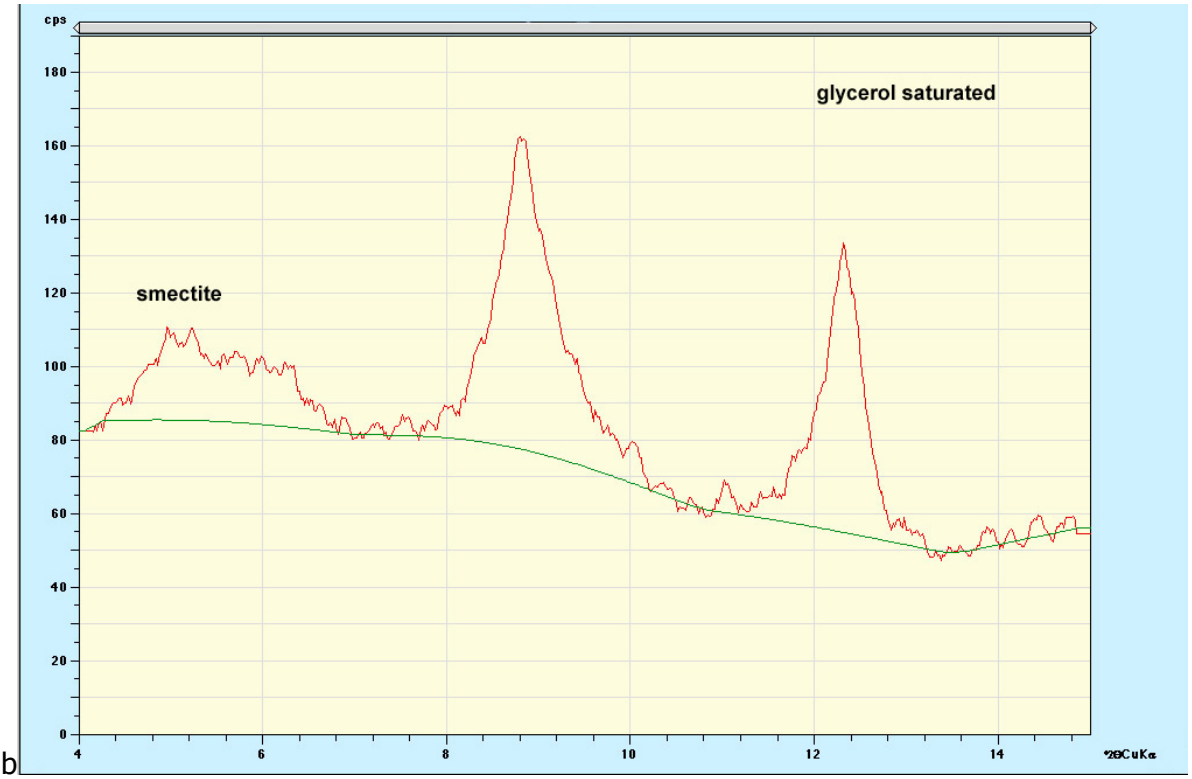

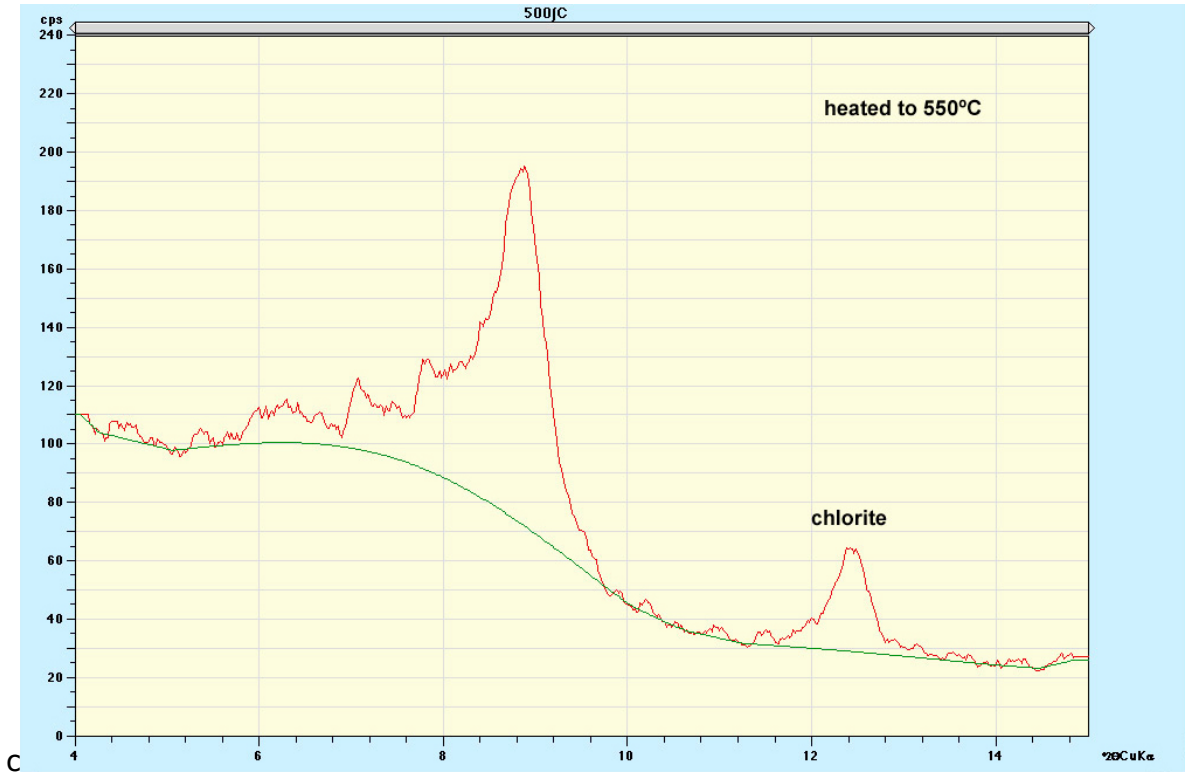

C

Figure 3.9. Diffractograms for the clay fraction of sediment trap sample 204-35 cup6 obtained with a Philips PANalytical diffractometer and analysed through MacDiff software, illustrating differences between different sample treatments: **a**) untreated sample, **b**) glycerol-saturated sample, **c**) glycerol-saturated sample heated at 500ºC for 90 minutes.

Kaolinite crystallinity index was determined as the ratio between the width measured at half-height of the 7 Å peak and the height of this peak, measured in air-dried specimens and after applying a correction for overlap of chlorite and kaolinite on the 7 Å peak. For illite crystallinity, the Kubler (1964) Index was used, determined as the width measured at half-height of the 10 Å peak. Well-ordered illite shows symmetrical and narrow basal reflections and consequently low values of the Kubler Index.

3.2.5. Resume of sample processing

Figure 3.10 summarizes the sample processing applied to sediment samples used in the present study and described above.

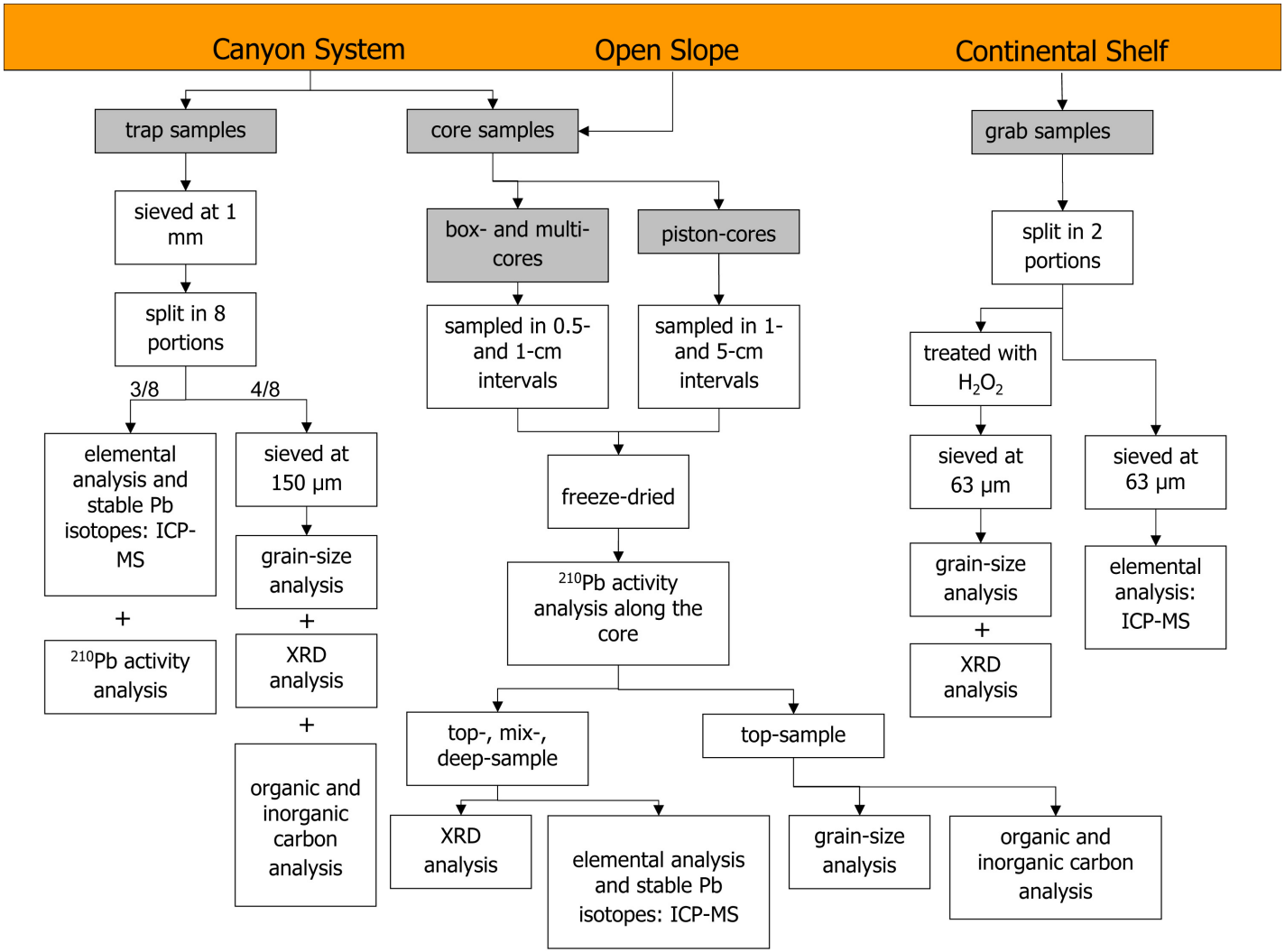

Figure 3.10. Flow diagram of the different steps of sample preparation and analysis (white boxes) applied to different types of samples (grey boxes).

3.3. Data processing and calculations

3.3.1. Horizontal sediment fluxes in the bottom boundary layer

Acoustic Doppler Current Profilers (ADCPs) are capable of yielding suspended sediment concentrations (SSC) estimates over the depth range ensonified at a high temporal and spatial resolution. ADCPs are non-intrusive, as the sediment suspension is being monitored at distance. The disadvantage of the acoustic approach is the dependence on sediment properties. In particular, irregularities in grain size distribution restrict the accuracy of acoustic SSC measurements (Mol, 2003). The ADCP used in the presented study collected data in 5-cm vertical intervals; the data presented here always refer to a level at 100-cm above the seabed. For the conversion of acoustic data into SSC estimates, the first step was to convert CTD profiles of optical backscatter to SSC, using filtered suspended matter samples for calibration. Then, optical backscatter values obtained by the BOBO lander were calibrated to SSC estimates from nearby CTD casts. Finally, the optical backscatter record of the BOBO lander, converted to SCC, was used for calibration of the acoustic backscatter. An exponential relationship was found between optical and acoustic backscatter from the BOBO lander. Since the influence of variations in particle characteristics during the measurement on optical and acoustic quantification of SSC is not known, the calculated sediment flux has to be regarded as a rough order of magnitude approximation.

3.3.2. Accumulation rates determined in sediment cores

The analysis of down-core ^{210}Pb activity is an important dating tool on a 100-yr time scale, providing a method for calculating recent sediment accumulation rates (SARs) in environments where a relatively undisturbed sediment record is preserved. In areas of low SARs and relatively intense bioturbation, the method is considered less suitable for dating, because it is often not possible to accurately correct for reworking (Carpenter *et al.*, 1982).

In the description of down-core profiles of ^{210}Pb activity three characteristic vertical zones are generally observed (e.g. Nittrouer *et al.*, 1979):

i) a surface mixed layer (SML), extending to a distance L below the water sediment interface, where sediments are actively mixed by physical and biological processes;
ii) a region where ^{210}Pb activities decrease logarithmically with depth in the sediment;
iii) a lower region of background activity, in equilibrium with ^{226}Ra.

For the present study sediment accumulation rates (SAR) were determined using the model of Constant Flux and Constant Sedimentation Rate (CF/CS; Appleby & Oldfield, 1992 *in* Boer *et al.*, 2006) and the model of Constant Flux and Constant Sedimentation Rate including a surface mixed layer (SML) on the top (CF/CSSML; Carpenter *et al.*, 1982; Boer *et al.*, 2006).

The first is a one-layered profile consisting of an exponential downward decline in excess (or unsupported) ^{210}Pb activity, on top of a background ^{210}Pb (supported ^{210}Pb) produced by decay of ^{222}Rn in the sediment. A Constant Flux and Constant Sedimentation rate (CF/CS) model is usually applied for dating, which assumes that the SAR remained constant and that reworking of sediment has been negligible (Appleby & Oldfield, 1992). The down-core total ^{210}Pb activity (A) can be described with the equation:

$$A_{m(tot)} = A_{0(xs)} \exp^{\frac{-\lambda m}{\omega}} + A_{(\sup)} \quad (2)$$

Where: A_m is the total ^{210}Pb activity (mBq g^{-1} dry sediment) at the cumulative mass depth m (g cm^{-2}), $A_{0(xs)}$ is the initial excess ^{210}Pb activity at the sediment-water interface (mBq g^{-1} dry sediment), λ is the decay constant of ^{210}Pb (0.0311 yr^{-1}), ω is the SAR (g cm^{-2} yr^{-1}) and $A_{(sup)}$ is the supported ^{210}Pb activity (mBq g^{-1}).

The CF/CSSML model is a two-layered profile consisting of an upper layer with a slow exponential downward decline in excess ^{210}Pb activity and a deeper layer characterised by a more rapid exponential downward decline. For these profiles, the usual assumption is that diffuse mixing caused by burrowing organisms generates a surface mixed layer (SML). The strength of the mixing processes in the SML is measured by the mixing coefficient (D_b) in units of g^2 cm^{-4} y^{-1}, assumed constant mixing rate throughout the mixed layer. This coefficient is incorporated into the equation for the SML:

$$A_{m(tot)} = A_{0(xs)} \exp^{\alpha m} + A_{(sup)} \quad (3)$$

Where:

$$\alpha = \frac{\omega + \sqrt{\omega^2 + 4\lambda D_b}}{2D_b} \quad (4)$$

The equation for layer 2 is similar to Equation (2), with the difference that $A_{0(xs)}$ is replaced by A_{mix} (at m_{mix}), which is the excess ^{210}Pb activity at the bottom of the SML. It is assumed that no reworking takes place below the SML, and that the SAR is constant through both layers ($\omega_{(SML)} = \omega_{(layer2)}$). The SAR is calculated from the layer below the SML.

Linear sedimentation rates are a function of porosity and SAR. As a result of sediment compaction, linear sedimentation rate decreases with depth in cores. To circumvent this problem of differential compaction, ^{210}Pb activity profiles were plotted against cumulative mass depth by intergrading dry bulk density values over depth (Figure 3.11). This provides SARs that are independent of compaction, which allows for better comparison between cores (Boer *et al.*, 2006).

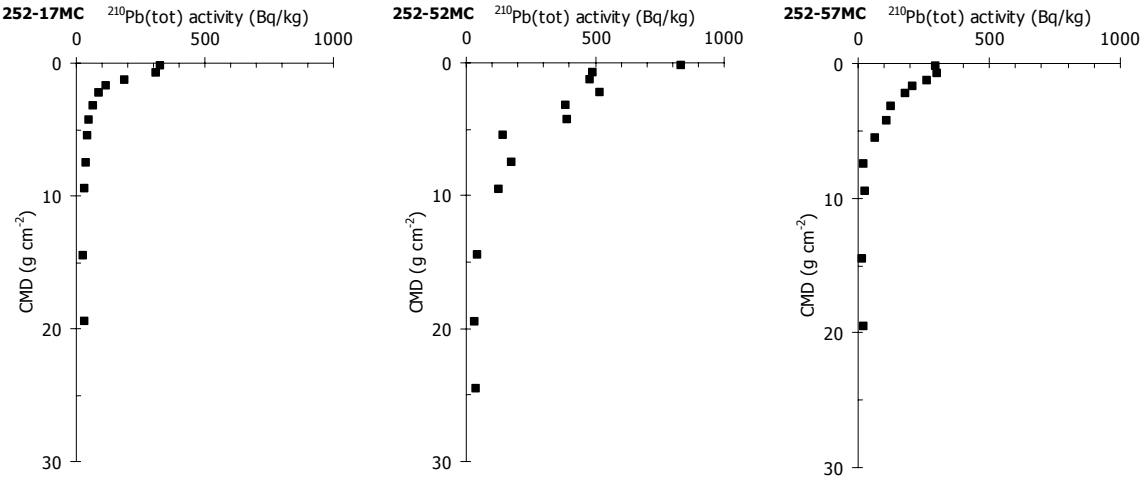

Figure 3.11. Three examples of total ^{210}Pb activity against down-core cumulative mass depth.

3.3.3. Trace metal enrichment factors (EF)

Trace metal enrichment in surface sediment and trap samples was assessed on the basis of normalised enrichment factors (EF), calculated relative to pre-industrial baseline values as follows:

$$EF(trace\ metal) = \frac{\left(\frac{[trace\ metal]}{[Fe]}\right)_{sample}}{\frac{\sum_{1}^{n}\left(\frac{[trace\ metal]}{[Fe]}\right)}{n}_{baseline}} \quad (5)$$

Pre-industrial baseline values were determined in subsurface sediment samples dated with ^{210}Pb as approximately 150 years old (cf. section 3.1.3). Baselines were determined separately for the Lisbon-Setúbal and Nazaré canyons (Table 7.1). These EFs compare present-day normalised trace metal contents with pre-industrial normalised contents of 150 years ago (cf. section 3.1.2).

As shown in Equation (5), Fe was used as the normaliser. Among various proxies for potential trace metal carriers, such as Al and Fe for terrigenous aluminosilicates, Ca and $CaCO_3$ for pelagic skeletal carbonate, and C_{org} for organic matter, Fe and Al showed the largest number of significant positive correlations with trace metals. However, as Fe had the highest accuracy and the strongest correlations to trace metals Fe was chosen for the normalisation of trace metals. No indication in the data was found referring secondary diagenetic enrichment of trace metals played a significant role. The selection of the normaliser is thoroughly discussed in Chapter 7, section 7.2.4. on pg. 195.

An EF value varying between 0.5 and 1.5 was interpreted to indicate a predominantly natural origin for the element in the sediment, while values greater than 1.5 indicate enrichment by either natural processes (e.g. contributions from biota) or anthropogenic influences. EF values lower than 0.5 can reflect mobilisation and loss of these elements relative to the conservative element, or could indicate an overestimation of the baseline metal contents (e.g. Zhang, 1995; Mil-Homens *et al.*, 2006).

3.3.4. Inventories and percentages of excess trace metals over the last 150 years

The difference between trace metal concentrations in the mix and deep sample (see section 3.1.3) corresponds to the excess metal content gathered over the last 150 years ([trace $metal_{xs}$]). Finally, inventories of excess trace metals were calculated by multiplying excess trace metal concentration with cumulative dry mass of the sediment column (CDM) considered in the mix sample:

$$trace\ metal_{xs}\ Inv\ \left(\mu g\ cm^{-2}\right) = \left[trace\ metal_{xs}\right]\left(\mu g\ g^{-1}\right) \times CDM\ \left(g\ cm^{-2}\right) \quad (6)$$

The excess of Pb, Zn and Cu deposited over the last 150 years was expressed as a percentage of total deposition of these trace metals as follows:

$$\%\left(Pb, Zn\ or\ Cu\right)_{excess} = \frac{trace\ metal_{xs}\ Inv}{trace\ metal_{tot}\ Inv} \times 100 = \frac{\left[trace\ metal_{xs}\right]}{\left[trace\ metal_{tot}\right]} \times 100 \quad (7)$$

These percentages are meant to quantify the relative contribution of anthropogenic metals to the natural background during the industrial period over the last 150 years.

Part II
Continental shelf and upper slope

4. MINERALOGY OF SHELF AND UPPER SLOPE SURFACE SEDIMENTS

4.1. Introduction

4.1.1. Different types of sediments and the importance of their study

The oceans of the world represent a natural depository for the dissolved and particulate products of continental weathering. After being discharged into the ocean by rivers, part of the dissolved load precipitates by biological and geochemical processes and is deposited on the ocean floor along with detritic sedimentary material.

Ocean sediments are heterogeneous with regard to their composition, displaying a considerable degree of geographical variation. Due to the origin and formation of the components various sediment types can be distinguished: lithogenic sediments which are transported and dispersed into the ocean as detrital particles, either as terrigenous particles (derived from land, which is most frequently the case) or as particles nourished by immersed outcrops (having only local importance); biogenic sediments which are directly constructed by organisms or are formed by accumulation of loose skeletal fragments; authigenic sediments which precipitate directly out of solution as new formations, or are a result of changes occurred when the pre-existing particles come into contact with the solution (Fütterer, 2006).

Lithogenic sediments on continental shelves reflect prevailing climatic conditions that affect chemical and physical weathering and transport processes, the geology of the source areas, and oceanographic processes. Coarse sediments (gravel and sands) are carried as bedload over the seabed and are deposited close to the mainland while finer particles (silt and clay) are transported in suspension and are therefore dispersed over large distances by currents. Part of the suspended matter transported over the shelf may settle and form ephemeral or more permanent fine-grained deposits on the shelf (Abrantes, 2005).

Minerals like plagioclases are good indicators of "fresh" lithogenic sediment because they are less resistant than most other common rock-forming minerals to weathering processes (Meunier, 2005), especially in the marine environment (Rothwell, 1989). Table

4.1 shows the total dissolution time of silica in minerals according to Lasaga (1984). Although this study does not refer to the marine environment it clearly illustrates the wide range of dissolution rates of various common minerals.

The provenance of sediments from different source areas with different lithologies may be distinguished through the assemblage of minerals present in the fine fraction. Especially minerals in the clay-size range are susceptible to erosion and dispersal by fluvial and aeolic transport, and transport by seabed currents and gravitational movements (Ehrmann *et al.*, 1992). Generally, clay minerals are not very susceptible to important mineralogical and chemical transformations during transport and after deposition in the marine environment. However, if the transport is over a long distance or if the minerals spend enough time in the marine environment, subtle changes do occur (referred to as "crystallographic scarring" by Millot, 1964 and Segonzac, 1969). An example is the increase of illite crystallinity order with increasing exposure to the marine environment, resulting from incorporation of Al into the crystal structure (Nemecz, 1981; Millot, 1964; Oliveira *et al.*, 2002).

Table 4.1. (adapted from Lasaga, 1984 *in* Goudie, 1995) Total dissolution time of silicate minerals with 1 mm of diameter at 25ºC and pH = 5.

Mineral	Dissolution time (years)
Quartz	34 000 000
Muscovite	2 700 000
Forsterite	600 000
K-Feldspars	520 000
Albite (Plagioclase)	80 000
Enstatite	8 800
Diopside	6 800
Nefeline	211
Anortite (Plagioclase)	112

Based on these general observations, the distribution of fine-grained material in marine sediments and of clay mineral associations which characterise these fine fractions have been widely used in studies of recent sedimentary dynamics, as indicators for provenance, dispersal and deposition of fine-grained sediments (e.g. Karlin, 1980; Honjo *et al.*, 1982; Zöllmer & Irion, 1993; Berner & Wefer, 1994; Oliveira *et al.*, 2002; Kairyte *et al.*, 2005; Morais *et al.*, 2006; Oliveira *et al.*, 2007).

Studies of the biogenic component in the fine fraction of marine sediments have shown the potential use of calcareous nannoplankton and diatoms as tracers of specific water masses and as paleoenvironmental tracers (e.g. Findlay & Flores, 2000; Salgueiro *et al.*, 2008; Cochran & Neil, 2010).

4.1.2. Different types of sedimentary deposits on the shelf

Approximately 70 % of the continental shelf surface worldwide is covered with relict sediment, i.e. sediment deposited during the last glacial period under conditions different from today's, especially at times when the sea level was comparatively low (Emery, 1968). The fine-grained constituents of shelf sediments were eluted during the rise of the sea level in the Holocene and exported over the edge of the shelf to the adjacent continental slope. The remaining sediment, covering large areas of modern shelf seabed, consists of relatively coarse sandy material (Milliman *et al.* 1972; Milliman & Summerhays, 1975). It is therefore assumed that fine-grained sediments contained in present shelf deposits are of relatively recent age.

Similar to most other continental shelves worldwide (e.g. Emery, 1968), the central Portuguese shelf is characterised by the presence of various types of sedimentary deposits, which reflect the interplay of different processes (e.g. long-term variations in sea level, sediment discharge from rivers, reworking of sediments by tides and currents, sheltering from main swell by capes). The fine fraction was chosen to be studied as it is the sediment fraction which is common to all shelf deposits. In addition, it is the prevailing fraction in sediments of deeper areas like the adjacent submarine canyons and open slopes, which are subject of Part III of this thesis.

4.1.3. Objectives of Chapter 4

The main objectives of this chapter are:

1) to describe the bulk and clay mineralogy of the fine fraction (< 63 µm) from surface sediments collected in the Lisbon, Setúbal and Sines shelves and upper slopes;
2) to compare results from the Lisbon-Setúbal-Sines shelf with those from other areas of the Portuguese shelf with a different regional setting;
3) to identify the main sources of fine-grained sediments in the study area, and gain insight in prevailing dispersal processes acting on the shelf.

4.2. General composition of surface sediments

Surface sediments from the Lisbon-Setúbal-Sines shelf are dominated by sand-sized material. Below 80 m WD (~outer shelf), fine-grained sediments are considerably more abundant on the Lisbon and Setúbal shelves compared to other areas of the Portuguese

shelf. Gravel occurs in low percentages in this area, contrasting with the adjacent Estremadura shelf. According to Dias (1987) the percentage of mica in surface sediments of the Lisbon and Setúbal shelves is relatively high not only for the Portuguese shelf but also comparing to other shelves around the world. Most of the shelf sediment has bulk carbonate contents below 30 % and sediments with higher contents of carbonates correspond to sandy deposits of the middle part of the Sines and Setúbal shelves and of the outer shelf / upper slope more in general (Figure 2.4).

4.3. Grain size in the fine fraction of surface sediments

The mean grain size of the fine fraction of surface sediments of the Lisbon-Setúbal-Sines continental shelf shows no obvious geographic trend in distribution. Relatively higher values occur in different parts of the study area such as the upper reaches of the Cascais, Lisbon and Setúbal Canyon, off the Sado Estuary and also in the southernmost part of the study area close to Cape Sines. The mean grain size values seem therefore to have no relationship with water depth or to the type of sedimentary deposits. Mean grain size values range from 6.1 to 7.4 μm on the Lisbon shelf and between 4.9 and 7.7 μm and 5.0 and 9.8 μm on the Setúbal and Sines shelves, respectively. Modal grain sizes span a narrow range of values on the Lisbon shelf (6.5 – 7.8 μm) compared to the Setúbal and Sines shelves (4.6 – 11.0 μm and 4.6 – 31.2 μm, respectively). These modal grain sizes do not show a relationship with water depth (data not shown).

On the other hand, contents of clay-sized particles show clear spatial distribution patterns (Figure 4.1). Relatively low contents of clay-sized particles (17 to 23 %) are found on the Lisbon shelf. In accordance, contents of silt are higher on the Lisbon shelf compared to those from the Setúbal and Sines shelves. However, a more reliable comparison between different shelf areas is made when sediments from similar sedimentary deposits are compared. Figure 4.2a compares the grain size spectra of the fine fraction of surface sediments from the Tagus and Sado mud patches (fine fraction > 90 %). Sediments from the Sado mud patch appear slightly finer-grained than those of the Tagus mud patch, with fine fraction modes of, respectively, 8 – 9 μm and 9 – 11 μm (Figure 4.2a).

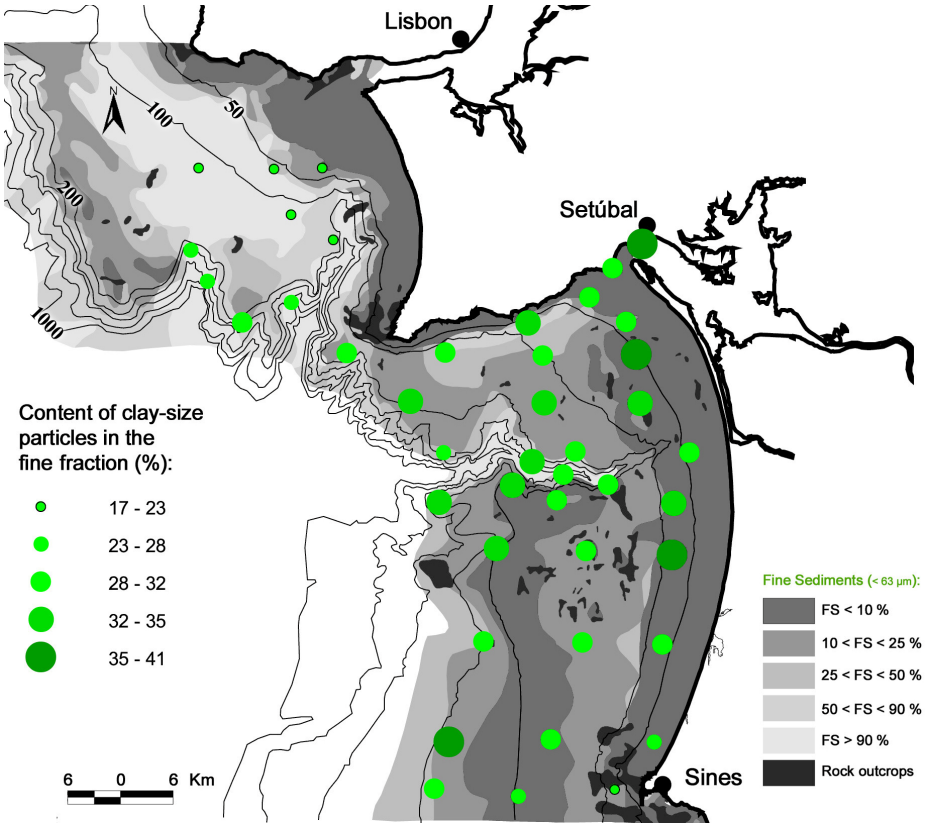

Figure 4.1. Content of clay-sized particles in the fine fraction of surface sediments from the Lisbon-Setúbal-Sines shelf and upper slope.

The relative proportions of clay and silt in the fine fraction shows considerable spatial variation in the area. Paradoxically, the higher percentages of clay-sized material are found in deposits with overall low content of fine sediment (< 63 µm), whereas low percentages of clay-size material occur in deposits rich in fine-grained material (Figures 4.1 and 4.2b). The reasons for this inverse relationship will be discussed in section 4.6.3.

4.4. Fine-fraction bulk mineralogy

Lithogenic detrital components of marine sediments, despite all regional variability, are composed of only a few common minerals. Next to quartz, which remains largely unaltered, even after prolonged weathering, phyllosilicates (most of them clay minerals) represent the most common end product of complete weathering of metamorphic and igneous rock. Consequently, this group represents the most important mineral constituent in sediments, next to quartz and biogenic minerals. To a lesser degree, terrigenous detritus contains unweathered minerals like feldspars. In general, the biogenic minerals

contributing most to sediment formation are carbonate minerals in the form of calcite, Mg-calcite and aragonite, and biogenic opal in the form of amorphous $SiO_2 \cdot nH_2O$.

Consequently, the bulk mineralogy of fine fraction shelf surface sediments of the Lisbon-Setúbal-Sines shelf is qualitatively monotonous. Although varying in relative abundance, only seven different minerals / groups of minerals were identified (Table 4.2): Quartz (Qz), Calcite (Cc), Phyllosilicates (Phy), Plagioclases (Plg), K-Feldspars (K-F), Aragonite (Arg) and Mg-Calcite (Mg-Cc).

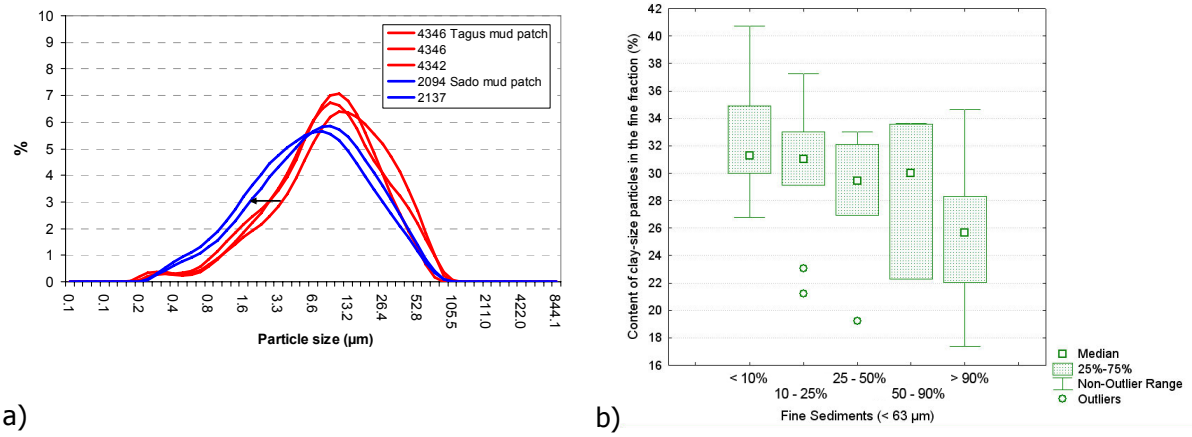

a) b)

Figure 4.2. a) Grain size spectra of the surface sediments' fine fraction from the Sado and Tagus mud patches (for spatial location of samples cf. Figure 3.1). **b)** Box-plots showing percentages of clay-sized particles in the fine fraction of surface sediments against different classes of sedimentary deposits classified according to the weight percentage of fine sediments (< 63 µm).

4.4.1. Quartz

Quartz constitutes between 12 and 51 % of the fine sediment fraction of the Lisbon-Setúbal-Sines shelf (Figure 4.3). On the Lisbon shelf, the highest contents are found at shallower water depths, and the lowest contents at the shelfbreak and in the upper reaches of the Lisbon and Cascais canyons. On the Setúbal shelf the highest contents of quartz appear in the northwestern part, almost in connection with areas of high quartz contents on the Lisbon shelf, and also in sandy deposits off the Sado Estuary. On the Sines shelf quartz contents are highest in sandy deposits of the inner shelf (< 50 m WD). Figure 4.11a shows the statistical distribution (median, percentiles 25 and 75 and extremes) of fine fraction quartz content for different classes of fine sediment content (< 63 µm). The classes of sedimentary deposits are also the ones indicated in Figure 4.3.

Sedimentary deposits composed of more than 25 % of fine sediment fraction have the highest contents of quartz in the fine fraction (Figure 4.11a).

Table 4.2. Basic statistics of the minerals / group of minerals identified in the fine fraction of 98 surface samples from the Lisbon-Setúbal-Sines shelf.

Minerals / Group of minerals	Median (%)	Range (%)	P25-P75 (%)
Quartz	31	12 - 51	26 - 37
Calcite	29	6 - 62	17 - 37
Phyllosilicates	19	3 - 59	14 - 24
Plagioclase	8	2 - 25	5 - 10
K-Feldspars	5	0 - 25	3 - 8
Aragonite	2	0 - 24	0 - 3
Mg-Calcite	0	0 - 36	0 – 2

4.4.2. Phyllosilicates

Concentrations of phyllosilicates between 26 and 32 % are found in the Tagus mud patch and even higher contents (> 40 %) are found in the Lisbon Canyon (Figure 4.4). On the Setúbal shelf three areas show enrichments in phyllosilicates: sediments in the outlet of the Sado Estuary (59 %); the Sado mud patch (reaching 40 %) and the upper Setúbal Canyon (reaching 39 %). On the Sines shelf, percentages of phyllosilicates tend to be lower than 20 % and only on the inner shelf off the central coastal arc contents are higher than 25 % (Figure 4.4).

In general, phyllosilicates seem to accumulate in areas that are relatively sheltered from intense wave and current energy, like in submarine canyons, on mud patches off the Tagus and Sado rivers and in estuaries. Since these are also the areas where fine-grained sediments tend to accumulate, phyllosilicate content in the fine fraction, and content of fine fraction in the total sediment appear positively correlated (Figure 4.11b). However, higher percentages of phyllosilicates are also found in some sandy samples (FS < 10 %) located close to phyllosilicate sources (e.g. the outlet of the Sado Estuary and the inner shelf off the central coastal arc between Tróia and Sines).

Despite this positive relationship between phyllosilicate content and the amount of fine fraction in shelf deposits, a negative correlation was found between the clay content and the amount of fine fraction in the total sediment (Figure 4.2b). These two

observations seem not to be in accordance since clay minerals constitute a large portion of the family of phyllosilicates. However, a large portion does not mean all. Muscovites are phyllosilicates of which the size ranges from 0.4 to 100 μm and they represent an important mineral constituent of the samples here presented and can be identified even in the bulk mineralogy (cf. Figure 3.8). Therefore, all muscovites contained in the fine fraction contribute to the phyllosilicates while only a part of these muscovites (those that have a diameter less than 2 μm) are counted as clay fraction. Muscovites in the clay fraction are counted as illite since there is no way of differentiating both minerals through normal XRD procedures.

4.4.3. Feldspars

Plagioclase in the fine fraction has a relatively well-defined spatial distribution pattern. High concentrations occur on the Lisbon shelf, especially close to the outlet of the Tagus Estuary, and extend to the northwest Setúbal shelf (Figure 4.5). High contents of plagioclase also occur on the inner Sines shelf (15 – 23 %). In general, the higher mean concentrations of plagioclase in the fine fraction are found in deposits with contents of fine fraction higher than 25 % (Figure 4.11c).

In the same way as plagioclase, contents of K-feldspar generally decrease with water depth (Figure 4.6). The highest values occur in the sandy deposits of the inner shelf especially at the shallowest depths.

4.4.4.Carbonates

In general, contents of calcite are below 25 % on the Lisbon shelf, and above 25 % and up to 62 % on the Setúbal and Sines shelf, except near the shore (Figure 4.7). There is no relationship between the content of this biogenic mineral and the amount of fine fraction in the sediment. The areas with higher terrigenous input near the outlets of the Tagus and Sado estuaries are well highlighted by concentrations of calcite lower than 25 % (see pink dots in Figure 4.7).

Aragonite occurs in significant amounts (> 3 %) on the inner and middle Setúbal shelf, but it is less common on the Sines shelf, and virtually absent in the sampled area of the Lisbon shelf (Figure 4.8). Across the Setúbal and Sines inner shelves there is a

southward decrease in aragonite content. Aragonite content is clearly inversely related to the amount of fine fraction (Figure 4.11f).

Significant contents of Mg-calcite (> 5 %) only occur on the inner and middle shelves. The distribution is rather scattered on the Setúbal and Sines shelves, without clear geographical pattern. As for aragonite, Mg-calcite occurs mainly in sandy deposits (Figure 4.9).

The lithogenic against biogenic mineral (L/C) ratio (Phy+Qz+Felds/CC+Mg-Cc+Arg) highlights the areas most affected by fresh lithogenic sediment input. The whole Lisbon shelf in general shows high values for this ratio (> 3). On the Setúbal and Sines shelves, high values (> 3) occur in the Sado mud patch, in the Sado outlet and on the inner shelf bordering the central and southern part of the coastal arc between Tróia and Sines (Figure 4.10).

4.4.5. Comparison to the adjacent open slope and canyon environments

The bulk mineralogy of the fine fraction of surface sediments from the Lisbon-Setúbal-Sines outer shelf and upper slope (100–500 m WD) is quite variable, displaying strong along-shelf gradients. Lithogenic/carbonate ratios are comparable on the Sines outer shelf (100 - 200 m WD) and upper slope (200 – 500 m WD) (Figure 4.10), with ratio ranging from 0.5 to 2.0 and from 0.5 to 1.5, respectively. As shown in Chapter 6, the surface sediment layer (0 - 0.5 cm) of two multicores collected from the Sines upper slope (280 and 490 m) had comparable L/C ratios (0.9 and 1.1) to those in grab samples from the Sines upper slope.

Further down the Sines open slope, in depths > 1000 m, the L/C ratio increases to values between 1.2 and 1.5 as a result of an increase of phyllosilicates and slight decrease of calcite relative to upper slope sediments (compare Figure 4.4 and 4.7 with Figure 6.10). Surface sediments from the lower Setúbal Canyon (> 2000 m WD) show even higher L/C ratios between 1.7 and 2.0 (Figure 6.12a), similar to values found for surface sediments from the Lisbon shelf and certain parts of the Setúbal shelf (Figure 4.10).

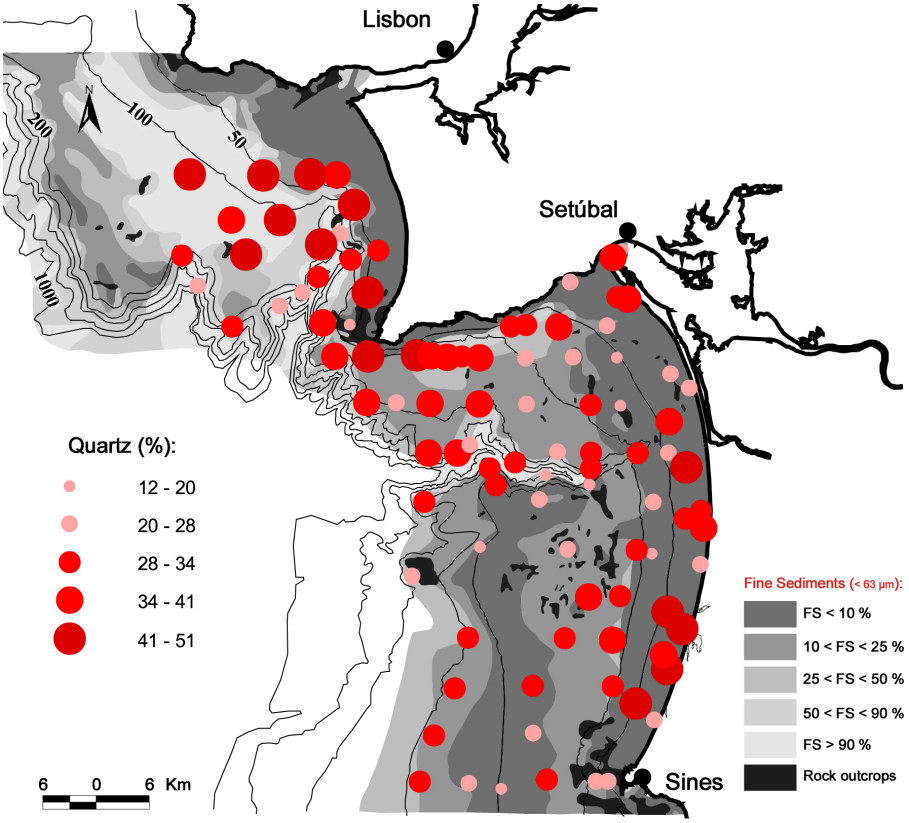

Figure 4.3. Content of quartz in the fine fraction of surface sediments from the Lisbon-Setúbal-Sines shelf and upper slope.

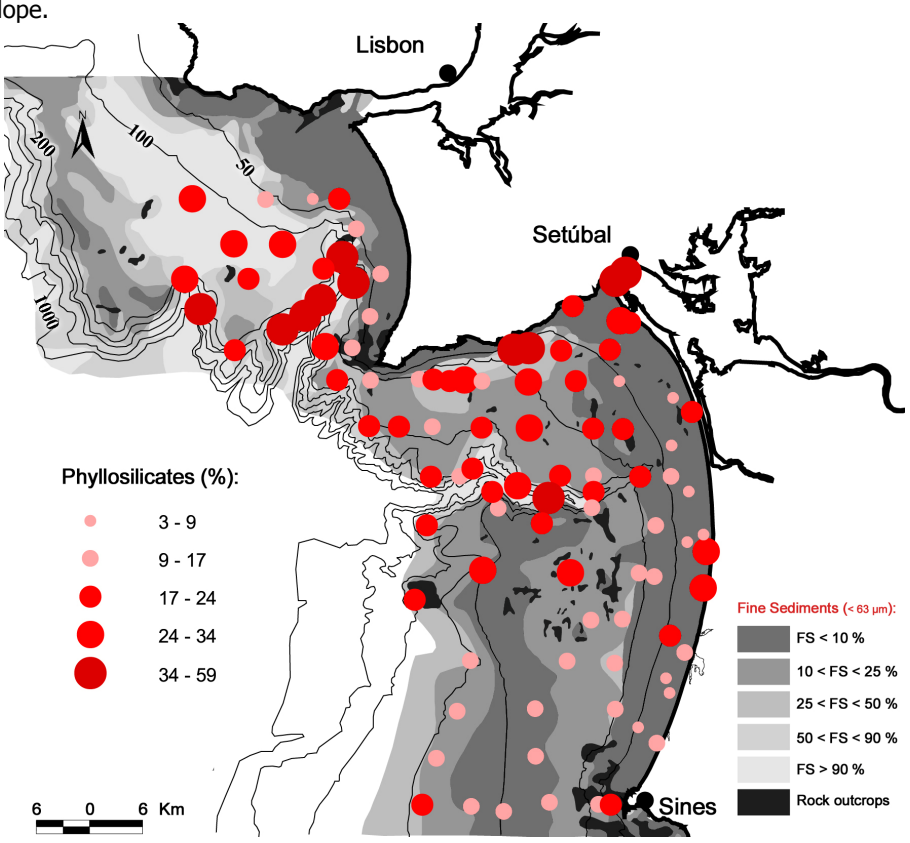

Figure 4.4. Content of phyllosilicates in the fine fraction of surface sediments from the Lisbon-Setúbal-Sines shelf and upper slope.

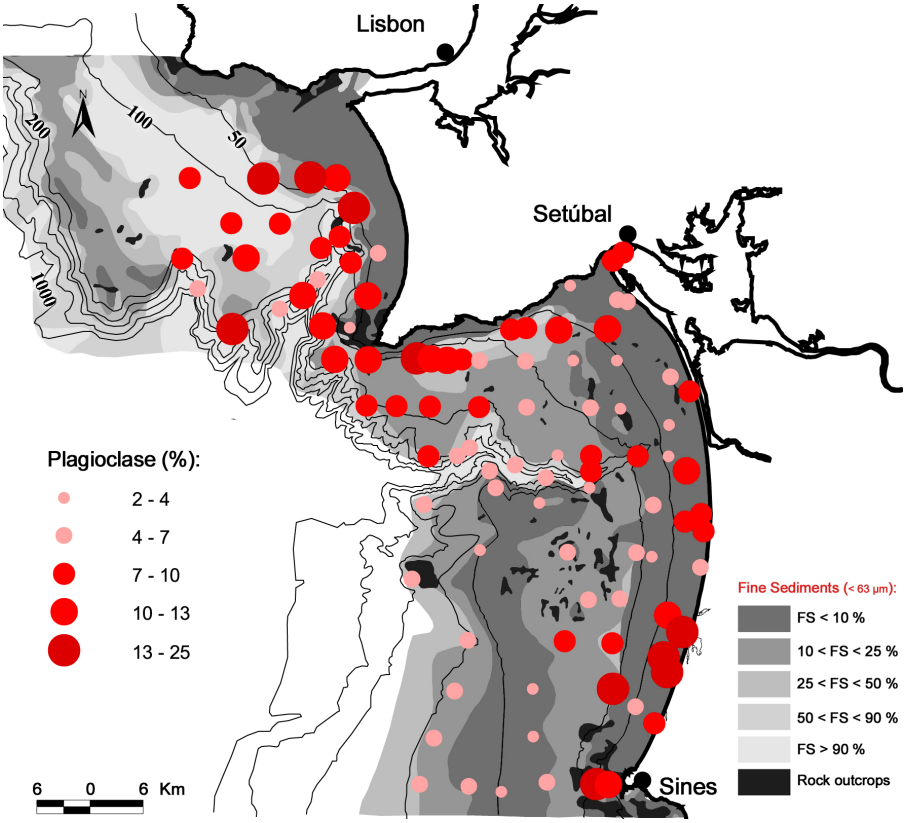

Figure 4.5. Content of plagioclase in the fine fraction of surface sediments from the Lisbon-Setúbal-Sines shelf and upper slope.

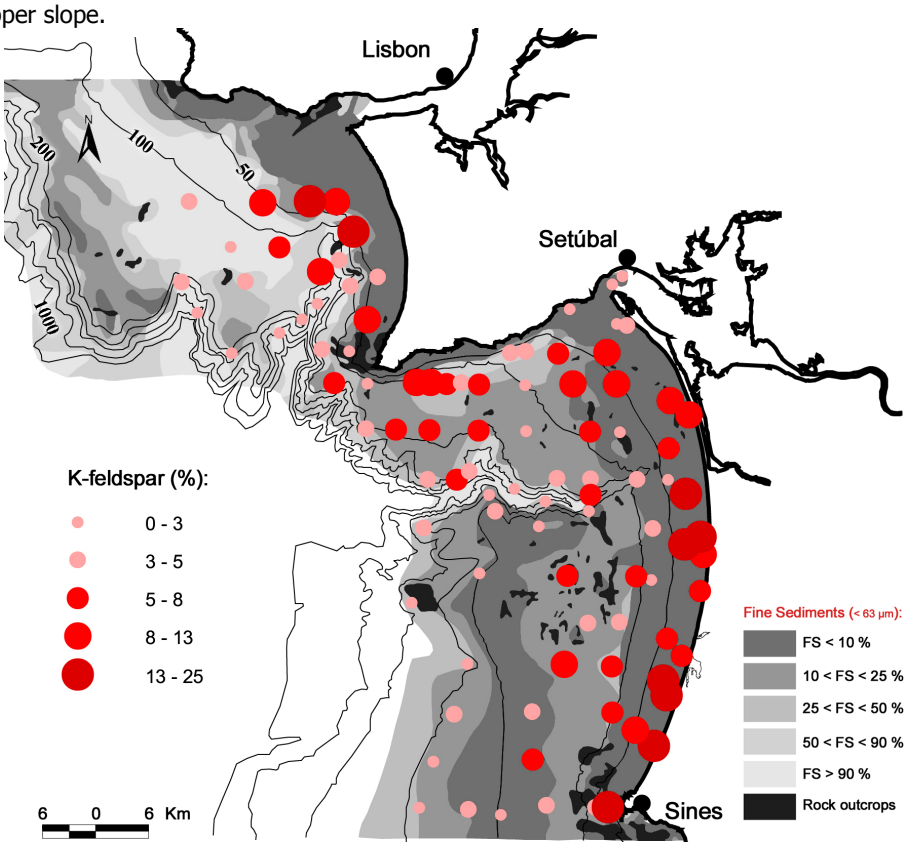

Figure 4.6. Content of K-feldspars in the fine fraction of surface sediments from the Lisbon-Setúbal-Sines shelf and upper slope.

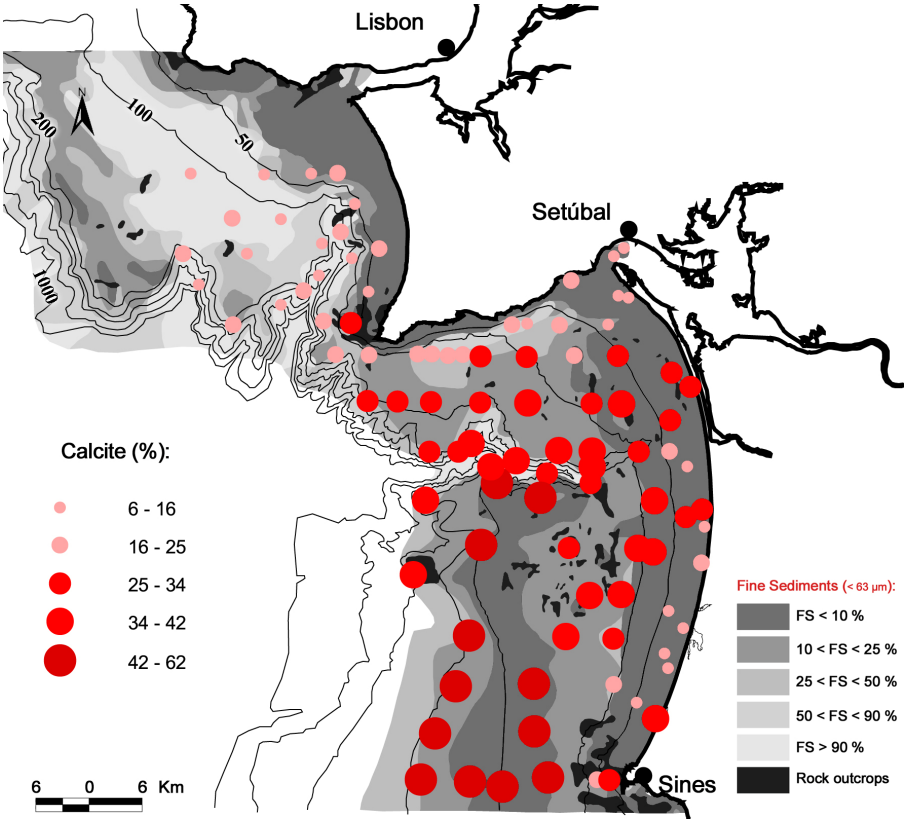

Figure 4.7. Content of calcite in the fine fraction of surface sediments from the Lisbon-Setúbal-Sines shelf and upper slope.

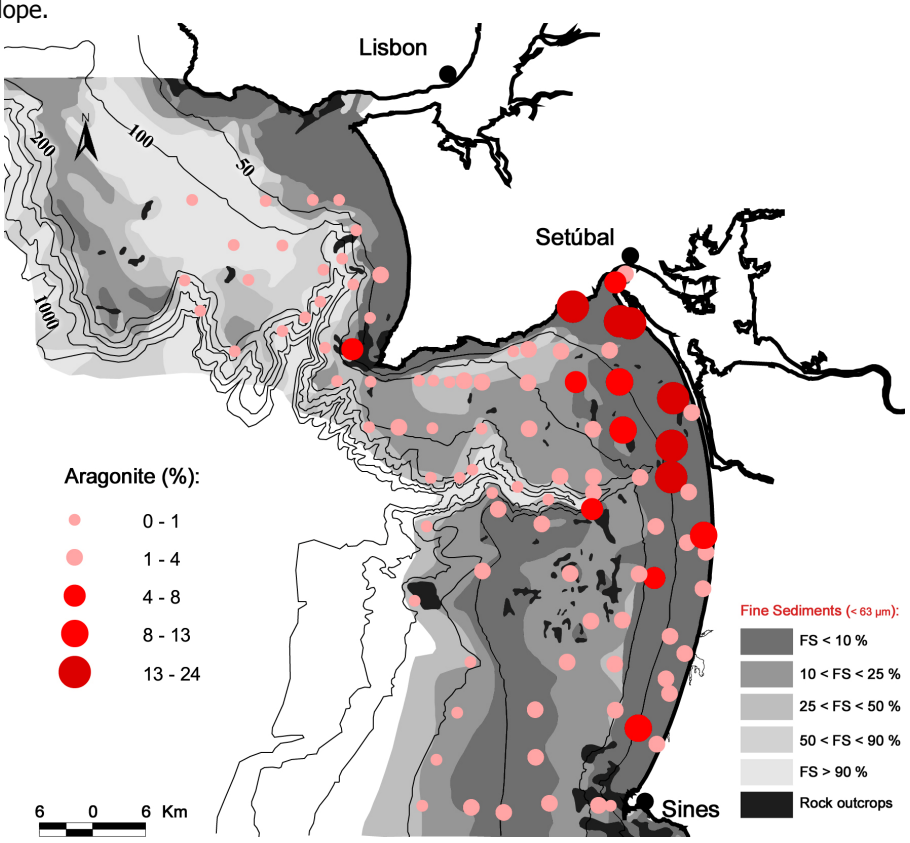

Figure 4.8. Content of aragonite in the fine fraction of surface sediments from the Lisbon-Setúbal-Sines shelf and upper slope.

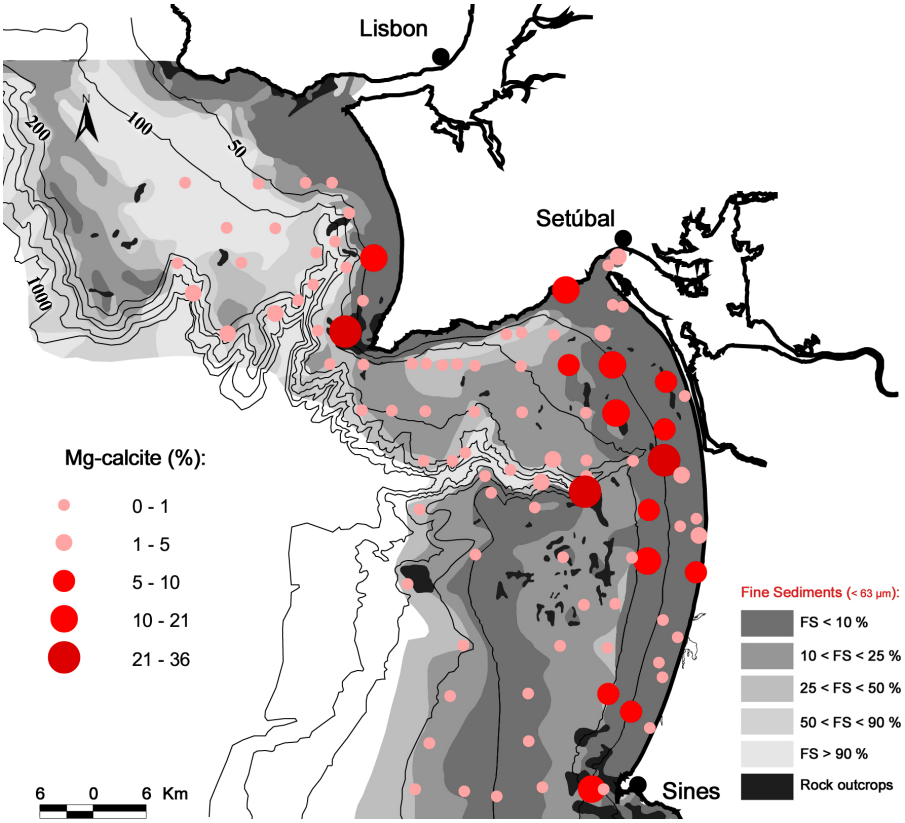

Figure 4.9. Content of Mg-calcite in the fine fraction of surface sediments from the Lisbon-Setúbal-Sines shelf and upper slope.

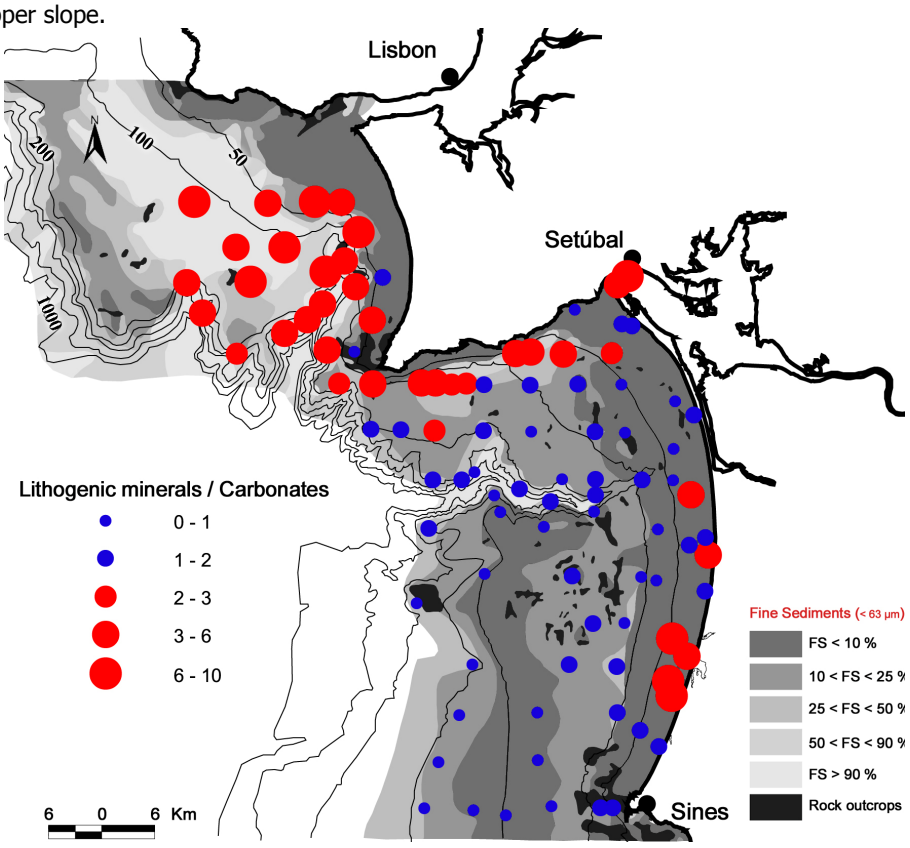

Figure 4.10. Ratio of lithogenic minerals against carbonates (L/C) in the fine fraction of surface sediments from the Lisbon-Setúbal-Sines shelf and upper slope.

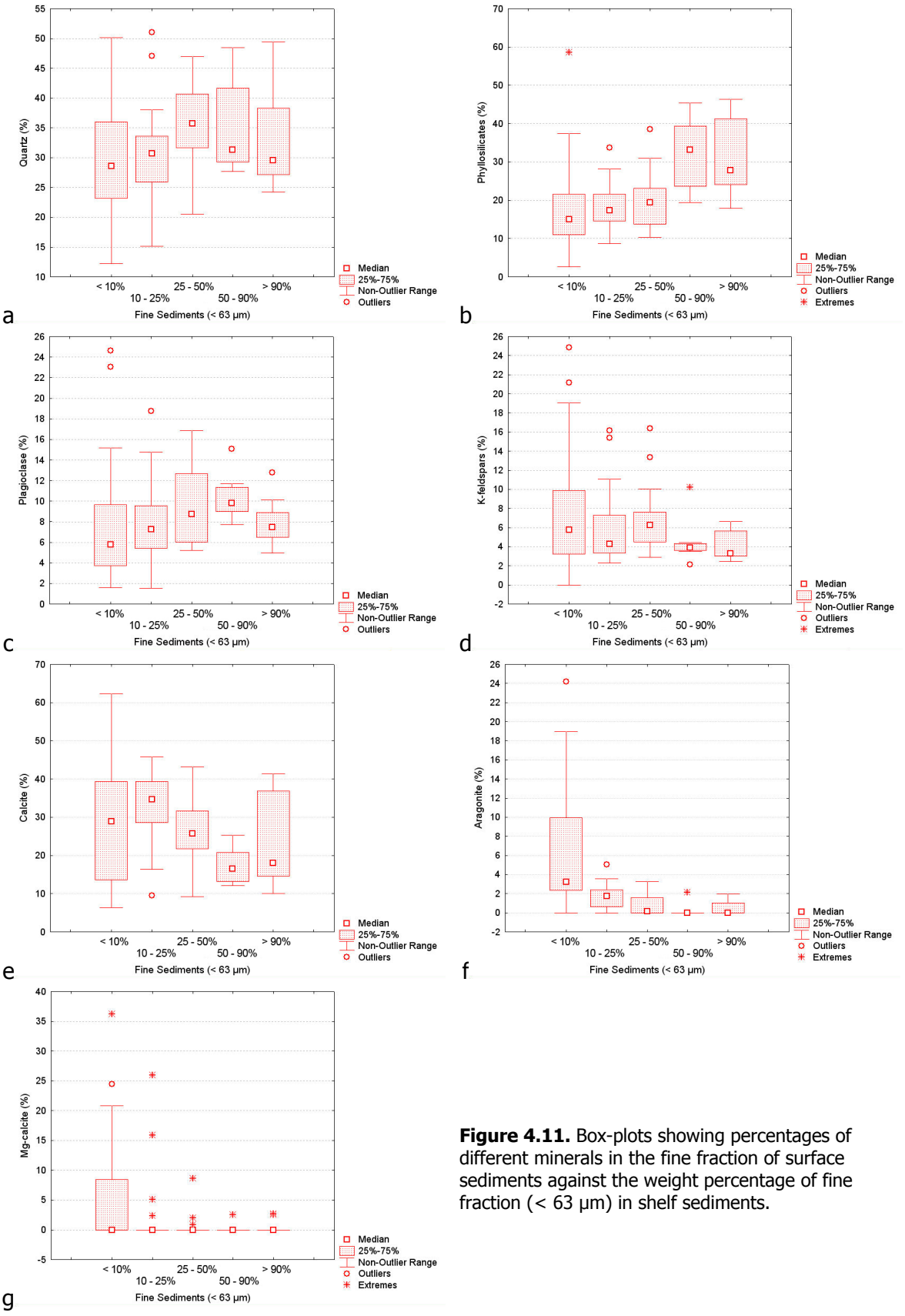

Figure 4.11. Box-plots showing percentages of different minerals in the fine fraction of surface sediments against the weight percentage of fine fraction (< 63 µm) in shelf sediments.

4.5. Clay-fraction mineralogy

Clay minerals are of special importance, not only because they constitute the largest portion of fine-grained and non-biogenous sediment, but also because they have the special geochemical property of absorbing and easily giving off ions, a property which will be further discussed in Chapter 5. Clay minerals are mostly formed by the weathering of primary, rock forming aluminous silicates, like feldspar, hornblende and pyroxene, or volcanic glass. Kaolinite, chlorite, illite, and smectite, representing the four most important groups of clay minerals, are typically formed under very different conditions of weathering. Consequently, the analysis of their qualitative and quantitative distribution may allow to make inferences on origin and transport, weathering and hydrolysis, and therefore on climate conditions of the source region of the clay minerals (Biscaye, 1965; Chamley, 1989).

The mineralogy of the clay fraction of shelf sediments is qualitatively monotonous. Only four different groups of minerals were identified yet, their percentages can vary significantly (Table 4.3): illite (54 – 80 %), kaolinite (18 – 40 %), smectite (1 – 12 %) and chlorite (0 – 3 %).

Table 4.3. Basic statistics of the group of minerals identified in the clay fraction of 64 surface samples from the Lisbon-Setúbal-Sines shelf and upper slope.

Group of minerals	Median (%)	Range (%)	P25 – P75
Illite	67	54 – 80	64 – 71
Kaolinite	30	18 – 40	26 – 32
Smectite	2	1 – 12	2 – 3
Chlorite	1	0 – 3	0 – 1

4.5.1. Illite

Illite is the most abundant clay mineral in ocean sediments. As a typical terrigenous mineral, it occurs in distinctly higher concentration in sediments at mid-latitudes of the northern oceans, which are surrounded by great land masses.

Contents of illite in the study area show a southward increase and also some enrichment with increasing water depth. Both Tagus and Sado mud patches have contents between 61 and 69 % while values over 72 % occur almost exclusively on the Sines shelf (Figure 4.12). Excluding deposits with less than 10 % of fine sediments, it

seems that contents of illite are inversely related to the amount of fine fraction present in shelf deposits (Figure 4.13a). As such, the distribution of illite seems the opposite of that of kaolinite, which tends to have higher contents in fine-grained deposits fed by river input.

In the study area the Esquevin Index (EI) varies between 0.24 (Fe-rich illites) and 0.67 (Al-rich illites). In shallow sandy deposits EI values are higher while in the predominantly fine-grained deposits of the shelfbreak, the mud patches and the upper canyon reaches values tend to be lower, which means that Fe-rich illites predominate.

The Kubler Index (KI) shows higher values, representing lower crystallinity in deposits with higher contents of fine fraction. The highest KI values (lower crystallinity) occur on the Lisbon shelf where fine-grained sediments predominate (Figure 4.15).

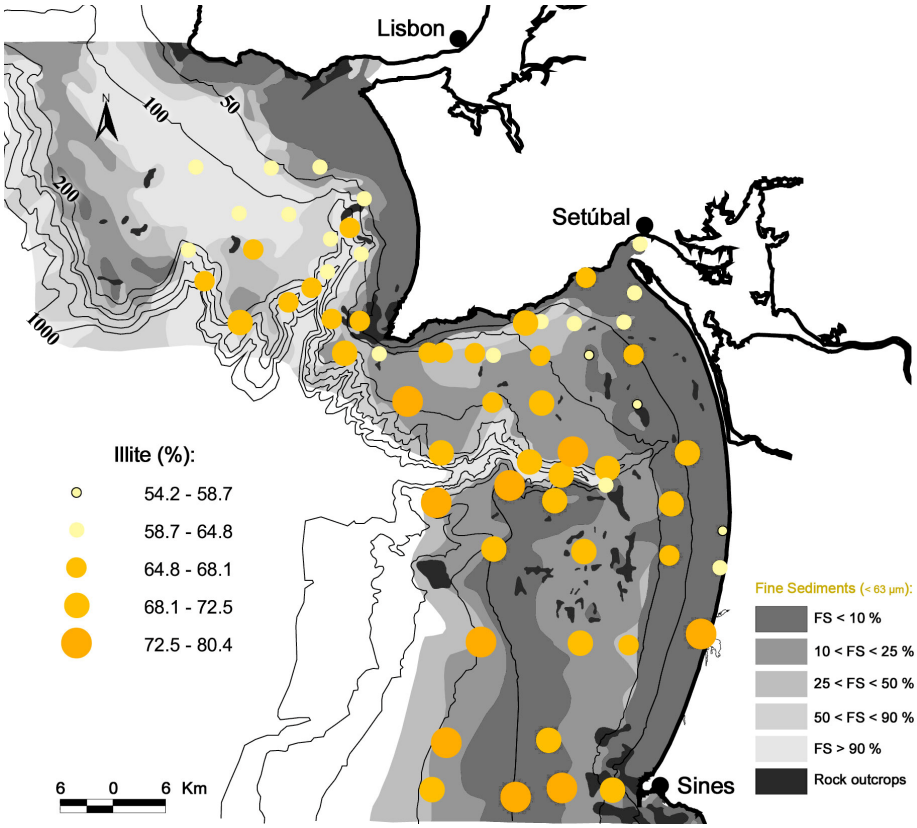

Figure 4.12. Content of illite in the clay fraction of surface sediments from the Lisbon-Setúbal-Sines shelf and upper slope.

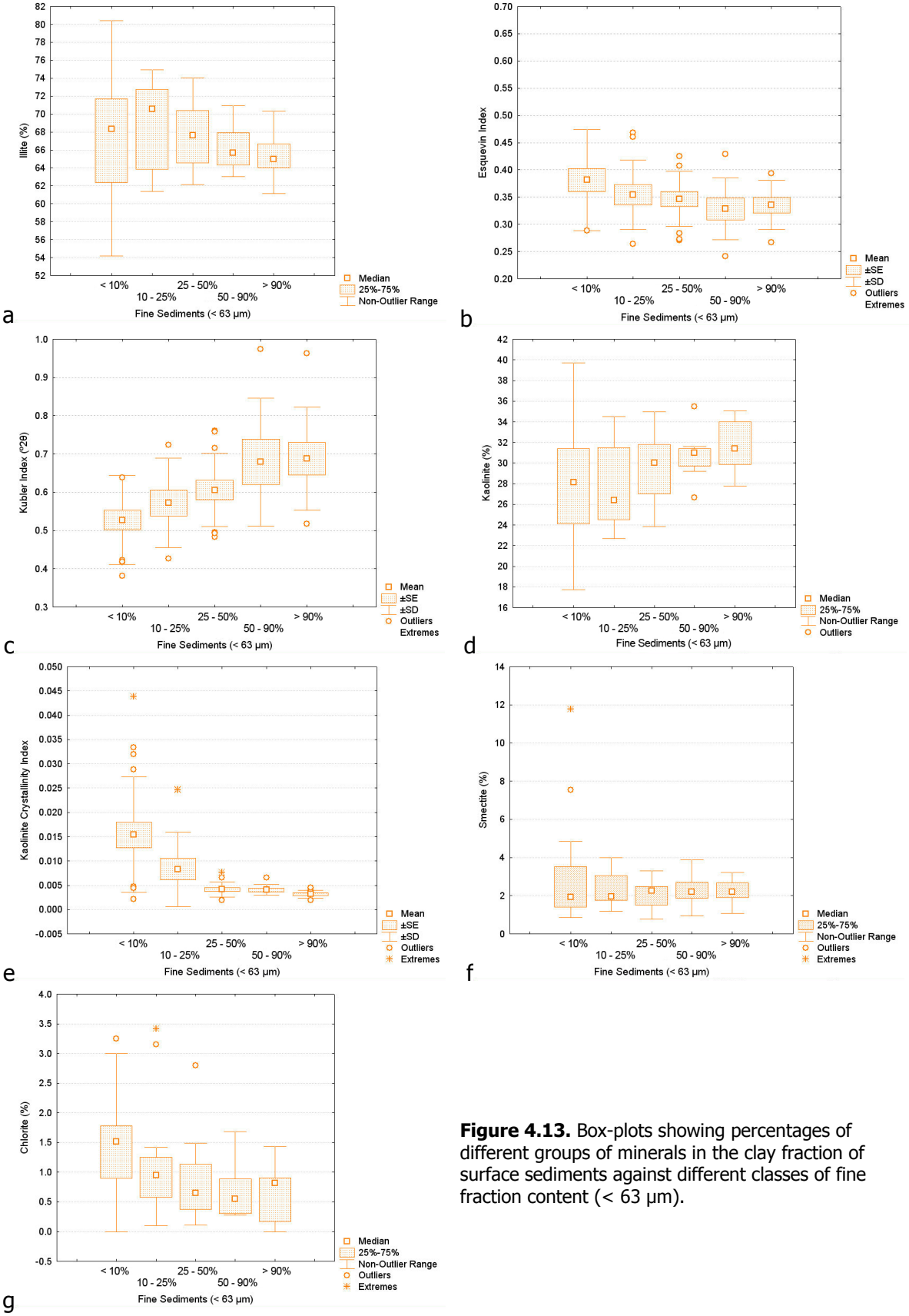

Figure 4.13. Box-plots showing percentages of different groups of minerals in the clay fraction of surface sediments against different classes of fine fraction content (< 63 µm).

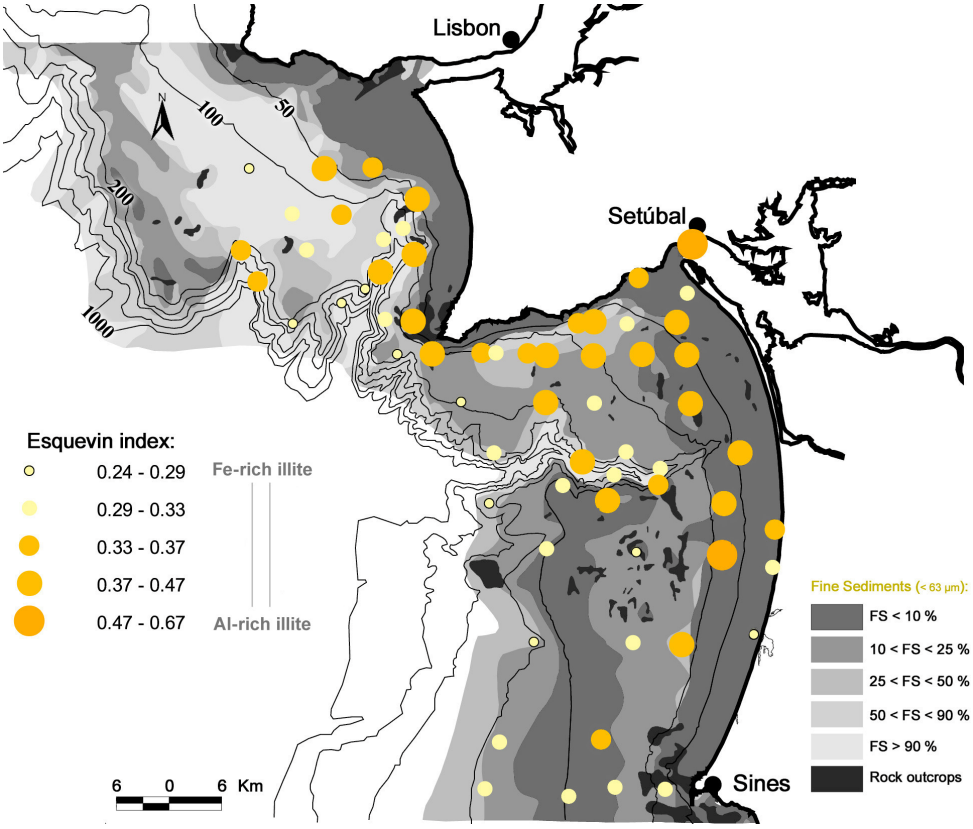

Figure 4.14. Esquevin Index for illites in surface sediments from the Lisbon-Setúbal-Sines shelf and upper slope.

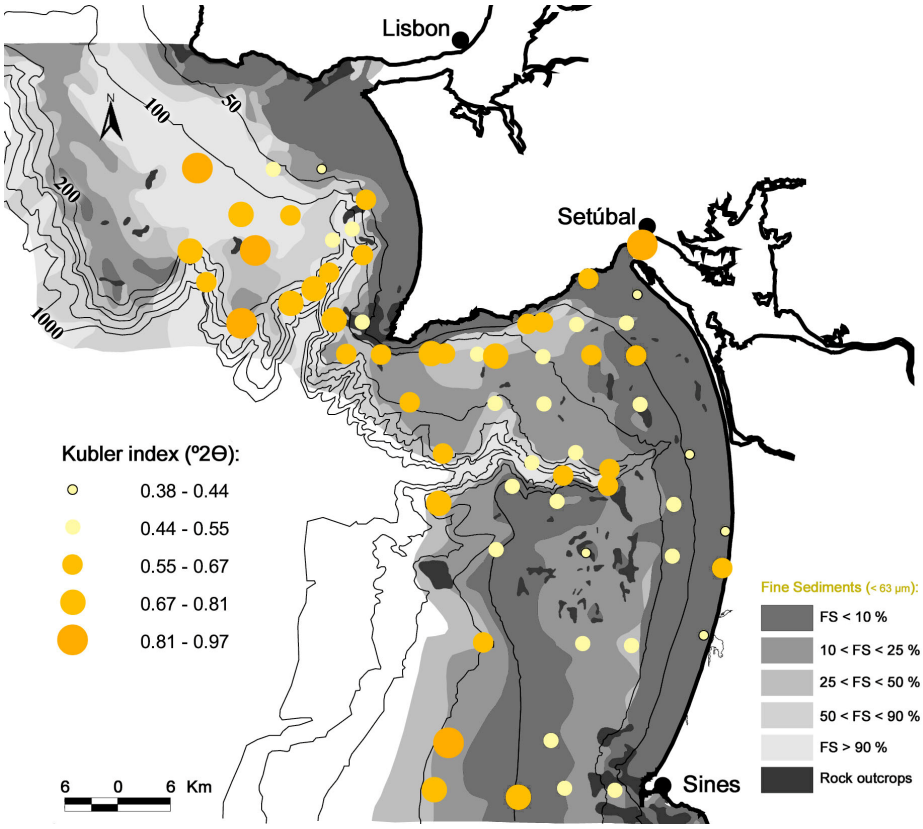

Figure 4.15. Kubler Index for illites in surface sediments from the Lisbon-Setúbal-Sines shelf and upper slope.

4.5.2. Kaolinite

The distribution of kaolinite in marine sediments depends on the intensity of chemical weathering in its source region and the essential patterns of eolian and fluvial transport. Due to its concentration at equatorial and tropical latitudes, kaolinite is usually referred to as the "clay mineral of low latitudes" (Griffin *et al.*, 1968).

As already mentioned above, the distribution of kaolinite shows opposite trends to that of illite, decreasing in southward direction. The highest concentrations are associated to the outlets of the Tagus and Sado estuaries. Conspicuously high contents, reaching 32 % are also found just offshore of the central part of the Tróia – Sines coastal arc (Figure 4.16).

For an easy description on the variation of the kaolinite crystallinity index (KCI) the author divided the index values in 5 classes according to Figure 4.17. This classification is based solely on the data from the present thesis. Kaolinite on the Lisbon shelf is mostly of relatively "crystalline" nature (low indexes). On the Setúbal and Sines shelf areas the crystallinity is more variable, with KCI values indicating the occurrence of both relatively "crystalline" and "very degraded" kaolinites. The latter are found mostly in shallower sandy deposits near the shore (Figure 4.13c).

4.5.3. Smectite

Smectite is generally considered as an indicator of a "volcanic regime" (Griffin *et al.* 1968). High smectite concentrations are usually observed in regions of volcanic activity, distant from major landmasses so that dilution with terrigenous sediment including other clay mineral is low. The low smectite concentration in the North Atlantic is due to terrigenous detritus inputs which are rich in illites and chlorites (Fütterer, 2006).

In the study area smectite concentrations are higher on the Lisbon shelf and in the northern part of the Setúbal shelf (Figure 4.18). The highest values (8 – 12 %), however, are found just offshore the central part of the coastal arc between Tróia and Sines.

4.5.4.Chlorite

Worldwide the distribution of chlorite in deep-sea sediments is essentially inversely related to the pattern of kaolinite. Although chlorite is distributed relatively

homogeneously over the oceans, its highest concentration is measured in the polar regions, and therefore chlorite is referred to as the "high latitude mineral" (Griffin *et al.* 1968).

In the study area the spatial distribution of chlorite is a bit scattered with no clear trend (Figure 4.19). This may be related to its low abundance (0 – 3 %), on which the error associated to the XRD measurements (~1 %) has a relatively large effect. Nonetheless, median contents of chlorite tend to decrease with increasing contents of fine fraction in shelf deposits (Figure 4.13g).

4.5.5. Comparison to the adjacent open slope and canyon environments

Kaolinite is a good tracer for the dispersal of fine-grained sediment from the shelf to the open slope and canyon environments, since its distribution clearly reflects lithogenic sediment input from land, and it is degraded with time in the marine environment. On the Sines outer shelf/upper slope, percentages of kaolinite vary between 18 and 29 % (Figure 4.16), comparable to contents found on the Sines open slope (490 - 3900 m WD) which vary between 21 and 27 %. In the middle and lower reaches of Setúbal Canyon (> 2000 m WD), surface sediments have kaolinite contents that span a narrower range of values (26 - 27 %). Although contents of kaolinite show little variation throughout the Sines margin the kaolinite crystallinity index (KCI) varies considerably. On the outer shelf/upper slope the KCI goes from 0.0039 to 0.0160 (from relatively crystalline to more degraded kaolinites, respectively) with some tendency to decrease with increasing water depth. On the adjacent open slope the crystallinity index reflects a similar variation between crystalline to degraded kaolinites (KCI 0.0038 – 0.0180). Finally, kaolinite in surface sediments from the lower Setúbal Canyon has relatively high crystallinity (KCI 0.0025-0.0045).

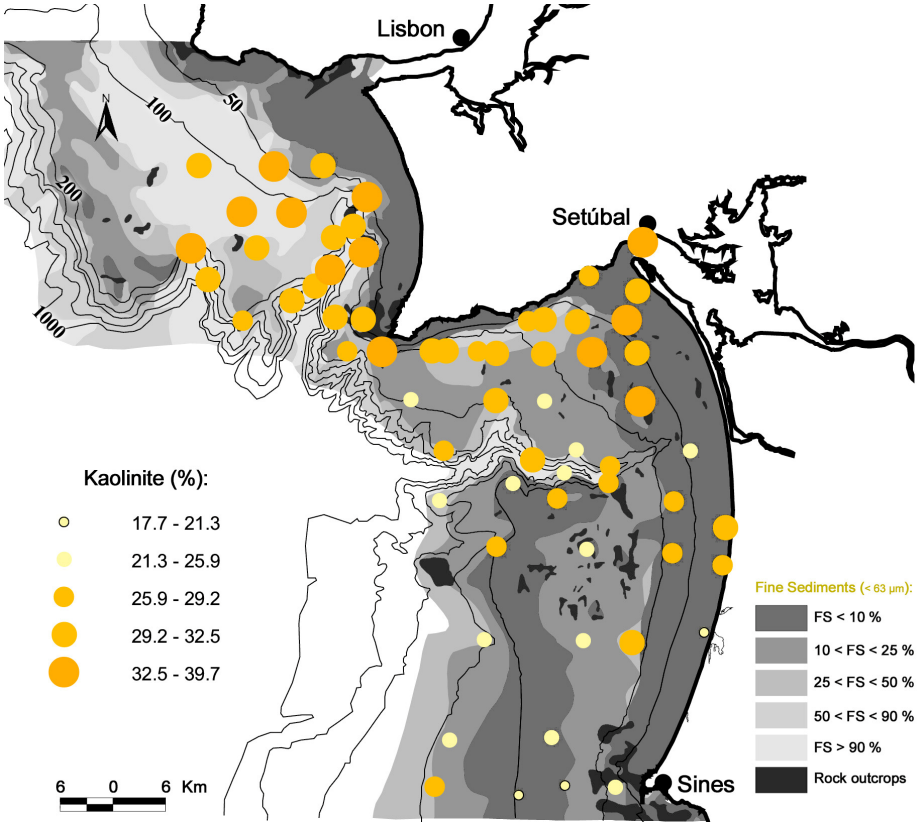

Figure 4.16. Content of kaolinite in the clay fraction of surface sediments from the Lisbon-Setúbal-Sines shelf and upper slope.

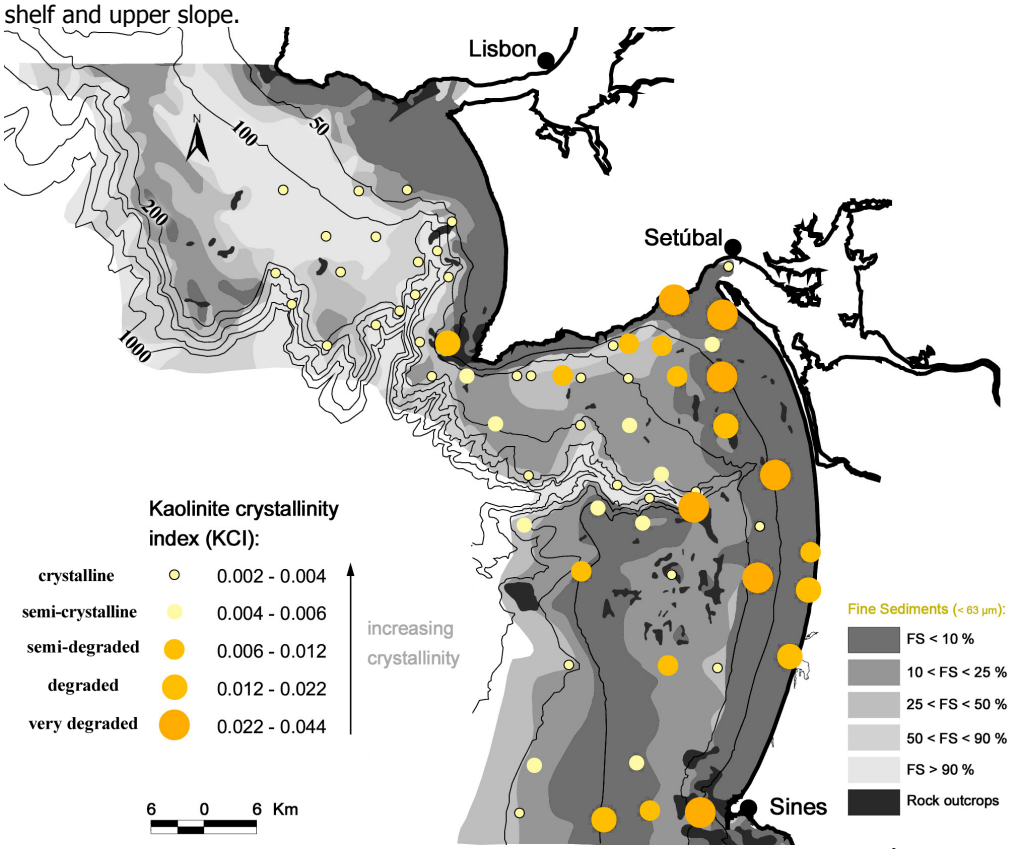

Figure 4.17. Kaolinite crystallinity index of surface sediments from the Lisbon-Setúbal-Sines shelf and upper slope.

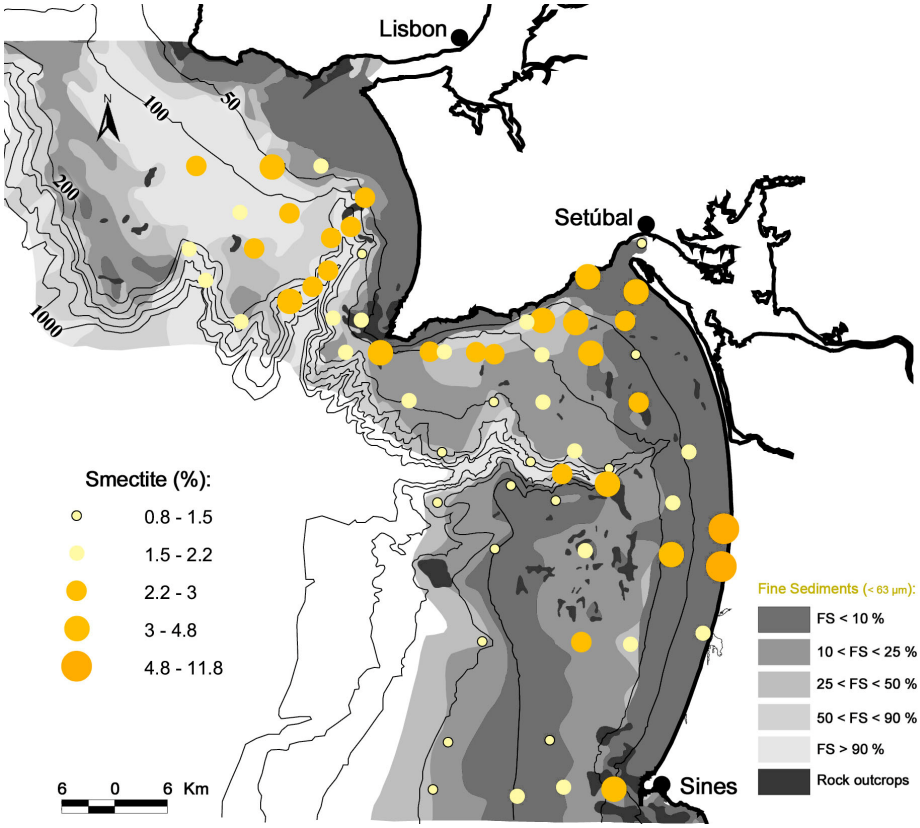

Figure 4.18. Content of smectite in the clay fraction of surface sediments from the Lisbon, Setúbal and Sines shelves.

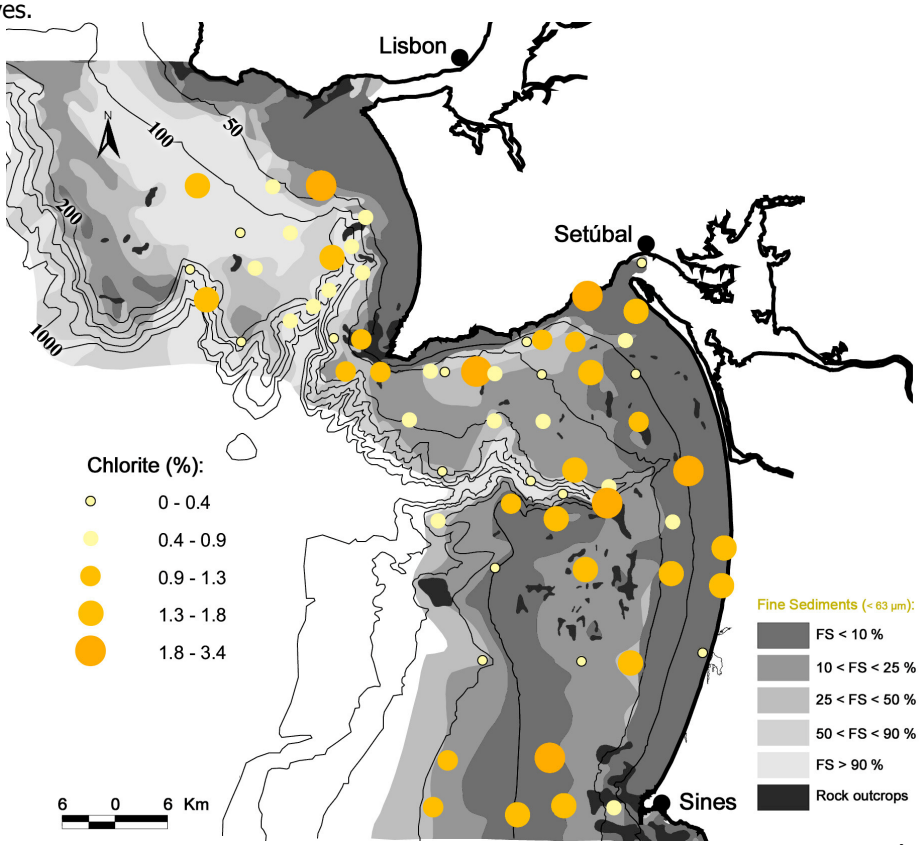

Figure 4.19. Content of chlorite in the clay fraction of surface sediments from the Lisbon, Setúbal and Sines shelves.

4.6. Discussion

4.6.1. The clay mineralogy context of the Lisbon and Setúbal shelves

Exhaustive data on clay mineral distribution in the world ocean sediments were successively provided by Biscaye (1965), Griffin *et al.* (1968) and Rateev *et al.* (1969). These data, augmented with subsequent information published by different authors, were reviewed and discussed by Windom (1976), who proposed average percentage values for the four major groups of clay minerals identified in surface deposits of the world main ocean basins (Chamley, 1989). Such average values have so far not been published for the bulk mineralogy of the fine fraction (< 63 μm).

The relative proportions of the various clay minerals in marine sediments is a function of their original source, the climate conditions of the source region, their mode of transport to the area of deposition – aeolian or volcanic transport, or transport by means of water currents or ice – and finally the route of transportation (Petschick *et al.*, 1996). On a global scale, the particular influence which, climate, weathering on the continents, wind patterns, riverine transport, and oceanic currents have on the distribution of different clay minerals (kaolinite, illite, smectite, and chlorite) is relatively well-defined.

The assemblage of clay minerals and their proportions in the study area (Table 4.3) are in accordance with what Windom (1976) described as typical for the principal clay mineral groups in the < 2 μm fraction of seabed sediments for the North Atlantic: illite > 50 %, kaolinite 10 - 20 %, smectite < 20 % and chlorite < 10 %. This assemblage of minerals reflects limited influence of hydrolytic processes, which are more important in low-latitude humid climate areas, and the predominance of direct physical rock erosion under colder climatic conditions.

On a regional scale, clay mineralogical variability is less obvious given the relatively small geographic area it comprises. When comparing between muddy deposits from different parts of the western Iberian margin, some differences in clay mineral assemblages are still observed. The clay mineralogy of the Tagus and Sado mud patches (Figure 4.20) is different from that of the northern mud patches located on the shelf off Porto and Galicia (Figure 4.20). The Douro mud patch is located to the northwest of the mouth of the Douro River in water depths of 65–130 m. It is about 8–18 km wide and 42 km long, and its western boundary is delimited by rocky outcrops. The Galicia mud patch is situated further north off the Minho River at a water depth of 110–120 m. It is a

narrow north-south oriented strip of 50 km long and 2–3 km wide (Dias *et al.*, 2002a). The Douro mud patch consists mostly of silty material, whereas the Galicia mud patch is constituted of finer grained silty-clayey material at its centre (Dias *et al.*, 2002b and Oliveira *et al.*, 2002).

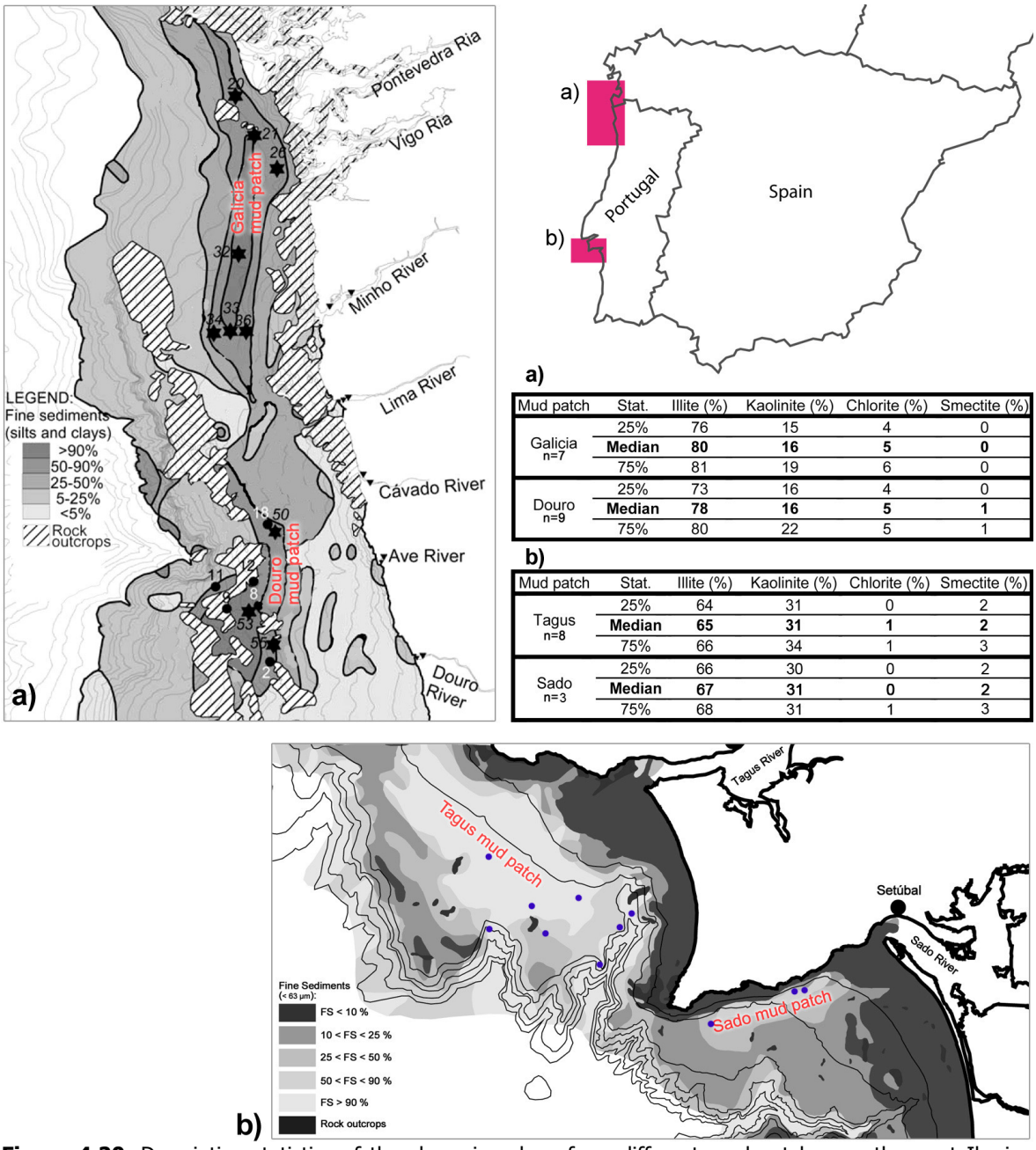

a)

Mud patch	Stat.	Illite (%)	Kaolinite (%)	Chlorite (%)	Smectite (%)
Galicia n=7	25%	76	15	4	0
	Median	**80**	**16**	**5**	**0**
	75%	81	19	6	0
Douro n=9	25%	73	16	4	0
	Median	**78**	**16**	**5**	**1**
	75%	80	22	5	1

b)

Mud patch	Stat.	Illite (%)	Kaolinite (%)	Chlorite (%)	Smectite (%)
Tagus n=8	25%	64	31	0	2
	Median	**65**	**31**	**1**	**2**
	75%	66	34	1	3
Sado n=3	25%	66	30	0	2
	Median	**67**	**31**	**0**	**2**
	75%	68	31	1	3

Figure 4.20. Descriptive statistics of the clay mineralogy from different mud patches on the west Iberian shelf: a) Galicia, Douro (Oliveira *et al.*, 2002); b) Tagus and Sado mud patches. The location of samples studied from these mud patches is shown.

In these northern deposits the contents of kaolinite and smectite are lower than those found in the Tagus and Sado mud patches (Figure 4.20), whereas contents of illite

and chlorite are higher than in the southern mud patches. A relative increase of illite and chlorite toward more northerly latitude is what would generally be expected according to Windom (1976), yet in this case the geology of the river basins draining to those areas is the more likely reason for the differences between northern and southern mud patches. Low-grade metamorphic rocks (e.g. micaschists) and chloritic shales, and granite, potential sources of chlorite and illites, respectively, dominate the watersheds of the Douro, Minho and Vigo rivers (Ribeiro *et al.*, 1979), whereas these lithologies are uncommon in both the Tagus and Sado basins (see Chapter 2). On the other hand, the geology of the Tagus and Sado basins is characterised by abundant outcrops of Tertiary sedimentary rocks enriched in kaolinite and smectite (Pimentel, 1997). Although both kaolinite and smectite are commonly available in the watersheds of the Tagus and Sado rivers, the increase of kaolinite in deposits of the central Portuguese shelf is more evident than that of smectite, probably because the latter remains longer in suspension whereas kaolinite settles more rapidly. This difference is due to the small size (< 1 μm) of smectite crystallites and to their ability to agglomerate into low-density aggregates (Meunier, 2005).

4.6.2. Bulk mineralogy of the fine fraction of surface sediments of the central Portuguese shelf

In order to study the mineralogical characteristics of the Lisbon-Setúbal-Sines shelf in a broader, regional context, data on fine-fraction mineralogy obtained in the present study were compared with data from the shelf adjacent to the Nazaré Canyon published by Oliveira *et al.* (2007), and data from the Aveiro shelf published by Abrantes (2005). The methodology used in the laboratory to analyse the samples was the same in all three studies. However, different from the present study, the other two studies considered also the accessories minerals (i.e. minerals occurring with a mean concentration < 1 % such as siderite, opal, haematite, pyrite). To make the data sets comparable, the percentage of each mineral from the other areas was recalculated after removing the accessories minerals.

The bulk mineralogy of the fine fraction of surface sediments as described by the above authors is qualitatively similar to that found in the Lisbon, Setúbal and Sines shelves. All the main minerals found in the southern area are also present on the shelf

adjacent to the Nazaré Canyon and on the Aveiro shelf (Table 4.4). However, dolomite was only identified on the shelf immediately north of the Nazaré Canyon and on the Aveiro shelf. This mineral, which occurs in high concentration (> 8 %) in both areas at depths greater than 100 m, is considered to be derived from dolomitic rocks outcropping in both areas (Abrantes, 2005 and Oliveira *et al.*, 2007). On the other hand, Mg-calcite was only identified in the Lisbon, Setúbal and Sines area on the inner and middle shelf. The remaining minerals are the same in both areas: phyllosilicates, quartz, calcite, K-feldspars, plagioclase and aragonite. Concentrations of feldspars (plagioclase and K-feldspars) are higher in the shelf areas adjacent to the Nazaré Canyon (median of 10 % for each of both groups of minerals) than on the Lisbon-Setúbal-Sines shelf (mean of 8 and 5 %, respectively) and the Aveiro shelf (7 and 6 %, respectively). Conversely, phyllosilicates have higher median concentrations in the southern area. Mean concentrations of quartz are similar for the Lisbon-Setúbal-Sines shelf and the shelf adjacent to the Nazaré Canyon (Table 4.4) while values are lower on the Aveiro shelf. This is probably a result of dilution by calcite which is extremely high (> 80 %) in some parts of the Aveiro shelf where rock outcrops predominate.

Table 4.4. Median (and range) concentrations (in %) of different minerals identified in the fine fraction of surface sediments from different areas of the central Portuguese shelf.

Minerals / Group of minerals	Lisbon-Set.-Sines (n = 98)	Shelf adj. to the Nazaré Canyon (n = 75)*	Aveiro (n = 181)**
Quartz	31 (12 - 51)	29 (11 – 73)	23 (2 – 49)
Calcite	29 (6 - 62)	19 (3 – 62)	42 (1 – 96)
Phyllosilicates	19 (3 – 59)	9 (0 – 35)	12 (0 – 50)
Plagioclase	8 (2 - 25)	10 (2 – 19)	7 (0 – 22)
K-feldspars	5 (0 - 25)	10 (1 – 27)	6 (0 – 37)
Aragonite	2 (0 - 24)	0 (0 – 2)	0 (0 – 9)
Mg-calcite	0 (0 – 36)	Not identified	Not identified
Dolomite	Not identified	4 (1 – 22)	2 (0 – 34)
Water depth of samples (m)	113 (1 – 572)	135 (33 - 296)	92 (11 - 497)

* Data adapted from Oliveira *et al.* (2007); ** Data adapted from Abrantes (2005).

The Lithogenic minerals/Carbonates ratio (Qz+Phy+Felds/Cc+Mg-Cc+Dol+Arg) reach values of 52 on the Aveiro shelf, 25 on the shelf adjacent to the Nazaré Canyon and only 12 in the studied area of the Lisbon-Setúbal-Sines shelf. It should be noted, however, that

in the latter area the shallowest sediment samples are more than 10 km away from the Tagus outlet. In the northern shelf areas these high ratios (> 6) are achieved in the inner shelf (less than 5 km from the coast) and rapidly decrease to constantly lower values (< 6) in the middle and outer shelf while in the Lisbon shelf values around 12 are still found close to the shelfbreak (~30 km from the Tagus Estuary). This dispersal of the L/C ratio suggests a more efficient transport of terrigenous sediments from the mainland to the shelfbreak in the Lisbon shelf compared to the other northern shelf areas.

The highest L/C values on the Aveiro shelf are found north from the Ria de Aveiro coastal lagoon (Figure 4.21), where they seem to be related to areas of important coastal erosion. In this area the highest rates of coastal retreat of the Portuguese coast are measured, with values between 3 and 9 m $year^{-1}$ (Andrade *et al.*, 2006); for the period between 1947 e 1958 Oliveira *et al.* (1982) determined a rate of retreat of 8 m $year^{-1}$.

Contents of phyllosilicates are higher on the Lisbon-Setúbal-Sines shelf than on the shelf adjacent to Nazaré Canyon and the Aveiro shelf (Table 4.4), as illustrated by the Phy/Qz+Felds ratio (Figure 4.22). This is consistent with the observation that sedimentary deposits with fine fraction contents higher than 90 % are more widespread in the southern area (Figure 2.2). But even when sedimentary deposits with similar contents of fine sediments are compared those of the Lisbon-Setúbal-Sines shelf still have higher contents of phyllosilicates than the shelves further to the north. Deposits with fine fraction contents between 50 and 90 % have average contents of phyllosilicates of 12 % in the northern area, compared to 31 % in the southern area. This difference in phyllosilicates contents is most likely primarily related to the presence of rivers debouching on the southern shelf area, especially the Tagus River, delivering large volumes of fine-grained suspended sediment to the shelf. Differences in hydrodynamic regimes of northern and southern shelf areas may play an additional role. Whereas the Lisbon, Setúbal and part of the Sines shelves are sheltered by the Estremadura mainland from the prevailing swell coming from N and NW, favouring the settling of fine-grained material rich in phyllosilicates, the northern shelf is directly exposed to the highly energetic swell (Magalhães, 2001).

4.6.3. Sources of fine-grained sediment and its deposition on the Lisbon, Setúbal and Sines shelves

Significance of the fine fraction in Lisbon-Setúbal-Sines shelf deposits

The Lisbon-Setúbal-Sines shelf areas display a high variability of sedimentary deposits in terms of the dominant grain size. These sedimentary deposits show a general along-shelf gradient of decreasing fine fraction content from the Lisbon shelf to the Sines shelf, as well as an across-shelf gradient of decreasing grain size from the coast outward to deeper water.

The along-shelf gradient is directly related to the supply of fine-grained material to the Lisbon shelf by rivers, and the sheltered position of this area. Given the present high sea-level stand, sediment discharged from estuaries to the shelf mainly consists of fine-grained suspended material (e.g. Magalhães, 2001; Ferreira *et al.*, 2008). From north to south, the Tagus River debouches on the Lisbon shelf, the Sado River (a smaller river) debouches on the Setúbal shelf, whereas the Sines shelf has no connection to any important river.

The across-shelf gradient is easily explained by grain size sorting across the shelf as sediment is transported from the mainland to the deep sea and also by decreasing influence of wave energy on the seabed as water depth increases.

Within the fine fraction of shelf deposits, significant variability is observed in terms of mineralogy and grain size distribution (and geochemistry as will be discussed in the next chapter) which essentially follow the above-mentioned general patterns.

Mineralogical characteristics of the fine-grained sediment fraction reflect a general increase in sediment maturity from deposits with overall high content of fine sediment to deposits poor in fine-grained material:

- There is a progressive increase of the KI and decrease of the EI (Figures 4.13b, c) from sandy deposits (fine-grained sediments < 10 %) to mud deposits (fine-grained sediments > 90 %) which indicates that fresher illites occur in the latter deposits. This conclusion results from the fact that the more time the illites spend in the marine environment the higher order (lower KIs values) they achieve in their crystallographic structure by incorporating K^+ (Millot, 1964; Nemecz, 1981). This same observation was made by Oliveira *et al.* (2002) in the northern Portuguese shelf. Furthermore, illites enriched in Fe (EI < 0.3) are less

resistant in the marine environment than Al-enriched illites (EI > 0.4) and therefore are the first to suffer modifications. Thus, fresh clay contents have higher contents of Fe-enriched illites (assuming all original illites for a given area have similar contents of Fe);

- The kaolinite crystallinity index shows less degraded kaolinites in the muddy deposits (Figure 4.13e);
- Plagioclase contents also indicate less mature sediments in the muddy deposits however in this case the relationship is not so obvious in Figures 4.5 and 4.11c because, as it will be seen below, high contents of plagioclase are also present in some areas of the inner shelf (coarse sediment deposits) as a result of inputs from nearby sediment sources.

Grain size characteristics of the fine-grained sediment fraction also show differences according to the overall contents of fine sediments. Higher percentages of clay-sized material are found in deposits with overall low content of fine sediment, whereas low percentages of clay-size material occur in deposits rich in fine-grained material (Figures 4.1 and 4.2b).

Sand deposits have therefore more mature fine fractions and have higher contents of clay-size particles while muddy deposits have less mature fine sediments and lower contents of clay-size particles.

The most likely explanation for the relative increase in clay-sized particles within the fine fraction towards coarser deposits is that these particles cohesively attach to sand-sized particles, making their removal from waves and currents more difficult. Since nowadays the hydrodynamic conditions do not allow the deposition of clay-size particles where sand deposits occur, clay-size fraction material seem to be mainly relict particles, which were deposited during times when sea level was lower. On the other hand, sediments within the range of "sortable silt" (10-63 μm) were eluted from these sand deposits during the sea-level rise in the Holocene. Mud patches on the shelf and mud deposits found on the upper slope have a higher content of particles within the "sortable silt" range (Figure 4.23). Possibly, these particles include both recent material sourced by present-day estuaries as well as relict material removed from the shallower deposits and transported offshore during the course of the Holocene sea-level rise.

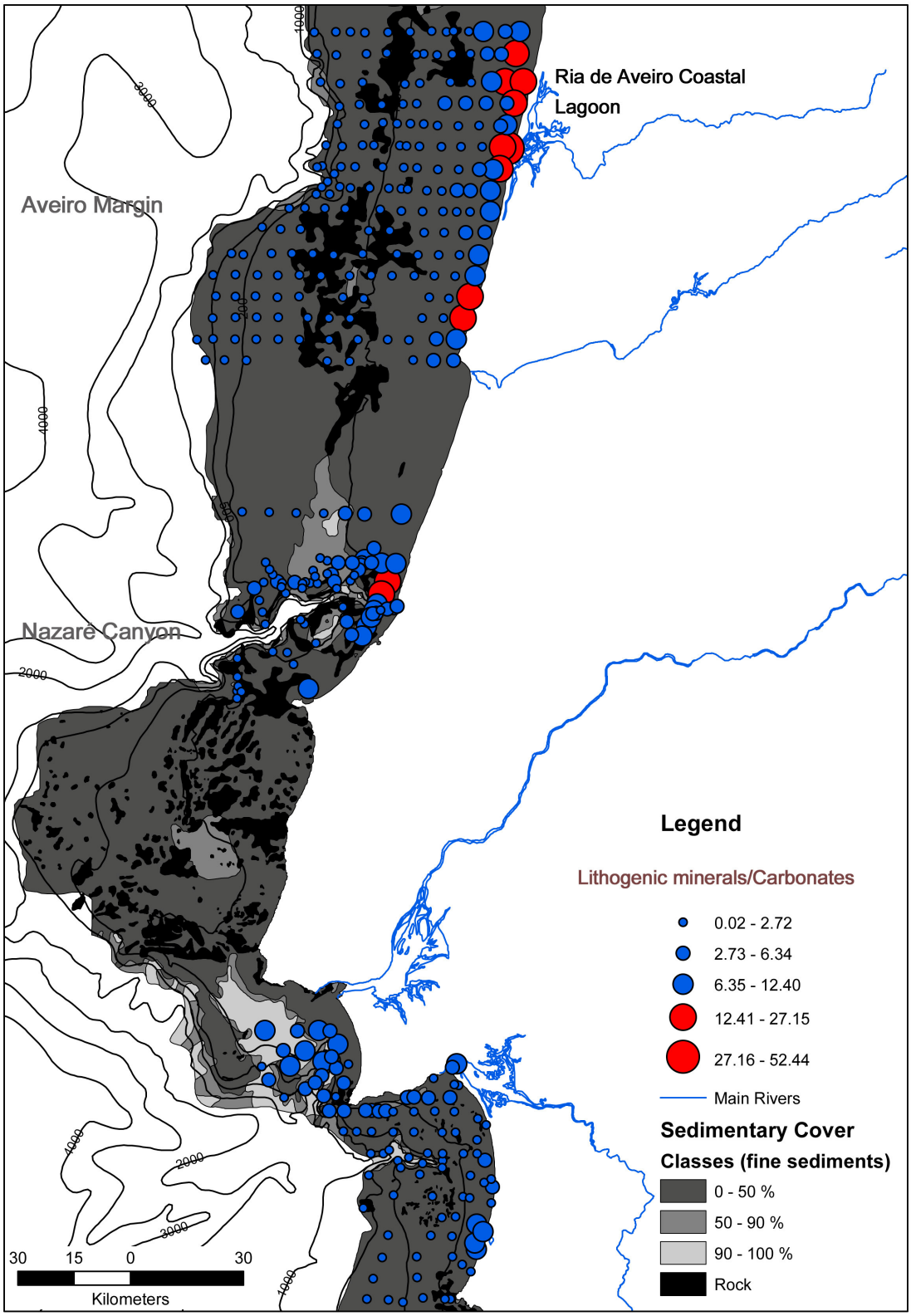

Figure 4.21. Lithogenic minerals/carbonates (L/C) ratio in the fine fraction of surface sediments from different areas of the central Portuguese shelf: the Aveiro shelf (from Abrantes, 2005), shelf adjacent to Nazaré Canyon (from Oliveira *et al.*, 2007) and the Lisbon-Setúbal-Sines shelves (this study).

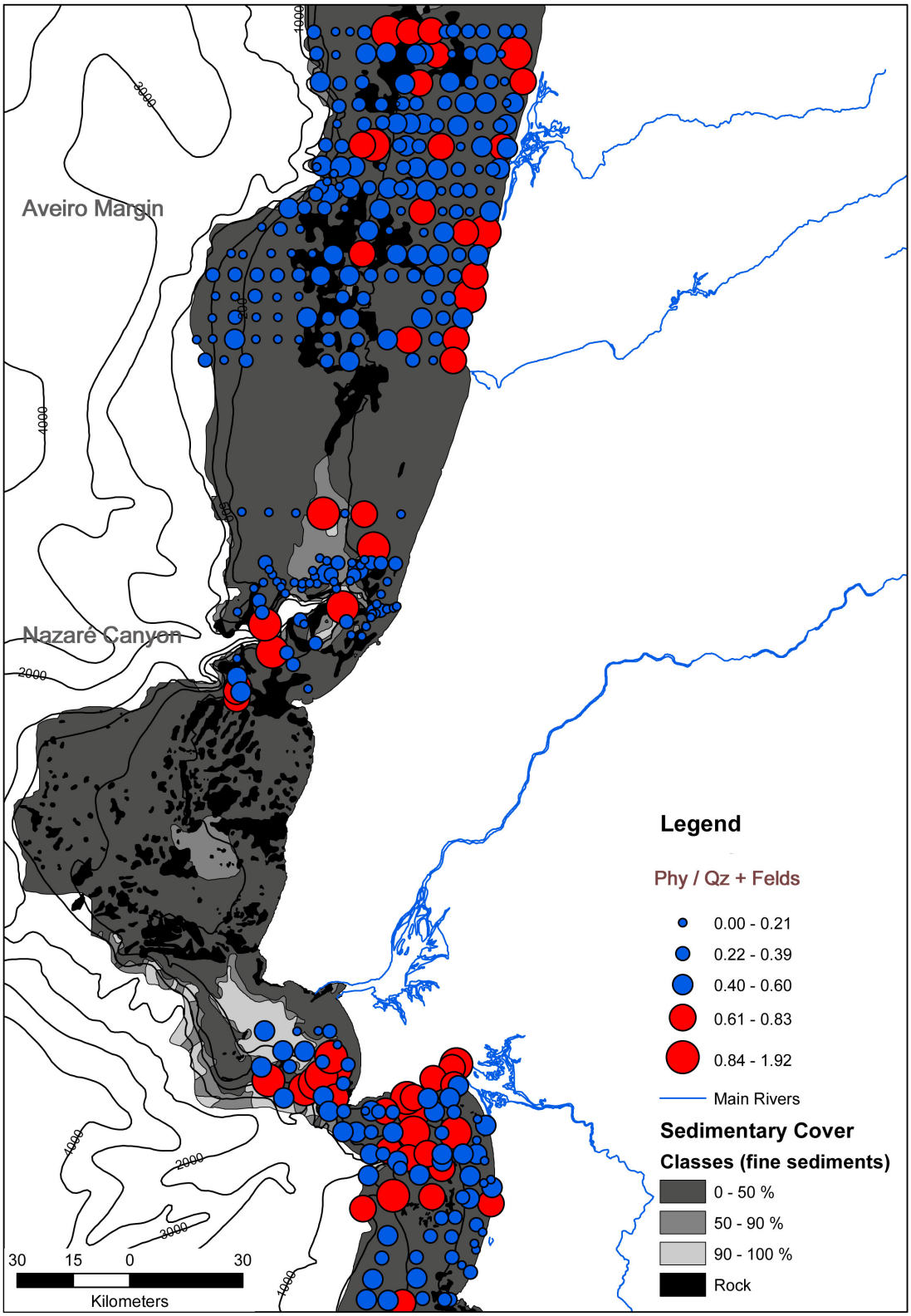

Figure 4.22. Ratio of phyllosilicates against quartz and feldspars in the fine fraction of surface sediments from different areas of the central Portuguese shelf: the Aveiro shelf (from Abrantes, 2005), the shelf adjacent to the Nazaré Canyon (from Oliveira *et al.*, 2007) and the Lisbon-Setúbal-Sines shelf (this study).

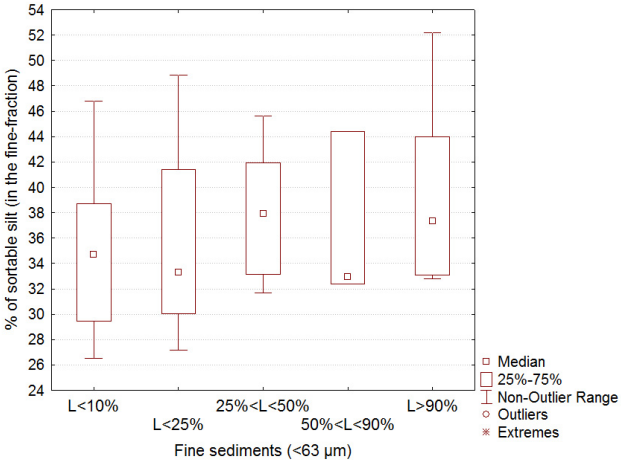

Figure 4.23. Percentage of "sortable silt" in the fine fraction against weight percentage of fine fraction in shelf sediments.

Identification of fine sediment sources based on mineral distribution

The mineralogy of the fine fraction reflects the variable input of two main marine sediment components: lithogenic material and biogenic carbonate. Generally, the importance of biogenic components only increase in areas where lithogenic input (from rivers, erosion of the coast, desert dust, etc) is not important. In accordance, the general southward increase of calcite on the Lisbon-Setúbal-Sines shelf indicates a decreasing input of lithogenic material from the area off Tagus Estuary towards Cape Sines (Figure 4.25). The following discussion referring to the identification of fine sediment sources based on mineral distribution will focus on each shelf area (Lisbon, Setúbal and Sines) at a time.

On the Lisbon shelf (and upper slope), considering sediments from deposits with contents of fine sediments > 50 %, plagioclase has a negative correlation with water depth (Figure 4.24a). This points to a progressive distance to the sediment source, in this case mainly the Tagus Estuary. Plagioclases are good indicators of "fresh" lithogenic sediment because, from the mineralogical assemblage found in the bulk mineralogy, they are the less resistant minerals to weathering processes (Meunier, 2005), especially in the marine conditions (Rothwell, 1989).

Despite the obvious contributions of kaolinite from the Tagus River to the shelf this mineral does not show a negative correlation with water depth as plagioclases (Figure

4.24b). It seems therefore that in the Lisbon shelf another sediment source is contributing as well with sediments enriched in kaolinite.

In the adjacent coastal area an important well known sediment source to the beach system are the sea-cliffs. The Mio-Pliocene deposits outcrop as sea-cliffs throughout the entire coastal arc between Traferia and Cape Espichel but only constitute part of the beach profile in the southern half of the coastal arc between Fonte da Telha Beach and Cape Espichel (Figure 2.12). Between Fonte da Telha Beach and the Albufeira Lagoon, cliffs are made of Plio-Pleistocene detritic deposits, have slopes higher than 45º and accumulate considerable amounts of sediments as dejection cones at the base of the cliff. In contrast, south of the Albufeira Lagoon, Miocene clayey deposits predominate and cliffs get slopes around 70º with much smaller cones of dejection (Teixeira, 1990). In accordance, this author reports that the Plio-Pleistocene cliffs contribute with more sediment to the beach system than the Miocene cliffs as they are less resistant to aerial erosion.

If one assumes the cliffs made up on Plio-Pleistocene deposits have a similar clay mineralogy signature to those cliffs with the same age found in the neighbour coastal arc between Tróia and Sines (Table 4.5) they may well be an additional source of kaolinites to the Lisbon shelf when storms remove sediments from the beach system. Since these same deposits are depleted of plagioclase they cannot represent a source of these minerals to the shelf.

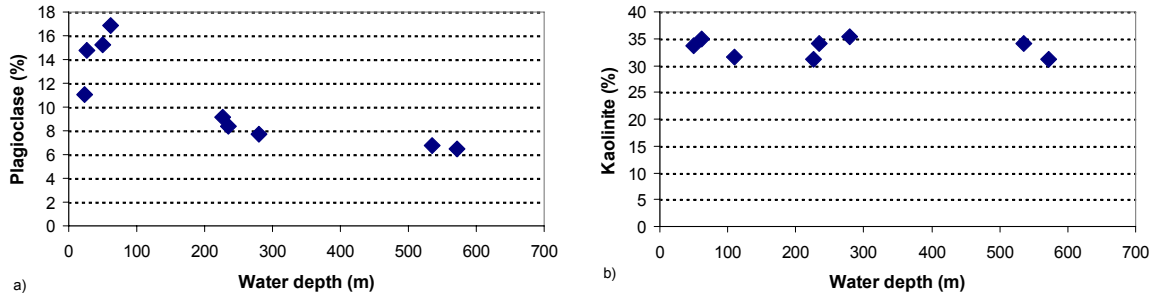

Figure 4.24. Contents of **a)** plagioclase and **b)** kaolinite in samples from the Lisbon shelf and upper slope with contents of fine sediments > 50 %, plotted against water depth.

The relatively high contents of plagioclase and kaolinite on the Lisbon shelf extend to the northwestern part of the Setúbal shelf (Figures 4.5 and 4.16) indicating that there might be some input of sediments from the Lisbon shelf to the northwestern Setúbal shelf. Relatively high contents of quartz on the Lisbon shelf also seem to extend to

northwestern Setúbal shelf (Figure 4.3). Jouanneau *et al.* (1998) also considered the possibility of exchange between the two shelf areas based on the distribution of As, Se, Ni, and Mo in shelf sediments. In their view the Sado shelf (here referred to as Setúbal shelf) forms a specific domain where contributions from the Tagus River can be noticed but are of relatively minor importance compared to contributions from the Sado River.

On the Setúbal shelf contents of carbonates are higher than on the Lisbon shelf, reflecting a decrease in lithogenic input. However, locally enhanced concentrations of plagioclase and kaolinite, highlight certain areas of the Setúbal shelf as terrigenous sediment depocentres, for example the Sado mud patch and the upper Setúbal Canyon. High contents of calcite, Mg-calcite and aragonite in the fine fraction of sandy deposits close to the inlet of the Sado Estuary (maximum values of 22, 13, and 24 %, respectively) indicate that terrigenous suspended sediment coming from the Sado Estuary is bypassing the sandy deposits of the inner shelf and only deposits on the Sado mud patch. Probably the upper Setúbal Canyon also receives some input from the Sado Estuary, although the estuarine signal is much weaker here than on the mid-shelf mud patch. This may either reflect an absolute decrease in particles reaching the upper canyon or a relative decrease due to dilution with particles coming from the shelf south of the canyon which have a different mineralogical signature (see Figures 4.5 and 4.7 for plagioclase and calcite, respectively). Most conceivably, mixing of material from the two sediment sources together creates a new mineralogical signature in the upper Setúbal Canyon. The sediment input to the Setúbal Canyon is further discussed in Chapter 6.

On the Sines shelf, in general, lithogenic sediment input appears low and therefore carbonates, especially calcite, reach their highest values. There are several areas though where lithogenic input can be traced, especially on the inner shelf (Figure 2.25):

1) The coastal area adjacent to the Sines shelf is characterised by beach-cliff profiles alternating with beach-dune profiles. The presence of Plio-Pleistocene sea-cliffs along the southern half of the coastal arc is the result of erosion of the coast which, according to Marques (1999), can reach coastal retreat rates around 0.5 m $year^{-1}$. From the morphology of the sea-cliff [cf. photos iii) and iv) of Figure 2.13] it appears that the erosion of these cliffs is mainly caused by run-off, producing dejection cones at the base of the cliffs. Characteristics of the fine-fraction and clay-fraction mineralogy of these sea-

cliffs are presented in Table 4.5. High contents of phyllosilicates and relatively high contents of K-feldspars are found in the fine fraction, and high contents of kaolinite in the clay fraction. The beach sediments between Tróia and Sines are characterised by high contents of kaolinite in the clay fraction, especially in the central portion of the coastal arc (Jesus *et al.*, 2006). According to Freitas *et al.* (1999) cliff debris contribute with up to 90 % of the sediments in the beach system. Sea-cliffs are therefore an important sediment source for the beach system in this area. The transfer of these sediments to the shelf occurs during winter storms, when waves wash sediments off the backshore area of the beach. Studies of sediment dynamics in the coastal zone show that storm waves cause offshore sediment transport while fair-weather waves and swell return the sediments shoreward (e.g. Komar, 1976; Wright & Short, 1984; Lee *et al.*, 1998; Van Rijn, 2009). Sand-sized particles are normally not transported deeper than the closure depth (the depth beyond which there is no significant seabed changes due to seasonality or to storms; it is around 6 and 15 m at Tróia and close to Sines, respectively – Quevauviller, 1988) while most of the fine-grained particles are washed from the sands and carried off to the inner shelf or even deeper. This is especially true for the southern half of the Tróia-Sines coastal arc where sea-cliffs are present and contribute with significant amount of fine material to the beach.

Table 4.5. Fine-fraction and clay-fraction mineralogy (in %) of sediments from Plio-Pleistocene sea-cliffs in the southern half of the coastal arc between Tróia and Sines.

Fraction	Group of minerals	Sea-cliffs in the central area of the coastal arc (north of the Melides Lagoon) n = 7	Sea-cliffs in the southern part of the coastal arc (Norte Beach) n = 3
Fine fraction*	Quartz	34 (22 – 44)	18 (17 – 19)
	Calcite	0	0
	Phyllosilicates	49 (33 – 60)	67 (66 – 68)
	Plagioclase	0	1 (0 – 1)
	K-feldspars	9 (4 – 12)	8 (7 – 8)
	Goethite	6 (5 – 8)	4 (4 - 4)
Clay fraction	Illite	25 (12 – 35)	14 (10 – 21)
	Kaolinite	71 (64 – 79)	82 (79 – 88)
	Smectite	1 (0 – 5)	1 (0 – 1)
	Chlorite	3 (0 - 9)	2 (0 - 7)

* as reported in Jesus *et al.* (2007)
For location of sample collection and procedures used consult Miranda (2007) or Jesus *et al.* (2007).

Contributions of sediments from the sea-cliffs to the shelf are best tracked by the K-feldspar contents (Figure 4.26). On the inner shelf concentrations of this mineral reaches values higher than those found in the cliff sediments. This apparent enrichment results from sorting by the high hydrodynamic energy conditions found on the inner shelf. The more easily resuspendable minerals like phyllosilicates are selectively removed to settle in calmer areas. In addition to enrichment by winnowing, other sources of K-feldspars may contribute to high contents in inner shelf surface sediments, as discussed below.

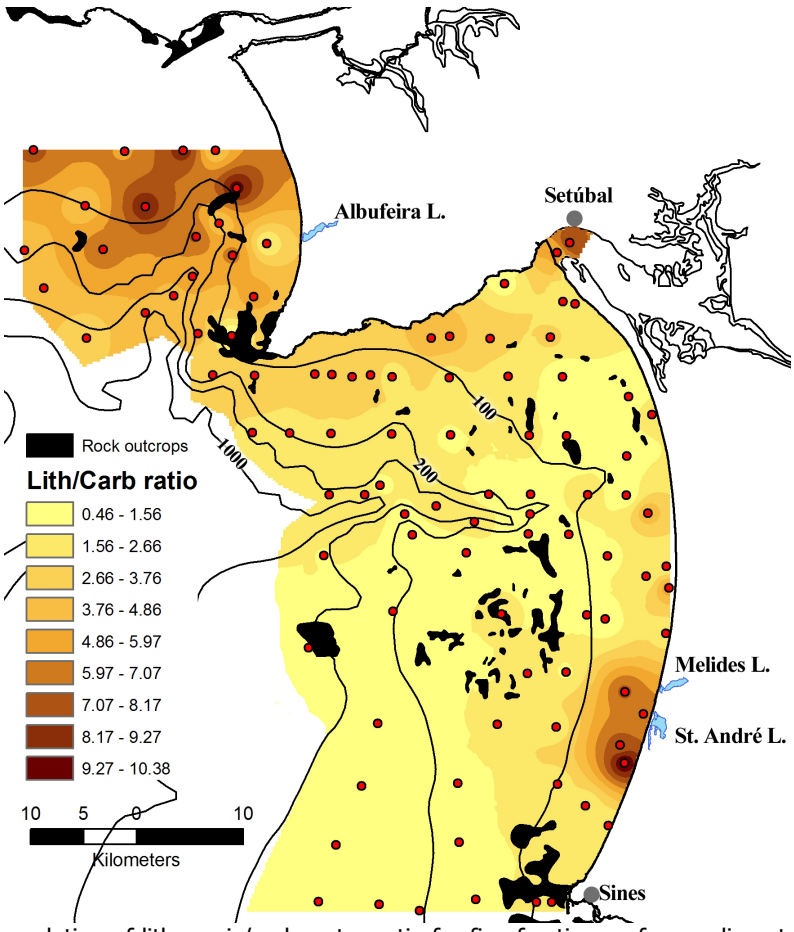

Figure 4.25. Interpolation of lithogenic/carbonates ratio for fine fraction surface sediments using an inverse distance weighted technique.

2) The Santo André and Melides lagoons may represent another source of lithogenic sediment input to the shelf, even though their connections to the sea are closed during most of the year. An artificial inlet is opened every year in order to exchange the water of the lagoons. The mineralogy and geochemistry of bottom sediments from the Santo André Lagoon was studied by Jesus *et al.* (2007). The fine fraction of surface sediments from this lagoon is characterised by high contents of phyllosilicates (39 – 62 %) and

quartz (21 – 34 %), while plagioclase contents vary from 2 to 11 %. Sediment input from these coastal lagoons may be tracked more clearly by plagioclase contents. Once again as a result of hydrodynamic sorting, contents of plagioclase in inner shelf sediments are higher than those from the source.

Jesus *et al.* (2007) found that the Santo André Lagoon has a specific geochemical signature (high contents of Mn and Pb) which can be tracked in the adjacent beach system. That study showed that even though the lagoon is opened to the sea only once per year it does leave a measurable signature in the sediments of the adjacent shelf. In the next chapter this topic will be discussed further.

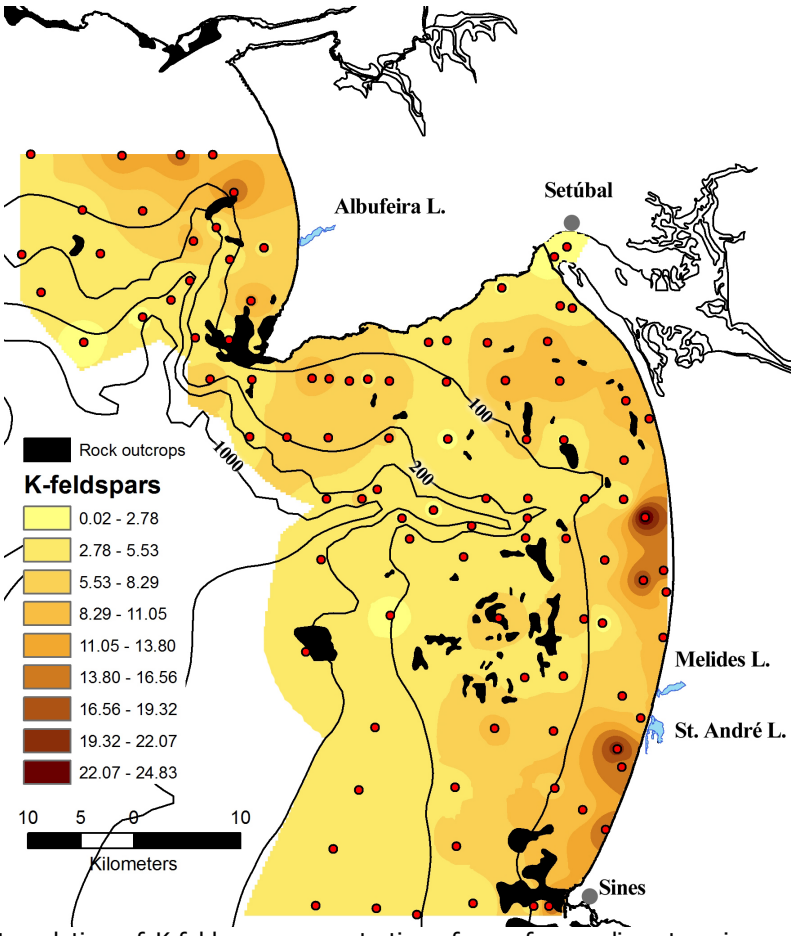

Figure 4.26. Interpolation of K-feldspars concentrations for surface sediments using an inverse distance weighted technique.

3) The Sines sub-volcanic complex represents a third distinct source of lithogenic sediments that can be tracked in the southern part of the coastal arc. Part of the complex constituting the protruding Cape Sines crops out below sea-level, on the shelf adjacent to the cape. Since this massif is made of exotic rocks in comparison to the surrounding

geology its imprint is relatively easy to track. In the fine fraction the most obvious mineral related to the Sines sub-volcanic complex is plagioclases. This mineral must be derived from the massif because the sea-cliffs contain only very low amounts of plagioclase (Table 4.5). Plagioclase is enriched in the inner shelf (Figure 4.27) and in beach sediments close to the cape (Jesus *et al.*, 2007). When studying the heavy mineral fraction of beach deposits between Tróia and Sines, Miranda *et al.* (2007) also found the signature of the Cape Sines subvolcanic complex in a marked increase in amphiboles and pyroxenes in the southernmost 10 km approaching the cape. Pombo *et al.* (2004) found a similar assemblage rich in amphiboles and pyroxenes in the inner shelf of the same area.

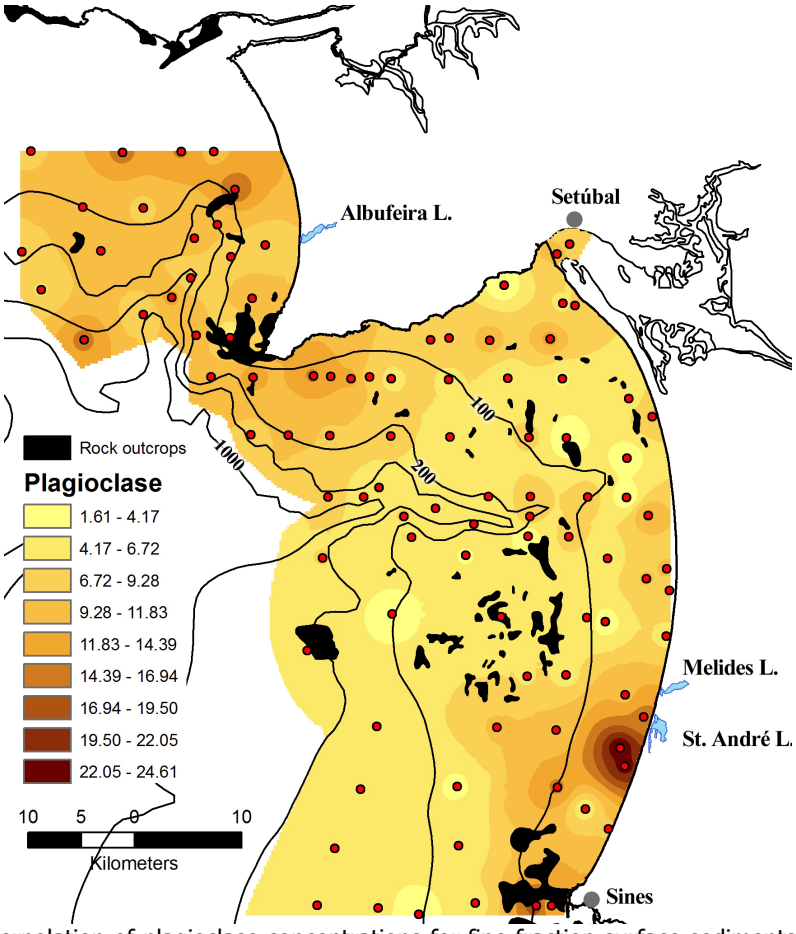

Figure 4.27. Interpolation of plagioclase concentrations for fine fraction surface sediments using an inverse distance weighted technique.

Whereas on the Sines inner shelf lithogenic input from the sea-cliffs, Sines subvolcanic massif and the coastal lagoon can be distinguished on the basis of characteristic mineral signatures, also confirmed by other studies using geochemical and

heavy mineral markers, these different sediment sources can not be distinguished further offshore on the middle shelf area below about 100 m WD (Figure 4.25).

The above inferences on dispersal of inner shelf sediments nourished by the sea-cliffs and coastal lagoons are in accordance with current models of sedimentary dynamics for this coastal area. According to the SNIRLit (2010) (and references therein) the net longshore drift of sediments in the coastal area between Tróia and Sines is directed towards the south in most of the coastal stretch. For instance, Silva *et al.* (2007) reported southward longshore drifts in the Comporta Beach (15 km south from Tróia) and Maretec (2008) confirmed the southward drift for the southern part of the coastal arc. This last study included ADCP current measurements recorded throughout a year (April 2007 – April 2008) covering the entire water column above the inner shelf (40-60 m WD). In this area mean currents are parallel to the coastline and directed preferentially towards the south with current speeds mainly between 10 and 30 cm s^{-1}, reaching 60 cm s^{-1} at the water surface at higher wind speed. Similar results were obtained with MOHID numerical model, considering the wind from different directions (Figure 4.28).

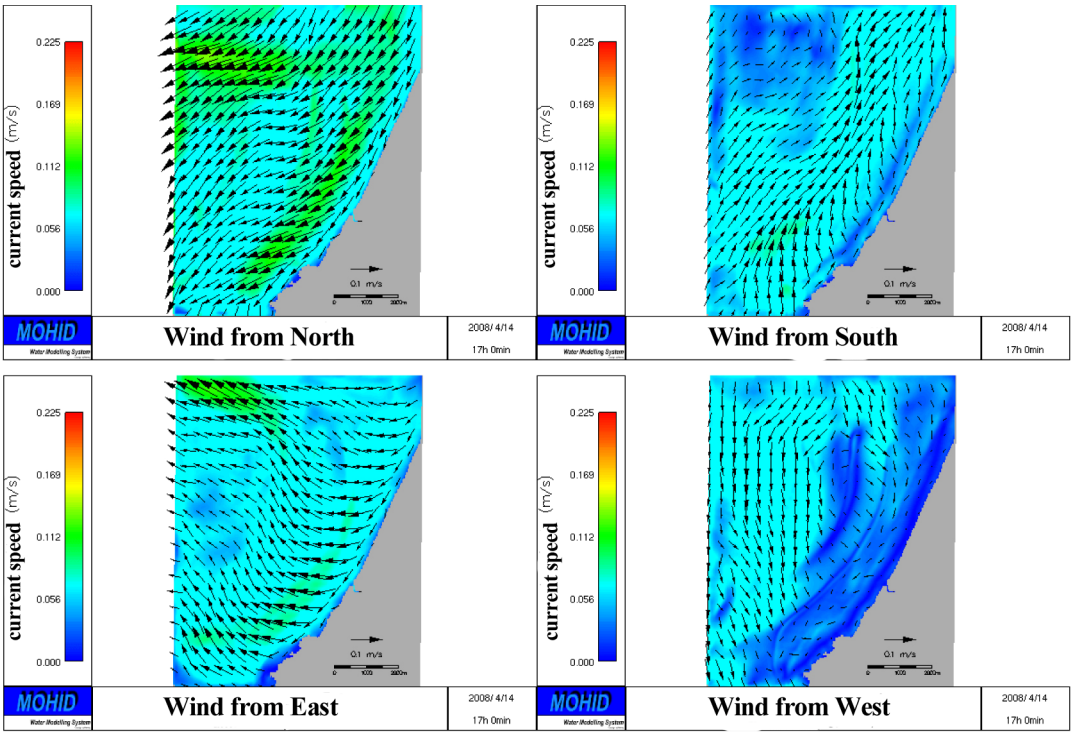

Figure 4.28. (adapted from Maretec, 2008) Mean current field for surface water in coastal area north of Cape Sines considering different scenarios of wind direction, and uniform wind speed of 3.6 m s^{-1}.

Only in the northernmost part of the coastal arc (Tróia Peninsula) where waves are refracted northeastward across the Sado submarine delta, net longshore drift of sediments is directed towards the north. In addition, during winter storms (representing a few days per year) the sediment transported otherwise southwards may undergo important redistribution towards the north as the longshore drift of sediments is temporarily reversed (Quevauviller, 1987).

The sediment samples collected in the inner shelf correspond to a sediment column of ~15 cm and therefore contains an integrated signal which covers seasonal and interannual variability. The high contents of plagioclase in the inner shelf south of Santo André Lagoon is possibly related to contributions from the coastal lagoons when these are opened to the sea and also as a result of northward transport of sediments from the surrounding area of the Sines massif.

In the following chapter elemental concentrations from surface sediments from the Lisbon-Setúbal-Sines shelf will be presented. As referred to above, the combination of mineralogical data with elemental concentration data will allow a better identification of sediment sources and assessment of sediment dispersal.

5. TRACE METALS IN SURFACE SEDIMENTS OF THE SHELF AND UPPER SLOPE

5.1. Introduction

The elemental composition of marine sediments is determined primarily by the mixture of particulate components that make up the bulk of the sediment. These components include lithogenic material derived from continental erosion, their composition reflecting the geology of the source area, as well as biogenic material produced in the marine environment. Trace elements, generally occurring in very low abundance at the Earth's surface, may become enriched in certain marine deposits, due to their high affinity to particulate matter, and under influence of physical sediment sorting and diagenetic alteration. In general, enhanced concentrations of trace metals in recent surface sediments, especially in the continental shelf environment, reflect anthropogenic input of trace metals in addition to input from natural sources. The distinction of contributions from both sources and the study of the anthropogenic fraction of elements may be relevant not only for assessment of anthropogenic impact in marine environment but also to highlight pathways of recent sediment transport. For the latter purpose, particle-reactive chemical species which are adsorbed to the surface of particles are especially good tracers. Since the majority of anthropogenic contaminants are derived from the mainland they may be used to track recent input of terrigenous sediments and to identify the main depocentres of recent sediments. The potential of these tracers increases as the signatures of the potential sources are better known.

A common misconception is to interpret environmental impact of trace metal contaminants and dynamics of their dispersal and accumulation solely on the basis of total concentration within the surface sediment. From this simplistic perspective, deposits with the highest concentration are considered to pose the greatest risk to the ecosystem and to represent the depocentres of recent sediments. However, the risk posed by trace metal contaminants is not merely a function of their concentration in the sediment, but also of their mobility and reactivity in the environment, the latter depending on chemical

characteristics of both the contaminant and the sedimentary substrate. Whereas trace elements may be loosely bound and bioavailable in one type of sediment, they may be tightly bound in another type of sediment (Horowitz, 1991). In addition to that, higher contents of trace metals in certain areas may be related to the presence of source-rocks which are naturally rich in these elements. In such case inferences on sediment transport assuming that trace metal enrichment is due to anthropogenic input will lead to erroneous results.

The distinction of the natural and anthropogenic fraction through bulk concentrations is complicated by the unequal distribution of trace metals over different grain size fractions and different components of the mineral and organic matrix. For this reason, trace metal contents are usually assessed within a defined grain size fraction, and normalized against a common major element representative for the natural sediment fraction. Such normalization procedures are especially important where samples from different sedimentary settings are compared. After normalization, trace metal contents in contaminated recent sediments can be compared with contents in older, non-contaminated sediments from a similar environmental setting. The observed recent excess in trace metal content can then be directly interpreted as the anthropogenic input.

The main goals of the present chapter are:

1) To determine concentrations of major and trace elements in the fine fraction of surface sediments from the Lisbon-Setúbal-Sines shelf area;

2) To assess the geographic patterns of trace metal enrichment in the studied shelf area;

3) To infer about sources of trace metals and sediments in order to gain insight into the pathways of recent sediment transport in the studied shelf area.

5.2. Spatial distribution and relationships between elements

Table 5.1 shows the main descriptive statistics of major and trace element concentrations in surface sediments of the Lisbon, Setúbal and Sines shelves. Overall, mean concentrations of Fe, Al, Ti, Mg, Mn, Pb, Cu, Zn, As, Th and U are highest on the Lisbon shelf and lowest on the Sines shelf, whereas the reverse pattern is observed for Ca, Cr and Ni. Intermediate values are found on the Setúbal shelf. By closer inspection of distribution patterns of these elements in the different shelf areas, four groups of

elements with different distribution patterns can be distinguished (Figures 5.1 and 5.2; for those elements not shown in these figures consult Appendix 3):

1) Ca;

2) Fe, Al, Mg, Ti, Th, U;

3) Cu, Pb, Zn, As, Mn;

4) Cr, Ni.

Table 5.1. Descriptive statistics of the elemental composition of sediment samples collected in the Lisbon-Setúbal-Sines continental shelf and upper slope.

	Lisbon shelf (N=23) (Water depth: Mean=193 m Range = 23 – 572 m)		Setúbal shelf (N=40) (Water depth: Mean=123 m Range = 1 - 527 m)		Sines shelf (N=43) (Water depth: Mean=139 m Range = 11 – 480 m)	
	Mean± Std. Dev.	Min-Max	Mean± Std. Dev.	Min-Max	Mean± Std. Dev.	Min-Max
Ca (%)	5.0±3.5	2.6-19.5	10.5±4.7	3.3-22.8	11.0±4.0	3.2-22.4
Al (%)	7.9±1.5	3.7-9.6	6.2±1.8	2.2-9.0	5.2±1.5	2.0-7.5
Fe (%)	3.7±0.6	2.0-4.8	3.2±0.9	1.4-5.2	2.7±0.9	1.1-4.8
Mg (%)	1.2±0.1	1.0-1.6	1.1± 0.2	0.6-1.8	1.0±0.3	0.4-2.0
Ti (%)	0.4±0.1	0.2-0.8	0.3±0.1	0.1-0.6	0.3±0.1	0.1-0.5
Mn ($\mu g\ g^{-1}$)	407±231	220-1194	413±663	129-4452	296±165	118-1105
Zn ($\mu g\ g^{-1}$)	190±66	93-353	153±69	57-405	91±20	36-146
Cr ($\mu g\ g^{-1}$)	86±88	49-400	105±113	38-559	139±146	33-651
Pb ($\mu g\ g^{-1}$)	91±54	40-273	75±54	19-295	56±47	21-237
Ni ($\mu g\ g^{-1}$)	50±58	24-266	64±65	20-303	95±103	12-431
Cu ($\mu g\ g^{-1}$)	29±7	15-45	27±12	13-74	21±7	12-52
As ($\mu g\ g^{-1}$)	24±13	12-60	18±8	8-42	15±6	8-41
Th ($\mu g\ g^{-1}$)	21±21	9-102	14±8	4-34	10±4	5-23
U ($\mu g\ g^{-1}$)	4.4±3.3	2.1-17.1	3.1±1.3	1.2-6.4	2.5±0.9	1.2-4.4

The lowest concentrations of Ca occur on the Tagus and Sado mud patches, yet on the latter contents are slightly higher. Calcium occurs in highest concentrations in the fine fraction of inner shelf sandy deposits. Despite these generally high contents of Ca, adjacent to the Santo André and Melides lagoons concentrations decrease to concentrations similar to those found in the Tagus and Sado mud patches. Concentrations of Fe, Al, Mg, Ti, Th and U are relatively low in inner shore sandy deposits, increasing

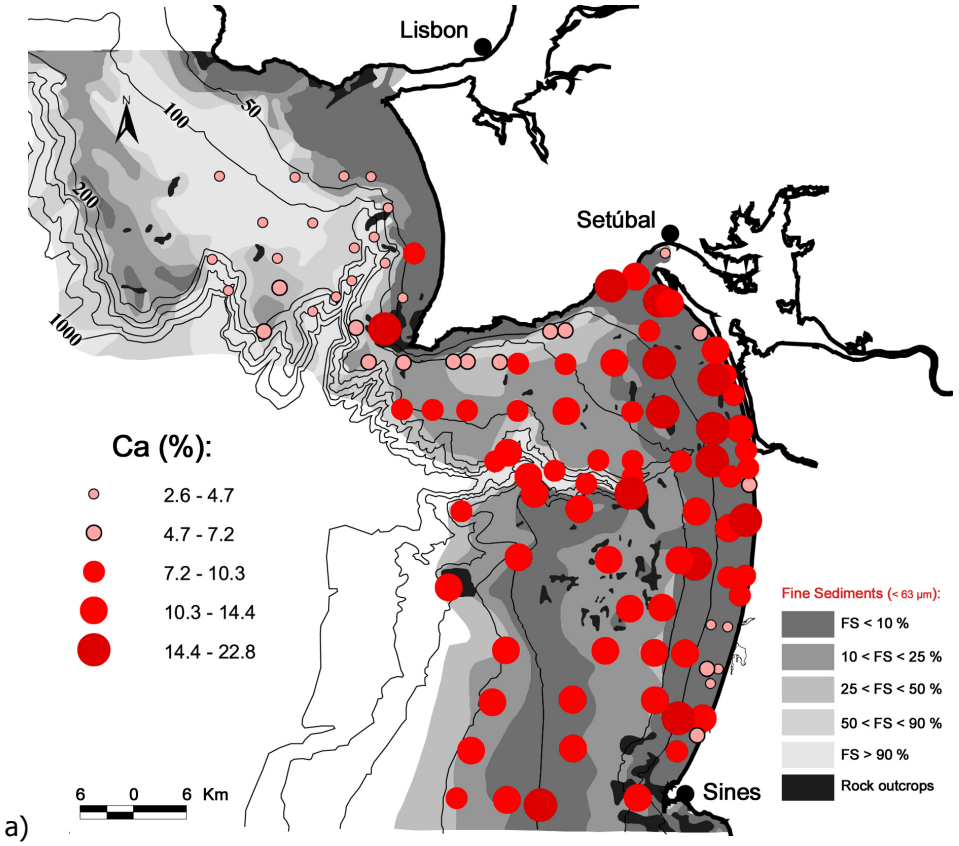
Lisbon
Setúbal
Sines
50
100
200
1000
Ca (%):
2.6 - 4.7
4.7 - 7.2
7.2 - 10.3
10.3 - 14.4
14.4 - 22.8
6 0 6 Km
Fine Sediments (< 63 µm):
FS < 10 %
10 < FS < 25 %
25 < FS < 50 %
50 < FS < 90 %
FS > 90 %
Rock outcrops

a)

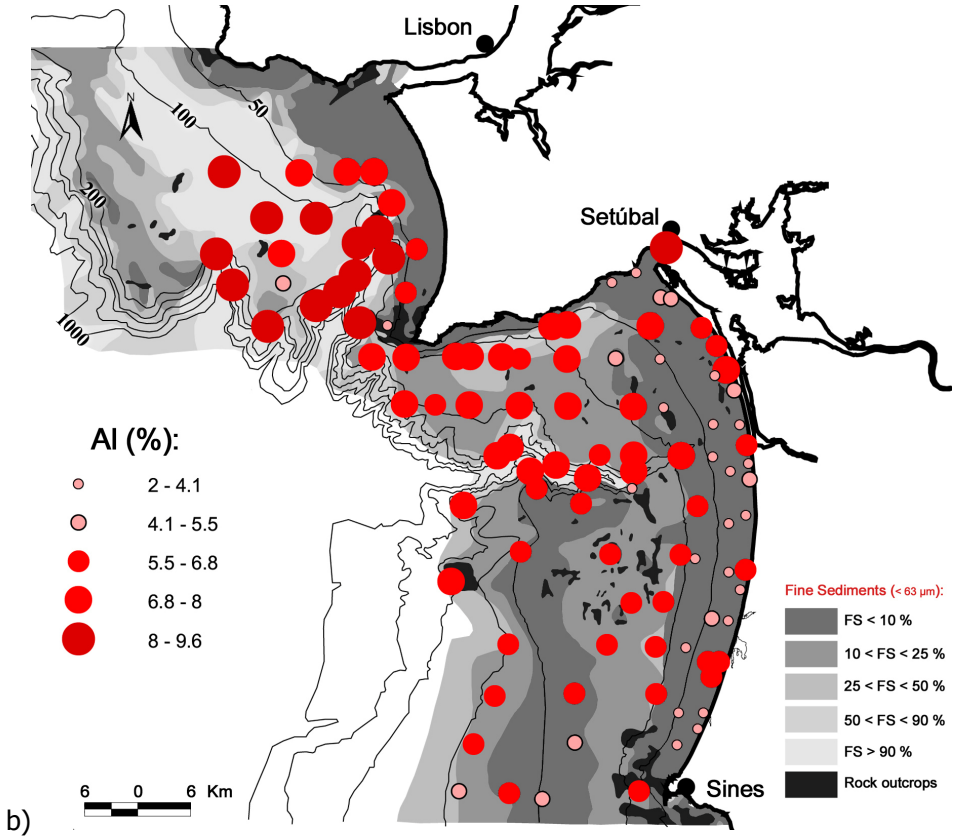
Lisbon
Setúbal
Sines
50
100
200
1000
Al (%):
2 - 4.1
4.1 - 5.5
5.5 - 6.8
6.8 - 8
8 - 9.6
6 0 6 Km
Fine Sediments (< 63 µm):
FS < 10 %
10 < FS < 25 %
25 < FS < 50 %
50 < FS < 90 %
FS > 90 %
Rock outcrops

b)

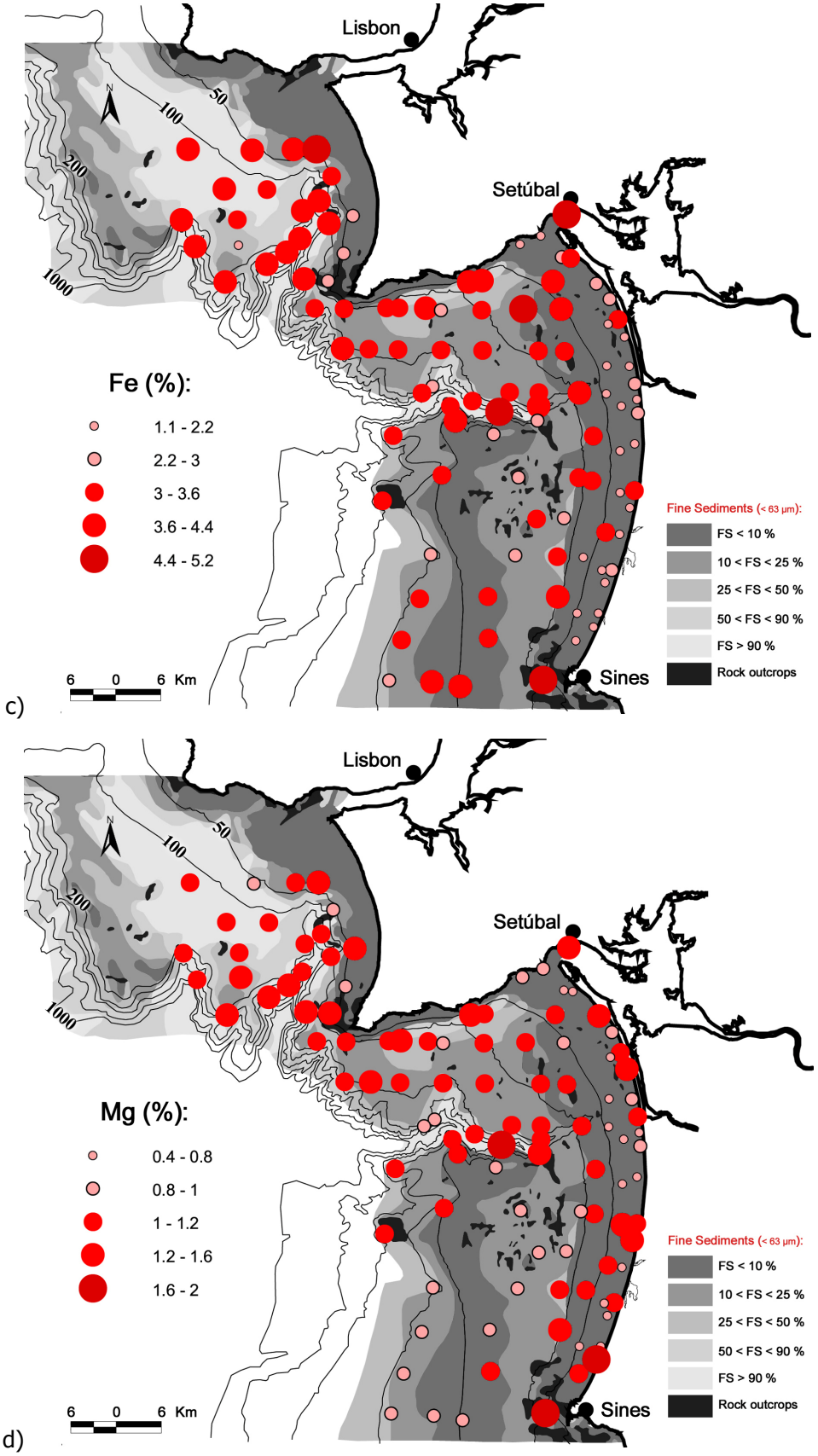

Figure 5.1. Spatial distribution of major elements Ca (**a**), Al (**b**), Fe (**c**) and Mg (**d**) in surface sediments from the Lisbon-Setúbal-Sines shelf and upper slope.

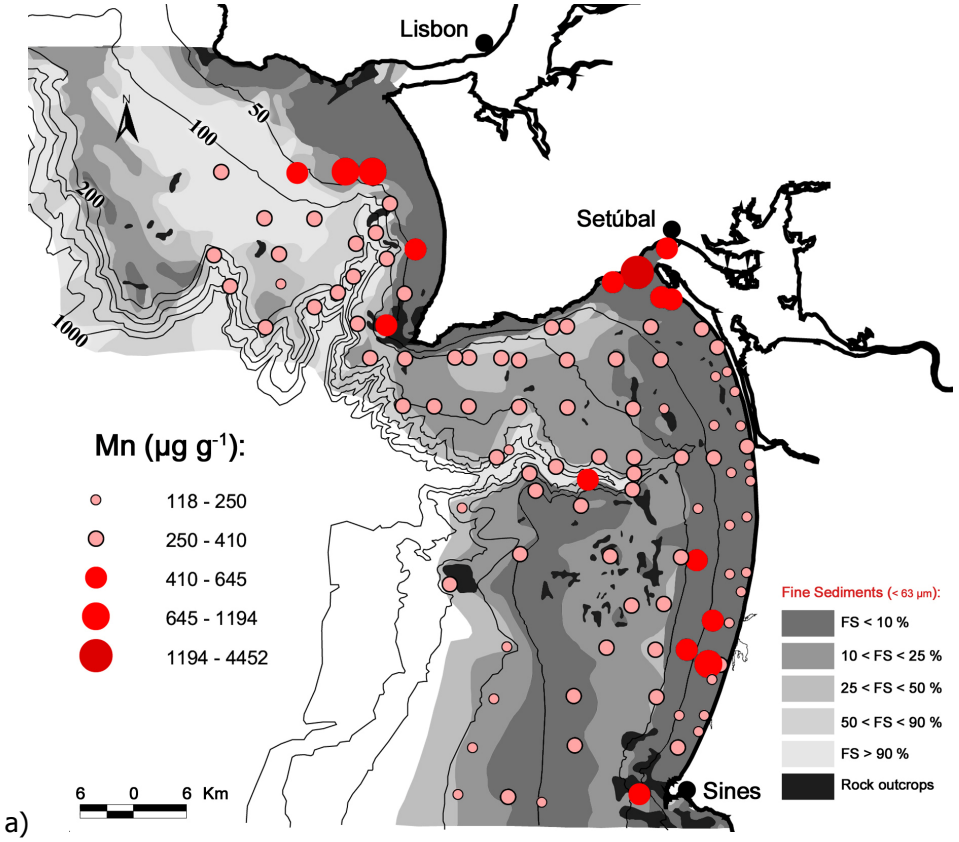
Lisbon
Setúbal
Sines
50
100
200
1000
Mn (µg g-1):
118 - 250
250 - 410
410 - 645
645 - 1194
1194 - 4452
6 0 6 Km
Fine Sediments (< 63 µm):
FS < 10 %
10 < FS < 25 %
25 < FS < 50 %
50 < FS < 90 %
FS > 90 %
Rock outcrops

a)

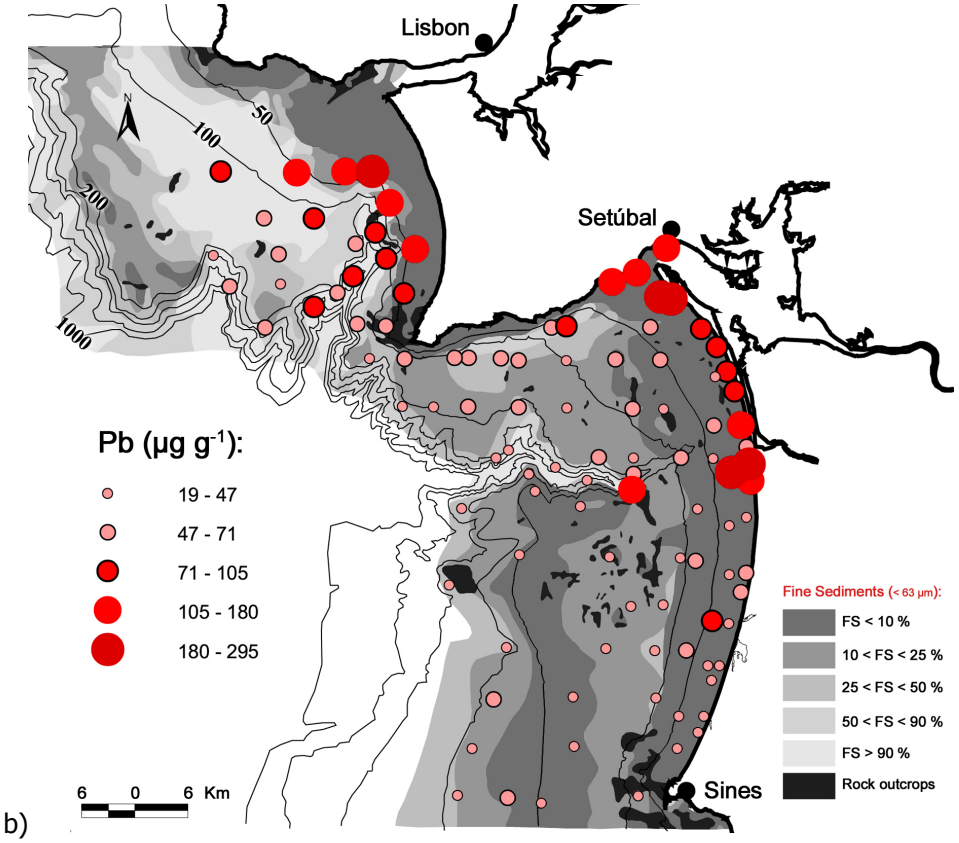
Lisbon
Setúbal
Sines
50
100
200
1000
Pb (µg g-1):
19 - 47
47 - 71
71 - 105
105 - 180
180 - 295
6 0 6 Km
Fine Sediments (< 63 µm):
FS < 10 %
10 < FS < 25 %
25 < FS < 50 %
50 < FS < 90 %
FS > 90 %
Rock outcrops

b)

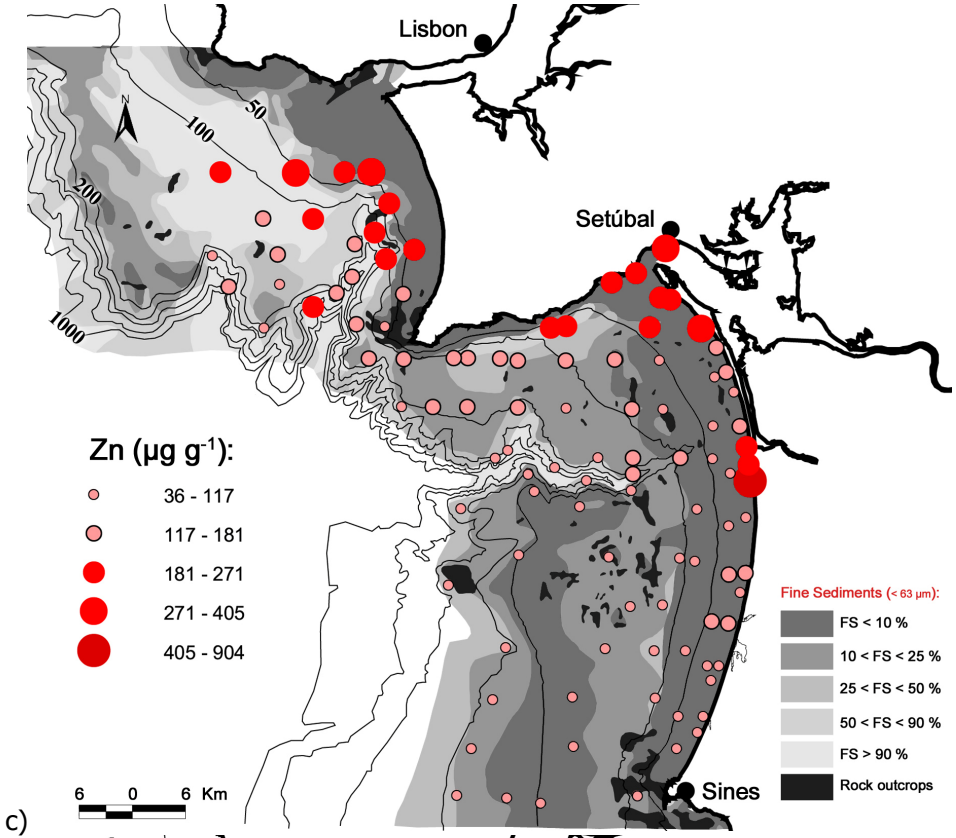
Lisbon
Setúbal
Sines
50
100
200
1000
Zn (µg g-1):
36 - 117
117 - 181
181 - 271
271 - 405
405 - 904
6 0 6 Km
Fine Sediments (< 63 µm):
FS < 10 %
10 < FS < 25 %
25 < FS < 50 %
50 < FS < 90 %
FS > 90 %
Rock outcrops

c)

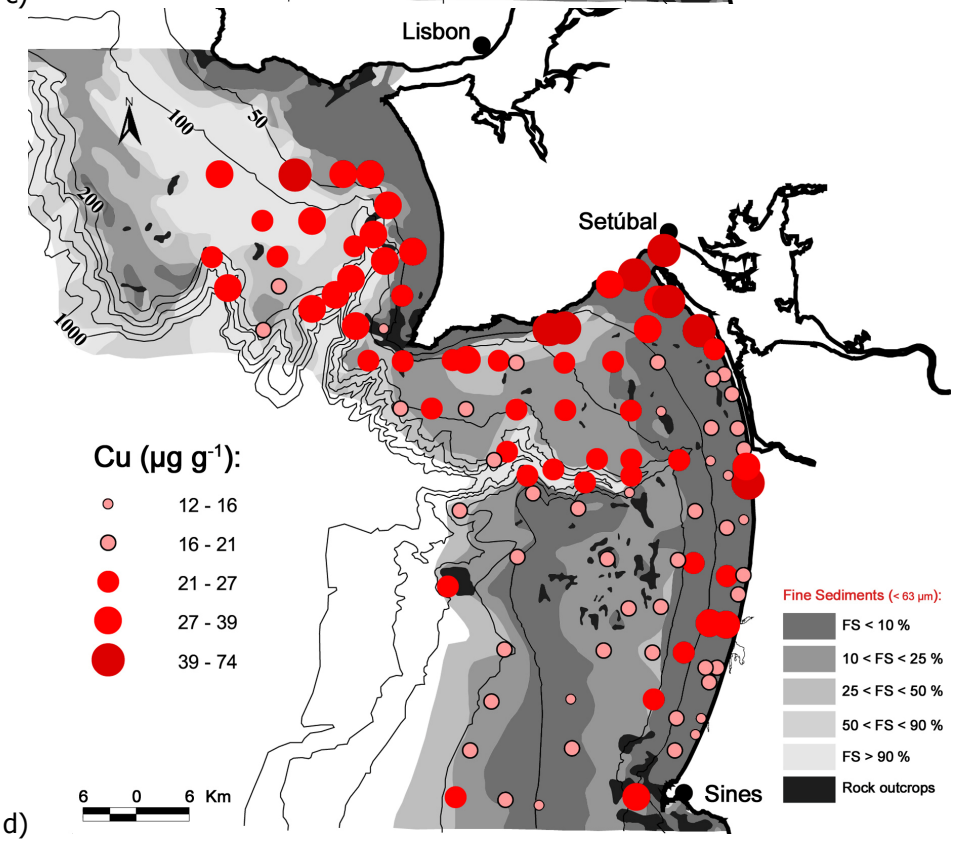
Lisbon
Setúbal
Sines
50
100
200
1000
Cu (µg g-1):
12 - 16
16 - 21
21 - 27
27 - 39
39 - 74
6 0 6 Km
Fine Sediments (< 63 µm):
FS < 10 %
10 < FS < 25 %
25 < FS < 50 %
50 < FS < 90 %
FS > 90 %
Rock outcrops

d)

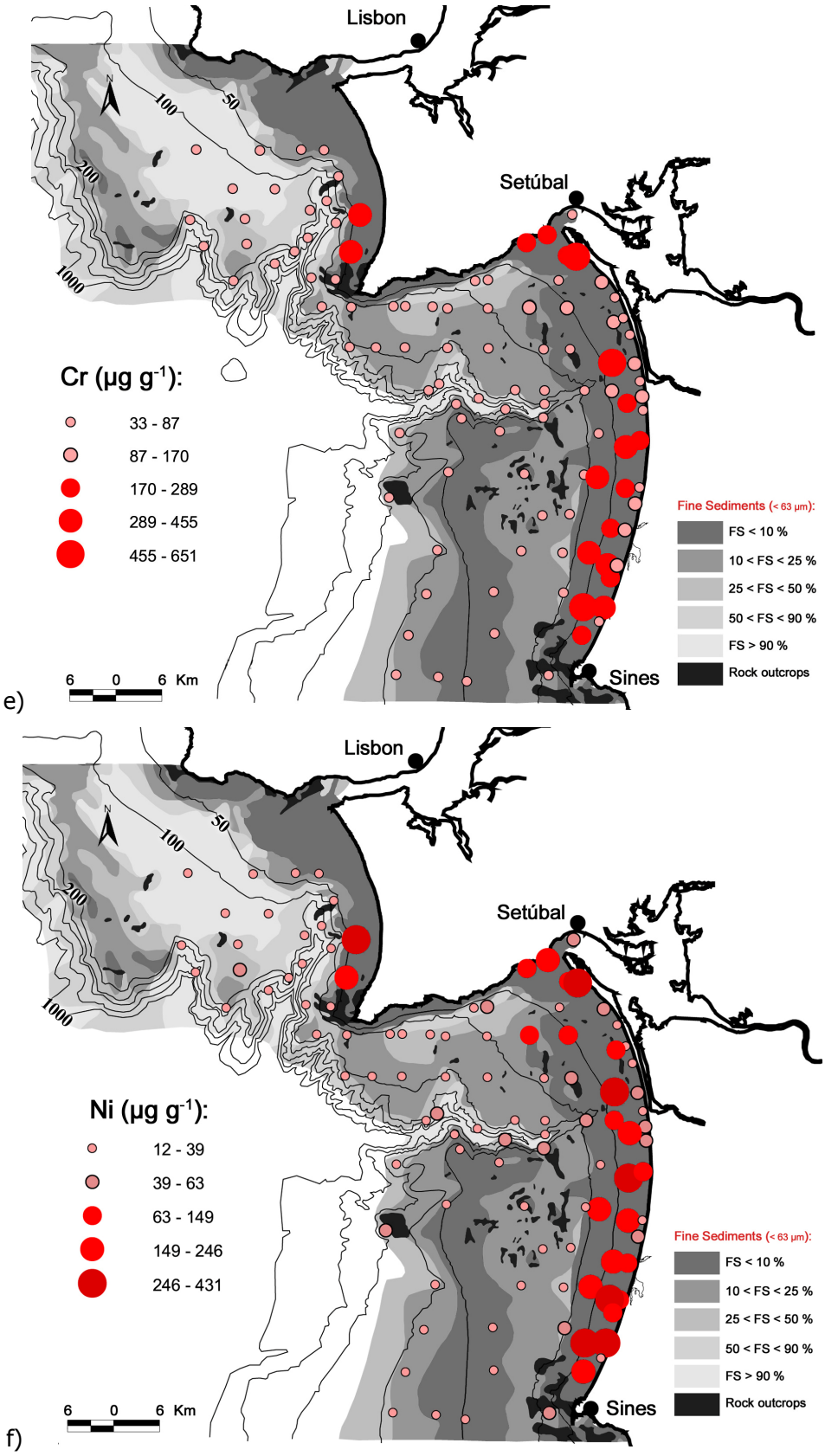

Figure 5.2. Spatial distribution of Mn (**a**), Pb (**b**), Zn (**c**), Cu (**d**), Cr (**e**) and Ni (**f**) in surface sediments from the Lisbon-Setúbal-Sines shelf and upper slope.

with water depth, along with the general increase of fine fraction contents towards the open slope. Despite the general trend increasing northwards, highest concentrations of Cu, Pb, Zn, As and Mn are observed on the inner shelf close the mouths of the Tagus and Sado rivers. The highest Cr and Ni contents are associated with inner shelf sandy deposits of the Setúbal and Sines shelf. On these inner shelf areas there is a southwards increase of both these elements. The groups established according to their distribution patterns also appear from Spearman correlation analysis, as schematically represented in Figure 5.3.

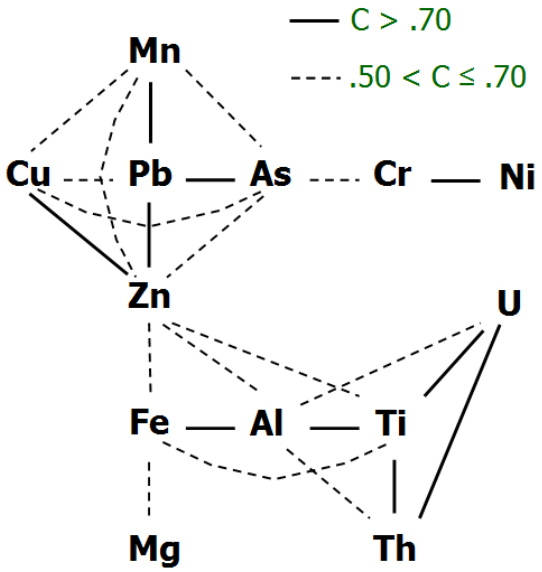

Figure 5.3. Schematic diagram showing the positive Spearman correlations (C) between major and trace elements in surface sediments from the Lisbon-Setúbal-Sines shelf and upper open slope. Note: Ca is not represented in the diagram, due to its negative correlation with all other elements except Cr and Ni.

Principal component analysis (PCA) applied to the complete dataset including all studied elements and all samples from the shelf and upper open slope reduced the spatial variation of the 14 analysed elements to 4 factors, which explain in total 80 % of the data variability.

Factor 1 (42 %) appears to primarily distinguish between elements that prevail in sediments of contrasting grain size; Ti, U, Th, Al and Fe with negative loadings on Factor 1 are most abundant in fine-grained deposits on the Lisbon shelf, whereas Ca, Ni and Cr with positive loadings on Factor 1 are most abundant in sandy deposits of the inner Sines shelf (Figure 5.4a and 5.5a).

Factor 2 (19 %) distinguishes between elements that prevail in nearshore *versus* more offshore areas; Cr and Ni, most abundant in inner shelf sandy deposits, and Pb, As and Mn, most abundant in fine-grained deposits near the major river mouths, load negatively on Factor 2. Fe, Al and Mg, which have a wider, less confined distribution extending toward deeper water load positively on Factor 2 (Figure 5.4a and 5.5b).

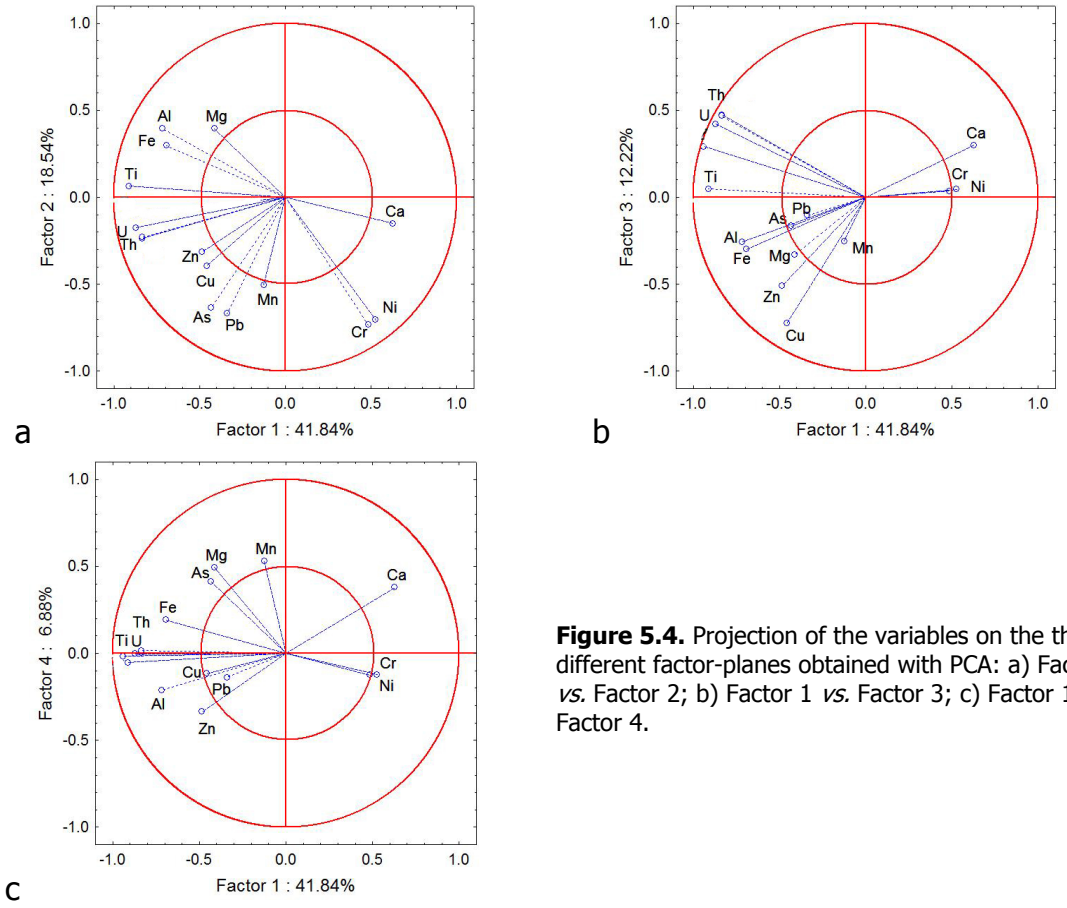

Figure 5.4. Projection of the variables on the three different factor-planes obtained with PCA: a) Factor 1 *vs.* Factor 2; b) Factor 1 *vs.* Factor 3; c) Factor 1 *vs.* Factor 4.

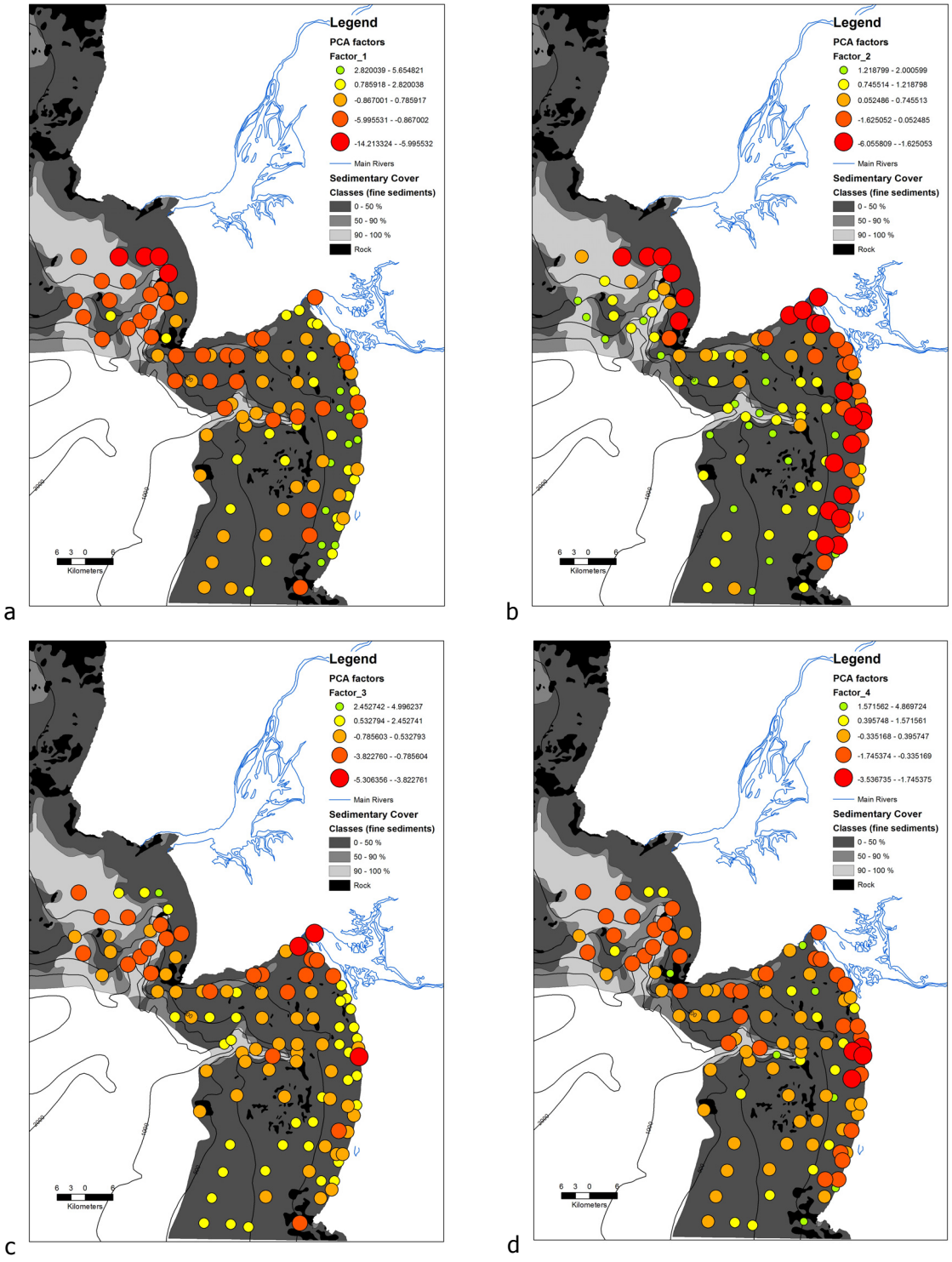

Figure 5.5. PCA factor coordinates of surface sediment samples: a) Factor 1; b) Factor 2; c) Factor 3 and d) Factor 4.

Factor 3 (12 %) is determined mostly by negative loadings of Cu and Zn, which have higher concentrations in localised fine-grained sediment deposits offshore the major river mouths (Figure 5.5c). This factor is interpreted as showing the areas more affected by

anthropogenic input of trace metals. Of these two elements Cu is the one with the highest negative score for this factor meaning that it is the one with the better defined spatial distribution, with high contents in specific areas and low contents in most of the remaining area. As will be shown below, Cu is the least widespread of the trace elements showing recent enrichment.

The formation of Factor 4 (7 %) is not entirely understood. Except Al, all elements scoring negatively on Factor 4 (all below 0.5) are trace elements which show anthropogenic enrichment (Figure 5.4c). The elements scoring positively are mostly the major elements with no evidence for enrichment.

5.2.1. Comparison between shelf and deeper environments

As discussed above, spatial variability in major and trace elemental concentration in sediments of the Lisbon-Setúbal-Sines shelf is considerable. However, no significant differences are found between elemental concentrations on the Sines outer shelf (100-200 m WD) and the Sines upper slope (200-500 m WD), except maybe for Pb which seems to increase offshore (see Table A4.1 in Appendix A4).

The surface sediments collected on the Sines slope (1000 – 3900 m WD) have consistently higher concentrations of Zn, Cu, Cr and Ni than the mean concentration found in the Sines upper slope (Figure 7.3 – pg. 194 *vs.* Table A4.1). Lead on the other hand has consistently lower concentrations on the Sines open slope than the mean value obtained for the upper slope. This difference between Pb and the other trace metals points out to different pathways of transport and will be discussed further in Chapter 7.

5.2.2. Selection of a normaliser

In order to calculate enrichment factors (EFs), trace metal contents were normalised using a conservative common element (cf. Chapter 3). Since both common elements Fe and Al showed no significant difference of number and level of correlations with trace metals (Figure 5.3) and the analysis of both showed a good accuracy (> 97 %), both appear suitable for normalising the trace element concentrations. Iron was chosen as normaliser in order to make enrichment factors calculated for shelf sediments comparable

to those obtained in Chapter 7 for the adjacent submarine canyons and open slope. For the latter there was a more specific reason for the use of Fe as normaliser.

5.3. Relationships between trace elements and mineralogy

It is commonly observed that trace metals and grain size show a linear relationship as trace elements tend to accumulate in the finer fractions (cf. section 5.1). In the present study, however, none of the studied elements shows a significant correlation higher than |0.45| with mean grain size, modal grain size or with the percentage of clay-sized particles (Table 5.2).

Table 5.2. Spearman correlation matrix: geochemistry against grain size and bulk mineralogy. Correlation coefficients higher than |0.50| are highlighted.

	% clay-sized part.	Grain size mean	Modal grain size	Phy	Qz	K-F	Plg	Cc	Mg-Cc	Arg
Cu	-	-	-	**0.56**	0.27	-	0.47	**-0.58**	-	-0.40
Pb	-0.35	-	-	0.24	0.26	-	0.30	**-0.67**	-	-
Zn	-	-	-	**0.58**	0.25	-	0.38	**-0.58**	-	-0.33
Ni	-	-	-	-	-	-	-	-0.26	0.36	0.29
Mn	-	-	-	0.22	-	-	0.24	-0.45	-	-
Fe	-	-	-	**0.50**	-	-	0.27	-0.24	-	-0.43
As	-	-	-	-	-	-	0.38	**-0.68**	0.23	-
U	-0.33	-	-	-	0.46	-	0.40	-	-0.44	**-0.56**
Th	-0.38	-	-	-	**0.55**	0.21	0.45	-	-0.45	**-0.58**
Ca	0.45	-	-	-0.45	**-0.52**	-	**-0.69**	**0.60**	0.40	**0.72**
Cr	-	-	-	-	-	-	-	-0.41	0.24	0.30
Mg	-	-	-	**0.54**	-	-	0.28	-0.21	-	-0.32
Ti	-0.38	-	-	0.32	0.49	-	**0.55**	-0.38	-0.31	**-0.65**
Al	-	-	-	**0.64**	0.29	-	0.44	-0.32	-0.36	**-0.74**

Phy – phyllosilicates; Qz – quartz; K-F – K-feldspars; Plg – plagioclase; Cc – calcite; Mg-Cc – Mg-calcite; Arg - aragonite

The relationship between major and trace elements and bulk mineralogy is also summarised in Table 5.2. Phyllosilicates correlate with some trace elements (Cu and Zn) and Al and Fe while, as expected, carbonates correlate with Ca. On the other hand, the relationship between the various elements and clay mineralogy is less obvious, at least

from a chemical point of view (cf. see below). Table 5.3 shows that kaolinite is the clay mineral with the highest positive correlations with trace elements while illite shows a negative correlation with trace elements. Smectite has some minor correlations with some trace elements.

The adsorptive capacities of the various clay mineral groups for trace elements is highly variable, depending on the negative charge on the broken edges of the layered sheets that result from the isomorphic substitution of Al^{3+} for Si^{4+} in the tetrahedral layer, and Mg^{2+} or Fe^{2+} for Al^{3+} in the octahedral layers. In the case of kaolinite, very little substitution occurs. Thus, its net negative surface charge, and its potential to adsorb cations to external surfaces, is limited. This factor explains its relatively low cation exchange capacity (CEC) because the exchange process is limited to external surfaces. In contrast, isomorphic substitution can be extensive in the 2:1 smectite clay mineral group, particularly within the octahedral layers. As a result they exhibit a relatively high net surface charge that promotes cation adsorption. Moreover, smectites tend to exhibit a relatively high CEC because the individual sheets are weakly bound together, and cations and water can penetrate between the sheets and participate in exchange processes. Despite the above, in the study area kaolinite shows better correlation with trace metals than smectite. This may be partly related to the narrow range of values observed for smectite content (P25 - P75 = 2 - 3 %). In addition, as already seen in Chapter 4, kaolinite distribution on the Lisbon and Setúbal shelves appears to reflect input more closely than smectite. Since conceivably the rivers are also the main source of trace metals, it seems logical that trace metals are carried off the estuaries in association with aggregates formed by the more common kaolinites. Coatings of organic matter and Fe and Mn hydroxides precipitated on clay particles may further enhance the adsorptive capacity of clay minerals (Jenne, 1976).

Table 5.3. Spearman correlations between major and trace elements and different clay minerals in surface sediments from the Lisbon-Setúbal-Sines shelf and upper slope. Correlations higher than |0.50| are highlighted.

	Ca	Fe	Mn	Pb	Zn	Cu	Cr	Ni	As
Kaolinite	**-0.51**	0.38	0.36	**0.62**	**0.70**	0.48	0.35	-	**0.52**
Illite	0.43	-0.29	-0.40	**-0.74**	**-0.71**	-0.47	-0.38	-	**-0.56**
Smectite	-	-	0.27	0.49	0.33	0.28	-	-	0.37
Chlorite	0.35	-0.31	-	-	-	-	-	-	-

5.4. Anthropogenic enrichment of trace metals in surface sediments

5.4.1. Comparison to sediment quality guidelines

The sediment quality guideline (SQG) of the National Oceanic Atmospheric Administration (NOAA), developed to assess biological effects of metal contamination, classifies different levels of metal concentration as "Effects Range-Low" (ERL) and "Effects Range-Medium" (ERM). These ERL and ERM represent, respectively, the 10^{th} and 50^{th} percentiles of the available dataset for different trace metal components (Long *et al.* 1995). The ERMs are supposed to represent concentrations above which adverse biological effects are expected to be common, whereas ERLs represent concentrations below which effects are expected to be rare. Between these values effects are expected to happen occasionally. Obviously, this classification is rather arbitrary since it is merely based on the statistics of the available data, and chemical concentrations do not directly correspond to sediment toxicity (O'Connor & Paul, 2000).

Concentrations of the trace elements considered in the present study (As, Pb, Zn, Cu, Cr and Ni) are found to exceed the ERL value in a considerable number of samples from the Lisbon-Setúbal-Sines shelf (Table 5.4). Concentrations of Pb, Cr and Ni exceed the ERM value in a number of samples in all three shelf areas. Lead, Zn and Cu show a southward decrease in the percentage of samples with contents above the ERL (Table 5.4) whereas Cr shows a southward increase of samples exceeding the ERL and ERM. Nickel and As concentrations are above the ERL value in almost all samples, and Ni exceeds the ERM in a considerable number of samples, increasing towards the south.

Table 5.4. Percentage of samples above the ERL and ERM.

	Lisbon shelf (N=23)		Setúbal shelf (N=40)		Sines shelf (N=43)	
	ERL (%)	ERM (%)	ERL (%)	ERM (%)	ERL (%)	ERM (%)
Zn ($\mu g\ g^{-1}$)	78	0	43	0	7	2
Cr ($\mu g\ g^{-1}$)	13	4	30	5	37	9
Pb ($\mu g\ g^{-1}$)	87	4	75	5	26	5
Ni ($\mu g\ g^{-1}$)	100	9	98	28	98	37
Cu ($\mu g\ g^{-1}$)	22	0	18	0	5	0
As ($\mu g\ g^{-1}$)	100	0	98	0	98	0

ERL/ERM concentrations ($\mu g\ g^{-1}$) for different trace elements according to the marine sediment quality guidelines of NOAA: Pb: 47/218; As: 8.2/70; Cr:81/370; Ni: 21/52; Cu: 34/270; Zn: 150/410.

5.4.2. Enrichment factors

The level of trace metal enrichment in sediments can be assessed through different indexes and methods (e.g. Loring & Rantala, 1992). In this study, the enrichment of trace metals in surface sediments from the shelf was assessed through enrichment factors using Fe as the normaliser (cf. Chapters 3 and 7) and using trace metal concentrations of pre-industrial sediment (older than ~150 years) as baseline (cf. Chapter 3). Since a pre-industrial baseline was not determined for As, enrichment could not be calculated for As.

Lead, Zn, Cu, Cr and Ni are variably enriched throughout the continental shelf and upper slope (Figure 5.6 and Table 5.5), locally by a factor 25 in the case of Pb. Zinc and Pb show a considerably higher percentage of samples which are significantly enriched (43 and 88 %, respectively) than Cu, Cr and Ni. Most of the samples not enriched in those trace metals occur on the Sines shelf, especially on the outer shelf and upper slope, and in the upper Setúbal Canyon. While sediments enriched in Pb extend over most of the study area, the area with significant enrichment in Zn appears to be more restricted to the Lisbon shelf and a relatively narrow area close to the coast on the Setúbal and Sines shelves. The highest EFs of Pb (7 - 25) occur in the Sado and Tagus pro-delta deposits while the highest EF of Zn (3 - 12) occur in the Sado pro-delta deposit, along the coastal arc between Tróia and Sines and in the Tagus mud patch (Figure 5.6a, b).

Enrichment of Cu, Cr and Ni appears especially associated with sandy deposits of the inner shelves (Table 5.5). From the five trace metals considered Ni and Cr are the ones with the lowest percentage of samples enriched (25 and 28 %, respectively). Yet, these elements show the highest EFs (22 and 26, respectively) in the inner shelf sandy deposits of the Sines shelf. Most likely, however, the baseline used is not appropriately representing the fine fraction of these sandy deposits. Thirty percent of the surface samples are enriched in Cu, most of which are from sandy inner shelf deposits and only few from mud patches on the Lisbon and Setúbal shelves. Among various other areas on the inner shelf, high EFs of Cu occur close to the Sado River mouth in the Sado pro-delta deposit (Figure 5.6c).

Enrichment factors of Pb and Zn (and Cu to some extent) decrease with increasing water depth, whereas a relationship with water depth is not observed for Cr and Ni (Figure 5.6).

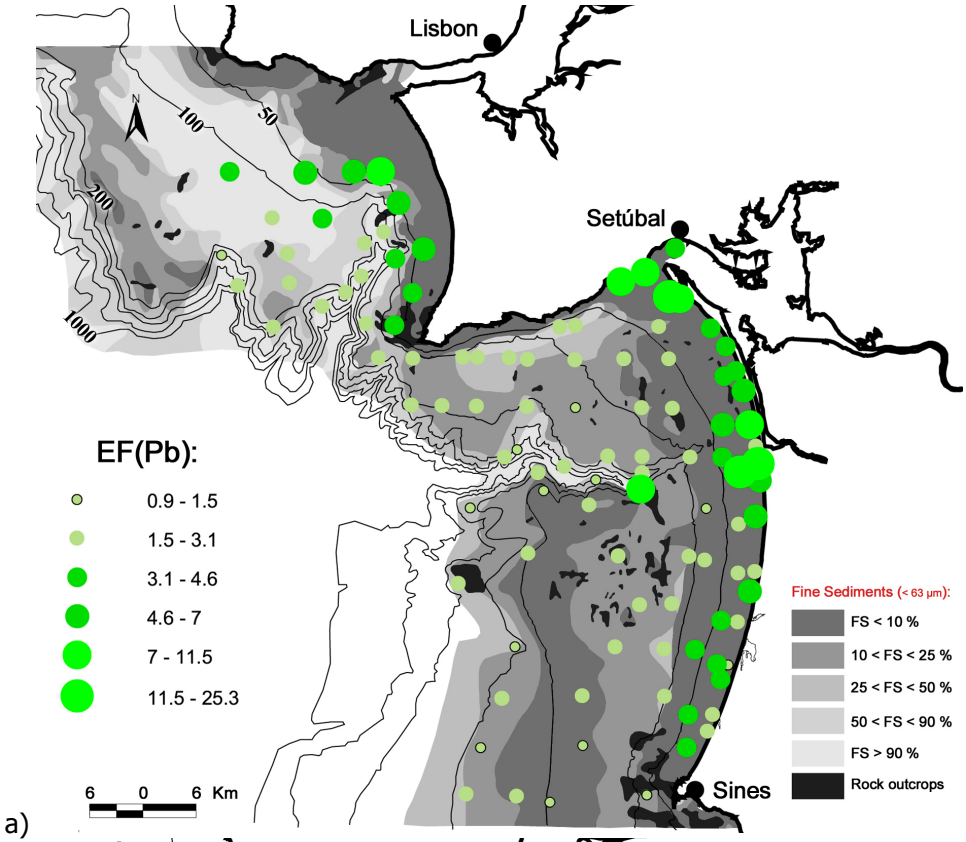
Lisbon
Setúbal
Sines
100
50
200
1000
EF(Pb):
0.9 - 1.5
1.5 - 3.1
3.1 - 4.6
4.6 - 7
7 - 11.5
11.5 - 25.3
6 0 6 Km
Fine Sediments (< 63 µm):
FS < 10 %
10 < FS < 25 %
25 < FS < 50 %
50 < FS < 90 %
FS > 90 %
Rock outcrops
a)

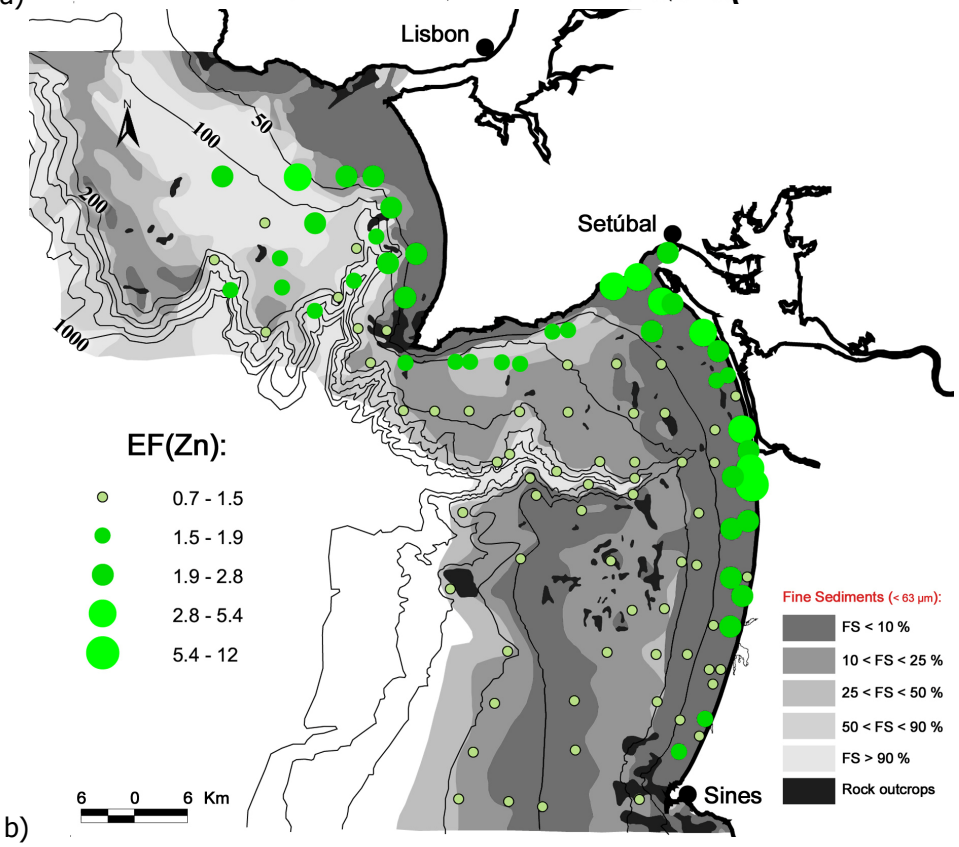
Lisbon
Setúbal
Sines
100
50
200
1000
EF(Zn):
0.7 - 1.5
1.5 - 1.9
1.9 - 2.8
2.8 - 5.4
5.4 - 12
6 0 6 Km
Fine Sediments (< 63 µm):
FS < 10 %
10 < FS < 25 %
25 < FS < 50 %
50 < FS < 90 %
FS > 90 %
Rock outcrops
b)

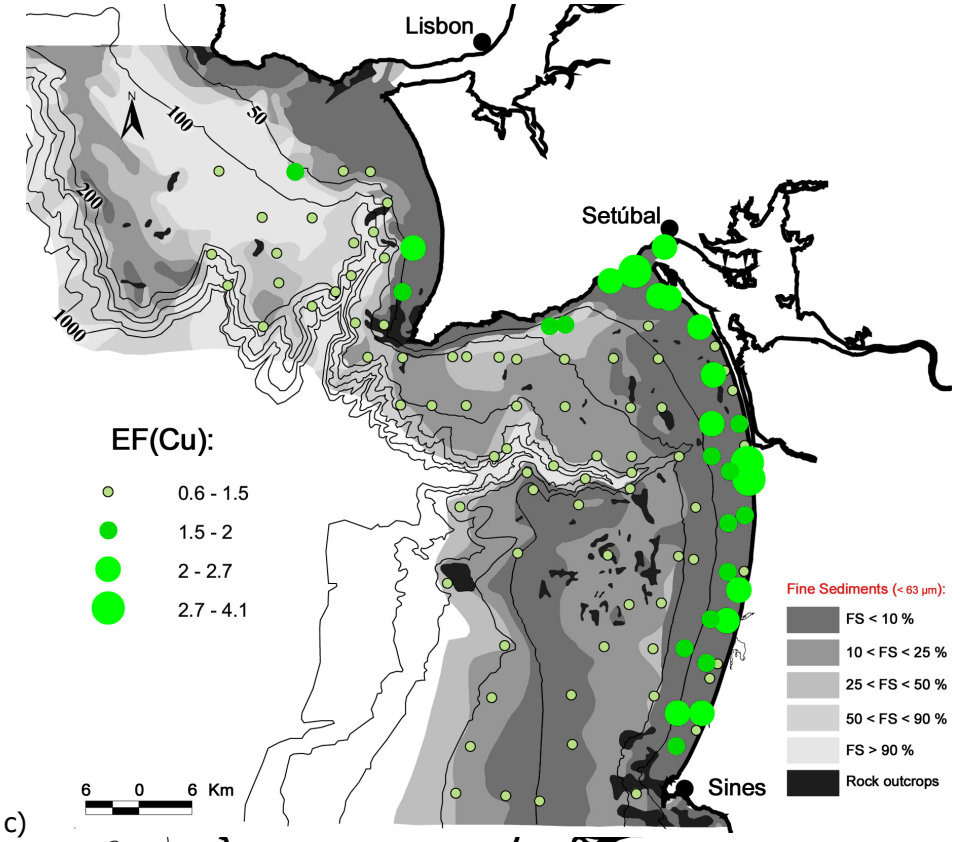
Lisbon
Setúbal
Sines
100
50
200
1000
EF(Cu):
0.6 - 1.5
1.5 - 2
2 - 2.7
2.7 - 4.1
6 0 6 Km
Fine Sediments (< 63 µm):
FS < 10 %
10 < FS < 25 %
25 < FS < 50 %
50 < FS < 90 %
FS > 90 %
Rock outcrops

c)

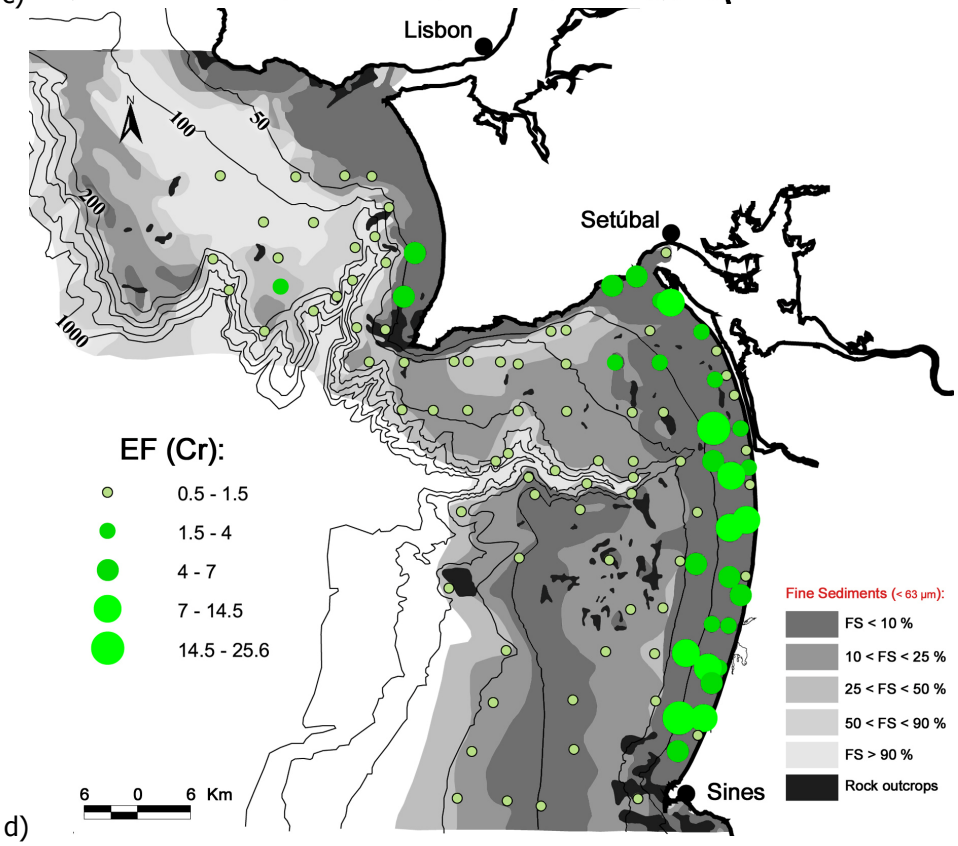
Lisbon
Setúbal
Sines
100
50
200
1000
EF (Cr):
0.5 - 1.5
1.5 - 4
4 - 7
7 - 14.5
14.5 - 25.6
6 0 6 Km
Fine Sediments (< 63 µm):
FS < 10 %
10 < FS < 25 %
25 < FS < 50 %
50 < FS < 90 %
FS > 90 %
Rock outcrops

d)

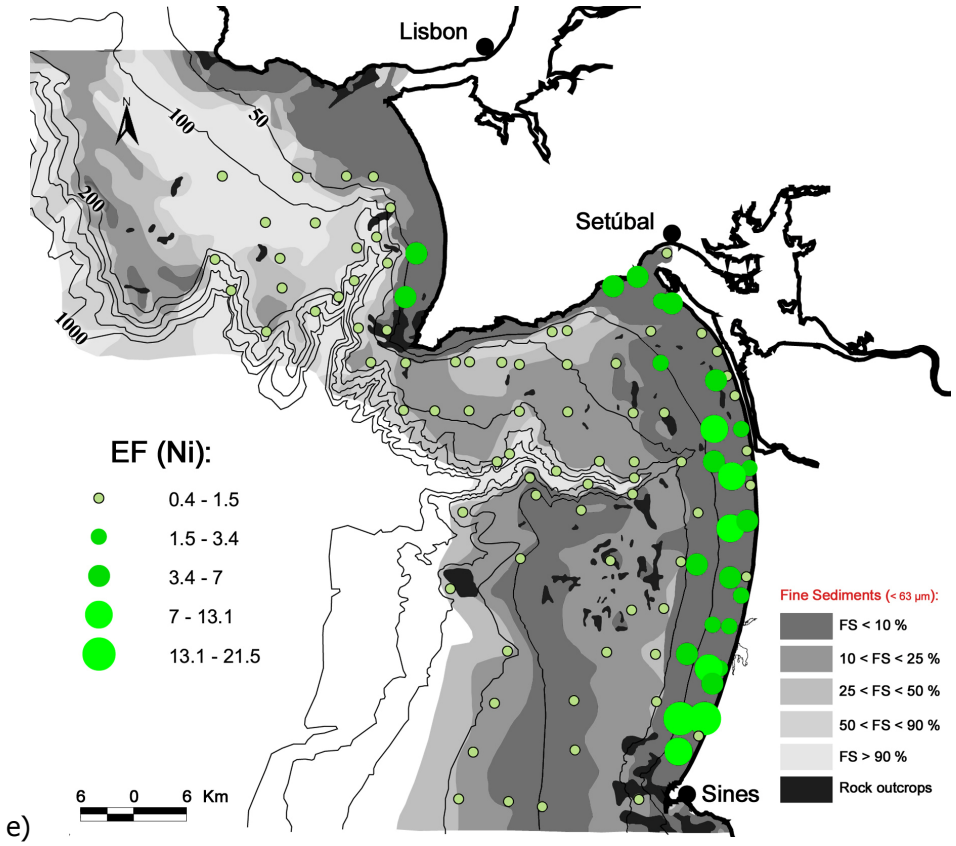

Figure 5.6. Spatial distribution of Pb (**a**), Zn (**b**), Cu (**c**), Cr (**d**) and Ni (**e**) enrichment factors in surface sediments of the Lisbon, Setúbal and Sines shelves.

Table 5.5. Mean enrichment factors, differentiated per inner-, middle-, and outer shelf and upper slope, for the three studied shelf areas. Mean enrichment factors higher than 1.5 are highlighted in grey.

		EF (Pb)	EF (Zn)	EF (Cu)	EF (Cr)	EF (Ni)
Lisbon	Inner (n = 4)	5.8	2.3	1.6	2.6	2.0
	Middle (n = 4)	4.9	2.2	1.5	2.0	1.4
	Outer (n = 6)	2.8	1.7	1.2	0.7	0.5
	Upper slope (n = 9)	2.4	1.6	1.2	0.8	0.6
Setúbal	Inner (n = 15)	6.6	2.5	2.0	4.0	3.2
	Middle (n = 7)	2.2	1.4	1.1	1.2	0.9
	Outer (n = 10)	2.1	1.5	1.2	0.8	0.6
	Upper slope (n = 9)	1.9	1.1	1.0	0.8	0.7
Sines	Inner (n = 17)	5.7	2.6	2.0	7.2	6.5
	Middle (n = 3)	2.8	0.9	1.4	5.1	3.9
	Outer (n = 13)	1.6	1.0	1.0	0.7	0.6
	Upper slope (n = 10)	2.5	1.0	1.0	0.8	0.7

5.5. Discussion

On the Lisbon-Setúbal-Sines shelf the elemental geochemistry of the fine-grained sediment fraction appears to a large extent determined by the amount of fine fraction. The Lisbon shelf is largely covered by fine-grained deposits of the Tagus mud patch, while towards the south, on the Setúbal and Sines shelves, deposits rich in fine-grained material are less widespread (Figure 2.3, page 22). In accordance, elements typically associated with fine-grained sediments (Al, Fe, Ti and U) show a southward decrease in mean concentrations (Table 5.1). As a result of the low input of fine-grained lithogenic sediments in the southern area, relatively coarse sediments with high contents of shells dominate the area. This is in turn expressed in the fine fraction by generally high concentrations of Ca.

Although trace metals are in general mostly associated with lithogenic input, trace metal distribution on the Lisbon-Setúbal-Sines shelf show spatial patterns that differ from the distribution of elemental proxies of lithogenic and biogenic material. The differing patterns of trace metals and proxies of lithogenic material such as Al indicate that there must be other trace metal carriers involved and/or a portion of the contents of trace metals cannot be explained by the existing concentrations of metal carriers, and may represent anthropogenic enrichment. Considering the spatial distribution pattern of the studied trace metals and the correlations among them, two groups with different behaviour can be distinguished: i) Cu, Pb, Zn, As, Mn and ii) Ni, Cr.

5.5.1. Copper, lead, zinc, arsenic and manganese

The most obvious difference between the distribution patterns of Cu, Pb, Zn, As, Mn and that of Ni and Cr is that elements from the first group show higher concentrations in sediments close to the inlets of estuaries and coastal lagoons (Figure 5.2). This is most conceivably related to co-precipitation of these trace elements with Mn and Fe (hydr)oxides. The efficiency of Mn oxides as trace metals scavengers in the lower estuaries is well documented (e.g. Zwolsman and van Eck, 1999 and reference therein). However, the trace metals which are affected by this scavenging process may be different from estuary to estuary depending on the prevailing chemical, physical, biological and hydrological characteristics of the estuary (Byrd *et al.*, 1990). Cortesão (2002) studied the reactivity of Cd, Cu, Cr, Ni and Co in the lower Sado Estuary and concluded that Mn co-

precipitation is the main process affecting particulate Co. This author considers however that this process may well be critical in the coastal area as well. Unfortunately, Pb, Zn and As were not considered in the referred study.

Within the group made by Cu, Pb, Zn, As and Mn different affinities between elements are observed. Zinc and Cu appear more closely related to lithogenic material, as represented by Al, Fe and phyllosilicates, than Pb, As and Mn (Tables 5.2 and 5.3). Apparently Zn and Cu are less controlled by precipitation of Mn oxides than the former trace metals and may be more affected by terrigenous materials and/or organic matter forming aggregates with clay minerals. Zinc and Cu accumulation in sediments may to some extent also be biologically controlled in relation to primary production. The relationship of Cu with primary production is further discussed in Chapter 7, dealing with trace metal distribution in sediments of deeper areas of the continental margin. However, on the shelf this process seems of less importance as shown by the close relationship of Cu and Zn with Al, Fe and phyllosilicates.

Enhanced concentrations of Cu, Pb, Zn, As together with Mn are also observed on the inner shelf adjacent to the Melides and St. André lagoons. These coastal lagoons are naturally closed off from the sea by a sand bar but every spring (March/April) both lagoons are artificially opened to promote water exchange with the open sea, with the objective of preventing eutrophication. According to Freitas *et al.* (1999) the artificial opening of some SW Portuguese coastal lagoons (Melides, St. André and Albufeira) is a common practice since the 18^{th} century. The subsequent closing of the inlet by natural processes may take days (Melides), weeks (St. André) or even months (Albufeira) (Freitas *et al.*, 2000). Natural overwash of the sand bar used to occur in the past during storms and high water levels within the lagoon, but has become less frequent due to increased regulation of the maximum levels of inundation of the lagoons.

While closed off from the open sea, the stagnant waters of the lagoons become distinctly stratified, as expressed in vertical gradients in temperature, salinity, turbidity, pH and dissolved oxygen. Depletion of dissolved oxygen in the bottom water, observed during prolonged periods of stagnation (e.g. Freitas *et al.*, 2000; Cearreta *et al.*, 2002) leads to lowering of the redox potential, and as a consequence reduced Fe and Mn are released from the bottom sediments to the overlying water. When the lagoon is again opened to the sea, precipitation of Mn oxides will occur as water flowing from the lagoon mixes with well-oxygenated sea water. In addition, the opening of the bar causes localised erosion and remobilization of superficial sediments and organic matter from the

bottom of the lagoon, and export to open sea (Freitas *et al.*, 2000). Jesus *et al.* (2005) found high contents of Mn and various trace metals in beach sediments from the area adjacent to these lagoons, distinctly higher than in other areas of the coastal arc between Tróia and Sines. The high contents of trace metals and Mn in beach and adjacent shelf sediments may additionally result from precipitation of Mn oxides as lagoonal water percolates through the permeable sand of the bar and emerges on the beach, driven by water level differences between lagoon and sea. However, the high contents of plagioclase found in the fine fraction of beach and shelf sediments from this area, supposedly sourced by the Santo André and Melides lagoons, suggest that indeed the opening of these lagoons to the sea has an impact on the composition of beach and shelf sediments from the surrounding area.

Apart from the above-mentioned mechanism enhancing the export of trace metals to the shelf and beach system, the St. André Lagoon is by itself rich in Mn, Zn and Pb (Freitas *et al.*, 2000; Piedade *et al.*, 2004; Jesus *et al.*, 2007). The relatively small drainage basin discharging into the lagoon comprises schists and volcano-sedimentary rocks which are relatively rich in the above-mentioned elements (Figure 2.18, pg.47). Manganese and Fe were even extracted in the past from the now abandoned Saramaga mine (Santos Oliveira *et al.*, 2002). Similar lithologies rich in trace metals are not found in the drainage basins discharging to the Melides and Albufeira Lagoons, and as a consequence these lagoons are probably less important as trace metal sources to the shelf than the St. André Lagoon.

5.5.2. Nickel and chromium

The correlation between Ni and Cr seems to be very strong, whereas the two elements show only a very weak correlation with any of the other studied elements (Figure 5.3). Cortesão (2002) reported this same relationship between Cr and Ni for the suspended particulate matter from the Sado Estuary (both upper and lower estuary) and the adjacent coastal area water. This same strong positive relationship between both elements was also found, for instance, in suspended particulate matter of the Scheldt and Rhine estuaries (Zwolsman & van Eck, 1999 and van de Meet *et al.*, 1985, respectively) and in surface sediments of the Sena and Mondego estuaries (Boust, 1981 and Vale *et al.*, 1994). All these examples point to a common process of incorporation of these two

elements in the particulate phase, yet the mechanism involved is not revealed by the data here presented. Since the highest values are found in sandy deposits of the inner shelf rich in biogenic carbonate it may be that Cr and Ni are enriched by a biological process or simply by weathering of some heavy mineral concentrated in the coarser fractions.

5.5.3. Enrichment of trace metals

The percentage of samples showing significant trace metal enrichment (EF > 1.5) per element follows the sequence: Pb (88 %) > Zn (43 %) > Cu (30 %) > Cr (28 %) > Ni (25 %). Generally, the enrichment of trace metals tends to decrease with increasing water depth, suggesting that the excess of trace metals must be derived from land (Figure 5.6 and Table 5.5).

The areas of the Lisbon-Setúbal-Sines shelf most affected by enrichment of trace metals include the entire Lisbon shelf, the Sado mud patch and the inner shelf between Tróia and Sines.

Enrichment of Pb and Zn on the Lisbon shelf and the Sado mud patch, and of Cu in the latter area points to the nearby Tagus and Sado estuaries as the likely sources of enrichment. Indeed, high trace metal concentrations in water, sediments and biota due to anthropogenic activities have been reported for both estuaries (e.g. Cotté-Krief *et al.*, 2000; Caeiro *et al.*, 2005; França *et al.*, 2005).

On the inner shelf between Tróia and Sines, decreasing levels of enrichment of Pb, Zn and Cu in southward direction, along with the prevailing longshore drift of sediments towards south (except in the northern most portion) (SNIRLit, 2010 and references therein) suggests once more that the Sado Estuary is the most likely source for these trace metals. Since enrichment of Cr and Ni on the inner shelf decreases in opposite, northward direction, and since these elements are not enriched in the Sado mud patch nourished by the Sado Estuary, it seems that these elements are not sourced by the Sado Estuary, but rather seem to come from the south. Two different sources of particles may explain this enrichment:

1) The enrichment of Cr and Ni may be due to relatively abundant presence of heavy minerals in these sediments nourished by the Sines sub-volcanic complex. In a study of the heavy mineral fraction in beach deposits between Tróia and Sines, Miranda *et al.* (2007) also found the signature of sub-volcanic rocks, in the form of an increase in

amphiboles and pyroxenes in the southernmost 10 km of the coastal arc. Pombo *et al.* (2004) found this same assemblage in the inner shelf of this same area. If there is indeed a natural source of enhanced Cr and Ni contents in sediments of this area, the calculated enrichment factor (EFs ~20 in some areas) is very likely too high because the baseline value used for the calculation refers to pre-industrial sediments from deeper areas (see Figure 3.2, pg. 52) where heavy minerals are rare.

2) Another source of Cr and Ni might be the Sines submarine outfall located ~2 km northwards from Sines which started to operate in 1978 (Cardoso & Palma, 2007). It mainly discharges industrial wastewater from an important industrial complex in the vicinity of Sines. The structure reaches to 3.2 km offshore and releases wastewater at 40 m WD (Maretec, 2008). At the time when the sediment samples were collected another outfall in the city of Sines was still operational and discharging in front of Cape Sines. Nowadays it is deactivated. Two monitoring studies done in sediments from the surroundings of the first outfall (Cardoso & Palma, 2007; Maretec, 2008) showed that there is no important enrichment of trace metals in the bulk sediments, which in this case are coarse sands. These studies are of limited use, however, to evaluate the possible impact of these releases on sediment samples shown in the present study because: i) The above-mentioned studies refer to the bulk sediment < 2 mm, while the present study is considering the fine fraction (< 63 μm); ii) Presently, the wastewater discharged by the Sines submarine outfall undergoes secondary treatment but possibly the treatment was less extensive at the time when the sediment samples here presented were collected (1980-1987). This input of trace metals to the inner shelf would have affected the area northwards from the submarine outfall especially during storms when the longshore drift is reversed to a northward direction.

From the two hypotheses, the first seems the more likely in view of the observed enrichment of heavy minerals in beach and shelf sediments from the southern half of the coastal arc, and also in view of the lack of correlations between Cr and Ni and other elements (Figure 5.3).

Since the enrichment of Pb is found to extend over a much wider area of the shelf and upper open slope than that of other trace elements, it can be deduced that other sources of excess Pb must exist apart from the rivers discharging terrigenous sediments to the shelf. Another source of contamination potentially involving the whole studied shelf area concerns atmospheric input. This subject will be further discussed in section 7.4.1 of

Chapter 7 where stable lead isotope signatures are used to identify potential sources of lead in the canyons.

As mentioned before, the sediment samples from the shelf here presented were collected between 1980 and 1987, which implies that they may not represent the present state of contamination of the shelf. Present-day shelf sediments could be expected to be less contaminated with trace metals, after improvement of industrial and domestic effluent treatment and closing of some industrial point sources in both the Tagus and Sado estuaries during the past two decades. During this time leaded gasoline was also gradually phased out, starting in the early 1990s and completely eliminated only in 1999 (Roma-Torres *et al.*, 2007). However, Mil-Homens *et al.* (2009), in a study of trace metal accumulation in sediments from the Tagus mud patch during the last 80 years (1920 - 2000), concluded that sediments dated between 1980 and 2000 show constant enrichment values of trace metals, presumably due to the homogenising effect of bioturbation in the surface mixed layer. EFs between 1980 and 2000 obtained by these authors are indeed very similar to those obtained in the present study for the same area (Table 5.6).

Table 5.6. Comparison of enrichment factors of Pb, Zn and Cu in sediments of the Tagus mud patch, as obtained in the present study for grab samples collected between 1980 and 1988, and those obtained by Mil-Homens *et al.* (2009) in samples collected between 1980 and 2000.

Tagus Mud Patch	Water depth	EF (Pb)	EF (Zn)	EF (Cu)
Present study	50-100 m (Sample 4346)	6.5	3.1	2.0
	> 100 m (Samples:	3.7	2.1	1.5
	4342	2.6	1.5	1.1
	4285			
	4282)	3.4	2.2	1.4
Mil-Homens *et al.* (2009)	50-100 m	~ 5-6.5	~ 2.5-3.5	~ 2.5-3.5
	> 100 m	~ 4	~ 1.8-2.5	~ 2.5

In addition, the enrichment factors found in grab samples from the outer shelf/upper slope (Chapter 5) are comparable to those found in the same area in the top 0.5 cm of

cores collected with box- and multi-corers (Chapter 7). This comparison will be further discussed in section 7.2.6 of Chapter 7.

The good agreement between the two independent studies, as shown in Table 5.6, gives reason for confidence that results presented in this Chapter are a good representation of the enrichment of trace metals in surface sediments over the last 20 years.

Part III
Submarine canyons and open slope

6. SEDIMENT TRANSPORT AND DEPOSITION IN THE LISBON-SETÚBAL CANYON AND ADJACENT CONTINENTAL MARGIN

6.1. Introduction

Despite of being a major topographic feature of the Portuguese margin, the Lisbon-Setúbal Canyon system so far was not studied in detail with regard to modern sediment transport and deposition. This is in contrast with the relatively geographically close Nazaré Canyon. Recently, studies by Arzola *et al.* (2008) and Lastras *et al.* (2009) focused on the general morphology and large-scale sedimentary structures of the above canyons, on the basis of analysis of seafloor geophysical data. Inferences about late glacial to Holocene sedimentation in the middle and lower reaches of the canyons were made, based on the analysis of piston-cores. Even more recently García *et al.* (2010) published a study on bioavailable organic matter in suspended aggregates and surface sediments, sediment deposition rates and mixing intensities in the Lisbon-Setúbal Canyon.

This chapter is intended to give more insight into the recent sedimentary processes acting in the Lisbon-Setúbal Canyon system by looking at:

1) up- and down-canyon horizontal sediment fluxes obtained by near-bottom measurements of turbidity and current velocities;
2) sediment deposition fluxes measured with sediment traps;
3) sediment accumulation rates measured in cores using ^{210}Pb geochronology;
4) general composition and grain size of surface sediments and suspended particulate matter;
5) bulk and clay mineralogy of surface sediments and suspended particulate matter.

Data on surface sediments from the Cascais Canyon are presented for comparison with the Lisbon-Setúbal Canyon system in terms of sediment accumulation rates, general composition and mineralogical contents of surface sediments. Comparisons with the

Nazaré Canyon will be frequent since a similar approach making use of data collected with sediment traps and surface sediment cores was previously applied to this canyon by De Stigter *et al.* (2007b), covering the entire canyon structure.

6.2. Near-bottom hydrodynamics, horizontal sediment flux and mass deposition flux

BOBO (BOttom BOundary) benthic landers were deployed in the Lisbon-Setúbal Canyon to record current dynamics in the near-bottom water layer, in combination with temporal variation of temperature, salinity, turbidity and mass deposition flux. Seven deployments were done at different depths along the canyon axis: three were done in the Lisbon Canyon (497, 1070 and 1858 m WD), two in the upper Setúbal Canyon (972 and 1324 m WD), one in the middle canyon (2716 m WD) and one in the lower Setúbal Canyon (4402 m WD). One deployment was done on the Afonso de Albuquerque Plateau (1213 m WD).

BOBO lander records of near-bed current dynamics show moderately strong currents in the entire Lisbon-Setúbal Canyon, directed predominantly along the canyon axis and typically alternating in up- and down-canyon direction with a semi-diurnal frequency. Mean current speeds varied between 6.2 and 12.1 cm s^{-1} and were generally higher in the upper canyon reaches (Table 6.1).

In the Lisbon Canyon, deployments at 497 and 1070 m WD (stations 269-02 and 252-34, respectively) were of short duration (7 and 12 days, respectively) and done during summer time (May 2007 and September 2006, respectively). For both deployments, sharp peaks in turbidity, indicating resuspension of sediment from the seabed, occurred when current speed exceeded 20 cm s^{-1} (Figure 6.1a, b). Whereas higher average current speeds and mass deposition fluxes were measured in the deployment at 497 m (269-02) (Table 6.1), both deployments displayed a net up-canyon SPM transport of around 4000 g m^{-2} d^{-1}. Figure 6.2 shows the location of the three BOBO deployments in the Lisbon Canyon.

A different sedimentary setting was found in the lower part of the Lisbon Canyon during a deployment of 12 months at 1858 m water depth (station 225-03). Peaks of current speed above 25 cm s^{-1} were common and only at these current peaks a clear relationship of turbidity and current speed was observed (Figure 6.1c). Although current

speeds recorded during this deployment were similar to those measured in the upper canyon, much lower horizontal and mass deposition fluxes were measured (Table 6.1; Figure 6.4). As illustrated in Figure 6.2, there is a clear decrease of horizontal fluxes with increasing depth along the canyon axis.

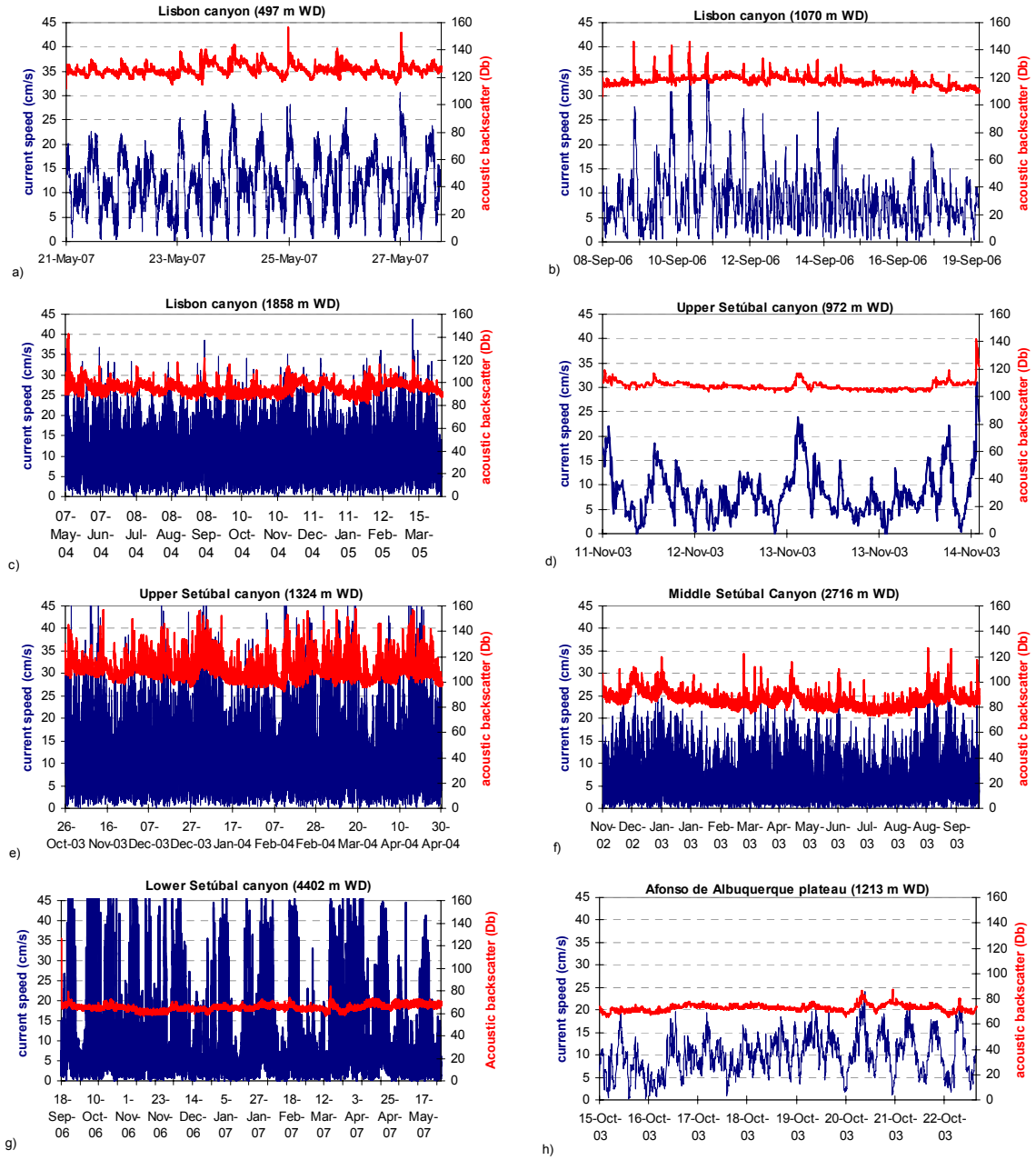

Figure 6.1. Current speed and turbidity (acoustic backscatter) at 1 m a.b., recorded by the BOBO benthic lander at different locations along the Lisbon-Setúbal Canyon system. 6.1a – g refer to canyon axis deployments while 6.1h refers to a deployment made on the adjacent open slope.

Figure 6.3 shows the recorded horizontal fluxes towards different directions for the four deployments done in the Setúbal Canyon and the one at the Afonso de Albuquerque

Plateau. In Appendix A5, current direction, current speed and turbidity are shown for each deployment.

As in the Lisbon Canyon, a general down-canyon decrease of horizontal fluxes (Figure 6.3a, b, c, d) and mass deposition fluxes (Table 6.1, Figure 6.4) was also observed along the axis of the Setúbal Canyon. Considering the entire Setúbal Canyon, a net down-canyon horizontal flux was only recorded at 1324 m WD, representing a net flux of about 2000 g m^{-2} d^{-1} (Table 6.1). The other three deployments displayed negligible horizontal net fluxes (< 100 g m^{-2} d^{-1}). Despite this apparent lack of sediment transport, especially in the middle and lower canyon, the deepest deployment at 4402 m WD recorded relatively high current speeds reaching peaks of 50 cm s^{-1} (Figure 6.1g). These

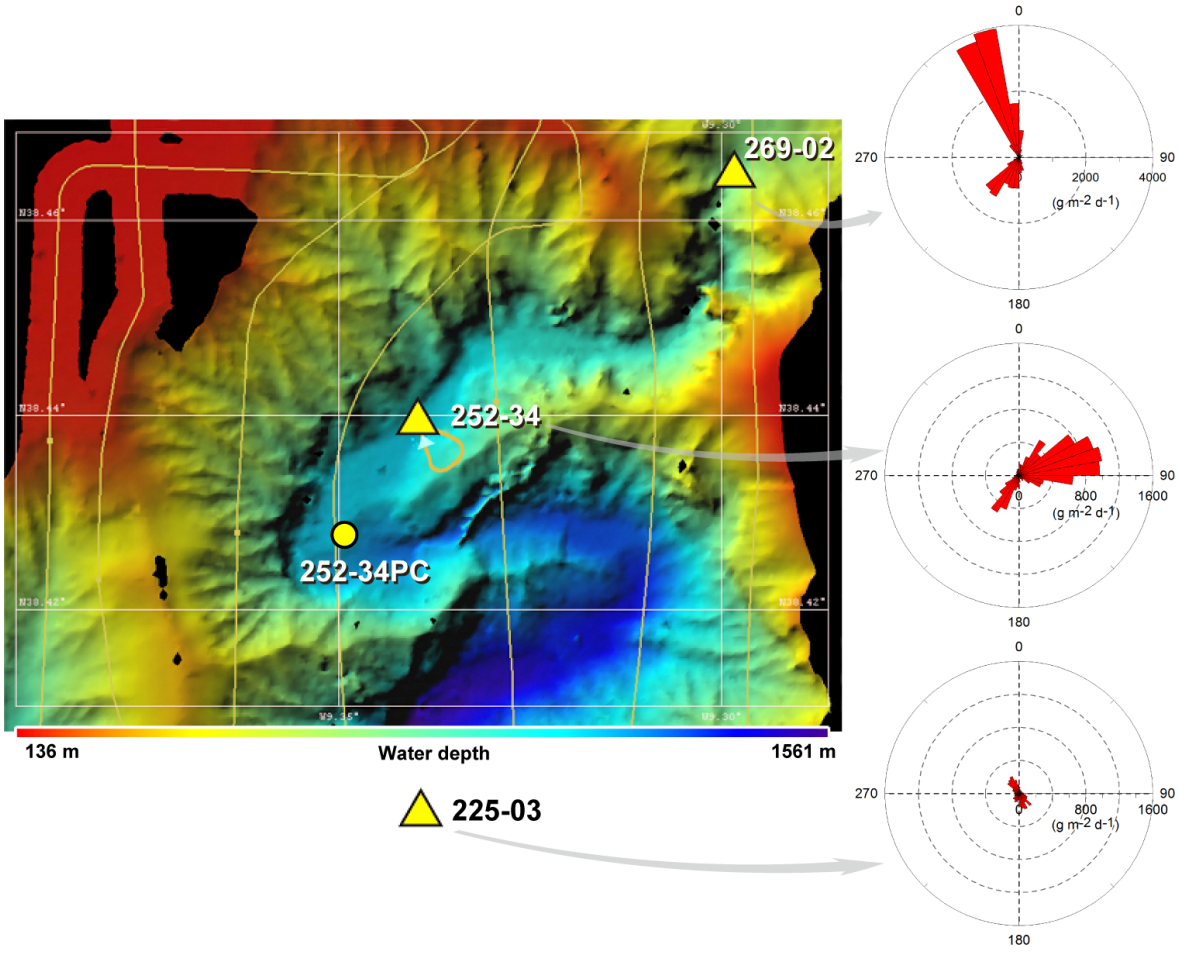

Figure 6.2. A sharp meander bend in the Lisbon Canyon as mapped with the EM300 multibeam echosounder of RV Pelagia (De Stigter *et al.*, 2007a). Depicted area is about 9.5 X 7 km. Yellow circle and triangles indicate positions of BOBO lander deployments and piston core 252-34, respectively. On the right, rose diagrams represent horizontal sediment fluxes in different directions recorded in each deployment of the BOBO lander. Note the different scales used for plotting the fluxes from deployment 269-02 and for the other two (252-34 and 225-03).

peaks in current speed were accompanied by relatively low and stable values of turbidity showing no signs of resuspension. Possibly there was little material to resuspend at this site, in contrast with the upper canyon where fine mud is always abundantly present. Accordingly, sediment deposition rates measured in the sediment trap at 4402 m WD were between 0.4 – 1.4 g m^{-2} d^{-1}, the lowest values measured in the entire canyon and comparable to those measured on the adjacent open slope (see below). The strong along-canyon alignment of currents and their high speed noticed in this record (Appendix 5, Figure A5.2) are in agreement with the observation that the canyon thalweg at this depth lies confined between steep canyon walls of hundreds of meters high (cf. section 3 of Figure 2.6c, on pg. 25 of Chapter 2). Arzola *et al.* (2008) and Lastras *et al.* (2009) reported localised grooving at the Lisbon-Setúbal Canyon mouth (4170 m WD) and related those with enhancement of turbidity currents as a result of narrowing of the canyon by a debris avalanche.

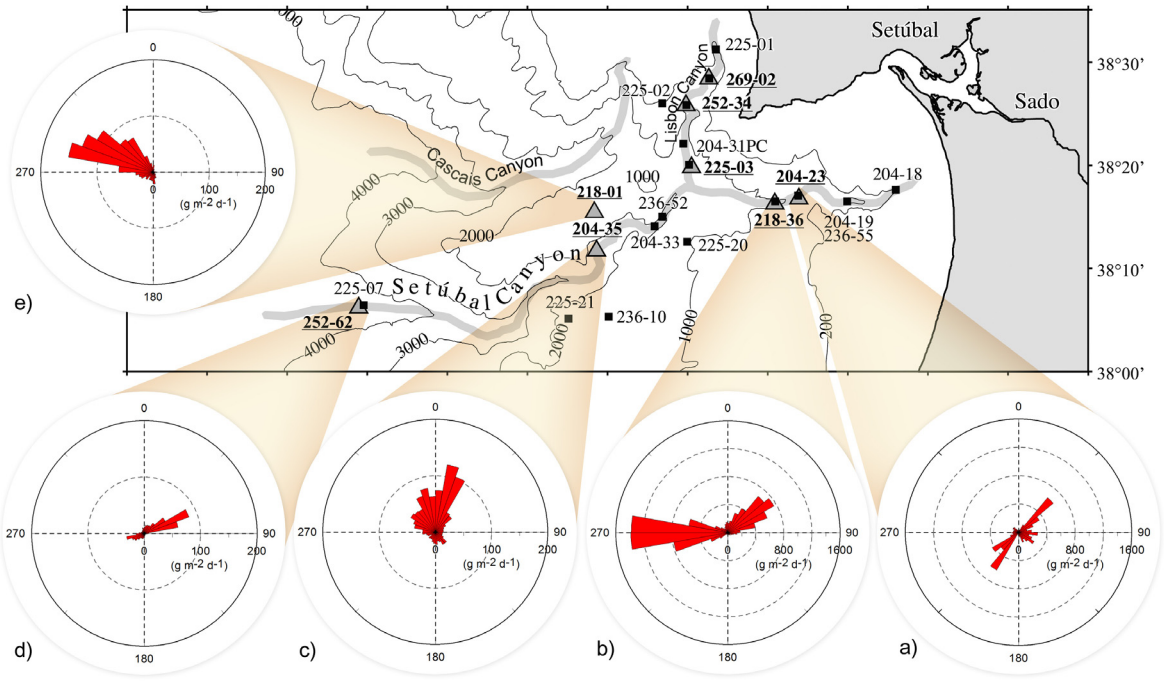

Figure 6.3. Distribution of horizontal sediment fluxes in different directions measured at different deployments along the Setúbal Canyon axis (a-d) and on the adjacent open slope of the Afonso de Albuquerque Plateau (e). Note the different scales used for plots.

During the 8-day deployment at 1213 m WD on the open slope of the Afonso de Albuquerque Plateau (cf. Figure 6.3e) current speed showed a very regular semi-diurnal variation with peaks of current speed above 15 cm s^{-1} occurring almost every cycle. Corresponding peaks in turbidity, indicating resuspension of sediment from the seabed,

Table 6.1. Descriptive characteristics of the near-bottom water masses and particulate fluxes obtained for different deployments done along the Lisbon-Setúbal Canyon system.

Area	Lisbon Canyon			Upper Setúbal Canyon		Middle Setúbal Canyon	Lower Setúbal Canyon	Open slope
Deployment	64PE269-02	64PE252-34	64PE225-03	64PE204-23	64PE218-36	64PE204-35	64PE252-62	64PE218-01
Period	May 21-28 2007	Sep. 09-19 2006	May04 – Mar.05	Nov. 12-14 2002	Oct.03 – Apr.04	Nov.02 – Oct.03	Sep.06 – May05	Oct. 16-23 2003
Water depth (m)	497	1070	1858	972	1324	2716	4402	1213
Mean Temperature (ºC)	12.2 ± 0.1	11.2 ± 0.1	5.7 ± 0.3	11.7 ± 0.04	9.9 ± 0.6	3.1 ± 0.2	2.5 ± 0.01	11.2 ± 0.05
Avg. current speed (cm s^{-1})	12.1 ± 5.7	8.7 ± 5.5	11.4 ± 5.6	8.3 ± 4.9	12.1 ± 7.3	6.2 ± 3.8	8.2 ± 8.3	10.0 ± 4.3
Residual current speed (cm s^{-1})	5.1	4.0	0.9	2.1	4.3	2.4	2.3	6.7
Residual direction (ºN)	295	84	207	133	311	351	49	288
Avg. up-canyon SPM flux (g m^{-2} d^{-1})	10.7 X 10^3	5.5 X 10^3	1.2 X 10^3	2.0 X 10^3	3.0 X 10^3	0.3 X 10^3	0.3 X 10^3	n.d.
Avg. down-canyon SPM flux (g m^{-2} d^{-1})	6.3 X 10^3	1.3 X 10^3	1.3 X 10^3	1.9 X 10^3	4.9 X 10^3	0.3 X 10^3	0.1 X 10^3	n.d.
Net SPM flux (g m^{-2} d^{1})	+ 4.4 X 10^3	+ 4.3 X 10^3	- 0.1 X 10^3	+ 0.1 X 10^3	- 1.9 X 10^3	< - 0.1 X 10^3	+ 0.1 X 10^3	n.d.
Range of mass deposition fluxes (g m^{-2} d^{-1})	42 - 57	27 - 46	4 - 9	9 - 12	14 - 42	1 - 5	0.4 – 1.4	0.3 – 1.2

Fluxes and water displacements – positive values represent up-canyon net results while negative values indicate down-canyon net results. N.d. – not determined.

occurred when current speeds exceeded ~20 cm s^{-1} (Figure 6.1h). Figure 6.3e indicates NW - WNW directed net sediment fluxes in the area, generally along with the poleward flow of the Mediterranean Outflow Water (MOW) along the slope. During this short period of deployment mass sediment deposition fluxes between 0.3 and 1.2 g m^{-2} d^{-1} were recorded.

6.3. Sediment accumulation rates (*vs.* mass deposition fluxes)

Sediment accumulation rates (SAR) measured in cores using ^{210}Pb geochronology vary from 0.8 to 20.8 g m^{-2} d^{-1} in the canyons while on the open slope values range from 0.5 to 2.7 g m^{-2} d^{-1} (Figure 6.4). The relatively lower sediment accumulation rates measured on the open slope (and in the lower canyon) are most probably overestimates. Since a surface mixed layer could not be distinguished from an unmixed subsurface layer, sediment accumulation rates were calculated under the (probably incorrect) assumption that bioturbation is negligible. Even so, the above ranges of values indicate preferential deposition of sediments in the Lisbon-Setúbal and Cascais canyons rather than on the adjacent open slope.

Of the six cores in the Lisbon Canyon for which SARs were determined, the highest value of 20.8 g m^{-2} d^{-1} was measured at ~1100 m water depth while SARs of 15.2 and 3.9 g m^{-2} d^{-1} were measured in other cores collected at 367 and 1856 m WD, respectively. In the upper Setúbal Canyon a similar pattern was observed with the highest sediment accumulation rate around 1300 m WD; however, comparing both upper canyons, values are consistently higher in the Lisbon Canyon (Figure 6.4). Down-stream after the merging of the two canyon branches, SARs tend to decrease with depth reaching a value of 0.8 g m^{-2} d^{-1} around 4400 m WD. In the Cascais Canyon there is a regular offshore decrease of sediment accumulation rates from 11.0 g m^{-2} d^{-1} at 445 m WD down to 1.4 g m^{-2} d^{-1} at 3900 m WD.

SARs on the Sines open slope are comparable to those in the slope adjacent to the Lisbon-Setúbal Canyon, ranging between 0.5 and 3.1 g m^{-2} d^{-1}. On the Estremadura and Mondego open slopes, located northwards of the above canyon, SARs are generally lower than at comparable depths on the Sines open slope.

By dividing the dry bulk density of the 0-0.5 cm slice of sediment cores by the SAR values obtained for the cores, average linear sedimentation rates of 0.39, 0.19, 0.13 and

0.06 cm yr.$^{-1}$ were determined for the upper (Lisbon and Setúbal), middle and lower canyon reaches, respectively, and 0.09 cm yr.$^{-1}$ for the adjacent open slope. Thus, 0.5 cm of sediment (the slicing interval for the surface sediment here considered) is equivalent to ~1.5 - 4 years of accumulation in the upper and middle Lisbon-Setúbal Canyon, and to ~6 - 8 years in the lower canyon and slope regions.

For both the Lisbon and Setúbal Canyon, sediment deposition fluxes measured in traps deployed upstream of 1500 m WD are higher than SARs determined for cores collected at corresponding water depths (Figure 6.4). This is most likely due to cumulative trapping of resuspended sediment clouds produced during consecutive tidal cycles. On the other hand, in the lower-canyon (and conceivably in the middle-canyon) where resuspension events are less common, sediment fluxes measured in traps span a range of values comparable to sediment accumulation rates obtained in nearby sediment cores.

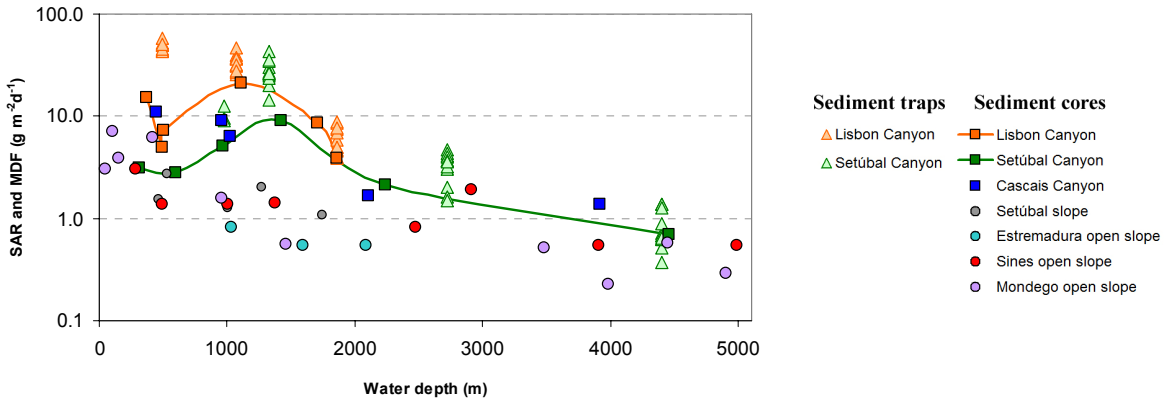

Figure 6.4. Sediment accumulation rates measured in the seabed sediment cores based on ^{210}Pb chronologies (SAR) and mass deposition flux (MDF) measured in traps against water depths in the Lisbon-Setúbal Canyon, Cascais Canyon and different open slope transects. Data for the Mondego open slope from Guerreiro *et al.* (unpublished data).

Episodic high sediment fluxes were not observed in the sediment trap time series for any of the seven deployments within the canyon, suggesting that sediment gravity flows like the ones described for the Nazaré Canyon by De Stigter *et al.* (2007b) are not frequent in the Lisbon-Setúbal Canyon. Over a time span that is comparable to that represented by the sediment traps of the present study, these authors observed a number of events occurring at various depths along the Nazaré Canyon axis, with sediment fluxes 5 to 50 times higher than the average flux for a given deployment.

6.4. General characteristics of surface sediments and suspended particulate matter (grain size, general composition and C_{org}/N ratios)

6.4.1. Surface sediments

Surface sediment cores brought up from the axis of the Lisbon-Setúbal Canyon consisted of soft muddy sediment with very little coarse material. Reduced dark grey to black sediment below a thin oxidized surface layer indicated a high content of organic matter. Piston-cores collected from the Lisbon and upper Cascais canyons (252-34 and 252-36, respectively) consisted also of dark olive grey silty clay, with intercalations of medium sand (De Stigter *et al.*, 2004 and 2007a). In a core collected from the lower Setúbal Canyon (225-07), a turbiditic sand layer at 15-20 cm depth indicates sporadic mass transport of sand-sized material. Multi-cores collected in the slope adjacent to the canyon (236-10, 225-20, 225-21) and at the open slope transects consisted of yellowish grey carbonate-rich silty clay with a well-developed oxidised layer (De Stigter *et al.,* 2004 and 2007a). Pteropod shells and living arborescent foraminifera were commonly found on the surface (Figure 3.6).

Surface sediments from the upper reaches of the Lisbon-Setúbal as well as the Cascais Canyon have modal grain sizes generally between 8 and 50 µm, and occasionally coarser than 50 µm, whereas finer modes less than 8 µm are found in the middle and lower reaches of these canyons (Figure 6.5). On the adjacent shelf and upper slope, coarser sediments are generally found with modes coarser than 65 µm, and locally at depths between 500 and 1500 m even coarser than 150 µm. At greater depths, open slope sediments have finer grain size modes below 8 µm. Surface sediments in the Nazaré Canyon tend to be slightly coarser than sediments at comparable depth in the other canyons, especially in the middle and lower reaches of the Nazaré Canyon where modes approach 50 µm. Only in the deepest cores from the canyon, fine grain size modes were observed, comparable to those in the lower reaches of the Lisbon-Setúbal and Cascais canyons and the lower slope.

Variation in surface sediment bulk composition is presented in Figure 6.6 for different bathymetrical transects (Lisbon-Setúbal and Cascais canyons and adjacent slope, Nazaré Canyon, Sines, Estremadura and Mondego open slopes). Canyon surface sediments are composed of 72 – 87 % non-carbonate lithogenic material, 10 – 25 % carbonate, and 1.4

– 5.0 % organic matter while surface samples from the adjacent slope are composed of 69 – 78 % non-carbonate lithogenic material, 20 – 27 % carbonate and 1.4 – 2.8 % organic matter. In both the Lisbon and Cascais canyons the highest contents of lithogenic material are found in the canyon head, decreasing down-canyon until around 2000 m water depth where contents reach values of 73 and 75 % respectively (Figure 6.6a, c). In the upper Setúbal Canyon, contents of non-carbonate lithogenic material are lower and also tend to decrease with increasing water depth, reaching values of 73 % already at 595 m water depth (Figure 6.6b). Below 2000 m water depth, contents of non-carbonate lithogenic material show a slight increase with depth in both the Lisbon-Setúbal and Cascais canyons. Contents of organic matter are higher in the canyon sediments than in sediments of the adjacent slope (Figure 6.6d). Along the canyon axis higher concentrations of organic matter appear in sediments collected around 500-1300 m WD in the Lisbon Canyon and upper Setúbal Canyon, corresponding to the areas with the highest sediment accumulation rates, and around 900-1000 m WD in the Cascais Canyon. Surface sediments from the Nazaré Canyon have contents of non-carbonate lithogenic materials consistently above 80 %. Biogenic silica, which in the present study is included in the non-carbonate fraction, presumably contributes very little to the bulk of surface sediment and sediment trap samples according to the XRD analysis. However, since most of the biogenic silica is amorphous and present in relatively low amounts, XRD analysis is not a good method to identify the presence of this mineral.

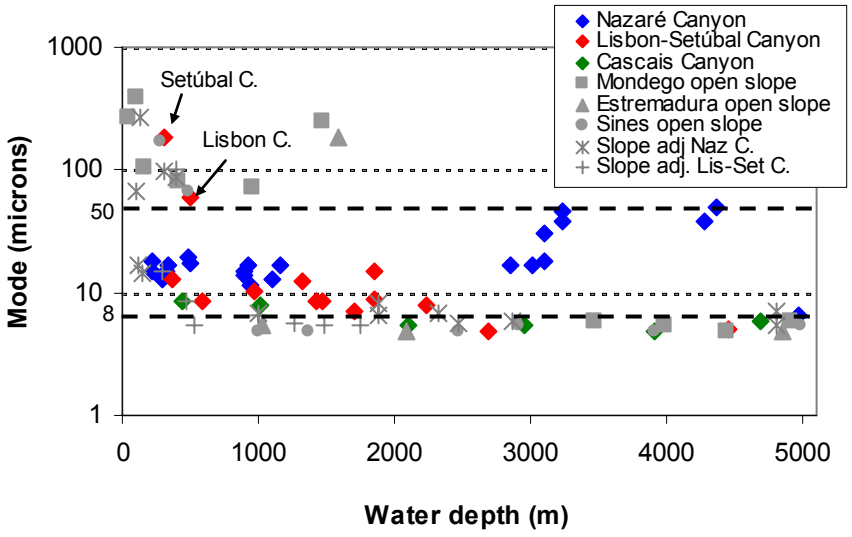

Figure 6.5. Modal grain size of surface sediments against water depth for different environments in the central Portuguese margin: Nazaré, Lisbon-Setúbal and Cascais canyons; Sines, Estremadura and Mondego open slopes. Data from the Mondego open slope from Guerreiro *et al.* (unpublished data).

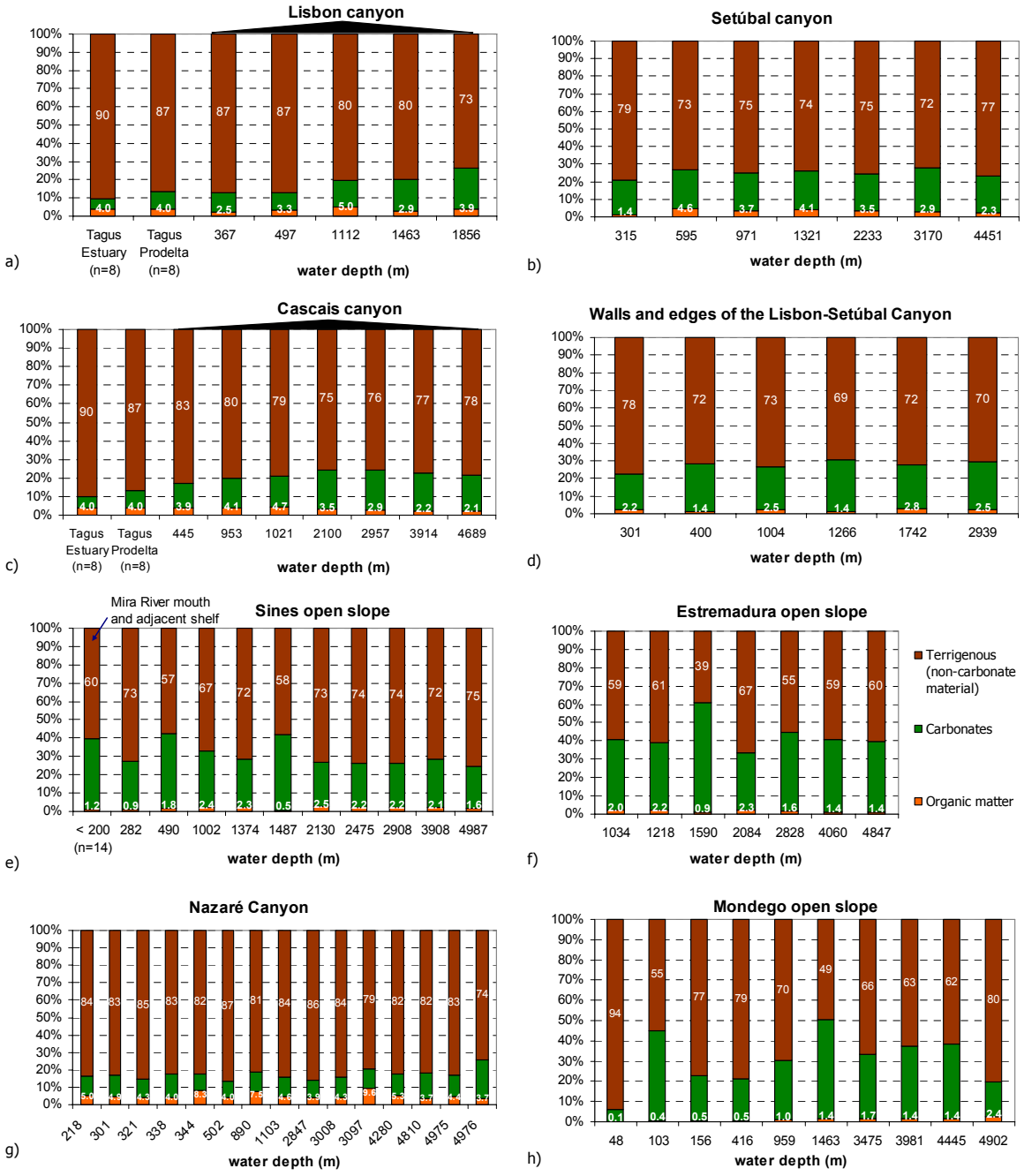

Figure 6.6. Variation in content of lithogenic material, carbonate and organic matter in surface sediments collected in different environments of the Portuguese margin (canyons, walls and edges of canyons and open slopes). The concentration of lithogenic material and organic matter is indicated within each bar. Data for the Tagus Estuary and prodelta (in 6.6 a, c) and Mira River mouth and adjacent shelf data (in 6.6 e) according to Alt-Epping *et al.* (2007). Data for the Mondego open slope from Guerreiro *et al.* (unpublished data).

Compared to canyon sediments, surface sediments from the open slopes of Sines, Estremadura and Mondego have lower contents of lithogenic material and organic matter, with the lowest contents occurring on the Estremadura open slope. In all three open slope

transects there is a conspicuous maximum in carbonate contents around 1500 m WD and also around 500 m WD in the Sines transect, which corresponds to relatively coarse winnowed sediments rich in foraminifera.

6.4.2. Suspended particulate matter (*vs.* surface sediments)

Particulate matter collected in sediment traps consisted of silt- to clay-sized material with very little coarser material. As an example, grain size analyses of twelve trap samples from deployment 218-36 (upper Setúbal Canyon, 1324 m) show volume percentages of clay-sized particles between 12 and 17 %, silt between 79 and 84 % and sand between 4 and 6 %. Figure 6.7 compares grain size spectra of sediment trap samples from deployment 218-36 with the grain size spectrum of the underlying surface sediment. The latter shows a relatively broad grain size mode around 10 µm, apparently integrating fluctuations in grain size of settling material with modes of 5 to 20 µm observed in the sediment trap samples.

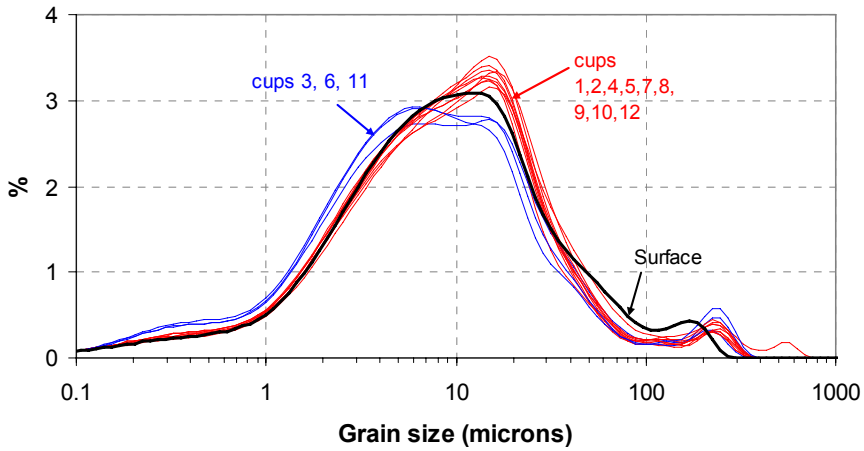

Figure 6.7. Grain size spectra of sediment trap samples from deployment 218-36 and underlying surface sediment.

The bulk composition of suspended particulate matter collected in sediment traps is presented in Figure 6.8. Composition did not vary much between samples from the same deployment, except for deployment 218-36 as discussed below. Clear differences, however, were observed between samples collected from different sites within the canyon. Suspended particulate matter collected in the sediment trap at 497 m in the Lisbon Canyon had the highest contents of lithogenic material and organic matter of all

deployments, and the lowest contents in carbonate. In this canyon, lithogenic contents were found to decrease down-canyon whereas carbonate content showed a relative increase, probably reflecting a reduction of terrigenous material input. Organic matter reached the highest values in the trap deployed at 1070 m WD. In general, the upper Setúbal Canyon showed the lowest contents of lithogenic material, and highest contents of carbonate, varying from 25 – 27 % at 972 m WD to 24 – 37 % at 1324 m WD. Highest contents of organic matter in the Setúbal Canyon were observed in the shallowest deployment (5.2 - 5.9 %). In the middle and lower Setúbal Canyon particulate matter collected in sediment traps had lithogenic and carbonate contents representing intermediate values relative to those of the two upper canyon branches. Organic matter increased further down-canyon from 3.6 – 4.9 % at 2716 m WD up to 4.9 – 5.7 % at 4402 m WD (Figure 6.8g and h).

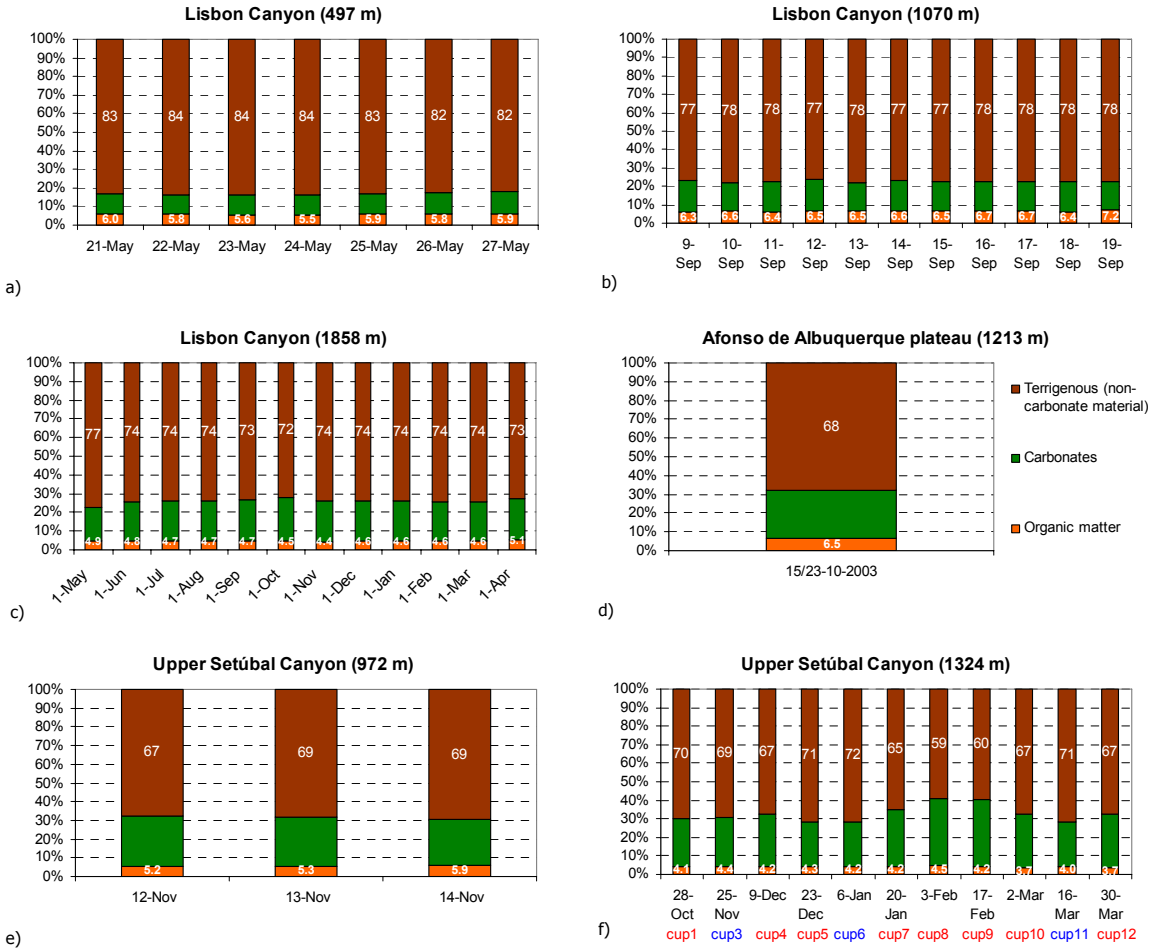

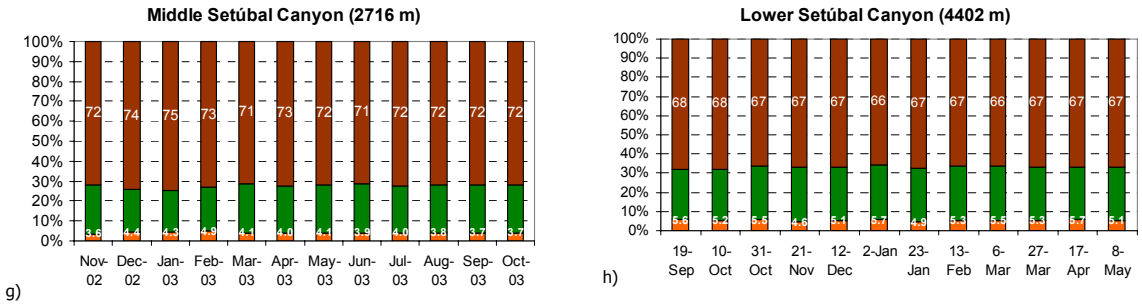

Figure 6.8. Variation in lithogenic, carbonate and organic matter contents of suspended particulate matter collected in sediment traps deployed at various depths along the axis of the Lisbon-Setúbal Canyon and on the Afonso de Albuquerque Plateau. The concentration of lithogenic material and organic matter is indicated within each bar. Numbering of cups and colour codes used in panel f correspond to those used in Figure 6.7.

In Figure 6.9 C_{org}/N ratio of organic material in sediment trap samples is plotted against carbonate content. The two parameters show a distinct negative relationship: samples with lowest carbonate content, and hence highest lithogenic content, contain organic material with C_{org}/N ratio around 10 indicative of organic material of mixed marine and terrigenous origin. Conversely, samples richest in carbonate, and hence lowest in lithogenic material, contain organic matter with low C_{org}/N ratio around 7, indicative of a prevalence of marine organic material. Whereas for most sediment trap deployments the samples tend to cluster closely together, the samples from deployment 218-36 show a conspicuously wide range of carbonate concentrations and C_{org}/N ratios, indicating a variable supply of terrigenous and marine material. For the entire set of sediment trap samples, carbonate content tends to be negatively correlated with mass deposition flux, suggesting that carbonate content is predominantly determined by dilution with terrigenous sediment rich in lithogenic material. This is not the case, however, for the samples of 218-36, where carbonate contents show no relationship with mass flux. This fact will be further discussed in section 6.7.1.

Whereas most sediment trap samples plotted in Figure 6.9 fall within a fairly narrow band of C_{org}/N *vs.* carbonate values, samples from traps in the lower Setúbal Canyon (252-62), the Afonso de Albuquerque Plateau (218-01) and the lower Nazaré Canyon (218-55) deviate from this general pattern by having organic matter with higher C_{org}/N ratio for similar carbonate content.

To illustrate trends in the relative proportion of lithogenic material (assumed to be mostly terrigenous) versus carbonate (assumed to be mostly of marine origin) the ratio of lithogenic material versus carbonate (L/C ratio) in sediment trap samples and surface sediments is plotted in Figure 6.10 against water depth. The high L/C ratio in the head of

the Lisbon and Cascais canyons, and its decrease down-canyon shows this ratio is a good indicator for terrigenous sediment input. In accordance, L/C ratios in the open slope samples are consistently lower than ratios obtained in the canyon surface samples for a given water depth.

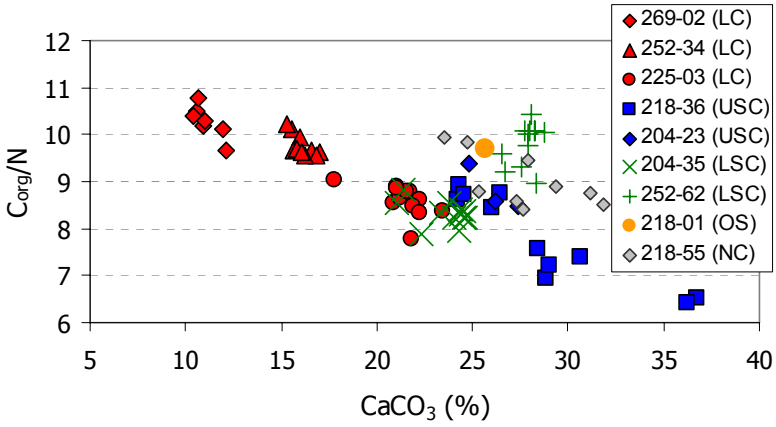

Figure 6.9. C_{org}/N ratio of organic matter in sediment trap samples plotted against carbonate content, for sediment traps deployed along the axis of the Lisbon-Setúbal Canyon and also the lower Nazaré Canyon and Afonso de Albuquerque Plateau. Red symbols: Lisbon Canyon branch (LC); blue: upper Setúbal Canyon branch (USC); green: lower Setúbal Canyon (LSC); grey: lower Nazaré Canyon (NC); orange: Afonso de Albuquerque open slope trap sample (OS).

Samples collected in the two shallowest traps of the Lisbon Canyon (269-02 and 252-34, respectively 497 and 1070 m WD) show lower L/C ratios than surface sediment samples at the same water depth in the canyon. Surface sediment samples with L/C ratios comparable to those of the trap samples are to be found at greater depth down-canyon, according to the trendline indicated in Figure 6.10. Assuming that most of the material trapped in the near-bottom water has undergone multiple cycles of resuspension from the seabed, the similarity of trap samples with down-canyon surface sediments samples would suggest temporary up-canyon SPM transport, as supported by observed up-canyon water transport illustrated in Figure 6.2. For the deepest sediment trap site in the Lisbon Canyon (225-03, 1858 m WD) eleven out of twelve samples have L/C ratios very similar to those found in surface sediments collected at comparable water depths. In the upper Setúbal Canyon, L/C ratios in sediment trap samples are lower than in surface sediment samples from nearby locations. Ratios in trap samples are comparable, however, to the ones obtained for surface sediments of the adjacent open slope, pointing out this area as a likely source of SPM as mentioned above (when referring to Figure 6.9). Further down-canyon at 2716 m WD (204-35), sediment trap samples collected in the course of an

entire year have ratios spanning a relatively narrow range of values and which are comparable to ratios for surface sediments at comparable water depths. Further seawards at 4402 m WD (252-62), the one-year series of trap samples shows consistently lower ratios (comparable to those of shelf/open slope surface sediments) than those of canyon surface sediments collected nearby.

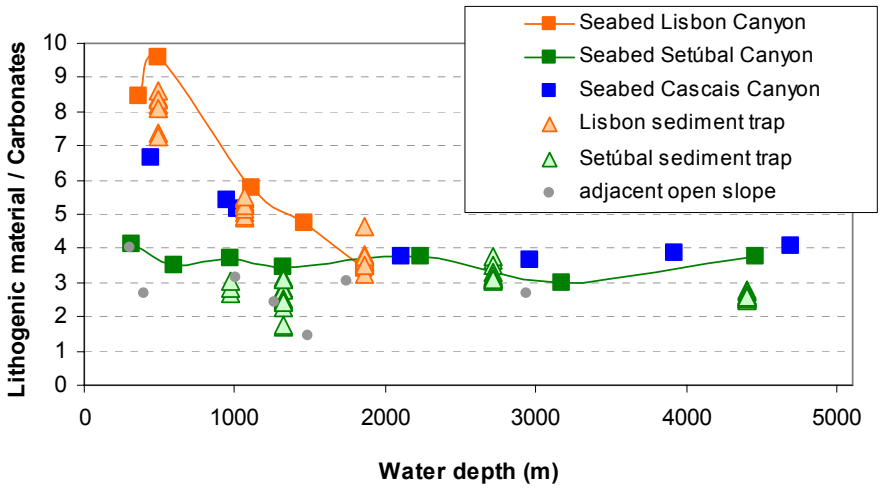

Figure 6.10. Lithogenic / Carbonate ratios in surface sediment and sediment trap samples collected along the Lisbon-Setúbal Canyon and L/C ratios in surface sediments from the adjacent open slope and the Cascais Canyon.

6.5. Bulk mineralogy of surface sediments and mineralogy of < 150 µm suspended particulate matter

Lithogenic detrital components of marine sediments, despite all regional variability, include only few basic minerals. With the exception of quartz, complete weathering, particularly the chemical weathering of metamorphic and igneous rock, leads to the formation of phyllosilicates. Consequently, this group represents, apart from quartz and biogenic sediments, the most important mineral constituent in sediments. To a lesser degree, lithogenic detritus contains unweathered minerals like feldspars. In general, the relevant biogenic minerals for sediment formation are only carbonate minerals in the form of aragonite, Mg-calcite and calcite, as well as biogenic opal in the form of amorphous $SiO_2 \cdot nH_2O$.

6.5.1. Bulk mineralogy of surface sediments from canyons and open slopes

Five main minerals/groups of minerals compose the bulk mineralogy of surface sediments of the canyons and open slopes: calcite, quartz, phyllosilicates, plagioclase and K-feldspars. The bulk mineralogy of the surface sediments from the Lisbon-Setúbal, Cascais and Nazaré canyons and open slope is very similar to the assemblage found in surface sediments from the shelves adjacent to these areas (Chapter 4), except aragonite and Mg-calcite were not identified in surface sediments from the canyons and open slope.

In the Lisbon-Setúbal and Cascais canyons there is an obvious relationship between bulk mineralogy and water depth. Generally calcite (Cc) and phyllosilicates (Phy) increase with water depth whereas quartz (Qz), K-feldspars (Fk) and plagioclase (Plg) follow the opposite trend (Figure 6.11). Throughout the Nazaré Canyon the bulk mineralogy of surface sediments does not have a clear trend with water depth. It is clear, however, that surface sediments in this canyon have an important component of lithogenic material (Cc < 28 % and Qz > 30 %) except around 5000 m WD where calcite is higher than 30 %, and feldspars and quartz are below 4 % and 20 %, respectively (Figure 6.11). With regard to the open slope environment each transect has its own pattern with increasing water depth. In addition to that, each transect comprises a different range of water depths which turns comparison more difficult, especially for the shallower water depths.

Nonetheless, one may observe a general trend in the open slope transects characterised by an increase in contents of phyllosilicates with water depth while quartz and feldspars tend to decrease. These trends are less obvious in the Estremadura transect which covers a smaller water depth range than on the other transects. Calcite content clearly increases with water depth on the Mondego open slope while on the Sines and Estremadura open slopes contents do vary across the open slope yet with no clear relationship with water depth.

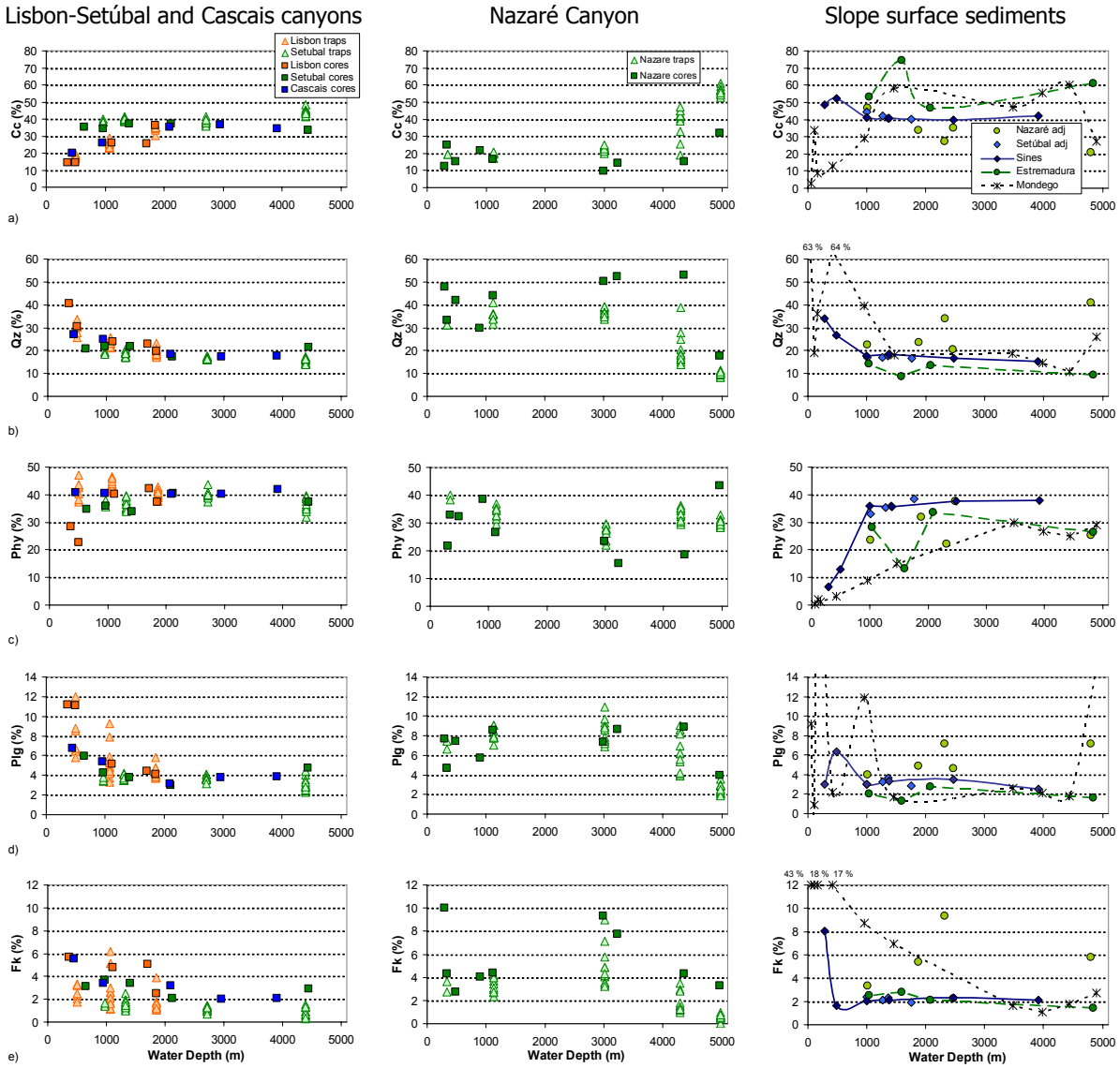

Figure 6.11. Variation with water depth of contents of Calcite - Cc (**a**), quartz - Qz (**b**), phyllosilicates – Phy (**c**), plagioclase – Plg (**d**) and K-Feldspars - Fk (**e**) in surface sediments and sediment trap particulate material collected along the axis of the Setúbal-Lisbon, Cascais and Nazaré canyons and on the open slope.

Some differences between different areas of the central Portuguese margin in general and between canyon and open slope environments in particular are apparent in the mineralogy of surface sediments.

Trends in contents of various minerals with water depth are very similar between the Lisbon-Setúbal and Cascais canyons, especially between the Lisbon and Cascais canyons, but they are generally different from those observed in the Nazaré Canyon. Whereas in the Lisbon and Cascais canyons calcite contents increase from ~15 % around 500 m WD to ~40 % at 2000 m WD, calcite contents remain more or less constant ~15 % in the Nazaré Canyon even at water depths around 4500 m WD. Only toward the deepest part of the canyon contents of calcite appear to increase (Figure 6.11a). In the Setúbal Canyon contents of calcite also remain virtually constant until 4500 m WD yet with higher contents of 34 – 37 %. Contents of quartz and feldspars tend to be higher in the Nazaré Canyon than at equivalent water depths in the southern canyons (Table 6.2 and Figure 6.11). This is especially clear for quartz which shows a difference in contents all the way through the canyons, whereas for feldspars similar contents are observed in the upper reaches of the canyons. Contents of phyllosilicates are again similar in the upper reaches of the canyons but further down-canyon contents are higher in the Lisbon-Setúbal and Cascais canyons compared to the Nazaré Canyon.

Comparing the three open slope areas, the Sines open slope transect has the lowest contents of calcite and highest in phyllosilicates for equivalent water depths. These contents are in good agreement with those of samples collected from the edges of the Lisbon-Setúbal Canyon (Figure 6.11a, c). The Mondego open slope is marked by conspicuously higher contents of quartz and feldspars compared to the other two open slope transects. The Estremadura open slope has the highest contents of calcite.

Lithogenic minerals versus calcite

The ratio of lithogenic minerals Qz+Phy+Fk+Plg against calcite (Cc) highlights the areas more affected by fresh input of terrigenous lithogenic input in a similar manner as the lithogenic/carbonate ratio described in 6.4.2, since normally carbonate contents only increase where input of lithogenic material is relatively low.

In the Lisbon Canyon a pronounced decrease of the Qz+Phy+Fk+Plg/Cc ratio with water depth is observed from the canyon head region down to about 2000 m WD, and a similar pattern is seen in the Cascais Canyon (Figure 6.12a). A markedly lower ratio is observed in the upper Setúbal Canyon, which remains more or less constant with

increasing depth down-canyon. In the Nazaré Canyon the Qz+Phy+Fk+Plg/Cc ratio is generally higher than in the former canyons, and no clear relationship with water depth is seen. All three canyons systems have higher values of the Qz+Phy+Fk+Plg/Cc ratio in the canyon thalweg compared to adjacent open slope areas.

The Qz+Phy+Fk+Plg/Cc ratios in sediments of the Estremadura and Sines open slopes are comparable or lower than those found on the edges and slopes of the canyons. The ratio is slightly higher in the Sines open slope transect compared to the Estremadura open slope and also to the Mondego open slope below 1500 m WD.

Phyllosilicates / Quartz + Feldspars ratio

The Phy/Qz+Feld ratio may give insight into the hydrodynamics of a given area since phyllosilicates tend to settle in calmer areas compared to quartz and feldspars. It might be used as well to track the mineralogical contributions of a given source of sediments.

In both the Lisbon-Setúbal and Cascais canyons there is a general increase of the Phy/Qz+Feld ratio with increasing water depth (Figure 6.12b). The lowest ratio of ~0.5 occurs in the Lisbon Canyon around 350 – 450 m WD, whilst it increases to more than 1.0 around 1100 m WD. In the Nazaré Canyon the ratio remains below 1.0 all the way to the lower canyon but around 5000 m WD the ratio doubles to around 2.0.

In the open slope environment this ratio tends to increase as well with increasing water depth (Figure 6.12b). Both in the Sines and Mondego transects the ratio starts with very low values of < 0.2 on the inner shelf, rapidly increasing to >1.5 at depths around 1000 m WD on the Sines open slope, whereas on the Mondego open slope a more gradual increase with water depth is observed, to values which are lower than on the Sines open slope at equivalent depths. Data for the Estremadura open slope are only available for depths below 1000 m WD, but here the ratio appears comparable to that observed on the Sines open slope. On the slope adjacent to the Nazaré Canyon the ratio is somewhat in between vales observed for the Mondego and Estremadura open slopes.

Feldspars / Phyllosilicates ratio

The ratio of feldspars against phyllosilicates may give insight into the maturity of sediments. Feldspars are less resistant to weathering than phyllosilicates and the former may be precursors of the latter. Since the two mineral groups have very different

hydraulic characteristics this ratio should preferably only be used for comparison of areas with comparable hydrodynamic regimes.

Through most of the Lisbon-Setúbal and Cascais canyons the Felds/Phy ratio in surface sediments gently decreases against water depth. A conspicuously high ratio is observed in sediment in the upper reaches of the Lisbon Canyon (Figure 6.12c).

In surface sediments from the Nazaré Canyon the ratio is more scattered with no clear relationship with water depth. Values are generally higher than those obtained for the southern canyons, which indicates a lower maturity of sediments in the Nazaré Canyon.

Ratios for the shelf and open slope as presented in Figure 6.12c seem to indicate a general decrease of Felds/Phy ratios from the Mondego to the Sines transect. Differences between the northernmost and southernmost transect are most pronounced on the shelf and upper slope, decreasing toward greater depths. Around 3500 m WD both transects have similar ratios. The other studied areas generally have intermediate values for this ratio. On the Mondego open slope there is again an increase of the ratio around 5000 m WD.

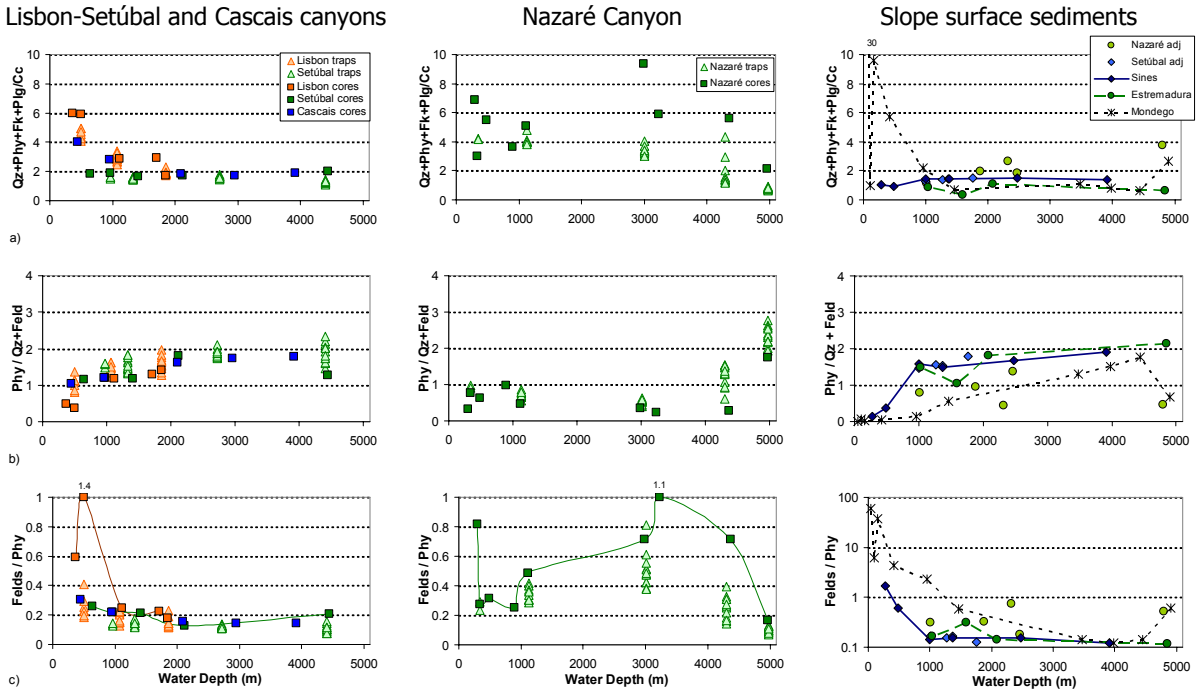

Figure 6.12. Variation with water depth of Qz+Phy+Fk+Plg/Cc ratio (**a**), Phy/Qz+Fk+Plg ratio (**b**), Felds/Phy ratio (**c**) in surface sediments and sediment trap particulate material plotted against water depth for the Lisbon-Setúbal, Cascais and Nazaré canyons and from open slope transects. Note different scales in graphs of panel c.

6.5.2. Mineralogy of < 150 µm suspended particulate matter (*vs.* surface sediments)

Generally the mineralogy of particulate material collected in sediment traps along the canyon axes shows similar trends against water depth to those defined by the surface sediments (Figure 6.11 and 6.12). However, as seen for bulk sediment components in section 6.4.2, contents of various components may differ systematically between trap samples and surface sediments.

Calcite contents in samples from individual sediment trap deployments commonly span relatively narrow ranges and are comparable to values observed in surface sediments at similar water depths, for as much as the upper canyon reaches are considered. However, in deeper areas of the canyons (~4500 m WD in the Lisbon-Setúbal Canyon and already at 3000 m WD in the Nazaré Canyon), sediment trap samples have higher contents of calcite compared to underlying surface sediments (Figure 6.11a). The Qz+Phy+Fk+Plg/Cc ratio shows this same trend along both Lisbon-Setúbal and Nazaré canyons being however more obvious in the Nazaré Canyon.

For phyllosilicates trap samples have normally higher contents than those found in underlying surface sediments. On the other hand, for coarser minerals as quartz and feldspars trap samples have lower contents compared to surface sediments at equivalent water depths. The Phy/Qz+Feld ratio summarises these differences between surface sediment and trap samples which can be tracked throughout the entire canyons, becoming nevertheless more evident in the lower reaches of the canyons. In the upper canyons resuspension processes caused by high bottom currents speeds occur frequently (see section 6.2) allowing coarser minerals to be caught in the sediment traps. In the deeper areas, however, differences between the mineralogy of suspended particulate material and surface sediments become more obvious since resuspension processes do not occur as frequently as in the upper canyon and material caught in the traps therefore represents mainly the pelagic sedimentation.

6.5.3. Comparison between surface sediments from the canyons and adjacent outer shelf and upper slope

Surface sediments from the upper reaches of the Lisbon and Cascais canyons (~350 – 500 m WD) have similar bulk mineralogy with only slight differences: contents of

phyllosilicates are higher in the Cascais Canyon and contents of quartz and plagioclase tend to be higher in the Lisbon Canyon (Figure 6.11). The Lisbon outer shelf and upper slope compared to these canyons has a mean content of phyllosilicates and quartz similar to those found in the Cascais Canyon head (38 and 30 %, respectively). The Lisbon Canyon head sediments, on the other hand have higher contents of plagioclase and quartz than sediments from these two other environments. In fact the Qz+Phy+Fk+Plg/Cc ratio is also higher in the Lisbon Canyon head (6) compared to the Cascais Canyon (4) and also to the outer shelf/upper slope sediments (4).

Surface sediments from the upper Setúbal Canyon branch have relatively constant concentrations of minerals composing the bulk mineralogy. These sediments are characterised by Qz+Phy+Fk+Plg/Cc ratios around 2 and the dominant minerals are calcite and phyllosilicates (~35 % each). It follows quartz, plagioclase and k-feldspars with ~21, 4-6, 3-4 %, respectively (Figure 6.11). The Setúbal outer shelf/upper slope has also a mean Qz+Phy+Fk+Plg/Cc ratio of 2 with similar contents of calcite and phyllosilicates (33 and 23 %, respectively) to those found in the canyon. The Sines outer shelf/upper slope has even lower mean contents of phyllosilicates (18 %), higher mean contents of calcite (43 %) and a mean Qz+Phy+Fk+Plg/Cc ratio of 1.

Table 6.2. Descriptive statistics of minerals determining the mineralogy of sediment trap samples and surface sediment samples collected along the axis of the Lisbon-Setúbal, Cascais and Nazaré canyons and from adjacent slopes and on the Sines, Estremadura and Mondego open slopes. Results are presented as: mean (range).

	Sines open slope	Lisbon-Setúbal Canyon system			Cascais canyon	Estremadura open slope	Nazaré Canyon system			Mondego open slope
	Open slope surface sediments (n = 6) WD Range = 282 – 3908 m	Sediment traps (n = 70) WD Range = 497 - 4402 m	Canyon surface sediments (n = 12) WD Range = 367 – 4445 m	Adjacent slope surface sediments (n = 4) WD Range = 1004 – 1760 m	Canyon surface sediments (n = 5) WD Range = 445 – 3914 m	Open slope surface sediments (n = 4) WD Range = 1034 – 4847 m	Sediment traps (n = 47) WD Range = 343 – 4975 m	Canyon surface sediments (n = 9) WD Range = 301 – 4969 m	Adjacent slope surface sediments (n = 5) WD Range = 1009 – 4798 m	Canyon surface sediments (n = 10) WD Range = 48 – 4902 m
Calcite (%)	44 (40 – 52)	35 (17 – 48)	30 (14 – 37)	33 (21 – 47)	30 (20 – 37)	59 (47 – 74)	35 (17 – 61)	18 (10 – 32)	42 (40 – 44)	34 (3 – 60)
Quartz (%)	21 (15 – 34)	20 (14 – 34)	23 (17 – 40)	28 (20 – 41)	21 (17 - 27)	11 (9 – 14)	25 (8 – 41)	41 (18 – 53)	17 (17 – 18)	31 (11 – 64)
Phyllosilicates (%)	28 (7 – 38)	40 (32 – 47)	36 (23 – 42)	28 (22 – 38)	41 (40 - 42)	25 (13 – 34)	31 (22 – 40)	28 (15 – 43)	36 (33 – 38)	14 (0 – 30)
Plagioclase (%)	4 (3 – 6)	4 (2 – 12)	5 (3 - 11)	6 (4 – 7)	5 (3 – 7)	2 (1 – 3)	6 (2 – 11)	7 (4 – 9)	3 (3 – 4)	8 (1 – 36)
K-feldspars (%)	3 (2 – 8)	2 (0 – 6)	5 (2 – 21)	5 (2 – 9)	3 (2 – 6)	2 (1 - 3)	3 (0 – 9)	6 (3 – 10)	2 (2 – 2)	12 (1 – 43)
L/C	1.3 (0.9 – 1.5)	2.1 (1.1 – 5.0)	2.7 (1.7 – 6.0)	1.4 (1.2 – 1.5)	2.5 (1.7 – 4.0)	0.7 (0.3 – 1.1)	2.5 (0.6 – 4.8)	5.2 (2.1 – 9.4)	2.3 (1.1 – 3.7)	5.5 (0.6 – 30.8)
Phy / Qz+Felds	1.2 (0.1 – 1.9)	1.6 (0.8 – 2.3)	1.2 (0.4 – 1.8)	1.6 (1.5 – 1.8)	1.5 (1.0 – 1.8)	1.6 (1.0 – 2.1)	1.2 (0.4 – 2.8)	0.6 (0.2 – 1.7)	0.8 (0.4 – 1.4)	0.6 (0.0 – 1.8)
Felds/Phy	0.47 (0.12-1.66)	0.15 (0.07 – 0.41)	0.30 (0.13 – 1.42)	0.15 (0.12 – 0.17)	0.19 (0.14 – 0.30)	0.18 (0.12-0.31)	0.30 (0.07 – 0.81)	0.53 (0.17 – 1.07)	0.20 (0.17 – 0.23)	11.23 (0.12 – 60.56)

6.6. Clay mineralogy

6.6.1. Clay mineralogy of canyon surface sediments

As in the surface sediments from the Lisbon, Setúbal and Sines shelves, four groups of minerals were identified in the clay fraction of surface sediments: illite (60 – 93 %), kaolinite (20 – 38 %), chlorite (0 – 5 %) and smectite (0 – 4 %).

Illite

As expected for sediments at mid-latitudes of the northern oceans illite is the dominant mineral in the clay fraction. For the Setúbal Canyon and lower Cascais Canyon as well as for the open slopes and walls and edges of the canyons contents of illite are higher than 70 % (Figure 6.13a). Contents of illite lower than 70 % occur throughout the Nazaré Canyon and also in the Lisbon Canyon and upper Cascais Canyon. For the different transects, contents of illite show no trend with water depth except in the Lisbon and Cascais canyons where there is a clear seaward increase of their contents.

In the southern canyons the Esquevin Index (EI) shows with consistence the following sequence across water depths until ~2000 m: Setúbal Canyon (more Al-rich illites) > Cascais Canyon > Lisbon Canyon (less Al-rich illites). For the Nazaré Canyon values are relatively constant with increasing water depth.

In the Mondego and Sines transects there is a decrease of the EI with increasing water depth until 4000 m WD; from this depth onwards it seems to increase for both transects.

In the southern canyons the Kubler Index (KI) is quite variable compared to the Nazaré Canyon where surface sediments have indices which gradually increase seawards. In the open slope transects of Sines and Mondego lower KIs occur in the shallowest and deepest samples. Across the Estremadura open slope transect the index is quite stable with increasing water depth (Figure 6.13c).

Kaolinite

Contents of kaolinite are generally higher in the Nazaré Canyon (28 – 38 %) than at equivalent depths in the southern canyons (22 – 31 %) and open slope areas (21 – 32 %). In the Setúbal Canyon contents are just slightly higher than those found in the studied open slope areas. The percentages of this mineral tend to decrease with

increasing water depth for the Lisbon and Cascais canyons. In the Setúbal and Nazaré canyons and open slope transects there are no clear trends with increasing water depth (Figure 6.13d).

The kaolinite crystallinity index (KCI) indicates the degree of order of the crystalline structure. The higher the value the less ordered the structure is. Referring to the classification defined in Chapter 4 (Figure 4.17, on pg. 95), KCI is low (crystalline kaolinites) throughout the Setúbal Canyon with no significant variation. Similar to what is observed on the Lisbon shelf (Chapter 4), crystalline kaolinites also occur in the upper reaches of the Lisbon and Cascais canyons (~300 m WD). At 1000 m WD in both canyons a conspicuous increase in the index indicates the presence of semi-degraded and degraded kaolinites. Further down-canyon, the KCIs decrease reaching again low values (crystalline kaolinites similar to those observed in the upper canyon) at 2000 m WD. From this point downwards the KCI stays relatively low only with a slight increase in the Cascais Canyon. In general, the Nazaré Canyon has low KCIs (crystalline kaolinites) comparable to those observed in the Setúbal Canyon with increments of the index around 400 – 900 m and below 3200 m WD. In the walls and slopes of the canyons values are comparable to those observed in the thalweg of the canyons. In the open slope environment values are more variable but tend to be higher than those from the canyons. Below 1000 m WD there is an increment of the index around 1500 m WD for the Sines and Estremadura open slopes. This fact will be discussed in section 6.7.3. The Mondego transect has more stable values below 1000 m WD than the above transects with a gentle increase of the KCI with water depth.

Smectite

Contents of smectite in surface sediments are low compared to the other clay minerals, with values ranging from 0 to 4 %. Most of the samples have smectite contents below 2 % except for the entire Mondego transect and between 900 and 1500 m WD in some of the other transects; from the seven transects studied, only in the Setúbal and Nazaré canyons and on the Mondego open slope this increase was not detected.

Chlorite

Chlorite contents span a relatively narrow range of values in surface sediments from the studied canyons (< 4 %) and open slope areas (< 6 %). The Setúbal and Nazaré canyons (< 2 %) have consistently lower contents of chlorite than the Cascais Canyon.

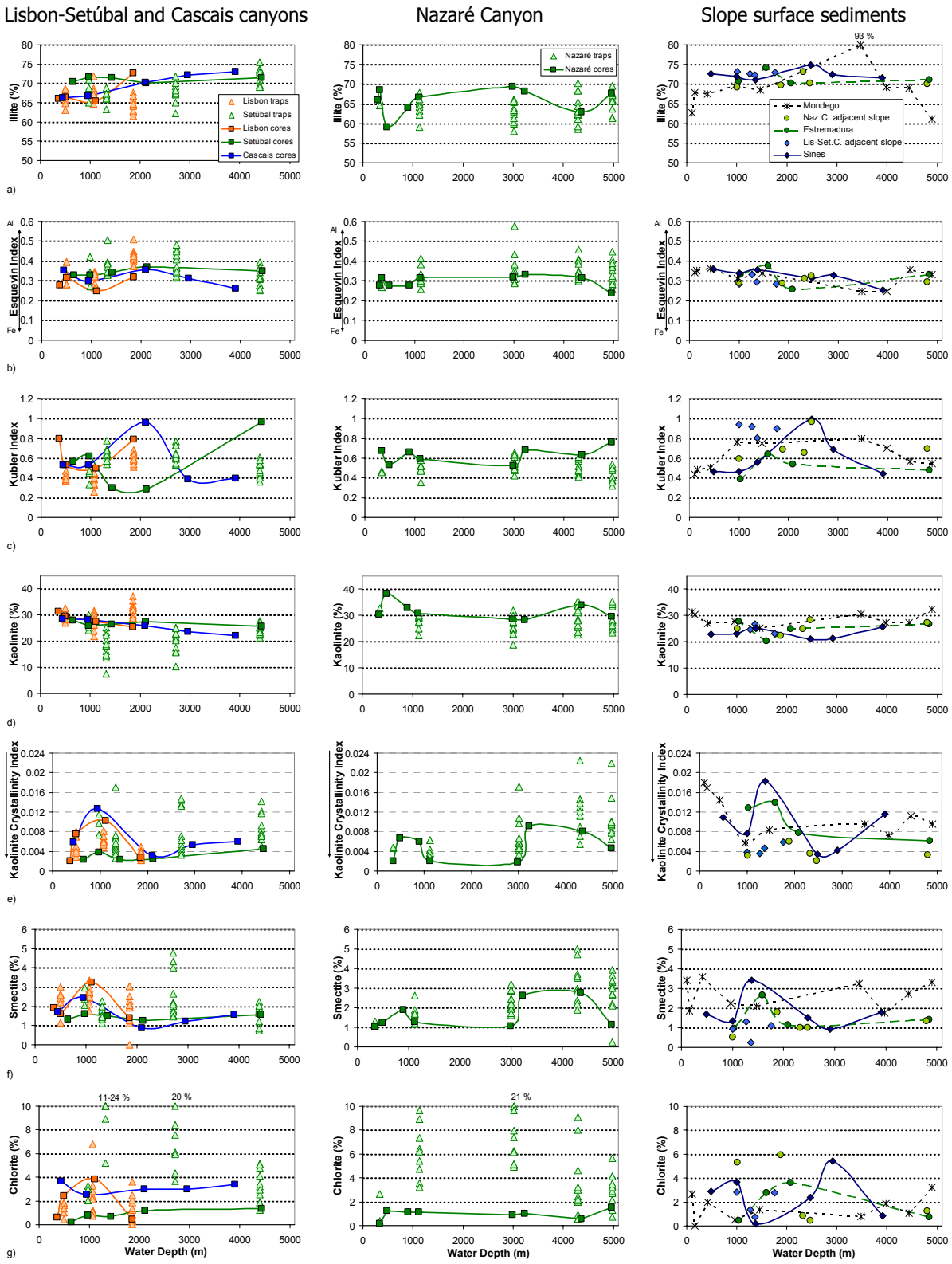

Figure 6.13. Variation with water depth of contents of illite (**a**), Esquevin Index (**b**), Kubler Index (**c**), contents of kaolinite (**d**), kaolinite crystallinity index (**e**), contents of smectite (**f**) and contents of chlorite (**g**) in surface sediments and sediment trap particulate material collected from the Setúbal-Lisbon, Cascais and Nazaré canyons and open slope.

The Lisbon Canyon shows a wider range of contents. Chlorite contents generally do not show a clear trend with water depth. Only in the Lisbon Canyon there is a conspicuous increase around 1100 m WD.

6.6.2. Clay mineralogy of suspended particulate matter

The clay mineralogy of particulate matter collected in sediment trap shows a wide variability and is also generally different from that of the underlying surface sediments (Figure 6.13). Generally, smectite and chlorite tend to have higher contents in sediment trap samples than surface sediments.

The only clear trend against water depth is observed for smectite, which in the Nazaré Canyon increase with increasing water depth.

In general, the Esquevin Index in sediment trap samples spans a wide range of values with tendency to be higher than in the underlying surface sediments. For the Kubler Index one may find the opposite trend in the Nazaré and Lisbon canyons: the index tends to be lower in the trap samples compared to underlying sediments. In the Setúbal Canyon this is only found in some areas of the canyon.

For the kaolinite crystallinity index values span a wide range of values and are generally higher (less ordered structure) in the trap samples compared to the underlying surface sediments.

6.6.3. Comparison between surface sediments from the canyons and adjacent outer shelf and upper slope

The clay mineralogy of surface sediments from the upper reaches of the Lisbon and Cascais canyons (~350 – 500 m WD) is very similar between both canyons. Illite and smectite contents are the same in both canyons with 66 and 2 %, respectively. Kaolinite has higher contents in the Lisbon Canyon than on the Cascais Canyon (31 and 28 %, respectively) while the opposite is true for chlorite (1 and 4 %, respectively). Mean concentrations of clay mineralogy from 9 surface sediments collected on the Lisbon outer

shelf/upper slope are very similar to those found in the upper reaches of the canyons with slightly higher contents of kaolinites (32 %).

The upper reaches of the Setúbal Canyon have more mature surface sediments compared to the Lisbon and Cascais canyons as seen by its lower kaolinites contents (28 %) and higher contents of illite (70 %). Chlorite and smectite compose the remaining 2 %. Both Setúbal and Sines outer shelves/upper slopes have similar clay compositions to the one found in the Setúbal Canyon. The Sines outer shelf/upper slope has slightly higher contents of smectite while the northern outer shelf/upper slope has slightly higher contents of kaolinite.

6.7. Discussion

6.7.1. Recent sediment transport and deposition in the Lisbon-Setúbal Canyon

Upper-canyon branches: Lisbon Canyon and upper Setúbal Canyon

Previous work on submarine canyons has established that they may constitute major pathways for the transport of sediment (and associated organic matter) from land to the deep ocean, depending on the interplay of various factors. Horizontal and mass depositional sediment fluxes are important indicators of the effectiveness of submarine canyons in capturing sediments and transporting them to deeper areas.

Relatively high sediment fluxes recorded in sediment traps and in seabed deposits of the canyons on the central Portuguese continental margin are clear evidence of the dynamic sedimentary environment present within these canyons. SPM concentrations (De Stigter *et al.*, in press) and sediment accumulation rates (SAR) in the upper canyon reaches are an order of magnitude higher than the ones measured at comparable depths on adjacent slope areas (Figure 6.4), and values reported from other parts of the western Iberian margin (Faugères *et al.*, 1984; McCave & Hall, 2002; Oliveira *et al.*, 2002; Van Weering *et al.*, 2002).

Sediment accumulation rates (SARs) measured in seabed sediment cores along the thalweg of the Lisbon-Setúbal Canyon show considerable variation with depth. The highest values occur between 1100 and 1400 m WD for the Lisbon Canyon and upper Setúbal Canyon. The highest sediment deposition fluxes measured in sediment traps from the Lisbon Canyon and upper Setúbal Canyon occur around 1100 and 1400 m WD, respectively. In the upper canyon reaches mass deposition fluxes estimated using sediment traps are consistently higher than SARs determined in the seabed. This is most likely due to cumulative trapping of resuspended sediment clouds produced during consecutive tidal cycles. In these same areas, De Stigter *et al.* (2004 and 2007a) detected well-developed bottom and intermediate nepheloid layers (BNLs and INLs) around the intersections of the canyon floor with the upper (500 m) and lower (1500 m) boundaries of the MOW while further down of the 1500 m isobath intermediate and deep waters apparently cleared up. The only exception was a bottom nepheloid layer of about 500 m

thick, observed in May 2004 at 2603 m WD (cruise 64PE225). The interaction of the MOW with the canyon seabed seems to favour resuspension of sediments which are potentially transported by internal tides cycles. At 500 m and between 1000 and 1500 m WD currents reach high speeds allowing cycles of deposition-resuspension.

Despite the high efficiency of the traps, as indicated in Chapter 3 (pg. 53), the comparison between mass deposition flux intercepted by sediment traps and SARs based on ^{210}Pb chronologies, as applied above for the upper canyons may raise questions because SARs are calculated on a longer time scale (~100 years) with regard to the daily/monthly/annual trap experiments here presented. Despite this, the comparison between both sets yields consistent information which is in accordance with other independent data such as near-bed current speeds.

Deployment 218-36 in the upper Setúbal Canyon, which lasted for around 6 months, recorded a considerable temporal variation in composition of the mass deposition flux. Different from what was observed in other deployments in the Lisbon-Setúbal Canyon, carbonate contents of trap samples of deployment 218-36 show no relationship with mass flux. The samples high in carbonate and with low C_{org}/N ratio (Figure 6.9) thus do not represent periods with reduced supply of lithogenic material through the canyon, but may reflect enhanced input of sediment from the adjacent open slope. Alternatively, but most unlikely as this was not seen in the other deployments, the higher concentrations of carbonate found between middle January and middle March 2004 (four samples) may represent a change in planktonic community in the water column (calcareous shelled groups *vs.* non-calcareous shelled groups), not necessarily accompanied by a change in primary productivity since concentrations of organic carbon did not increase significantly in this period (Figure 6.8f). In the upper Setúbal Canyon, surface sediments collected from the seabed have higher lithogenic material than particulate matter collected in sediment traps at equivalent water depths (by comparing Figure 6.6 with 6.8 and more explicitly in Figure 6.10). The mineralogical composition of surface sediments and trap sample also shows some differences. Smectite has higher contents in trap samples compared to the underlying sediments while the opposite is observed for kaolinite (Figure 6.13 d, f). Figure 6.10 shows how material collected in traps of two deployments in the upper Setúbal Canyon have similar L/C ratios as surface sediments from the adjacent open slope. Therefore, most of the material in trap samples collected in the upper Setúbal Canyon seems to be derived from the adjacent slope/shelf, probably from the southern

slope/shelf where surface sediments are characterised by low contents of lithogenic material (L/C < 2, compare Figure 4.11 with 6.12a); low kaolinite contents (< 30 %, compare Figure 4.16 with 6.13d) and relatively high smectite contents (> 1 %, compare Figure 4.18 with 6.13f). On the other hand, surface sediments of the upper Setúbal Canyon represent the integrated input of sediment over a longer period of time, with contributions from the Setúbal shelf (Sado mud patch or possibly directly from the Sado River) north of the canyon, as suggested by similarity in mineralogy in 6.5.3.

From the higher SARs determined for surface sediments, and higher contents of lithogenic material and more terrigenous C_{org}/N signature of organic matter, it appears that the Lisbon Canyon receives larger quantities of sediment from the near-shore area than the upper Setúbal Canyon. This is in accordance with the proximity of the Lisbon Canyon to the Tagus River, a much more important river in terms of annual mean discharge than the Sado River which feeds the upper Setúbal Canyon (cf. Chapter 2, pg. 40). As illustrated in Figure 6.6a, surface sediment from the Lisbon Canyon head shows a great similarity in composition with sediments from the Tagus prodelta (described by Alt-Epping *et al.*, 2007). Most of the L/C ratios obtained for the Lisbon shelf area range between 6 and 10 (Figure 4.11), comparable to L/C ratios between 8 and 10 found in surface sediments from the head of the Lisbon Canyon. Garcia (1997) reported bottom nepheloid layers on the Lisbon shelf directed towards the Lisbon Canyon under influence of waves and wind from southwesterly direction. Thus, these bottom nepheloid layers are conceivably caused by resuspension of shelf sediments, which can probably reach the Lisbon and Cascais canyons during SW storms. However, the conspicuous decrease in L/C ratio in surface sediments further down the Lisbon Canyon suggests that, despite the high input of terrigenous sediment to the canyon head, there is no substantial down-canyon transport of sediments down the canyon. Conceivably, the strong meandering of the Lisbon Canyon at water depths between 1000 and 1500 m may form an obstruction to down-canyon transport of sediments. In fact the highest SAR measured in the whole canyon (20.8 g m^{-2} d^{-1}) was measured in a piston core (252-34) collected just up-slope from where the canyon makes an almost complete 180º bend (Figures 6.2 and 6.4). In addition, the highest concentration of organic matter (5 %) is also found in this same core (Figure 6.6a) suggesting high input and rapid burial of organic material with little time for mineralization. The two BOBO lander deployments located up-slope from this meander bend recorded a net up-canyon water flow, and associated up-canyon SPM

fluxes around 4000 g m^{-2} d^{-1} in both deployments. However, surface sediments collected from nearby these lander deployments show a higher proportion of material derived from the shelf (expressed in e.g. L/C ratio, Felds/Phy ratio, Phy/Qz+Feld ratio) than the material collected in the sediment trap deployments. From this it can be inferred that up-canyon fluxes recorded with BOBO landers are intermittent in nature, and may alternate with periods with predominance of down-canyon transport. Obviously, the short duration of 7-10 days of the upper canyon deployments is not sufficient to determine whether the observed up-canyon flow is an intermittent feature, alternating with down-canyon flow, or is representative for the longer term circulation in the canyon. Nevertheless, surface sediment characteristics suggest a decrease in down-canyon transport further down the Lisbon Canyon, possibly as a result of the morphology of the canyon. In the latter case of more or less permanent up-canyon flow, it might be related to local diversion of the along-slope flow of Mediterranean Outflow Water as it encounters the canyon. Then, the conspicuous maximum in L/C ratio in surface sediments near the head of the Lisbon Canyon, and decrease further down-canyon, may in fact reflect the dumping of dredged sediments from the Tagus Estuary in the Lisbon Canyon, and subsequent up-canyon dispersal by currents. Recent information from the APL (Administração do Porto de Lisboa – Administration of the Harbour of Lisbon) shows that 8000 m^3 and 7500 m^3 of contaminated sediments dredged from the Tagus Estuary were discharged in the Lisbon Canyon in 2005 and 2007, respectively (Nemus, 2011). The area used has a radius of 200 m and central point at Longitude 09º 19' W and Latitude 38º 29' N (ED50) at around 400 m of water depth (Figure 6.14). According to the APL this same area has been used by other institutions for discharge of sediments (e.g. military institutions which also dredge the estuary). The relative impact of these discharges on the natural sedimentary system of the Lisbon Canyon may be assessed by comparing the total mass of dumped sediment to an order of magnitude estimate of the annual sediment accumulation in the canyon thalweg. Taking 38 km for the length of the canyon (Lastras *et al.*, 2009) and 1 km for maximum width of the thalweg and average sediment accumulation of around 8.75 g m^{-2} d^{-1} (section 6.3) yields an annual sediment accumulation in the Lisbon Canyon of around 12 x 10^{10} g dry weight. Assuming then that 15500 m^3 of known discharges of 2005 and 2007 had a dry bulk density of 1000 kg m^{-3} yields a total dry mass of dumped sediment of 1.55 x 10^{10} g, which is 12.8 % of the annual sediment accumulation in the Lisbon Canyon thalweg and 1.6 % of the annual sediment discharge from the Tagus Estuary into the adjacent shelf.

Middle and Lower Setúbal Canyon

Down-slope of the junction of the Lisbon and upper Setúbal Canyon branches mass depositional fluxes decrease one order of magnitude from 1 – 5 g m^{-2} d^{-1} at 2716 m WD to 0.3 – 1.4 g m^{-2} d^{-1} at 4402 m WD, whereas also SARs measured in surface sediments decrease (Figure 6.4). Low values of bottom water turbidity observed during both lander deployments in the middle and lower canyon (Figures 6.1f and g), and good correspondence between mass deposition fluxes measured in traps and seabed SARs in the lower canyon (Figure 6.4) indicate limited resuspension from the seabed and a prevalence of sedimentation in this part of the canyon. Therefore, in the middle and lower canyon internal tides do not appear to be very effective in transporting sediments in up- or down-canyon directions.

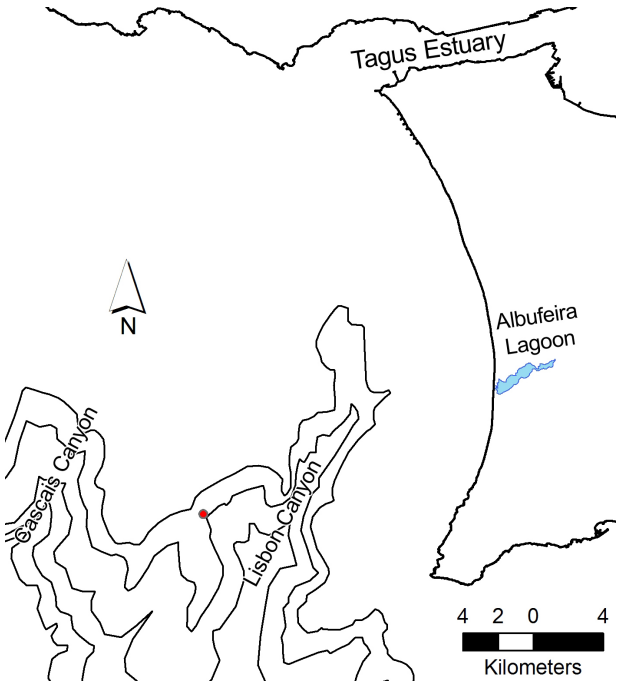

Figure 6.14. Location of the area used by APL and other institutions to discharge contaminated sediments dredged from the Tagus Estuary (marked as a red circle).

Surface sediments from the middle and lower Setúbal Canyon have lithogenic contents between 72 – 77 % (2200 – 4400 m WD) comparable or slightly higher than for sediments from an equivalent water depth range on the walls and edges of the canyon (70 % at 2939 m WD) and on the Sines open slope (72 – 75 %, between 2130 and 4987 m WD). L/C ratio and contents of kaolinite, which can be used as tracers for coastal and riverine inputs of sediments, have contents in surface sediments consistently higher in the Setúbal Canyon compared to the canyon edge and Sines open slope for equivalent

depths (Figures 6.10 and 6.13d). This may indicate that despite the low down-canyon transport of sediments from the upper-canyon, the funnel effect of the canyon may be enough to differentiate sediments from the canyon thalweg against those occurring in the open slope and even in the walls of the canyon. Conceivably, a larger input of lithogenic material from the adjacent shelf during winter months, due to increased river discharge and higher frequency of storms, may be included in the time-integrated record of seabed sediment, but may not be present in the suspended matter collected during comparatively shorter intervals sampled with the sediment traps (De Stigter *et al.*, in press). For the lower canyon, at 4402 m WD (252-62), the relatively high contents of lithogenic material in surface sediments compared to suspended material collected with sediment traps in the same area may also result from bioturbation causing the upward mixing of lithogenic-enriched turbiditic sediment buried at a few centimetres depth below the hemipelagic surface layer.

Low-frequency and high-energy processes like gravity flows are also capable of transporting considerable amount of sediments further down-canyon. They seem, however, very rare in the Lisbon-Setúbal Canyon. In fact, during the total time of five years and six months of BOBO deployments (2002 - 2007) no gravity flows were recorded in the Lisbon-Setúbal Canyon.

Overall, all collected data suggest that sediments are not transported effectively down to the lower canyon and rather accumulate in the upper canyon. The only evidence of relatively recent mass sediment transport from shallower areas to the lower canyon is a turbiditic sand layer, rich in quartz and mica, encountered below superficial mud in the lower Setúbal Canyon (225-07, 4445 m WD). According to ^{210}Pb geochronology it seems, however, to be related with the Lisbon 1755 earthquake (De Stigter *et al.*, in press). Representing the most recent recognisable event of mass transport, it shows that only powerful events like a major earthquake are capable of triggering sediment transport down to such water depths.

6.7.2. Lisbon-Setúbal Canyon *vs.* Nazaré Canyon (and others)

Despite of its proximity to the coast and to an important river, the Lisbon-Setúbal Canyon appears to be characterised by sediment accumulation rates (SAR) and mass deposition flux (MDF) one or two orders of magnitude lower than the relatively nearby

Nazaré Canyon (Figure 6.15) (De Stigter *et al.*, 2007b). SPM horizontal net fluxes estimated through the BOBO lander were also consistently higher in the Nazaré Canyon (De Stigter *et al.*, 2007b) for comparable water depths (5600 and 1200 g m^{-2} d^{-1} at 343 and 3010 m WD, respectively; cf. Table 6.1); however, around ~4300 m negligible net SPM transport was inferred for both canyons. In terms of SARs the Lisbon-Setúbal Canyon seems to be more similar instead to other canyons located at far distances from the main sediment source (e.g. Bari Canyon - Turchetto *et al.*, 2007). In accordance, the Cascais Canyon which has its multiple heads at the shelfbreak (~175 m WD) has comparable SARs to the former canyon (Figure 6.4).

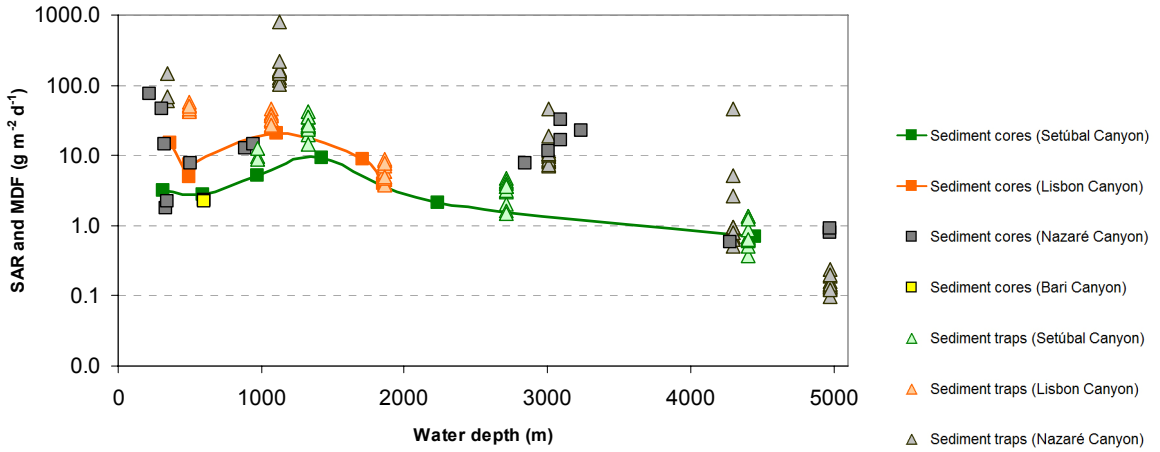

Figure 6.15. Sediment accumulation rates (SAR) measured in the seabed based on ^{210}Pb geochronology and mass deposition flux (MDF) measured in sediment traps, plotted against water depth in the Lisbon-Setúbal Canyon, Nazaré Canyon (De Stigter *et al.*, 2007b) and Bari Canyon (Turchetto *et al.*, 2007). Note the change of y-scale from Figure 6.4.

It is generally accepted that sediment entering the canyon head from fluvial and/or along-shelf/open slope transport sources accumulates in a sediment pile in the upper canyon over time, producing a temporary sediment reservoir (Mastbergen & Van den Berg, 2003). Failure of this sediment deposit, which may occur due to a number of processes, results in low frequency, high-energy, sediment gravity flows rather than continuous sedimentation (Arzola *et al.*, 2008). According to observations by De Stigter *et al.* (2007b) in the Nazaré Canyon, internal tides are a major force behind fine-grained suspended sediment transport from the canyon head to the middle canyon (2700 – 4000 m WD), whereas intermittent gravity flows are responsible for down-canyon transport from the middle canyon to the lower canyon occurring on a yearly or longer timescales. As referred above already, in the Lisbon-Setúbal Canyon no gravity flow was

recorded during the total time of five years and six months of deployments while for a similar period of time at least three important mass flux events were recorded in the Nazaré Canyon. This might suggest that gravity flows in the Lisbon-Setúbal Canyon are not as common as in the Nazaré Canyon, and therefore play a minor role in transporting sediment to the middle and lower Setúbal Canyon.

Surface sediments of the Nazaré Canyon show lithogenic contents consistently above 80 % down to depths around 5000 m WD (Figure 6.16), and kaolinite contents higher than 30 % and Feld/Phy ratios > 0.2 throughout the canyon, indicating effective transport of coastal sediments down to the lower canyon, in accordance with the hydrodynamic data. In the Lisbon-Setúbal and Cascais canyons such mineralogical characteristics only occur in the upper reaches of the canyons close to the canyon head (Figure 6.16).

Efficiency of the Nazaré Canyon in transporting sediments down to the lower canyon is also reflected in the supply of fresh organic matter to deeper ecosystems (Figure 6.17). García *et al.* (2010) compared organic matter content and its bioavailability in both the Nazaré and the Lisbon-Setúbal canyons and concluded that while in the Lisbon-Setúbal Canyon there are no major differences in C_{org} contents between the canyon and the adjacent slope, contents are considerably higher in the Nazaré Canyon compared to the adjacent slope. As shown in Figure 6.17 these differences can also be noticed in the data here presented. García *et al.* (2010) found, however, that quality of organic matter in both regions is similar for equivalent depths in the canyon and on the slope, which may be interpreted as an indication that lateral transport through the canyons occurs on a time scale that is too long to preserve the freshness of the organic material.

Even so, the fact that sediment accumulation rates determined for the axis of the Lisbon-Setúbal and Cascais canyons are consistently higher than SARs determined for the canyon walls and edges and for the Sines and Estremadura open slopes indicates that, for this area of the Portuguese margin, the Lisbon-Setúbal Canyon and the Cascais Canyon act as important depocentres of sediments. This relative importance of canyons as depocentres or geomorphological traps of sediments compared to the surrounding slope environments was already demonstrated for other submarine canyons: e.g. for the Nazaré Canyon (Portuguese margin), Schmidt *et al.* (2001), Van Weering *et al.* (2002) and De Stigter *et al.* (2007b); for the Bari Canyon (Adriatic Sea), Turchetto *et al.* (2007); for the Foix Canyon (Catalonia margin), Sanchez-Cabeza *et al.* (1999).

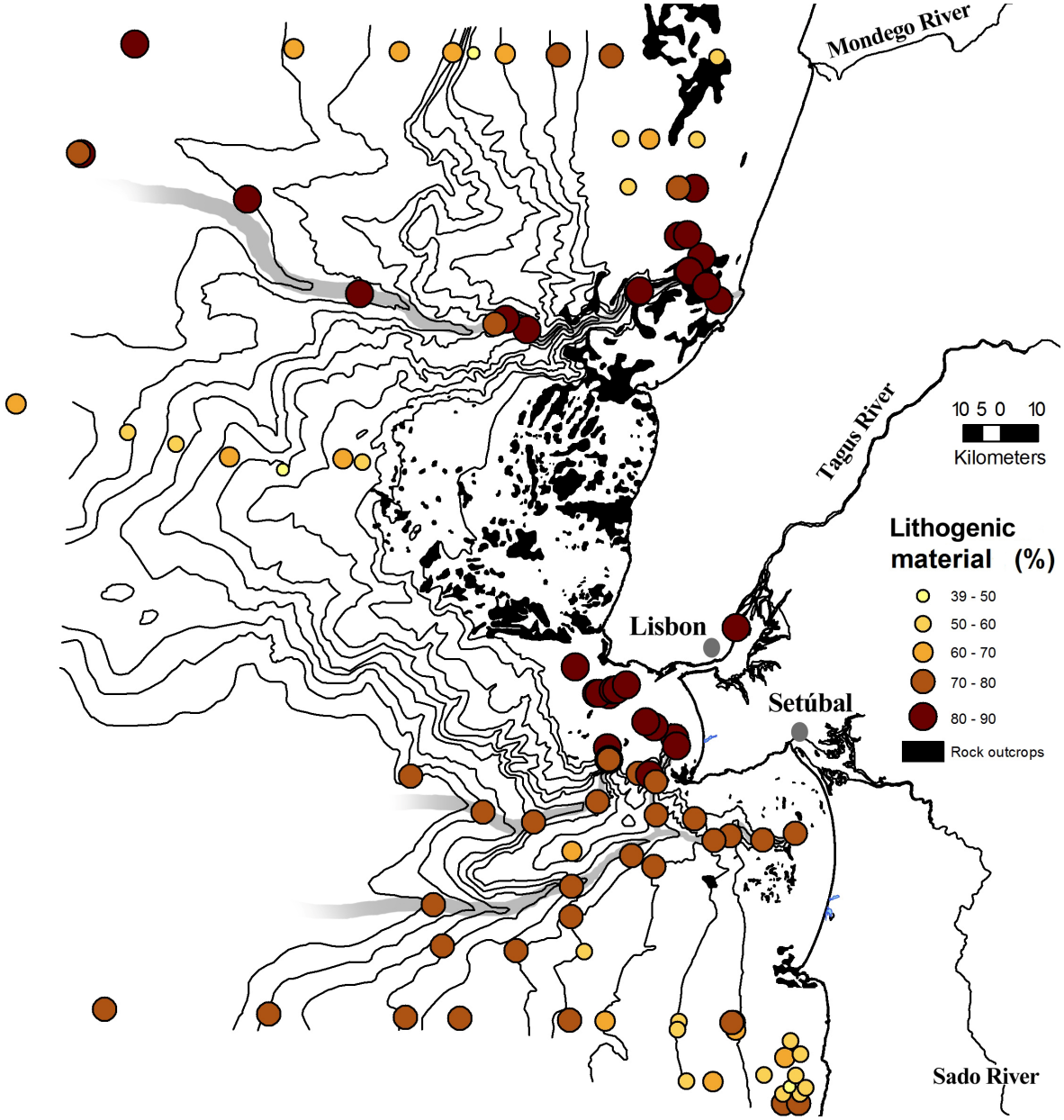

Figure 6.16. Contents of lithogenic material in surface sediments (0-0.5 cm) of the central Portuguese margin. Data for the Sines, Lisbon and Nazaré shelf and the Tagus Estuary from Alt-Epping *et al.* (2007) and for the Mondego transect from Guerreiro *et al.* (unpublished). Rock outcrops drawn after Sedimentary Cover Map 5 from Instituto Hidrográfico (2005) for shelf between Cape Sines and Cape Roca; from Balsinha (2008) for shelf between Cape Roca and the Nazaré Canyon and Pombo (2004) for shelf north of the Nazaré Canyon.

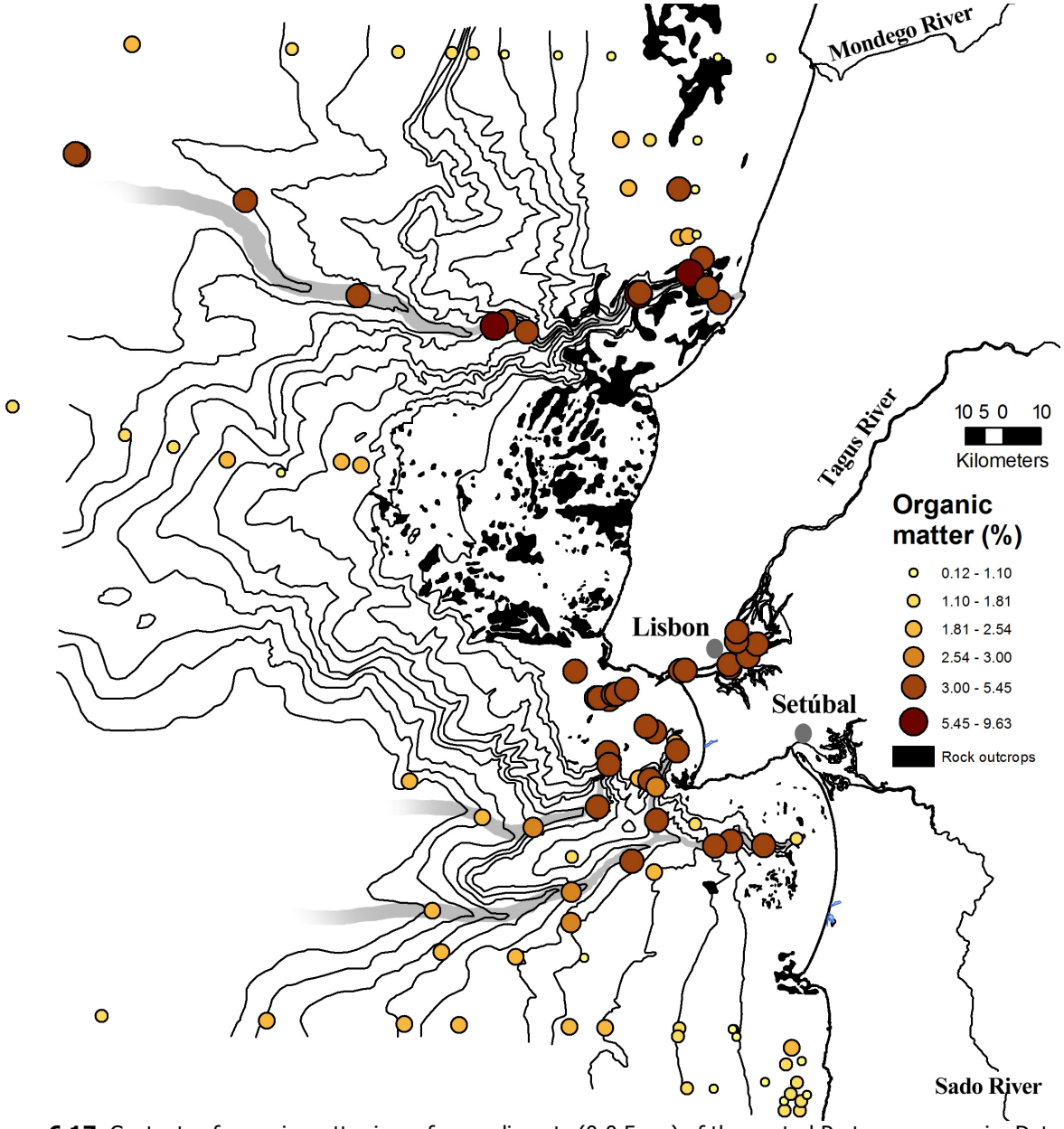

Figure 6.17. Contents of organic matter in surface sediments (0-0.5 cm) of the central Portuguese margin. Data for the Sines, Lisbon and Nazaré shelf and the Tagus Estuary from Alt-Epping *et al.* (2007) and for the Mondego transect from Guerreiro *et al.* (unpublished). Rock outcrops drawn after Sedimentary Cover Map 5 from Instituto Hidrográfico (2005) for shelf between Cape Sines and Cape Roca; from Balsinha (2008) for shelf between Cape Roca and the Nazaré Canyon and Pombo (2004) for shelf north of the Nazaré Canyon.

6.7.3. Open slope of the central Portuguese continental margin

The Lisbon-Setúbal, Cascais and Nazaré canyons act as natural boundaries dividing the central Portuguese margin in different sections of shelf and slope, here referred to as the Mondego, Estremadura, Lisbon, Setúbal and Sines shelf and slope, each with its specific pattern of sediment distribution.

From the three studied open slope areas (Mondego, Estremadura and Sines), the Sines open slope stands out for its higher SARs and higher contents of non-carbonate terrigenous materials (around 70 %) comparing equivalent water depths, while the Estremadura shows the lowest SARs and contents of non-carbonate terrigenous materials (around 60 %). The Mondego open slope has intermediate features regarding the above parameters being nonetheless the closest transect to a main river - Mondego River (Figures 6.4 and 6.6e, f, h). The differences between the Sines and Estremadura areas can be related to the following:

1) several studies (e.g. Ortiz & Mix, 1992; Thunell & Sautter, 1992) clearly show that maximum fluxes of planktonic foraminifera occur when upwelling is more intense. Salgueiro *et al.* (2008) show lower mean Sea Surface Temperature (SST) between 1985 and 2003 during summer time in the Estremadura margin compared with the SSTs from Sines margin (see Figure 2.11 on pg. 36 of Chapter 2). This suggests more intense upwelling occurring around the northern area. According to these same authors, higher planktonic foraminifera abundance occurs in the Estremadura margin, associated with the Cape Roca. This fact does explain higher $CaCO_3$ contents in the northern open slope but does not explain however higher SARs measured in the Sines open slope;

2) the progressive deposition of suspended fine-grained terrigenous material along entrained with the MOW along the Portuguese continental slope (Grousset *et al.*, 1988) must be higher in the Sines area than in the Estremadura area. This subject will be further discussed below.

The imprint of the Mediterranean Outerflow Water

The high distance from terrigenous sediment supply and winnowing of sediments on the upper slope can help to lower SAR and concentrate $CaCO_3$ contained in foram shells in the Estremadura open slope. The concentration of $CaCO_3$ may be also partially explained by relatively higher productivity of foraminifera in the Estremadura slope. Since no important rivers debouch on the coast facing the Sines open slope, it is contrary to

expectations that sediment accumulation rates and contents of lithogenic material are found to be higher on the Sines open slope than on the Estremadura and Mondego open slopes. Deposition of sediments entrained with the MOW may help explaining these higher SARs and associated higher contents of lithogenic material on the Sines open slope.

According to McCave & Hall (2002), the strong density gradients at the boundaries of the MOW favour internal wave activity and sediment resuspension. Suspended particles on the upper slope may be carried along with the poleward flowing MOW, forming a wide and permanent intermediate nepheloid layer over the upper slope, as observed on the Galician slope by McCave & Hall (2002). Moreover, as observed in south-western Gulf of Cadiz, settling of suspended sediment from the MOW may also be found in areas where the MOW flows detached from the seafloor, giving rise to the formation of hemipelagites.

Along-margin perspective

The Mediterranean Outflow Water (MOW) was clearly recognised in hydrographic profiles across the central Portuguese continental margin, as distinct salinity maximum between 500 and 1500 m WD (De Stigter *et al.*, 2004 and 2007a, Figure 2.10 on pg. 34). Along the Portuguese margin this water mass mixes with other less saline and colder waters as shown in Figure 2.10. Bower *et al.* (2002) show that there is a significant amount of mixing of the lower-core MOW around the south-western Iberian Peninsula and that a considerable portion of the lower-core water flows into the interior of the ocean after crossing the Lisbon-Setúbal Canyon as the large-scale orientation of the slope changes from north-south to northwest-southeast.

In the Gulf of Cadiz, Pierce & Stanley (1975) observed that smectite content in SPM in the MOW is twice as high as in the overlying surface water and two to four times higher than in the underlying surface sediments. The source for this smectite is thought to be the Guadalquivir River (Mélières, 1974; Grousset *et al.*, 1988; Schönfeld, 1997).

Although there are other sources of smectite in the area, the results of the present study show that there is a northward regional decrease of smectite contents, within the depth interval affected by the MOW flow. Between 1000 and 1500 m WD smectite contents in surface sediments decrease from 3.5 % on the Sines open slope, to 2.7 % on the Estremadura slope, to 2.1 % on the Mondego slope. Within the canyons, in the same depth interval, smectite contents were between 1.6 and 3.2 %. Grousset *et al.* (1988) also observed this general decrease of smectite contents along the Portuguese margin but

the percentages obtained in this study are not comparable to those reported here as different methodologies were used to quantify clay minerals.

Across-margin perspective

The across-margin changes in the mineralogy of surface sediments which may be related to the MOW include:

1) Enhanced contents of smectite between 1000 and 1500 m WD (Figure 6.13f);
2) Decrease of kaolinite's crystallinity between 1000 and 1500 m WD (Figure 6.13e);
3) Conspicuous increase of the carbonate contents around 1500 m WD (Figure 6.6e, f, h) in the open slope transects.

The across-margin changes of the clay mineralogy (point 1 and 2) are most conspicuous in the Sines and Estremadura open slope transects and in the Lisbon and Cascais canyons. The clay mineral signature of MOW seems almost lost or diluted in the Mondego transect and neither is it detected in the Nazaré Canyon, probably due to the more active down-canyon transport of sediments through this canyon. The reason why it is also not detected in the upper Setúbal branch is not clear. It could be due to a change of the course of the water mass in this area. Many studies have highlighted the important modifications that along-slope currents suffer when they encounter a canyon on their path (e.g. Durrieu de Madron, 1994; Puig *et al.*, 2000; Petrenko, 2003).

Suspended particulate matter of the MOW is not only enriched in smectite but also in kaolinite (Grousset *et al.*, 1988). This mineral, however, seems not a suitable tracer for this water mass because kaolinite enrichment in sediments from the central Portuguese margin may also be derived from other sources such as the Tagus and Sado rivers. However, crystallinity index of kaolinite across the open slope transects indicates the occurrence of more degraded kaolinites between 1000 and 1500 m WD. These kaolinites seem therefore to have a different and more distant source than those predominating at different water depths, conceivably transported by the MOW. The occurrence of the maximum in smectite contents and kaolinite crystallinity minimum in the 1000-1500 m depth interval indicates that SPM carried along the MOW settles in the lower part of the MOW.

Winnowing of surface sediments by enhanced currents associated with the MOW appears to be reflected by grain size distribution patterns across the open slope. Whereas at water depths below 2000 m surface sediments have relatively uniform grain size spectra with mode < 8 μm typical for hemipelagic sedimentation (Figure 6.18), sediments

between 500 and 2000 m WD have distinctly coarser modes indicating that pelagic sedimentation is not the main process affecting surface sediments. On the upper Sines slope, particle size mode at 500 m WD is coarser than at 1500 m WD (Figure 6.18). The above suggests that the fine grained sediment fraction is removed from the slope affected by the upper MOW and settles near the lower limit of the MOW limit together with suspended matter entrained by the MOW from more distant sources. As proposed by Schönfeld (1997) the reason for the enhanced sedimentation in the lower MOW core layer may be the rapidly decreasing or highly variable water turbulence at this level. This same author observed the accumulation of pteropod shells around 1500 m WD on the Sines open slope which may explain the conspicuous increase of carbonate contents around this depth as seen in the three open slope transects (Figure 6.6) and as indicated before in point 3.

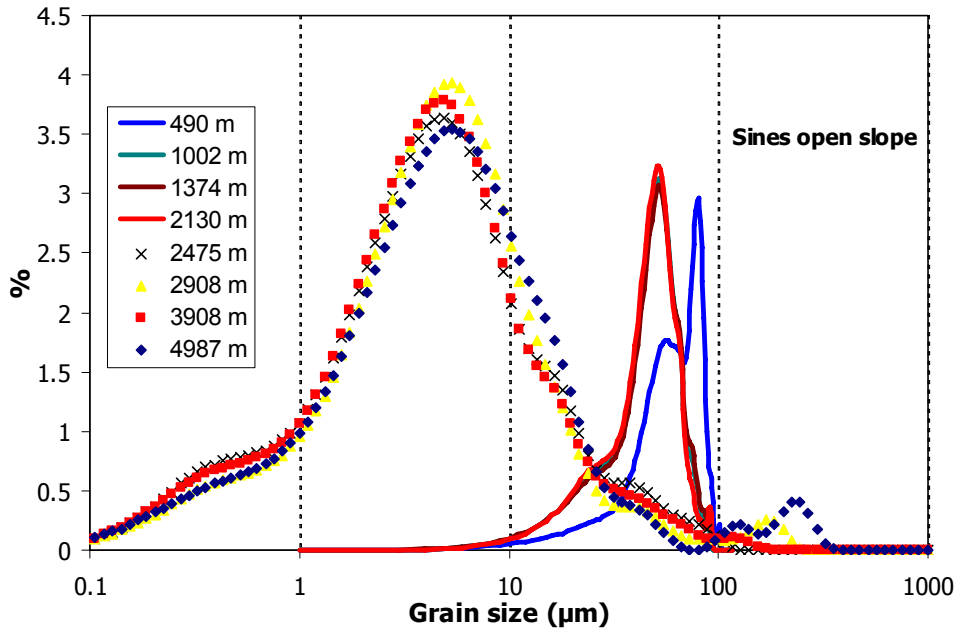

Figure 6.18. Grain size spectra of surface sediments (0-0.5 cm) collected along the Sines open slope transect.

As will be shown in the next chapter, on the Sines open slope the highest enrichment factors of Pb in surface sediments and highest contents of excess Pb and Zn deposited during the last 150 years occur exactly around the lower MOW boundary (Figures 7.10, 7.12 and 7.13) giving evidence of import of trace elements from an exotic source or concentration of these trace elements with a certain mineral fraction.

7. TRACE METALS IN SURFACE SEDIMENTS AND SUSPENDED PARTICULATE MATERIAL FROM THE CENTRAL PORTUGUESE CONTINENTAL MARGIN

7.1. Introduction

Contamination of the marine environment with anthropogenic trace metals has strongly increased over the last ~150 years as a result of the exponential growth in the world's population and industrial development. In the last few decades this contamination has become an issue of international concern, urging for research on the sources, dispersal pathways, and sites of accumulation of these trace metals. Since trace metals originating from human activity usually accumulate in sediments together with trace metals from natural sources, it is often difficult to quantify the contribution from the respective sources (Soto-Jiménez & Páez-Osuna, 2001). The problem is amplified by variable loadings of trace elements originating from these two sources, as well as the interaction of elements with sediment of variable grain size, mineralogy and organic matter content (Soto-Jiménez & Páez-Osuna, 2001). Several granulometric and geochemical procedures have been developed to compensate for such influence and to allow comparisons between samples with different characteristics. Geochemical procedures include normalisation in relation to a conservative element such as Al, Fe, Rb, Cs, Sc and Li (e.g. Grant & Middleton, 1990; Loring & Rantala, 1992).

Even then, knowing only the total concentrations and chemical/mineralogical context of trace metals is not strictly sufficient for a precise evaluation of contamination sources. In the present study lead stable isotopes are therefore introduced as "fingerprints" of environmental pollution, because it is the only trace metal pollutant known to exhibit

significant natural variation in the proportions of its isotopes - ^{204}Pb, ^{206}Pb, ^{207}Pb, ^{208}Pb (Dickin, 1995). The isotopic proportions, usually expressed as isotope ratios, display characteristic ranges for different natural Pb ores and are thought to be unaltered by smelting and other manufacturing processes (Flegal & Smith, 1995). Therefore, Pb isotope "signatures" have been increasingly used by environmental scientists as tracers to putatively identify the different natural and industrial contributions of Pb in humans and the environment (Sangster *et al.*, 2000).

Trace metals enter the ocean from sources located on continents via atmospheric transport or riverine input. Like many other contaminants, trace metals are removed from the sea water by biological and physico-chemical processes, including scavenging by suspended particulate organic matter, to become incorporated into sediments on the seabed (Boström *et al.*, 1981; Gibbs, 1986). Most of the contaminants discharged by rivers, sewers and pipelines are associated with fine-grained particles (Salomons & Förstner, 1984), including organic films, colloidal material or plankton cells (Fisher & Reinfelder, 1995). Thus, the fate of contaminants introduced to the sea is closely associated with the transport and deposition of particulate matter (Gibbs, 1973; Puig *et al.*, 1999).

Submarine canyons are important transport routes for the transfer of particulate matter from the coastal ocean to the deep sea. Although most submarine canyons are presently sites of sediment accumulation rather than of erosion, some studies show intermittent mass transport of sediments down canyons continuing to the present-day (e.g. Xu *et al.*, 2002; Palanques *et al.*, 2005; De Stigter *et al.*, 2007b). For the large submarine canyons of the central Portuguese margin, which are the subject of the present study, present-day intermittent down-canyon transport to depths greater than 4000 m has been confirmed for the Nazaré Canyon (De Stigter *et al.*, 2007b). Results presented in Chapter 6 indicate that down-canyon transport is less effective in the Lsibon-Setúbal Canyon, and probably as well in the Cascais Canyon. Mass down-canyon transport of sediments seems to occur only infrequently in these canyons, triggered by high energy seismic events. The latter two canyons, located close to densely populated and industrialized metropolitan areas and heading close to where the Tagus and Sado rivers debouch on the shelf, are likely to intercept riverine sediments and associated trace metals. By contrast, the Nazaré Canyon has no direct connection to a major river system, and is more remote from point sources of anthropogenic pollutants.

Trace metal contamination has been documented for the Tagus and Sado estuaries (e.g. Figuères *et al.*, 1985; Quevauviller, 1988; Cortesão & Vale, 1995; Gil & Vale, 2001; Caeiro *et al.*, 2005; França *et al.*, 2005; Vale *et al.*, 2008) and to a lesser extent, the adjacent open shelf (e.g. Jouanneau *et al.*, 1998; Cotté-Krief *et al.*, 2000; Mil-Homens *et al.*, 2009; Chapter 5). Little attention has been paid to the nearby canyons and deep slope environments. Even worldwide, studies involving the dispersal of trace metals through canyon systems are scarce.

The main objectives of the present chapter are to assess:

1) the geographic patterns of excess trace metals dispersal in three Portuguese canyons (Lisbon-Setúbal, Nazaré and Cascais) and open slope;

2) natural and anthropogenic sources of trace metals in the canyons and open slope of the central Portuguese margin, with especial focus on Pb;

3) the role of the Lisbon-Setúbal Canyon in channelling transport of anthropogenic trace metals to the deep sea. Data from the Nazaré Canyon will be used to establish comparisons with the Lisbon-Setúbal Canyon. The Nazaré Canyon was studied in more detail with regard to the dispersal of Pb by Richter *et al.* (2009).

The last objective will be approached through the comparison of enrichment factors obtained for trap samples and surface sediment cores and by integrating trace metal data with observations on near-bottom hydrodynamics and sediment dispersal from the Lisbon-Setúbal Canyon (Chapter 6) and the Nazaré Canyon (De Stigter *et al.*, 2007b).

7.2. Major, minor and trace element concentrations

In this section the distribution of eleven elements (Al, Fe, Ca, Mg, Pb, Zn, Cr, Mn, Ni, Cu and U) in surface sediments and sediment trap samples from the central Portuguese canyons and open slope will be evaluated and correlated with other relevant sedimentary parameters such as grain size, lithogenic content, calcium carbonate ($CaCO_3$) and organic carbon (C_{org}) / organic matter.

Subsequently, the enrichment with anthropogenic trace metals will be assessed, first for the most recent sediment deposit included in the top 0.5 cm of sediment cores and for sediment trap samples by using enrichment factors, and then for the last 150 years by looking at the relative contribution of excess trace metals to total trace metal inventories.

7.2.1. General characteristics of surface sediments and suspended particulate material

Surface sediments in the canyon thalweg and lower part of the walls comprise mostly hemipelagic clayey silt composed of terrigenous lithogenic material (72 - 87 %), calcium carbonate (10 - 25 %) and organic matter (1.4 - 5.0 %) (Figure 7.1a, b). Higher up the walls and edges of the canyons, surface sediments show lower concentrations of lithogenic materials (69 - 78 %) and organic matter (1.4 - 2.8 %) while carbonate contents are generally higher (20 - 27 %). True open slope surface sediments have even lower contents of lithogenic material (39 - 75 %) and organic matter (0.3 - 1.0 %) and higher carbonate contents (24 - 60 %). Canyon surface sediments generally have a modal grain size between 8 and 50 µm, while upper slope surface sediments often have modal grain size coarser than 50 µm, and sediments from the middle and lower slope have modes finer than 8 µm. Surface sediments from the walls and edges of the canyons usually have grain sizes within the range of open slope sediments, but may also have modal grain sizes between 8 and 50 µm. Generally, modal grain sizes decrease with depth down the canyons and on the adjacent open slope, but in the Nazaré Canyon modal grain size increases until 4500 m WD (Chapter 6, Figure 6.5 on pg. 152).

Suspended particulate matter collected in sediment traps along the canyon axes consists of clayey silt with minor coarse material (sand-sized particles never exceed 6 % of the total content). In general, carbonate contents increase with depth down-canyon, probably reflecting a reduction of lithogenic input. Contents of organic material are higher

in the lower reaches of both the Setúbal and Nazaré Canyon, as well as in the upper Lisbon-Setúbal Canyon (Figure 7.1a).

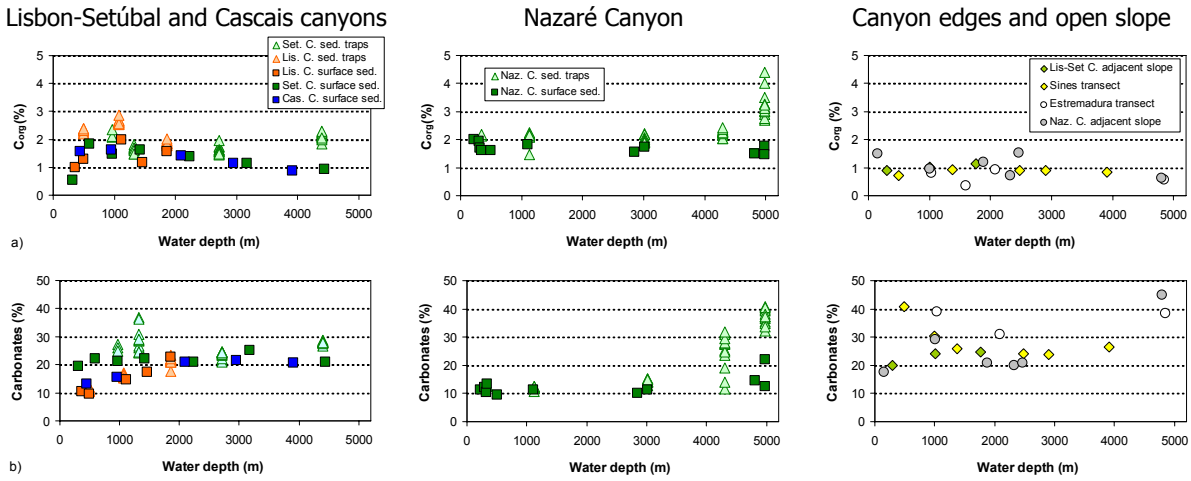

Figure 7.1. Organic carbon (**a**) and calcium carbonate (**b**) in surface sediments and sediment trap particulate material plotted against water depth for the Lisbon-Setúbal, Cascais and Nazaré canyons and adjacent canyon edges and open slopes.

7.2.2. Major elements Ca, Fe, Al and minor element Mn

With regard to major elements, the regional distribution of Ca closely matches the distribution of $CaCO_3$, with lower contents in canyons (especially in the Nazaré Canyon) and higher values on open slopes (Figure 7.2a). Concentrations of Al tend to be higher in canyons than on true open slopes (Table 7.1, Figure 7.2b). On the other hand, Fe shows more or less uniform mean concentrations for all environments (Table 7.1). Neither in canyons or open slopes are consistent trends with water depth observed for Ca, Fe and Al contents in surface sediments and trap samples, except that Ca has higher concentrations in trap samples from the lower canyons.

No major differences are found between contents of Mn in canyons and open slopes at comparable water depths (Figure 7.2d). Concentrations generally increase with increasing water depth both in canyons and slopes, but a conspicuous maximum is observed in the Lisbon-Setúbal Canyon just down-slope from where the upper canyon branches merge.

Table 7.1. Descriptive statistics of elemental composition, organic carbon and calcium carbonate contents of sediment trap samples and surface sediments collected along the axes of the Lisbon-Setúbal, Cascais and Nazaré canyons and adjacent canyon edges and from the Sines and Estremadura open slopes. Data presented are means ± standard deviation.

	Lisbon-Setúbal Canyon system				Sines open slope	Cascais Canyon	Estremadura open slope	Nazaré Canyon system			
	Sediment traps (n = 55-67)	Canyon surface sediments (n = 10-14)	Adjacent slope surface sediments (n = 4-5)	Baseline values (n = 9)	Open slope surface sediments (n = 6)	Canyon surface sediments (n = 5)	Open slope surface sediments (n = 4)	Sediment traps (n = 29-47)	Canyon surface sediments (n = 8-12)	Adjacent slope surface sediments (n = 5-7)	Baseline values (n = 5)
Ca (%)	8.4 ± 2.1	7.2 ± 2.5	9.7 ± 0.8	8.9 ± 2.8	11.2 ± 2.5	7.2 ± 1.8	17.9 ± 5.8	8.4 ± 4.3	5.9 ± 2.7	9.0 ± 3.4	7.1 ± 3.1
Al (%)	7.0 ± 1.0	6.0 ± 0.9	6.1 ± 0.6	6.3 ± 1.5	4.3 ± 0.6	4.8 ± 1.3	3.9 ± 1.1	6.9 ± 1.1	6.2 ± 2.0	6.9 ± 1.5	6.5 ± 2.0
Fe (%)	3.7 ± 0.3	3.2 ± 0.3	3.3 ± 0.3	3.0 ± 0.7	3.3 ± 0.5	3.7 ± 0.1	2.5 ± 0.7	3.2 ± 0.3	3.6 ± 0.7	3.5 ± 1.1	3.1 ± 0.6
Mg (%)	1.3 ± 0.1	1.0 ± 0.2	1.2 ± 0.2	-	1.2 ± 0.2	1.2 ± 1.3	1.0 ± 0.2	1.0 ± 0.2	1.1 ± 0.4	1.1 ± 0.4	-
Mn (μg g^{-1})	606 ± 158	603 ± 544	710 ± 141	-	811 ± 327	668 ± 308	571 ± 165	485 ± 143	439 ± 199	507 ± 278	-
Zn (μg g^{-1})	186 ± 162	210 ± 314	93 ± 11	78 ± 11	173 ± 33	244 ± 69	146 ± 13	113 ± 43	117 ± 51	95 ± 24	78 ± 12
Cr (μg g^{-1})	80 ± 9	67 ± 9	76 ± 6	57 ± 17	78 ± 20	81 ± 8	53 ± 19	67 ± 8	67 ± 17	73 ± 26	57 ± 8
Pb (μg g^{-1})	46 ± 8	46 ± 10	37 ± 6	20 ± 5	33 ± 8	48 ± 10	26 ± 10	42 ± 20	35 ± 6	32 ± 6	23 ± 6
Ni (μg g^{-1})	41 ± 11	34 ± 8	38 ± 9	43 ± 21	52 ± 19	52 ± 13	43 ± 20	27 ± 6	36 ± 15	41 ± 19	37 ± 22
Cu (μg g^{-1})	40 ± 10	27 ± 8	38 ± 30	19 ± 6	39 ± 15	40 ± 9	39 ± 18	70 ± 43	26 ± 12	27 ± 10	19 ± 12
U (μg g^{-1})	2.2 ± 0.6	2.6 ± 0.4	2.3 ± 0.2	-	1.9 ± 0.1	2.4 ± 0.4	1.6 ± 0.3	2.1 ± 0.5	3.1 ± 0.5	3.1 ± 0.4	-
C_{org} (%)	2.0 ± 0.4	1.4 ± 0.4	0.9 ± 0.3	-	0.9 ± 0.1	1.3 ± 0.3	0.7 ± 0.3	2.4 ± 0.6	1.8 ± 0.1	1.1 ± 0.4	-
$CaCO_3$ (%)	22 ± 6	19 ± 5	25 ± 4	-	29 ± 6	18 ± 3	42 ± 12	22 ± 11	12 ± 1	26 ± 10	-

7.2.3. Trace metal concentrations in surface and pre-industrial sediments and in suspended particulate material

Comparison of elemental contents in surface sediments in the three canyons reveals higher mean concentrations for most analysed trace metals (Pb, Zn, Cu, Cr and Ni) and Mn in the Cascais Canyon (Table 7.1). Surface sediments from the Nazaré Canyon display the lowest means for Pb, Zn, Cu and Mn and the highest for Al.

In surface sediments from canyons and open slopes, Pb and Zn concentrations generally decrease with increasing water depth (Figure 7.3a, b) while Cr and Cu show the inverse trend (Figure 7.3c, d). Nickel does not show any trend with water depth. Trap samples along the axes of the Lisbon-Setúbal and Nazaré canyons have concentrations comparable to underlying surface sediments, except in lower canyon sites where trap samples show consistently higher trace metal contents (Figure 7.3).

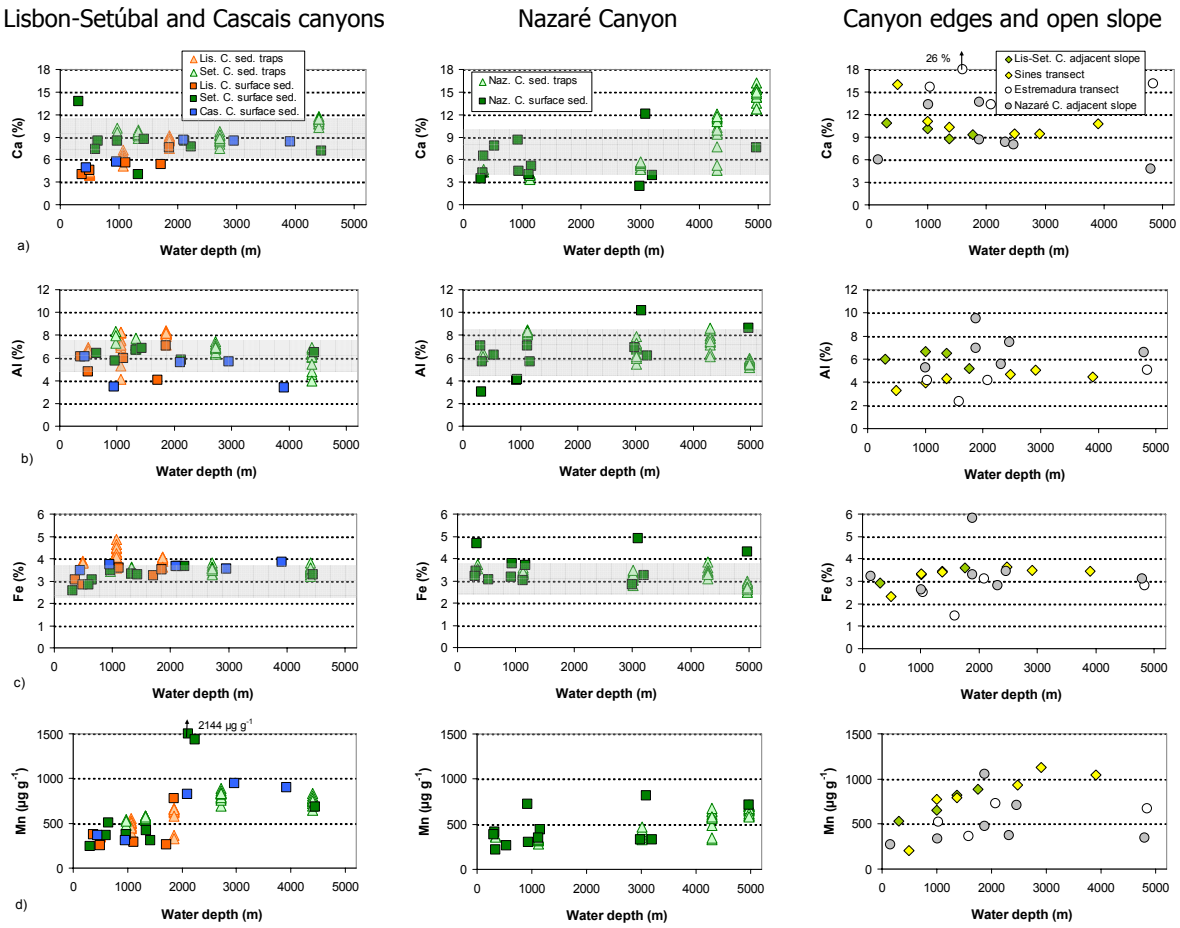

Figure 7.2. Calcium (**a**), Al (**b**), Fe (**c**) and Mn (**d**) concentrations in surface sediments and sediment trap particulate material plotted against water depth for the Lisbon-Setúbal, Cascais and Nazaré canyons and adjacent canyon edges and open slopes. Grey shaded bars represent pre-industrial concentrations (average ± standard deviation).

Pre-industrial sediments (~1850 AD) were analysed in deep samples from 14 cores from the Lisbon-Setúbal and Nazaré canyons and adjacent open slopes (see the location of selected cores in Figure 3.2). Baseline concentrations for the various elements were determined separately for the Lisbon-Setúbal area (9 samples) and the Nazaré area (5 samples), taking the simple average of all deep samples from the respective areas. The baseline values thus calculated for the Lisbon-Setúbal system (used also for the Cascais and Sines transect) and for the Nazaré system (used also for the Estremadura transect) are very similar for most of the analysed elements (Table 7.1).

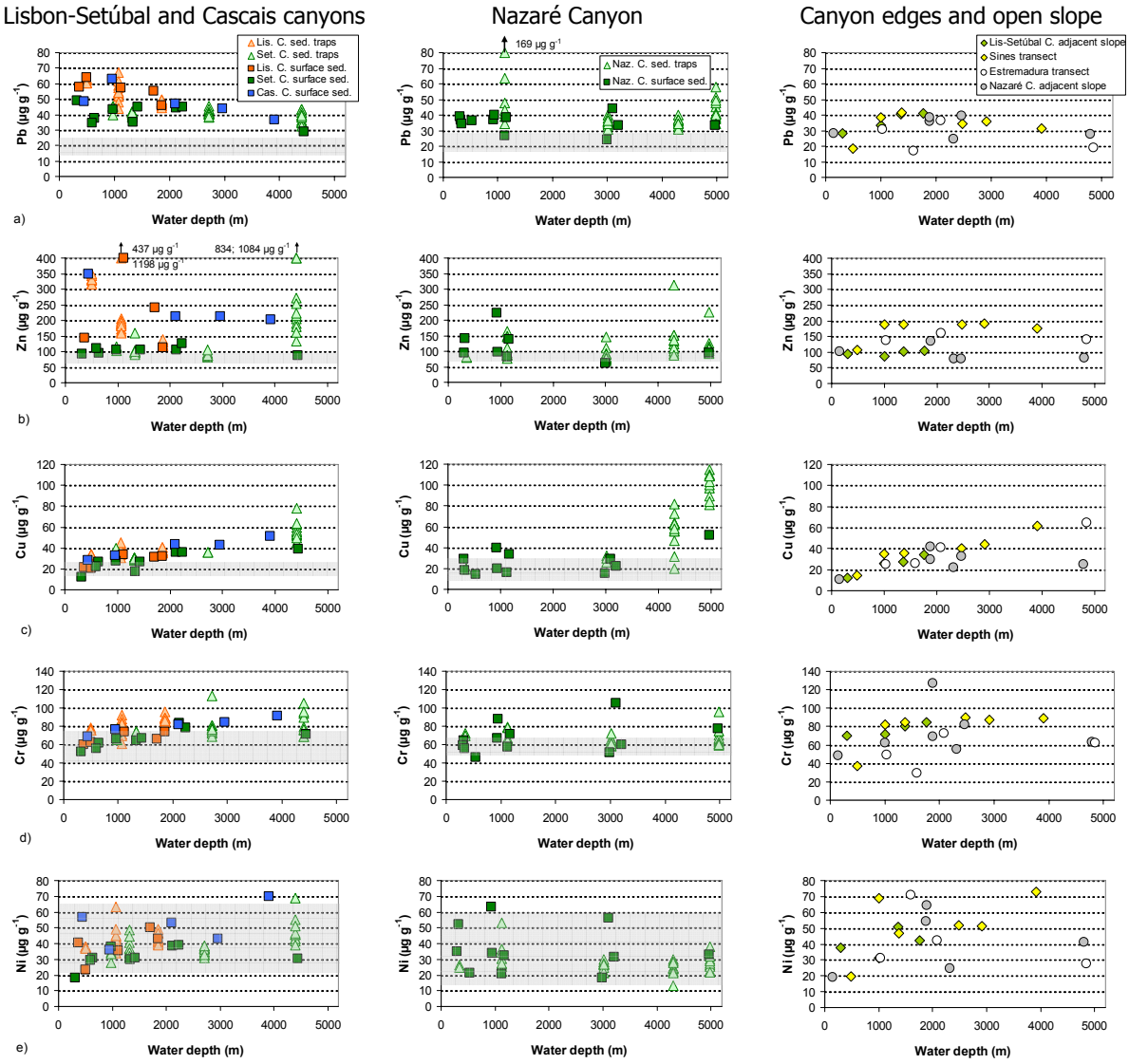

Figure 7.3. Lead (**a**), Zn (**b**), Cu (**c**), Cr (**d**) and Ni (**e**) concentrations in surface sediments and sediment trap particulate material plotted against water depth for the Lisbon-Setúbal, Cascais and Nazaré canyons and adjacent canyon edges and open slopes. Grey shaded bars represent pre-industrial concentrations (average ± standard deviation).

Surface sediment and sediment trap samples display consistently higher concentrations of Pb, Zn and Cu compared to pre-industrial concentrations (average ± standard deviation) presented as grey shaded bars in Figure 7.3. Chromium and Ni show comparable concentrations in surface sediments and trap samples as in pre-industrial sediments.

7.2.4. Selection of a normaliser for calculating enrichment factors

Temporal or spatial variation in trace metal distribution may to some extent be related to variation in supply of major sediment components with which the trace metals are associated. To compensate for this effect, normalisation is often applied relative to a proxy of the most important carrier. Correlations between trace metal and carrier proxies may help in identifying the most suitable carrier proxy to be used as normaliser. Among various proxies for potential trace metal carriers, such as Al and Fe for terrigenous aluminosilicates, Ca and $CaCO_3$ for pelagic skeletal carbonate, and C_{org} for organic matter, Fe and Al showed the largest number of significant positive correlations with trace metals, suggesting that terrigenous aluminosilicates are the dominant trace metal carriers in the study area. Spearman correlations calculated for all surface sediment samples (Table 7.2) from all the studied canyons and open slopes show positive correlation of Fe with Cr (0.78), Cu (0.57), Pb (0.40), Ni and Zn (0.33). Correlations between Al and trace metals are less strong than for Fe. Organic carbon is only correlated to Pb (0.44) while $CaCO_3$ has no positive correlation with any trace metal. Modal grain size only correlates positively with Zn (0.46) and negatively with Cu (-0.51). In general, the correlations between trace metals and trace metal carrier proxies do not seem to be strong when using the whole dataset of surface sediments. This is most conceivably because differences in anthropogenic trace metal input to different areas lead to variable trace metal/trace metal carrier ratios, disturbing the natural correlation between both. Correlations were therefore calculated separately for the Lisbon-Setúbal and Nazaré Canyon systems as shown in Tables 7.3 and 7.4, making further distinction between surface sediment and trap samples. Indeed these subsets of data yield more significant correlations than the entire dataset, but since the results do not differ much in qualitative sense they will not be discussed here for the separate datasets.

Table 7.2. Spearman correlation coefficient matrix showing significant correlations (p<0.05) between proxies of potential trace metal carriers and trace metals. The analysed dataset includes 58 surface sediment samples collected from the axis, walls and edges of the Lisbon-Setúbal and Nazaré canyons and adjacent open slopes.

	Fe	Al	$CaCO_3$	Grain size mode	C_{org}
Pb	0.40	0.53	-0.60	-	0.44
Zn	0.33	-	-	0.46	-
Cu	0.57	-	-	-0.51	-
Ni	0.33	-	-	-	-
Cr	0.78	0.34	-0.33	-	-
Mn	-	-	-	-	-
Fe	1	0.53	-0.60	-	0.52
Al	0.53	1	-0.53	-	0.57
Ca	-0.29	-	0.82	-	-0.67
$CaCO_3$	-0.60	-0.53	1	-	-0.68
C_{org}	0.52	0.57	-0.68	-	1

Normalisation to C_{org} is only useful when organic matter is relatively homogeneous in composition (predominantly of pelagic or terrestrial origin). However, according to our C_{org}/N ratios (Chapter 6, Figure 6.9 on pg. 157), the C_{org} in the canyon comprises a variable mixture of marine and laterally advected terrigenous organic matter. On the adjacent slope the C_{org} is predominantly of marine origin. Apart from that, there are differences in degradation state when comparing sediment trap material and surface or deep sediments (Figure 7.1a) which makes the use of C_{org} as normaliser problematic.

Since analytical results showed a better accuracy for Fe than for Al, and Fe showed the strongest correlations to trace metals, Fe was chosen for the normalisation of trace metals. Normalisation for Al yielded very similar results, albeit more scattered than for Fe, conceivably because of the lower accuracy of Al analyses. We found no indication in our data that secondary diagenetic enrichment of trace metals played a significant role. The few cores displaying distinct surface enrichment of Fe and Mn (225-22, 204-56, 236-14, 236-20 for Fe and 236-52, 204-33 for Mn) showed no corresponding enrichment in trace metals.

7.2.5. Trace metal concentrations in surface sediment and trap samples and NOAA sediment quality guideline

In all studied canyon systems there were surface sediments and sediment trap samples with concentrations of trace metals (Pb, Cr, Ni, Cu, Zn) exceeding the ERL (effect range-low) value, but there were no concentrations above the ERM (effect range-

Table 7.3. Spearman correlation coefficient matrix showing significant correlations ($p<0.05$) between element concentrations, C_{org}, $CaCO_3$ and modal grain size in surface sediment and sediment trap samples from the Lisbon-Setúbal Canyon system. Number of samples N is indicated between brackets.

		Pb	Ca	C_{org}	$CaCO_3$	U	Mn	Ni	Cu	Al	Cr	Zn	Fe	Mg	Mode	
Trap samples	Pb	**1.00**	-	-	-	-	-	-	-	-	-	0.66 (16)	-	-	-	Surface sediment samples
	Ca	-0.75 (67)	**1.00**	-	-	-	-	-	-	-	-	-0.70 (16)	-	-	-	
	C_{org}	0.56 (67)	-0.40 (67)	**1.00**	-	-	-	-	-	-	-	0.62 (12)	-	-	-	
	$CaCO_3$	-0.85 (67)	0.89 (67)	-0.53 (67)	**1.00**	-0.60 (14)	0.56 (14)	-	-	-	-	-	-	-	-	
	U	0.79 (67)	-0.58 (67)	0.71 (67)	-0.70 (67)	**1.00**	-0.58 (19)	-	-0.57 (19)	0.71 (16)	-0.57 (19)	-	-	-	-	
	Mn	-0.63 (67)	0.61 (67)	-0.59 (67)	0.56 (67)	-0.60 (67)	**1.00**	0.46 (19)	0.58 (19)	-	0.76 (19)	-	0.64 (19)	-	-	
	Ni	-	-	0.40 (65)	-	0.45 (65)	-	**1.00**	-	-	0.56 (19)	0.61 (16)	0.59 (19)	-	-	
	Cu	-	0.36 (55)	0.41 (55)	-	-	0.49 (55)	0.69 (55)	**1.00**	-	0.72 (19)	-	0.64 (19)	-	-0.77 (10)	
	Al	0.38 (67)	-	**-**	-	-	-	-	-	**1.00**	-	-	-	0.71 (16)	-	
	Cr	0.34 (65)	-	-	-	0.30 (65)	-	0.59 (63)	0.58 (53)	0.35 (65)	**1.00**	-	0.81 (19)	0.59 (19)	-	
	Zn	0.52 (65)	-0.25 (65)	0.80 (65)	-0.42 (65)	0.76 (65)	-0.46 (65)	0.52 (64)	0.49 (54)	-	0.34 (63)	**1.00**	-	-	-	
	Fe	0.87 (67)	-0.55 (67)	0.51 (67)	-0.73 (67)	0.70 (67)	-0.40 (67)	0.37 (65)	-	0.53 (67)	0.60 (65)	0.46 (65)	**1.00**	-	-	
	Mg	-	-	-0.28 (67)	-	-	0.43 (67)	-	-	0.51 (67)	0.69 (65)	-	0.37 (67)	**1.00**	**-**	

Table 7.4. Spearman correlation coefficient matrix showing significant correlations (p<0.01) between element concentrations, C_{org}, $CaCO_3$ and modal grain size in surface sediment and sediment trap samples from the Nazaré Canyon system. Number of samples N is indicated between brackets.

		Pb	Ca	C_{org}	$CaCO_3$	U	Mn	Ni	Cu	Al	Cr	Zn	Fe	Mg	Mode	
Trap samples	Pb	**1.00**	-	-	-	-	-	0.60 (16)	-	-	0.64 (18)	-	0.58 (18)	-	-	Surface sediment samples
	Ca	-	**1.00**	-	-	-	-	0.55 (16)	0.51 (17)	-	-	-	-	-	-	
	C_{org}	0.49 (45)	0.72 (47)	**1.00**	0.89 (10)	-	-	-	-	-	-	-	-	-	-	
	$CaCO_3$	-	0.98 (47)	0.71 (47)	**1.00**	-	-	-	-	-	-	-	-	-	-	
	U	-	-0.57 (45)	-0.34 (45)	-0.55 (45)	**1.00**	-	-	-	-	-	-	-	-	-	
	Mn	-	0.95 (47)	0.67 (47)	0.94 (47)	-0.62 (45)	**1.00**	0.76 (16)	0.83 (17)	-	0.70 (19)	-	-	-	-	
	Ni	0.35 (40)	-	-	-	0.43 (40)	-	**1.00**	0.72 (16)	-	0.77 (16)	-	0.58 (16)	-	-	
	Cu	0.71 (29)	0.91 (29)	0.82 (29)	0.91 (29)	-	0.86 (29)	-	**1.00**	-	0.77 (17)	0.59 (12)	0.59 (17)	-	-	
	Al	-	-0.70 (47)	-0.51 (47)	-0.72 (47)	-	-0.59 (47)	-	-0.70 (29)	**1.00**	-	-	-	0.82 (18)	-	
	Cr	0.43 (28)	-	-	-	-	-	-	-	-	**1.00**	-	-	-	-	
	Zn	0.37 (42)	0.33 (44)	0.51 (44)	-	-	-	-	-	-	-	**1.00**	-	-	0.68 (10)	
	Fe	-	-0.61 (47)	-0.41 (47)	-0.66 (47)	-	-0.49 (47)	-	-0.73 (29)	0.75 (47)	0.40 (28)	-	**1.00**	-	-	
	Mg	-	-	0.34 (47)	-	-0.43 (45)	0.29 (47)	-	-	0.41 (47)	-	0.45 (44)	-	**1.00**	**-**	

medium). In almost all analysed samples Ni exceeded the ERL, yet Long *et al.* (1995) argue that sediment guidelines for Ni have low accuracy.

In the Lisbon-Setúbal, Cascais and Nazaré canyons all analysed trace metals reached concentrations above the ERL in one or more samples. There are samples with concentrations of Pb above the ERL especially in the upper reaches of the canyons. Copper and Cr showed concentrations above the ERL in the walls of the canyons and in the lower canyons. For Zn the Cascais Canyon is highlighted since all samples collected had concentrations above the ERL.

On the Sines open slope, Cr, Cu and Zn showed contents exceeding the ERL in all samples from below 1000 m WD while Pb had no samples above the ERL. On the Estremadura open slope there were no samples with contents of Pb and Cr higher than the ERL. For Cu and Zn two samples of the four collected in this area had concentrations above the ERL.

Assessment of trace metal distribution by reference to NOAA guidelines highlights samples from all study areas with enhanced trace metal contents. In the southern canyons higher concentrations of trace metals were mainly encountered in surface sediments from the upper reaches of the canyons. In the northern area enhanced concentrations of all the considered trace metals were mostly found in sediment trap samples from the lower Nazaré Canyon.

Interpretations based on sediment quality guidelines must be treated with due caution since they do not take regional biotic and environmental variability into account nor the specific sediment composition. In the present study they are presented just as a preliminary step for the evaluation of trace metal dispersion.

7.2.6. Present-day trace metal enrichment

Lead and Zinc

In the Lisbon-Setúbal and Cascais canyons all surface sediment samples show EF (Pb) higher than 1.0 (Figure 7.4a). Highest EF (Pb) values above 2.5 are found in the upper reaches of these canyons, whereas EF values generally decrease further down-canyon. The lowest values (EF < 1.5) correspond to two samples collected on the open slope (225-02 and 225-20, EF = 1.4) and one in the lower part of the canyon (225-07, EF

= 1.3). Zinc enrichment has a largely comparable distribution as Pb though generally with lower EF values (Figure 7.4a, b). EF (Zn) values above 1.5 occurred only in the Lisbon Canyon. Both Pb and Zn showed highest enrichments in the Lisbon Canyon, followed by Cascais and upper Setúbal canyons.

In the Lisbon-Setúbal Canyon, EF (Pb) has an offshore logarithmic decrease in both canyon branches (r^2 = 0.60 and 0.57, respectively) while EF (Zn) only shows it for the Setúbal Canyon. Samples collected on the walls and edges of the canyons reveal consistently lower EFs than surface samples collected at equivalent water depths along the axis of the Lisbon-Setúbal and Cascais canyons.

EFs in surface sediments of the upper reaches of the Lisbon and Cascais canyons are comparable to those from surface sediments from the Lisbon outer shelf and upper slope (Chapter 5, Table 5.5 on pg. 133). EFs in surface sediments of the upper Setúbal Canyon, however, are higher than the mean values obtained for the Setúbal and Sines upper slopes for both Pb and Zn.

In the Nazaré Canyon, EF (Pb) and EF (Zn) above 1.5 are only found in the upper reaches of the canyon, at depths less than 1000 m WD. Lower values are found further down the canyon. Canyon surface samples show a slight EF decrease with water depth, especially for Pb, whereas open slope values are relatively constant for Zn and do not show a consistent pattern with water depth for Pb (Figure 7.4a, b).

Enrichment factors of Pb and Zn are slightly lower on the walls and edges of the canyons than on true open slope transects (Sines and Estremadura) (Figure 7.4a, b). Possibly this reflects dilution with pre-industrial sediment, either by hydrodynamic mixing or bioturbation. Comparing samples at equivalent water depths, the enrichment factors of Pb and Zn are higher in the Sines transect than for the Estremadura transect.

Copper

In contrast with Pb and Zn, Cu enrichment shows a logarithmic increase with water depth (r^2 = 0.67) in the Lisbon-Setúbal Canyon and the adjacent slope. For the Cascais Canyon EF (Cu) increases with increasing water depth as well but values are consistently lower than for the Lisbon-Setúbal Canyon (Figure 7.4c). Surface sediments from the upper reaches of the Lisbon and Cascais canyons have comparable EFs (Cu) to the mean value obtained for the Lisbon outer shelf and upper slope (1.2 each area). Surface sediments from the upper Setúbal Canyon have also comparable EFs (Cu) to those found on the Setúbal and Sines outer shelves and upper slopes (Table 5.5).

In the Nazaré Canyon, EFs (Cu) in surface sediments are more or less constant both along the canyon thalweg and on the adjacent slope.

On the open slopes, EFs (Cu) are generally higher near the edges of the canyons than on true open slope sediments (Figure 7.4c). No differences in Cu enrichment are observed between the Sines and Estremadura transects.

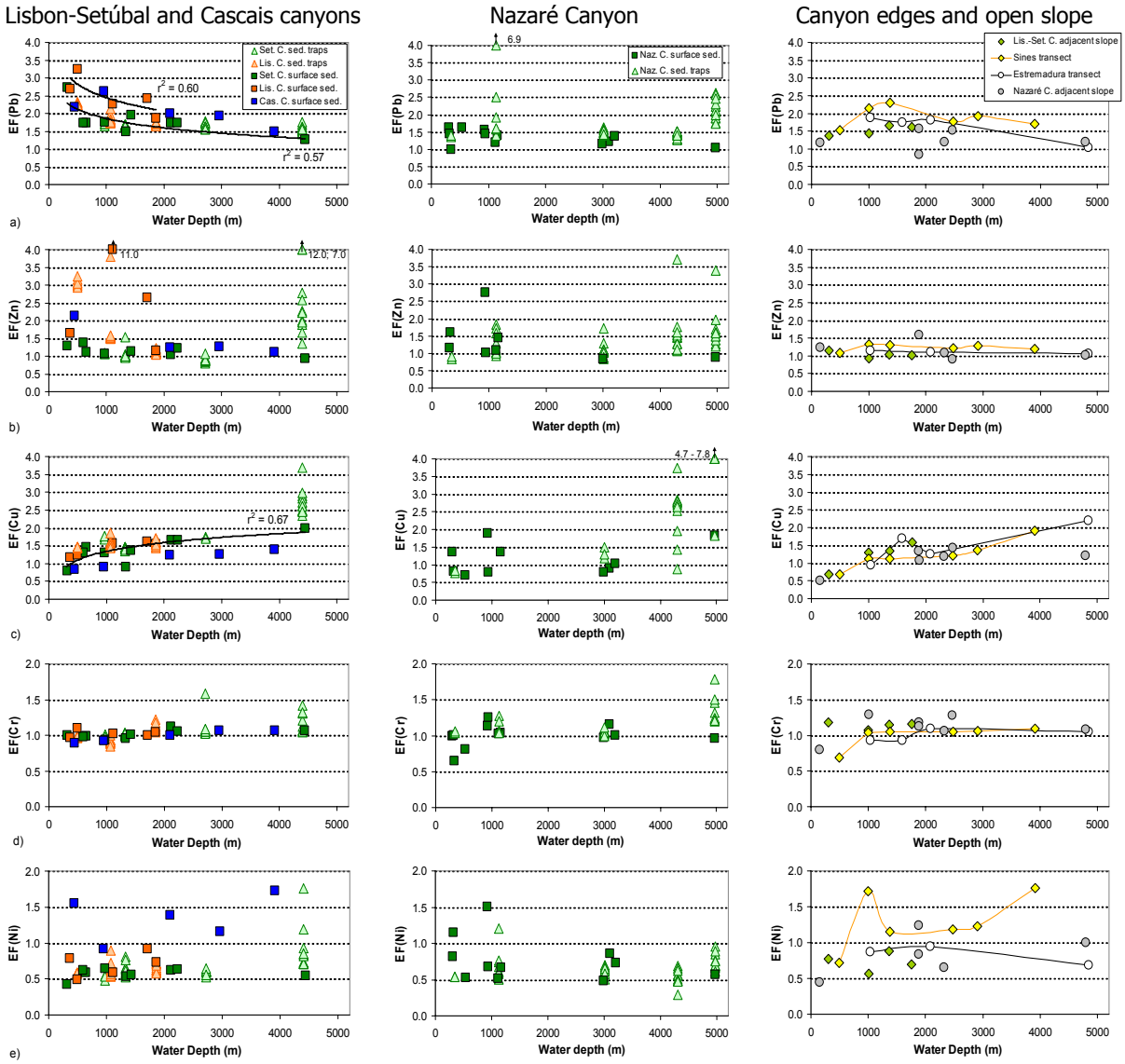

Figure 7.4. Enrichment factors for Pb (**a**), Zn (**b**), Cu (**c**), Cr (**d**) and Ni (**e**) in surface sediments and sediment trap particulate material plotted against water depth for the Lisbon-Setúbal, Cascais and Nazaré canyons and adjacent open slopes.

Chromium and Nickel

Whereas Pb, Zn and Cu are variably enriched throughout the central Portuguese canyons and open slope transects there is little if any evidence for surface enrichment of Cr and Ni in any part of the study area (Figure 7.4d, e).

Within the canyons there are no clear trends in enrichment factors with water depth for Cr and Ni, and neither are substantial differences observed in enrichment of these elements between the canyons, except that EF (Ni) seem higher in the Cascais Canyon compared to the other canyons. On the open slopes, no differences are observed in Cr enrichment, but Ni enrichments seem to be higher in the Sines transect.

EFs of Cr and Ni in sediments from the upper reaches of the Lisbon and Cascais canyons are comparable to those found in surface sediments from the Lisbon outer shelf/upper slope, but EF (Ni) values in the Cascais Canyon are considerably higher than those found in the upper slope. Surface sediments from the upper Setúbal Canyon have also comparable EFs (Cr and Ni) to those found on the Setúbal and Sines outer shelves/upper slopes (Table 5.5).

7.2.7. Excess and total metal inventories over the last 150 years

Inventories of excess Pb, Zn and Cu in sediments from the canyons range from values comparable to, to values two orders of magnitude higher than the ones recorded in open slope sediments for equivalent water depth (Figure 7.5, Table 7.5).

In general, the contributions of excess Pb, Zn and Cu relative to total inventories deposited over the last 150 years decrease with increasing water depth for both canyons and open slope (Figures 7.6, 7.7, 7.8). The contribution of excess Pb (Pb_{xs}) varies from a maximum of 56 and 41 % in the upper Lisbon and Setúbal canyons, respectively, to a minimum of 6 % in the lower canyon (4402 m WD). In the Cascais Canyon, percentages vary from 53 to 29 % from 953 to 3900 m WD. Sediments from the upper Nazaré Canyon have Pb_{xs} percentages between 37 and 42 %, similar to the ones from the upper Setúbal canyon (Figure 7.6). In general, percentages of Pb_{xs} are lower in the northern part of the study area, adjacent to the Nazaré Canyon and at the Estremadura transect, than in the southern part, for equivalent water depths. For example, between 2000 and 3000 m WD there is ~12 % more Pb_{xs} in the Sines open slope compared to the Estremadura open slope (Figure 7.6).

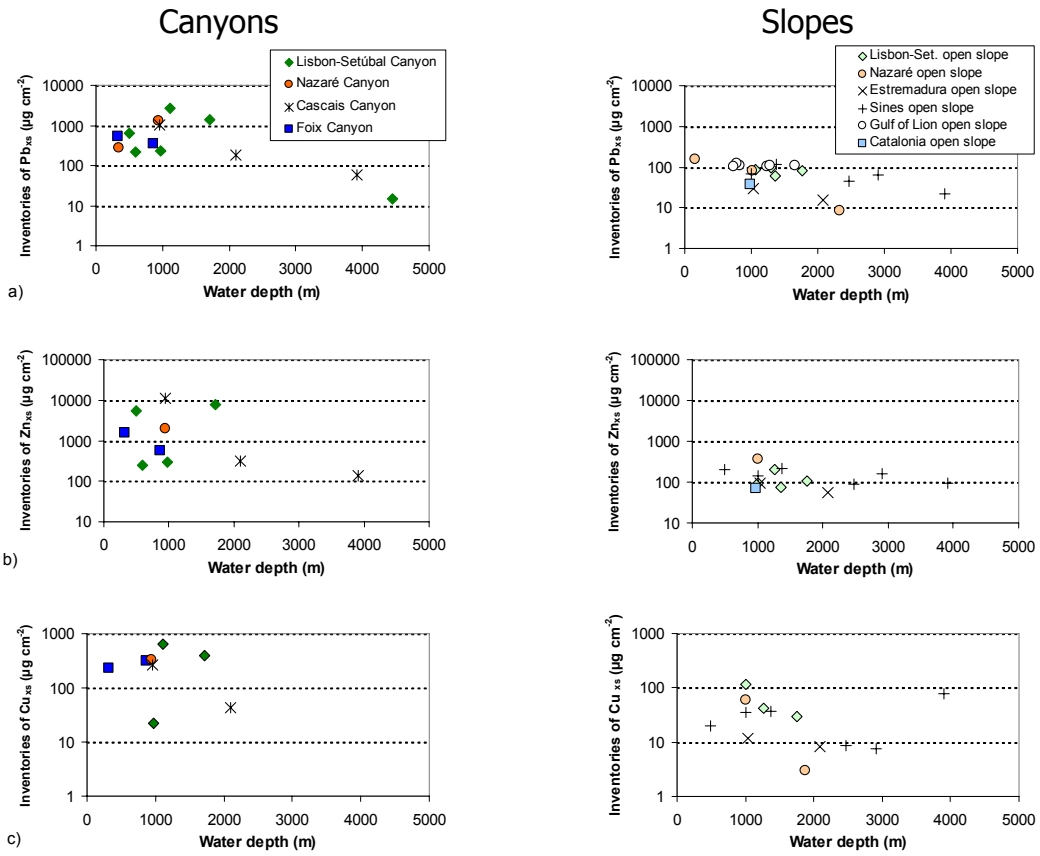

Figure 7.5. Inventories of excess Pb, Zn and Cu accumulated over the last 150 years in sediment deposits of canyons (left) and of slopes adjacent to canyons and open slopes (right), plotted against water depth. Catalonia margin inventories as reported by Palanques *et al.* (2008) and inventories of Pb for the Gulf of Lions open slope as reported by Miralles *et al.* (2006).

Percentages of excess Zn (Zn_{xs}) are clearly higher in the Lisbon Canyon (51 – 55 %) compared to the upper Setúbal Canyon (14 – 20 %). The only core in the Nazaré Canyon reliable for Zn, located at 941 m WD, has 21 % of Zn_{xs}, comparable to the upper Setúbal Canyon values (Figure 7.7, Table 7.5). In the Cascais Canyon a more complete set of Zn_{xs} percentages was obtained for the whole canyon range from 58 % (953 m WD) down to 10 % (3914 m WD). Excess Zn on the open slope transects has considerably lower values of 15 % (490 m WD) down to 6 % (3900 m WD). Values from the open slopes adjacent to the canyons span a wide range of 9 – 36 %.

Excess Cu (Cu_{xs}) reaches the highest values on the slope around 1000 m WD, 43 % in the Lisbon-Setúbal area and 27 % in the Nazaré area (Figure 7.8). At equivalent water depth in the canyons, lower values of 22 %, 21 %, 17 % and 6 % are found for the Cascais, Lisbon, Nazaré and Setúbal canyons, respectively.

Table 7.5. Inventories of total and excess trace metals and percentages of excess trace metal accumulated in sediment deposits of the central Portuguese margin over the last 150 years. NC - Nazaré canyon; NS - Nazaré slope; EOS - Estremadura open slope; CC - Cascais canyon; LC - Lisbon canyon; SC - Setúbal canyon; LSS - Lisbon-Setúbal slope; SOS - Sines open slope. * represent piston-cores being the other multi- or box-cores.

Location	Core	WD (m)	Total Pb Inv. (μg cm^{-2})	Excess Pb Inv. (μg cm^{-2})	Pb_{xs} (%)	Total Zn Inv. (μg cm^{-2})	Excess Zn Inv. (μg cm^{-2})	Zn_{xs} (%)	Total Cu Inv. (μg cm^{-2})	Excess Cu Inv. (μg cm^{-2})	Cu_{xs} (%)
NC	204-56	497	667	280	42.0	-	-	-	-	-	-
NC	236-13*	941	3537	1301	36.8	9516	1995	21.0	2030	335	16.5
NS	218-57	151	494	154	31.2	-	-	-	-	-	-
NS	225-27	1009	274	80	29.1	990	357	36.0	220	60	27.2
NS	204-49	1881	289	112	38.7	-	-	-	257	3	1.1
NS	204-60	2323	103	8	8.1	-	-	-	-	-	-
EOS	252-27	1034	158	29	18.3	901	92	10.2	166	12	7.1
EOS	252-16	2084	78	15	19.7	513	55	10.8	127	8	6.6
CC	252-36*	953	1931	1016	52.6	18718	10910	58.3	1205	268	22.3
CC	252-32	2100	370	182	49.2	1987	323	16.2	345	44	12.6
CC	252-30	3914	198	57	28.9	1327	133	10.0	-	-	-
LC	269-02*	497	1163	626	53.9	10725	5482	51.1	-	-	-
LC	252-34*	1112	4820	2703	56.1	-	-	-	2947	633	21.5
LC	204-31*	1710	3134	1418	45.2	13935	7722	55.4	2413	390	16.2
SC	204-19	595	532	218	41.0	1738	250	14.4	-	-	-
SC	204-23	971	559	230	41.2	1448	290	20.0	395	22	5.6
SC	225-07	4445	235	15	6.4	-	-	-	-	-	-
LSS	225-20	1004	308	85	27.8	1076	96	8.9	264	115	43.4
LSS	225-45	1266	295	95	32.1	913	204	22.3	262	43	16.4
LSS	236-10	1364	144	62	43.1	470	73	15.5	-	-	-
LSS	225-21	1760	201	79	39.5	574	104	18.2	196	30	15.2
SOS	252-57	490	-	-	-	1486	206	13.9	197	20	10.1
SOS	252-56	1002	221	69	31.2	1355	142	10.5	257	36	13.9
SOS	252-55	1374	274	116	42.4	1486	219	14.7	278	37	13.5
SOS	252-53	2475	173	45	26.2	1152	87	7.6	254	9	3.4
SOS	252-52	2908	274	65	23.8	1903	162	8.5	458	8	1.7
SOS	252-51	3908	214	22	10.3	1618	92	5.7	540	77	14.2

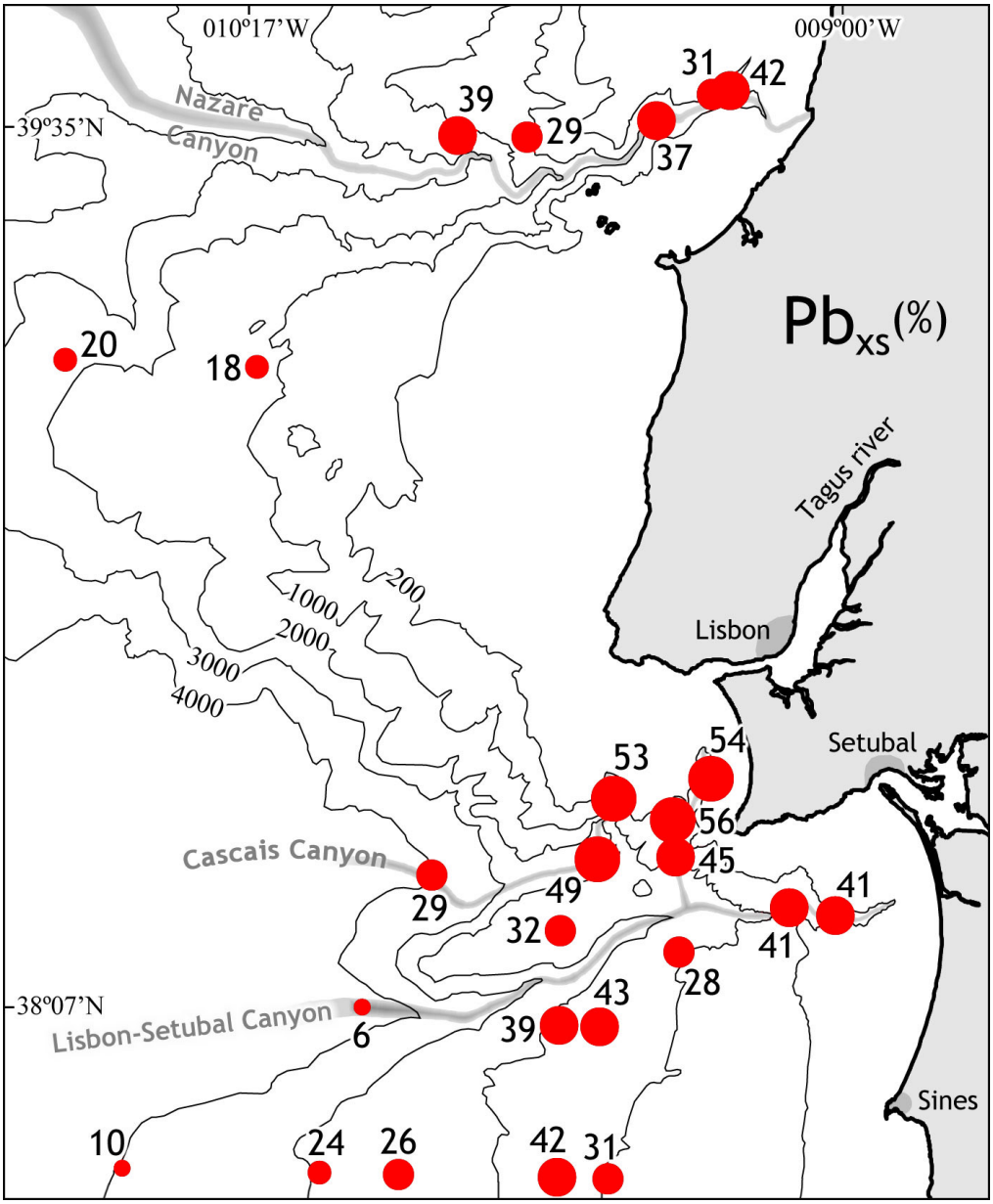

Figure 7.6. Geographic distribution of mean contribution of excess Pb as percentage of total Pb deposition over the last 150 years.

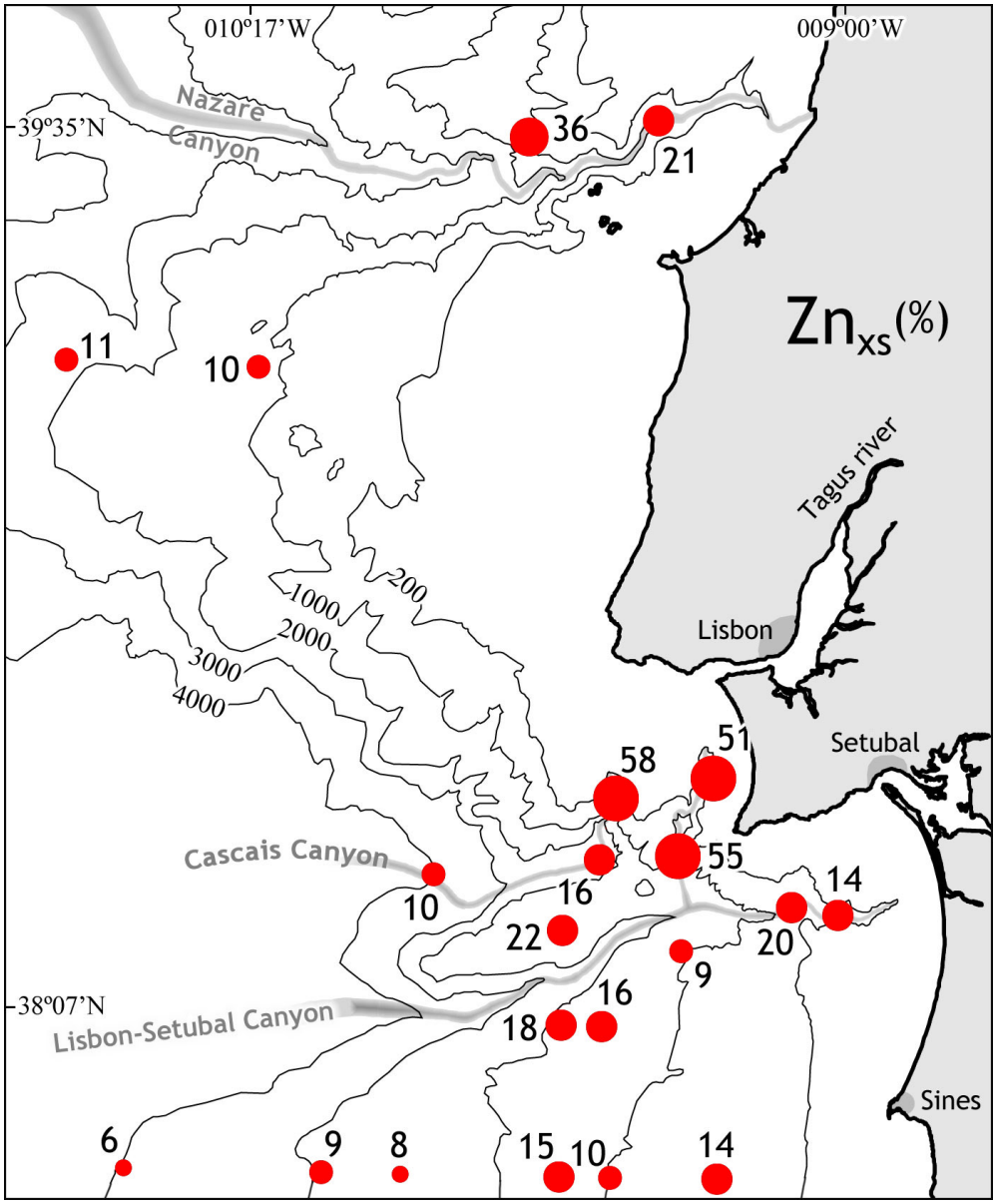

Figure 7.7. Geographic distribution of mean contribution of excess Zn as percentage of total Zn deposition over the last 150 years.

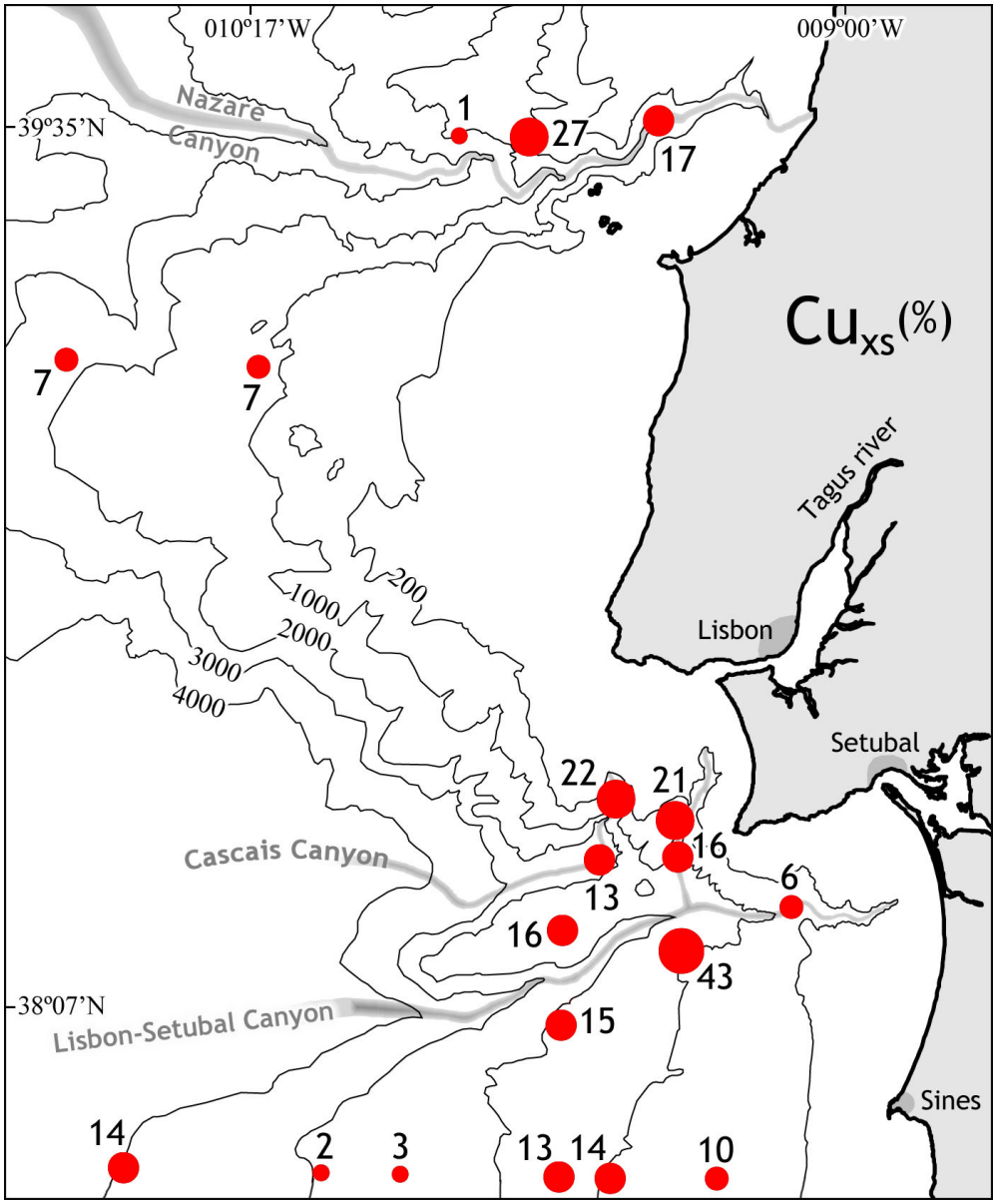

Figure 7.8. Geographic distribution of mean contribution of excess Cu as percentage of total Cu deposition over the last 150 years.

7.3. Discussion

7.3.1. Distribution patterns of excess trace metal accumulation in Portuguese canyons and open slopes

Contents of major elements Ca, Al and Fe and some trace metals like Cr and Ni in surface sediments appear largely similar to contents measured in pre-industrial sediments (Figures 7.2 and 7.3), meaning that in terms of bulk composition the sediment has not changed over the last 150 years. Pre-industrial concentrations of trace metals, Fe and Al are largely similar for the Lisbon-Setúbal and Nazaré Canyon systems (Table 7.1), whereas recent surface sediments and suspended particulate matter usually display higher concentrations of various trace metals, for some elements appreciably diverging between both areas. Surface sediments and suspended particulate matter in the Lisbon-Setúbal Canyon have higher mean concentrations of Mn, Zn, Pb, Cr and Ni (and Cu, Fe for surface sediments only) compared to the Nazaré Canyon (Table 7.1). Regarding only surface sediments, the highest mean concentrations for all trace metals are found in the Cascais Canyon.

Percentages of excess trace metal accumulated over the last 150 years in sediment deposits are also higher for the southern canyons, especially the Lisbon and Cascais canyons (Table 7.5). This is consistent with the proximity of the Lisbon and Cascais canyons to densely populated and industrialised areas, and with sediment input from the Tagus River, a potential major source of particle-bound pollutants.

The degree of trace metal enrichment found in sediments from the Lisbon and Cascais canyons is comparable or higher to what has been previously published from other canyon and slope areas (Figure 7.5), such as the Foix Canyon in the NW Mediterranean (Palanques *et al.*, 2008), the Gulf of Lions continental slope in the NW Mediterranean (Miralles *et al.*, 2006), and the Kaoping Canyon off Taiwan (Hung & Hsu, 2004).

Thus, the canyons of the central Portuguese margin represent different degrees of trace metal enrichment, with the upper Cascais and Lisbon canyons being the more affected by trace metal contamination, and the Nazaré Canyon the least. This applies not only for the most recent sediments but also for sediments deposited over the last 150 years.

On the other hand, comparing trace metals inventories in canyons and adjacent open slopes demonstrates that the upper canyons act as trace metal depocentres. Maximum excess inventories occur in the upper parts of the canyons between 500 and 1700 m WD (Figure 7.5 and Table 7.5), which is where trace metal loadings generally are highest and where active sediment depocentres are located (De Stigter *et al.*, 2007b; Oliveira *et al.*, 2007; Arzola *et al.*, 2008).

7.3.2. The Lisbon-Setúbal Canyon: trace metal enrichment and links to sediment input and transport

Contributions from the Tagus and Sado rivers to the canyon

As seen above the Lisbon and upper Setúbal canyons are hotspots of Pb and Zn enrichment relative to the deeper canyon reaches and adjacent open slopes. The Lisbon and Setúbal Canyon heads are located close to the mouths of the Tagus and Sado rivers, respectively, where high trace metal concentrations in water, sediments and biota due to anthropogenic activities have been reported (e.g. Cotté-Krief *et al.*, 2000; Caeiro *et al.*, 2005; França *et al.*, 2005).

A gradient of decreasing Pb and Zn enrichment, from the Tagus prodelta (Chapter 5 and Mil-Homens *et al.*, 2009) to the head of the Lisbon Canyon and then further down, strongly suggests that the excess Pb and Zn must be derived from land, with the Tagus River appearing as the most important local source. This is supported by observations by Jouanneau *et al.* (1998), who noted a southward gradient in intensity of bottom nepheloid layers on part of the Lisbon shelf, and in Pb and Zn concentrations in the underlying seabed sediments, from the Tagus River mouth to close the head of Lisbon Canyon. Much less sediment and associated trace metals appear to be transferred from the Sado River into the upper Setúbal Canyon, judging from the consistently lower enrichment of Pb and Zn in the latter canyon, as compared to the Lisbon Canyon, despite the fact that also the Sado Estuary is enriched in Pb and Zn. The less effective transfer may be explained by the much lower discharge of the Sado River and the greater distance between the river mouth and the canyon head.

Copper on the other hand shows signs of enrichment (EF > 1.5) especially in the deeper parts (> 2000 m WD) of both canyons and open slopes. Whereas Pb and Zn dispersal thus seem to be largely explained by terrigenous sediment transport from river

to canyon, a different mechanism may be involved in the dispersal of Cu. Although the significant correlation between Cu and Fe suggests that Cu is partly associated with terrigenous sediment, normalisation for Fe reveals another trend of increasing Cu enrichment with increasing water depth. Calcium seems to be involved in this other mechanism of Cu dispersal, in view of the positive correlation of EF (Cu) with Ca (r^2 = 0.73) in sediment trap samples from deep parts of the Lisbon-Setúbal Canyon which are less affected by resuspention (Figure 7.9). In different marine environments worldwide the distribution of Cu has been shown to correlate with major nutrients (Bruland, 1983) especially caused by coupled cycling of those nutrients mediated by assimilation and recycling by plankton (e.g. Bruland *et al.*, 1991; Löscher, 1999). In agreement with this, Caetano & Vale (2003) studying the composition of seston and plankton from the mouth of major estuarine systems in Portugal concluded that Cu accumulation in phytoplankton is the dominant process determining the distribution of this element in Portuguese coastal waters.

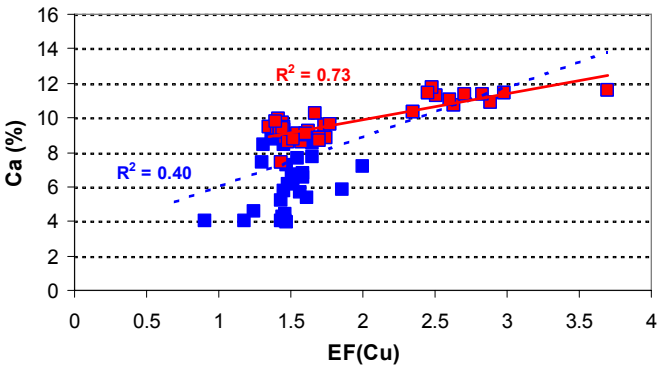

Figure 7.9. Concentration of Ca against EF (Cu) in sediment trap samples from the Lisbon-Setúbal Canyon. Blue symbols represent samples from shallower deployments (269-02, 252-34, 204-23, 218-36) where lateral supply of resuspended sediment is thought to dominate sedimentation, and red symbols represent samples from deeper sites (225-03, 204-35 and 252-62) where pelagic sedimentation is thought to prevail. The blue line represents the regression using all samples and the red line the regression using only the trap samples from deeper deployments.

Sediment transport along the Lisbon-Setúbal Canyon

On secular timescale, in the lower Setúbal Canyon, the contribution of excess Pb on the total accumulation of Pb (natural and anthropogenic) over the last 150 years is conspicuously low, and of the same order as the % Pb_{xs} calculated for equivalent depth on the Sines open slope (respectively 6 % and 10 %). This provides further confirmation that down-canyon transport of sediments and associated trace metals is not important in the Lisbon-Setúbal Canyon. As observed previously, the most recent event of mass

transport to the lower canyon, represented by a sandy turbidite layer, dates from before the start of the industrial era. In comparison to the low % Pb_{xs} in the lower Setúbal Canyon and Sines slope, the 29 % of Pb_{xs} calculated for the lower Cascais Canyon appears quite high, and may indicate more efficient transport through the latter canyon, or in general a higher fallout of Pb due to greater proximity to land.

On a decadal timescale, the logarithmic decrease of Pb and Zn EFs and increase of EF (Cu) in surface sediments down the course of the Lisbon-Setúbal Canyon indicate the inefficient down-canyon transport of sediments from the upper to the lower canyon. The geographic patterns of Cu, Pb and Zn enrichment indicate that most of the particulate matter coming from the coastal area and/or adjacent shelf is trapped in the upper canyons. In the lower canyon, lower and less variable EFs imply a change in the sedimentary setting, with reduced terrigenous input and increasing relative importance of pelagic settling as a source of sediments. In agreement, Mn concentrations in surface sediments from the canyon and open slope show a slow increase with water depth until around 2000 m where a conspicuous increase appears in the surface sediments from the canyon (Figure 7.2d). High contents of Mn in surface sediments are related to high oxidised states of seabed sediments caused by low sediment accumulation rates and low organic matter fluxes (Miller & Orbock, 2007).

According to the here presented geochemical data, the Lisbon-Setúbal Canyon thus seems to be characterised by limited down-canyon transport of sediments, and the system appears to be rather accumulating sediments and associated trace metals in the upper canyon. This is in accordance with data presented in Chapter 6 which show that, for this canyon, processes of down-canyon transport are not common on a decadal timescale. Down-canyon transport of trace metals to the lower canyon seems certainly more effective in the Nazaré Canyon due to its more active mechanisms of down-canyon sediment transport by sediment gravity flows (De Stigter *et al.*, 2007b). In fact, the enrichment of Pb and Zn in surface sediments from the Nazaré Canyon show a somewhat linear down-canyon decrease. This is in accordance with sedimentary material derived from the near-shore zone being trapped in the upper canyon and then being effectively transported down-canyon with increasing dilution by old sediments with pre-industrial trace metal concentrations.

Discharges of contaminated sediments in the Lisbon Canyon

Recent information from the APL (Administração do Porto de Lisboa – Administration of the Harbour of Lisbon) shows that 8000 m^3 and 7500 m^3 of contaminated sediments dredged from the Tagus Estuary were discharged in the Lisbon Canyon in 2005 and 2007, respectively (Nemus, 2011). The area used has a radius of 200 m and central point at Longitude 09º 19' W and Latitude 38º 29' N (ED50) at around 400 m of water depth (Figure 6.14). According to the APL this same area has been used by other institutions for discharge of sediments (e.g. military institutions which also dredge the estuary).

Sediments discharged by APL in this area were classified, according to the Portuguese law (Portaria nº1450/2007, de 12 de Novembro), as "moderately contaminated" (class 3). Table 7.6 shows the range of concentrations for different parameters in class 3.

Table 7.6. Concentrations of trace metals (µg g^{-1}) and organic compounds (µg kg^{-1}) in sediment classified as class 3 (moderately contaminated) according to the Portuguese law (Portaria nº1450/2007 de 12 de Novembro).

Parameters	Range of concentrations	Parameters	Range of concentrations
As	50 - 100	Ni	75 – 125
Cd	3 - 5	Zn	600 – 1500
Cr	100 – 400	PCB	25 – 100
Cu	150 – 300	PAH	2000 – 6000
Hg	1.5 – 3.0	HCB	2.5 - 10
Pb	150 - 500	-	-

The following is an exercise attempting to compare the input of anthropogenic trace metals from these sediment dumpings to the total annual input of anthropogenic trace metals in the Lisbon Canyon thalweg. Taking 38 km as the length of the canyon (Lastras *et al.*, 2009) and 1 km as maximum width of the thalweg, and average sediment accumulation in the thalweg as around 8.75 g m^{-2} d^{-1} (Chapter 6, section 6.3, pg. 143) with ~35 ug g^{-1} anthropogenic Pb content (sections 7.2.3 and 7.2.6) yields a deposition of 4.2 x 10^6 g of anthropogenic Pb per year. Known discharges of 2005 and 2007, together 15500 m^3 with average dry bulk density of 1000 kg m^{-3}, and considering a class 3 Pb contamination of 300 µg g^{-1} yields a total input of 4.7 x 10^6 g of dumped Pb. Spread out evenly over the Lisbon Canyon thalweg this means that the discharges represent 1.1 times the present-day annual deposition of anthropogenic Pb in the Lisbon Canyon thalweg. That is assuming that the surface enrichment of Pb found in the Lisbon Canyon itself is not the result of sediment dumping.

Concentrations of trace metals found in the Lisbon Canyon at sampling locations relatively close to the discharge area (surface sediment and sediment trap samples from site 252-34, collected in 2007) only approached class 3 level reported in Table 7.6 for Zn. The other analysed trace metals had lower concentrations (Figure 7.3). In addition, sediments collected in the same area in 2003 (Costa *et al.*, 2011) had concentrations of Pb, Cu, Cr and Ni comparable to those reported in the present study, implying that the mentioned discharges did not introduce considerable concentrations of these trace metals in the system. Only concentrations of Zn were effectively higher in sediments collected in 2007 compared to those collected in 2003 for similar water depths (1198 *vs.* 197 μg g^{-1}, respectively). This increase may indeed be related to the discharge of contaminated sediments into the Lisbon Canyon between 2005 and 2007. The exercise shown above about contributions of Pb in the Lisbon Canyon by the mentioned discharges is most certainly an overestimation as surface sediment concentrations of Pb did not increase between 2003 and 2007. However, it is possible that other discharges of Pb-contaminated sediments had already occurred in the canyon before 2003, before the collection of samples analysed by Costa *et al.* (2011).

The above exercise, even if very rough, implies that present-day trace metal concentrations in surface sediments in the upper Lisbon Canyon may not only originate from outflow from the Tagus Estuary and resuspension of sediments from the shelf, but may include a considerable contribution from dumping of moderately contaminated dredged sediments in the area. This subject certainly needs further investigation as to what concerns the type and level of contamination in the discharged sediments and the frequency and location of these discharges by other entities than the APL.

7.3.3. Atmospheric lead fallout recorded in Portuguese canyons and open slopes

Marine sediments are assumed to provide good records of atmospheric pollution (Miralles *et al.*, 2006). The sampling transects on the Estremadura and Sines open slope and sediment traps deployed in the lower reaches of the Nazaré and Lisbon-Setúbal Canyon (218-55 and 252-62, respectively, located 104 ± 2 km from the nearest shoreline) can be assumed to have only limited influence from rivers. In accordance, surface sediments from the open slopes and trap samples from the lower canyon sites show high

contents of calcium carbonate (Figure 7.1b). C_{org}/N ratios for the trap and surface sediments are between 6.9 and 8.5 (Chapter 6) which is indicative for organic matter of predominantly marine origin. In addition, the $^{206}Pb/^{207}Pb$ isotopic ratio of these traps samples falls in the range of that determined for regional surface waters (Richter *et al.*, 2009). Therefore, one may assume that trace metal fluxes determined from mix samples from open slope sediment cores (core interval where ^{210}Pb excess activity was still detectable) and from sediment traps, both collected in deep areas where pelagic sedimentation dominates, represent mainly atmospheric fluxes of trace metals over the last 150 years and at the present-day, respectively.

Comparison between the open slope transects shows consistently higher contents of Pb_{xs} in the Sines transect but no clear patterns for Zn_{xs} and Cu_{xs} (Figures 7.6, 7.7, 7.8). Sediment cores collected between 2000 and 3000 m WD contain ~12 % higher mean Pb_{xs} in the Sines transect (Figure 7.6). The deployments done in the Lisbon-Setúbal and Nazaré canyons around 4402 and 4975 m WD, respectively, yielded average values of excess Pb flux of 0.54 and 0.35 μg cm^{-2} yr^{-1}, respectively, representing 48 and 36 % of the total fluxes of Pb at these sites. Interestingly, the difference in anthropogenic contribution between both areas is again 12 %. It seems therefore that atmospheric Pb input in both areas was not only different in terms of cumulative flux over the past 150 years, including the interval when leaded gasoline was in use, but also in terms of present-day flux. In fact, after the complete ban on gasoline lead additives (as late as 1999 in Portugal, Roma-Torres *et al.*, 2007) one may presently notice the influence from various industrial activities as sources of Pb, as will be further discussed in the next section.

Our results are consistent with prevailing wind directions and more abundant point sources of anthropogenic Pb in the southern part of the study area. Over the second half of the last century, input from gasoline lead additives were certainly higher in the southern area since it is closer to major cities like Lisbon and Setúbal. In addition, atmospheric pollution produced in these cities is unlikely to be transported northwards since prevailing regional winds blow from N and NW directions (Freire, 1986; Gomes, 1992). Even closer to the Sines transect a major industrial agglomeration, which is the largest of the entire Iberian Peninsula, is located in the vicinity of Sines. This industrial area includes several companies, some operating since the late seventies, which represent potential sources of Pb to the environment, namely: Carbogal (produces raw material for tyres); Ibera (production of concrete); Kimaxtra (production of cement);

Metalsines (production and handling of metals); Petrogal (oil refinery); Recipneu (recycling of tyres) and Repsol polímeros e Repsol (petrochemistry plant).

The higher level of atmospheric pollution in the Sines area is confirmed by a study of biomonitors in northern, central and southern Portuguese cities by Baptista *et al.* (2008) which showed higher accumulations of Pb in biomonitors from Sines.

7.4. Lead stable isotopes (^{206}Pb, ^{207}Pb, ^{208}Pb)

7.4.1. Isotopic evidence for natural and anthropogenic sources of Pb

Estimated isotopic end members

The entire dataset, obtained for sediment trap and surface sediment samples from the central Portuguese margin, predominately suggests binary mixing between one component with high [Pb] and low ^{206}Pb/^{207}Pb and a second one with low [Pb] and high ^{206}Pb/^{207}Pb (Figure 7.10a). These are interpreted to represent anthropogenic pollutant and natural sources of lead, respectively. In such a situation, the isotopic composition of the pollutant end member can be estimated from the x-axis intercept on a plot *vs.* the inverse of the Pb concentration (Figure 7.10b). This yields ^{206}Pb/^{207}Pb ratios of 1.143 (1.134 – 1.149 at 95 % confidence interval) for the entire dataset or 1.150 (1.141 – 1.155) if samples from the two deepwater traps are excluded from the regression analysis. Conversely, the possible ^{206}Pb/^{207}Pb ratio of the natural end member can be constrained from the x-axis intercept on the isotopic ratio *vs.* concentration plot of 1.232 (1.226 – 1.240) or 1.228 (1.222 – 1.235). This represents an upper limit, because by definition the intercept at 0 µg g^{-1} Pb extrapolates beyond the isotopic signature of the actual end member with an unconstrained but non-zero Pb concentration.

Lead concentrations display an obvious, albeit slightly scattered, relationship with the ^{206}Pb/^{207}Pb isotopic ratio (Figure 7.10a). Only one data point from sediment trap site 236-07 in the upper Nazaré Canyon (1126 m WD) had a distinctly higher Pb concentration compared to the remainder of the dataset (169 µg g^{-1} *vs.* 24 - 64 µg g^{-1} for the other 112 samples) and was omitted for calculation of regression lines. This point could be considered as an outlier, although it was replicated by duplicate analysis and this trap site was generally characterised by highly variable Pb isotopic ratios and concentrations (cf. Figure 7.14b and Figure 7.3a, respectively).

Further deviations from the overall relationship between Pb concentrations and stable isotope ratios are partly systematic; i.e. points from individuals sites fall in distinct parts of the diagram. Notably, most trap samples from the lower Nazaré and Lisbon-Setúbal canyons (stations 225-22/4975 m, 218-55/4298 m and 252-62/4402 m WD) plot below the overall regression line, i.e. display a relatively low ^{206}Pb/^{207}Pb ratio for a given

concentration. These three trap sites are influenced mostly by pelagic fluxes from the overlying water column, with minor, if any, direct down-canyon transport (cf. section 7.4.3 below); the associated atmospheric lead fallout seems to be characterised by a distinct concentration-isotopic signature.

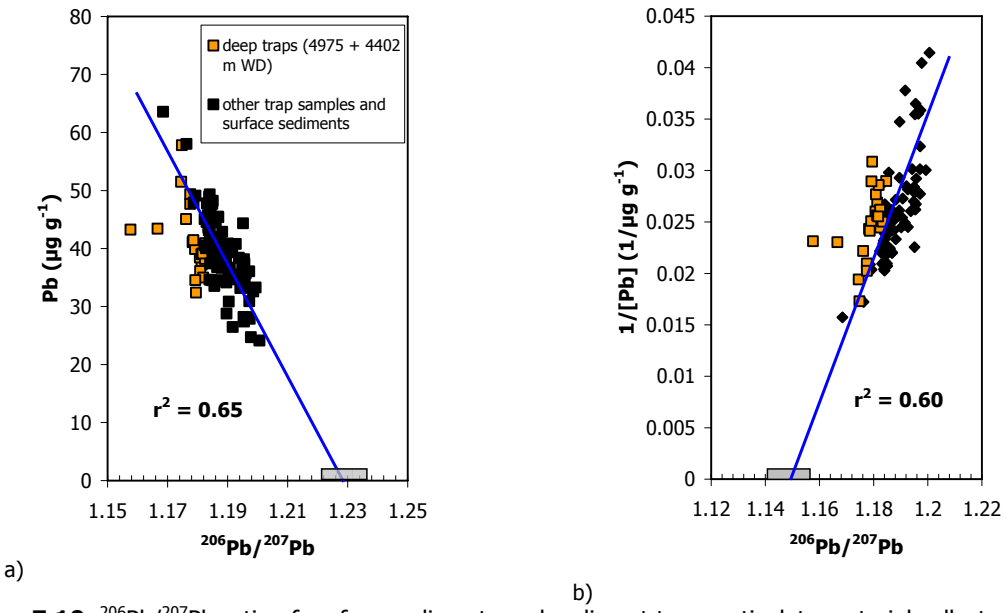

a) b)

Figure 7.10. $^{206}Pb/^{207}Pb$ ratio of surface sediments and sediment trap particulate material collected from the central Portuguese continental margin plotted against **a)** Pb concentrations and **b)** inverse of Pb concentrations. Orange squares – lower canyon sediment traps; black diamonds – all other samples. Solid lines are regressions excluding data from two lower canyon traps. Grey rectangles indicate combined 95 % confidence interval for x-axis intercepts, depicting possible signatures for natural (panel a) and anthropogenic contaminant (panel b) isotopic end members.

Potential sources of lead in Portuguese canyons

A three-isotope diagram ($^{206}Pb/^{207}Pb$ *vs.* $^{208}Pb/^{206}Pb$) puts isotopic results of the present study in context through comparison with potential natural and anthropogenic sources (Figure 7.11). As data on Portuguese pollutant lead are unfortunately not available, we assume that isotopic signatures from other western European countries are broadly representative for the area of the present study. Cumulatively, the well-defined overall linear regression through most data points indicates that binary mixing between two end members as outlined above can explain most of the Pb isotopic variability observed in the present study. End members might obviously be "mixed", themselves reflecting mixing of several sources, or slightly variable along the canyon axes (cf. above) or between sediment trap and core top samples (see below). More complex scenarios with additional "intermediate" sources along the mixing line also cannot be ruled out.

The estimated $^{206}Pb/^{207}Pb$ ratio of the anthropogenic end member in canyon sediments and particulate material collected in sediment traps (~1.14 – 1.15, cf. above) most closely corresponds to fly ashes from waste incinerators. Their Pb isotopic composition represents an average signature of industrial lead, as it is derived from mixing and burning of a wide range of Pb-containing products (Monna *et al.*, 1997). It is remarkably constant both for different European locations and different sampling sites (Döring *et al.*, 1997; Monna *et al.*, 1997; Deboudt *et al.*, 1999; Hansmann & Köppel, 2000) and also close to the average Pb isotopic ratio of all main worldwide Pb ores (Sangster *et al.*, 2000).

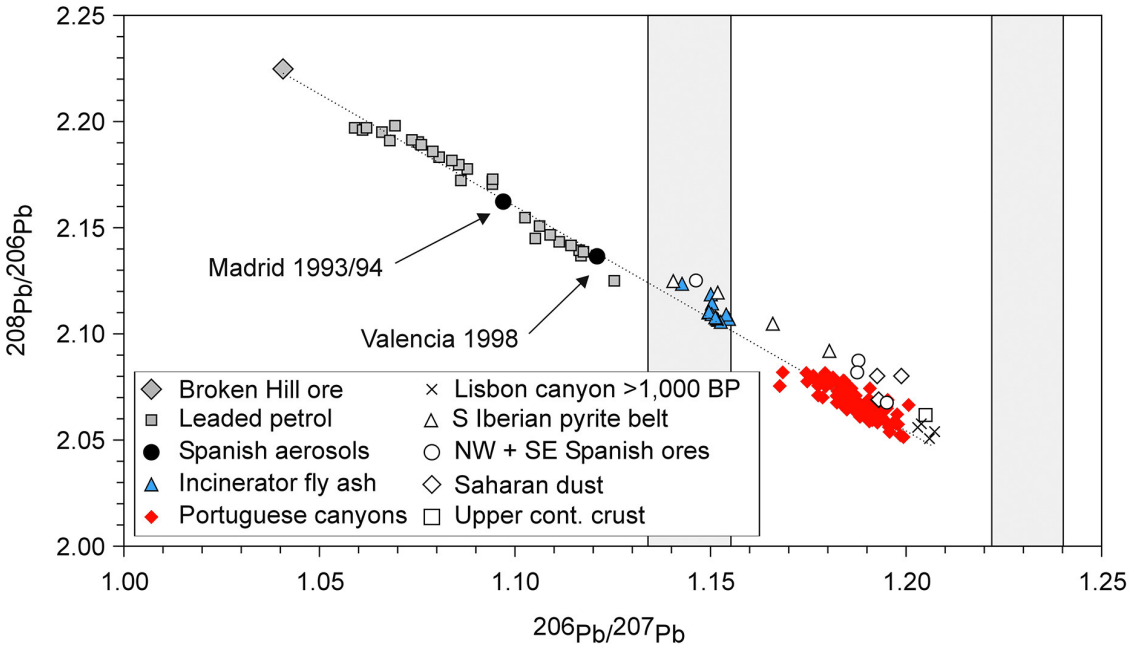

Figure 7.11. Three-isotope plot ($^{206}Pb/^{207}Pb$ *vs.* $^{208}Pb/^{206}Pb$) for surface sediments and sediment trap samples from central Portuguese canyons (red diamonds and black crosses, this study – samples from Sines open slope and trap 252-62 are not included) and various possible sources of Pb (literature data). Grey, blue and black symbols represent inferred primary potential contaminants, open symbols correspond to conceivable minor additional sources. Regression line (stippled line) determined for filled blue, red, black and grey symbols (r^2 = 0.99). Grey bars correspond to range of estimated $^{206}Pb/^{207}Pb$ for anthropogenic and natural end members in Portuguese canyons (see Figure 7.10 and text); the anthropogenic end member corresponds most closely to fly ashes from individual waste incinerators (blue triangles). Data sources: Broken Hill ore (Sangster *et al.*, 2000), European leaded petrol (Monna *et al.*, 1997; Hansmann & Köppel, 2000), Spanish aerosols (Bollhöfer & Rosman, 2001), Incinerator fly ashes (Döring *et al.*, 1997; Monna *et al.*, 1997; Deboudt *et al.*, 1999; Hansmann & Köppel, 2000), S Iberian pyrite belt (Santos Zalduegui *et al.*, 2004 [average values for four sample populations]), other Spanish ores (Sangster *et al.*, 2000), Saharan dust (Grousset *et al.*, 1994, 1995; Abouchami & Zabel, 2003), Upper continental crust (Millot *et al.*, 2004).

In Portugal, leaded gasoline was gradually phased out in the early 1990s but completely eliminated only in 1999 (Roma-Torres *et al.*, 2007). Some surface sediment samples of the present study integrate Pb input over the last ~10 years (prior to sampling

in 2002-2007); their Pb isotopic ratios may thus still be affected by this time-transient change in pollutant sources (cf. Grousset *et al.*, 1994). Available data (Monna *et al.*, 1997; Hansmann & Köppel, 2000) indicate that western European leaded gasoline has comparatively unradiogenic (not produced by radioactive decay) Pb isotopic signatures, reflecting mixing between Australian Broken Hill ore (Sangster *et al.*, 2000) and other Pb ores for production of gasoline lead additives. Considering the 95 % confidence interval for $^{206}Pb/^{207}Pb$ of the pollutant end members, some ongoing contribution from this source cannot be ruled out. Yet its current influence appears at most minor, and considerably reduced with respect to the late 20th century Spanish urban aerosols (Bollhöfer & Rosman, 2001).

Four samples from the lower part of Lisbon Canyon piston-core 204-31 (142 – 172 cm core depth) have more radiogenic lead isotopic signatures than all present-day samples and Pb concentrations of 14.3 ± 1.4 µg g^{-1}, which falls in the range of average continental crust (12 – 17 µg g^{-1}, Wedepohl, 1995). Planktonic foraminifera from an overlying sample (134 cm) were AMS ^{14}C-dated to 1410 ± 50 yrs., corresponding to ~1000 AD on a calendar age scale. Several previous studies provided evidence for continuous input of anthropogenic Pb since Greek and Roman times, after ~2000 BC (e.g. Shotyk *et al.*, 1998; Kylander *et al.*, 2005). However, after the decline of the Roman Empire, anthropogenic Pb was strongly reduced at the end of the first millennium AD. Thus, the lead isotopic composition of coeval samples from Portuguese canyons will provide another estimate for the natural unpolluted end member, conceivably a lower limit for $^{206}Pb/^{207}Pb$ if they include some anthropogenic Pb. These values ($^{206}Pb/^{207}Pb$ = 1.2050 ± 0.002, $^{208}Pb/^{206}Pb$ = 2.0546 ± 0.003) are close to the most recent global mean estimate (Millot *et al.*, 2004) for weathering products of the upper continental crust ($^{206}Pb/^{207}Pb$ = 1.2050, $^{208}Pb/^{206}Pb$ = 2.0618).

The Pb isotopic composition of Saharan dust (Grousset *et al.*, 1994, 1995; Abouchami & Zabel, 2003) and south Iberian pyrite belt ores (Sangster *et al.*, 2000; Santos Zalduegui *et al.*, 2004) falls above the general regression line shown in Figure 7.11. Accordingly, these sources are at most of minor importance for most of the Portuguese canyon samples.

7.4.2. Comparison of Lisbon-Setúbal and Nazaré canyon sediments

Lead isotope variability along and between canyons

To elucidate differences in natural and anthropogenic lead along the canyon axes and between the Lisbon-Setúbal and Nazaré canyon systems, the $^{206}Pb/^{207}Pb$ ratio in surface sediments is plotted against water depth in Figure 7.12.

Three trends are obvious from the figure:

First, samples from the Lisbon-Setúbal Canyon display consistently lower $^{206}Pb/^{207}Pb$ ratios than Nazaré Canyon samples, with hardly any overlap in isotopic ratios between the two areas. This indicates stronger anthropogenic influence in the southern study area; the single exception from this pattern is discussed below.

Second, along both canyon axes the $^{206}Pb/^{207}Pb$ ratio generally increases with increasing water depth, implying a decreasing anthropogenic lead input from the canyon heads, closest to potential source areas, to more offshore areas.

Third, samples from the shelf and slope adjacent to the canyons commonly exhibit higher isotopic ratios than samples from the canyon axes. Yet, in both study areas mean isotopic values of canyon *vs.* shelf/slope sediments slightly overlap within one standard deviation, essentially because divergences from the general pattern occur at intermediate water depths (see below).

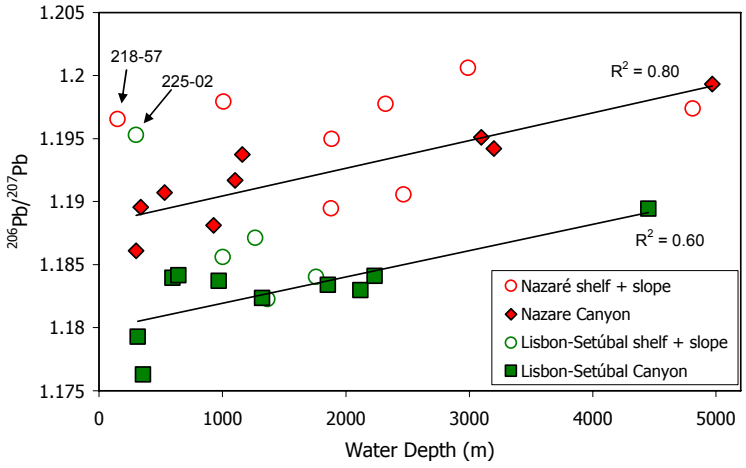

Figure 7.12. Surface sediment $^{206}Pb/^{207}Pb$ ratios plotted against water depth. Green and red symbols represent samples from the Lisbon-Setúbal and Nazaré study area, respectively, and filled and open symbols correspond to canyon axis and adjacent shelf and open slope samples, respectively. Regression lines are determined for canyon axis sediments in both study areas.

Divergent patterns between canyons and adjacent open shelf and slope are most obvious at shallow water depth (< 400 m): sediments from the Lisbon, Setúbal and Nazaré canyon heads (stations 204-18, 225-01 and 225-41) show by far the lowest isotope ratios for the respective areas, whereas distinctly higher ratios occur at comparable water depth outside of the canyons (stations 218-57 and 225-02). Interestingly, isotope ratios at station 225-02 are much higher than anywhere else in the southern study area; this single location displays values comparable to and even towards the upper limit of those measured in the Nazaré Canyon area. One may infer that the sediment collected at this upper slope location is of an older age, and that recent sedimentation is largely bypassing this site (Figure 3.2).

In contrast to the apparent weak anthropogenic influence detected in these upper slope samples, a relatively stronger influence was detected in some of the open slope stations at intermediate water depth (1300 – 2500 m), which have isotope ratios comparable to those observed inside the canyons. This possibly implies that material initially trapped inside the canyon spills over and escapes to the adjacent slope at intermediate water depths, as previously suggested for the eastern U.S. continental shelf and slope (Biscaye & Anderson, 1994) and northwestern Mediterranean continental margin (Puig & Palanques, 1998a).

At water depths > 4500 m in the Nazaré study area, $^{206}Pb/^{207}Pb$ ratios in surface sediments of the slope are also comparable to those of the Nazaré Canyon thalweg. However, as further discussed below in section 7.4.3, different processes may be responsible for the relatively minor influence of pollutant lead at both stations.

Quantifying natural and anthropogenic Pb

As discussed above, Pb isotopic ratios of samples from the central Portuguese margin, specifically their position along the mixing line in Figure 7.11, reflect the relative importance of natural *vs.* anthropogenic sources of lead. Assuming binary mixing between natural and anthropogenic end members of known and spatially constant lead isotopic composition, the percentage of anthropogenic lead (Pb_A) with respect to total Pb can be calculated from the following formula:

$$\%Pb_A = 100 * \frac{[Pb]_A}{[Pb]_{tot}} = 100 * \frac{R_N - R_S}{R_N - R_A}$$

In the right part of the formula, R represents the ratio $^{206}Pb/^{207}Pb$; subscripts A and N refer to the derived anthropogenic and natural end members, and subscript S to measured values of a given samples. Multiplying measured (bulk) Pb concentrations with the relative proportion of Pb_A yields estimates for the concentration of anthropogenic Pb in sediment samples.

The regression in Figure 7.10b yields a $^{206}Pb/^{207}Pb$ ratio of 1.143 (1.134 – 1.149, 95 % confidence interval) for the anthropogenic end member (see section 7.4.1). Two values are proposed for the natural end member: end member N1 ($^{206}Pb/^{207}Pb$ = 1.2050 ± 0.002) is based on the composition of sediments samples from piston core 204-31 dated as older than 1000 AD, whereas end member N2 ($^{206}Pb/^{207}Pb$ = 1.232 [1.226 – 1.240, 95 % confidence interval]) is derived from the x-axis intercept in Figure 7.10a. As discussed above, these represent lower and upper limits for the natural isotopic signature. Consequently, subsequent calculations using either of the two natural end members yield lower and upper limits for anthropogenic Pb, presumably bracketing its "true" contribution to canyon sediments. Based on natural end member N1, about 20 % (range 10 – 30 %) of total lead is of anthropogenic origin in the Nazaré Canyon, *vs.* 35 % (25 – 45 %) in the Lisbon-Setúbal Canyon and the Cascais Canyon. Using end member N2 results in values of 45 % (37 – 52 %) and 55 % (48 – 63 %) for the two canyon systems, respectively.

Uncertainties in these calculations dominantly relate to the possible isotopic range of natural and anthropogenic end members and presumably affect all samples equally. In absolute terms, they amount to 8 % or less (95 % confidence interval, e.g. 25 ± 8 % anthropogenic Pb). The influence of analytical uncertainties is variable and generally smaller (± 2.4 % on average) than the above-mentioned end member uncertainty. Differences between both study areas are robust, except for the unlikely case of distinctly different natural and/or anthropogenic end members for the Nazaré *vs.* Lisbon-Setúbal + Cascais canyon systems.

Inferred concentrations of natural Pb are relatively constant across the entire study area (19 ± 2.6 µg g^{-1} or 27 ± 3.5 µg g^{-1} using end members N1 and N2, respectively, n = 32). In both cases, natural Pb concentrations are slightly elevated compared to average upper continental crust (cf. above), which may reflect preferential incorporation of Pb into the fine fraction of marine sediments.

Differences in total (bulk) Pb concentrations thus essentially reflect variable input of anthropogenic Pb (Figure 7.13), superimposed on a nearly constant background of natural Pb. Spatial variability of anthropogenic Pb retains patterns described above, i.e. higher

concentrations in the Lisbon-Setúbal compared to the Nazaré Canyon and, for both canyon systems, generally higher concentrations within canyons compared to the adjacent shelf and slope. There is also a general decrease of anthropogenic Pb with increasing water depth. In Figure 7.13 data from the Cascais Canyon and open slope transects are also presented. The Cascais Canyon has slightly higher concentrations of anthropogenic Pb than the Lisbon-Setúbal Canyon for equivalent water depths. For the open slope transects, concentrations seem to be similar to those found on the walls and edges of the canyons at equivalent water depths.

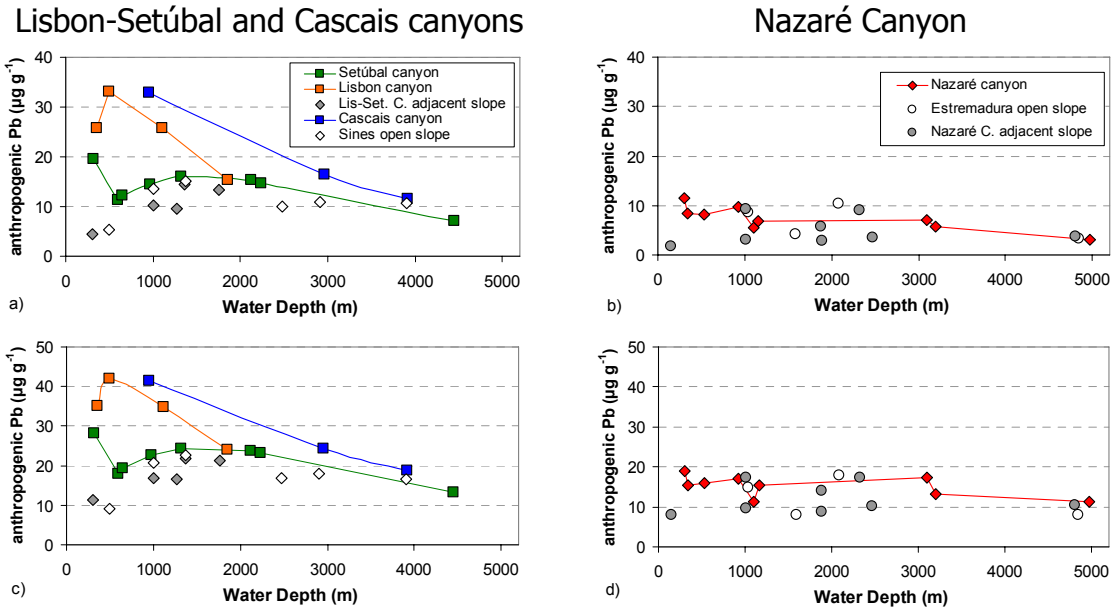

Figure 7.13. Concentrations of anthropogenic Pb in surface sediments of the Lisbon-Setúbal area (a, c) and the Nazaré area (b, d) obtained with $^{206}Pb/^{207}Pb$ = 1.143 for the pollutant end member and **a, b)** natural end member 1 ($^{206}Pb/^{207}Pb$ = 1.205), **c, d)** natural end member 2 ($^{206}Pb/^{207}Pb$ = 1.232).

In summary, both Pb isotopic ratios and derived concentrations of anthropogenic lead indicate stronger anthropogenic influence in the southern study area. This is consistent with sediment supply by major rivers, potentially carrying pollutant material, and with proximity of the southern area to heavily populated and industrialised areas. In particular, the Tagus River was previously identified as a major source of other pollutants metals including Hg, Cd, Cu, Ni and Zn (Figueres *et al.*, 1985; Cotté-Krief *et al.*, 2000).

7.4.3. Link with sediment transport processes (sediment trap *vs.* core top sediments)

Core top samples discussed above yield an integrated signal over annual to decadal timescales, whereas particulate material from sediment traps correspond to sampling intervals of one day in the upper canyon up to two to four weeks in the middle to lower canyon. Comparison of the two sample sets of the present study may yield clues on short-term depositional processes and their influence on the "final" sedimentary signal.

In most of the deployments done in the Lisbon-Setúbal Canyon and in the middle Nazaré Canyon, $^{206}Pb/^{207}Pb$ ratios for particulate material from individual sediment trap deployments commonly span relatively narrow ranges and are comparable to values observed in surface sediments at similar water depths (Figure 7.14). Hence, sediment trap data collected in these areas accurately reflect longer-term depositional conditions; the cases where this pattern was not found are discussed below.

For sediment trap samples from the Nazaré Canyon, Richter *et al.* (2009) noticed a conspicuous decrease of $^{206}Pb/^{207}Pb$ ratios with decreasing mass deposition flux (Figure 7.15b). This trend was shown by four of the five trap deployments; only the samples of deployment 236-07 showed a deviating pattern. Apparently, samples with highest mass flux, generally occurring in the upper reaches of the canyon, had the lowest relative contribution of anthropogenic Pb, whereas samples with lowest mass fluxes, occurring in the lower reaches of the canyon, showed the highest relative contribution of anthropogenic Pb. Intuitively, however, one would expect the opposite, with samples from the upper canyon, being nearer to source areas of anthropogenic lead on land, to have the highest relative contribution of anthropogenic lead. Richter *et al.* (2009) interpreted the lower anthropogenic contribution in the upper canyon samples as reflecting dilution of recent particulate material with reworked pre-industrial sediment, under influence of the vigorous tidal currents. Further down the canyon, where tidal currents are reduced in strength, the effect of dilution with reworked older sediments would become less pronounced.

Sediment trap samples from the Lisbon-Setúbal Canyon display a different relationship between mass flux and $^{206}Pb/^{207}Pb$ (Figure 7.15a). Excluding the samples from the lower Setúbal Canyon (252-62), there seems to be an opposite trend as observed for the Nazaré Canyon. Especially in the Lisbon Canyon $^{206}Pb/^{207}Pb$ ratios seem to increase with decreasing mass flux and increasing depth down-canyon, implying that

particulate matter settling in the deeper areas of the canyon contains a relatively lower contribution of anthropogenic Pb, which is in agreement with the expected decrease in input of terrigenous material with increasing depth down-canyon.

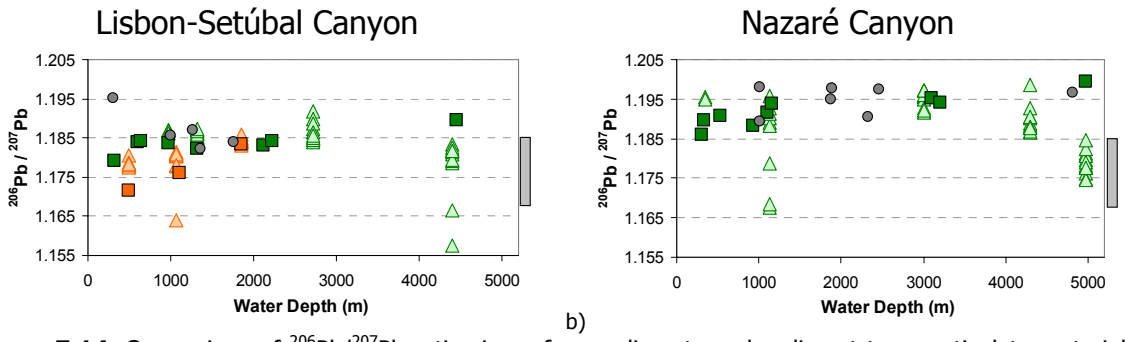

Figure 7.14. Comparison of $^{206}Pb/^{207}Pb$ ratios in surface sediments and sediment trap particulate material, plotted against water depth in **a)** Lisbon-Setúbal and **b)** Nazaré study areas. Squares, triangles and circles represent, respectively, core top and sediment trap samples from the canyon axes, and samples from the canyon walls and edges. In **a)**, orange and green symbols represent samples from, respectively, the Lisbon and Setúbal Canyon. Regional surface water data (Véron *et al.*, 1994; Weiss *et al.*, 2003) appear as grey rectangles plotted for comparison.

Pelagic fluxes and gravity flows in the lower canyons

Pronounced differences in $^{206}Pb/^{207}Pb$ ratios in surface sediments and sediment trap particulate material are observed at water depths > 4000 m in both the Lisbon-Setúbal and Nazaré canyons (Figure 7.14). $^{206}Pb/^{207}Pb$ ratios for the deepest traps in both canyons (stations 252-62 and 225-22, respectively) showing a relatively wide range of values, are distinctly lower than ratios in surface sediments from equivalent water depths. Low mass fluxes at these sites (0.37 – 1.38 g m^{-2} d^{-1} and 0.09 – 0.23 g m^{-2} d^{-1} in the Lisbon-Setúbal and Nazaré canyons, respectively, represent pelagic settling from the overlying water column. This is supported by closely similar ranges of $^{206}Pb/^{207}Pb$ ratios in trap particulate material and in late 20th century regional surface waters – the latter ranging between 1.1670 and 1.1850 (Véron *et al.*, 1994; Weiss *et al.*, 2003). The different isotopic signature of pelagic material settling in the lower Lisbon-Setúbal and Nazaré Canyon, compared to material collected in sediment traps further up-canyon and accumulated in surface sediments, is also expressed in a different relationship between isotopic ratio and Pb concentration as illustrated in Figure 7.10. Largely unaffected by contributions of older sediment resuspended from the seabed, this pelagic material likely represents the most undiluted form of recent Pb input to the open ocean environment.

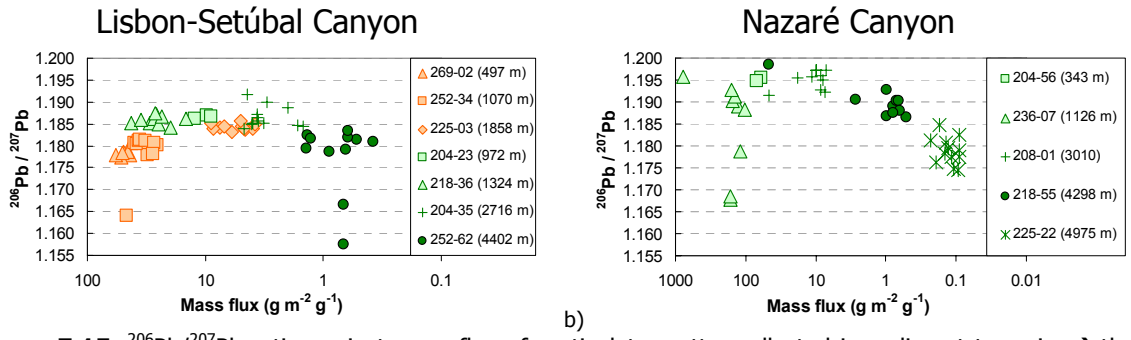

Figure 7.15. $^{206}Pb/^{207}Pb$ ratio against mass flux of particulate matter collected in sediment traps in **a)** the Lisbon-Setúbal and **b)** the Nazaré Canyon. In a orange and green symbols represent samples from the Lisbon and Setúbal Canyon, respectively. Note inversed logarithmic x-axis for comparison with previous plots with water depth on x-axis (mass fluxes generally decrease with increasing water depth).

Surface sediment samples from comparable water depths in the lower Setúbal and Nazaré Canyon and adjacent canyon edge (respectively, 225-07, 225-22 and 225-25) display distinctly higher $^{206}Pb/^{207}Pb$ ratios implying lower relative contributions of pollutant lead. For the two sites in the canyon axis, the relatively lower contribution of anthropogenic lead may be attributed to lateral supply of reworked older sediments. This seems to be confirmed by observed higher lithogenic content of canyon axis sediments, compared to the material collected in sediment traps (Chapter 6). For station 225-25 located on the southern edge of the Nazaré Canyon, however, lateral supply of reworked sediment can be assumed to be negligible. High carbonate content observed at this location (45 % compared to 22 % inside the canyon; see below Figure 7.17b) also implies that sediments are derived from vertical settling through the overlying water column rather than lateral advection of resuspended canyon sediment rich in lithogenic material. Low sediment accumulation rate of 0.1 g m^{-2} d^{-1}, derived from planktonic foraminiferal biostratigraphy in a piston core from the same location (De Stigter *et al.*, 2007b), which is similar to mass deposition flux measured in the deepest sediment trap deployment in the lower Nazaré Canyon, implies that the sediment layer representing the last 150 years of industrial development can only be a few mm thick which makes reworking of pre-industrial sediment by recent bioturbation very likely. Hence, the relatively high $^{206}Pb/^{207}Pb$ in open slope surface sediment may be attributed to biological mixing with underlying unpolluted sediments.

In the canyon thalweg, the long-term accumulation rate of 0.8 g m^{-2} d^{-1} in sediment core 225-22 (De Stigter *et al.*, 2007b) is almost one order of magnitude higher than mass fluxes observed in the trap at the same location. It seems therefore that the surface sediment represents not only material derived from pelagic settling, but in addition

material supplied by intermittent sediment gravity flows. A sediment gravity flow event was recorded at the shallower trap site 218-55 (4298 m WD); the corresponding sample showed a markedly higher mass flux than all other samples from the same deployment (46 g m^{-2} d^{-1} *vs.* 0.5 – 2.7 g m^{-2} d^{-1}). Compared to other samples collected by the same trap, material delivered during this sedimentation event was distinctly coarser-grained and displayed lower carbonate content. In this respect, it resembles particulate matter collected by upper and middle canyon traps, strongly suggesting down-canyon transport rather than local slumping from canyon walls (for more information cf. De Stigter *et al.*, 2007b).

The $^{206}Pb/^{207}Pb$ ratio for the sediment trap sample corresponding to the sediment gravity flow event is closely similar to the Pb isotopic ratio of surface sediments in the lower Nazaré Canyon. It seems therefore that episodic sediment gravity flows dominate the integrated sedimentary signal in the lower canyon. It is worth noting that $^{206}Pb/^{207}Pb$ ratio of the trap sample corresponding to the gravity flow event is higher than all samples from shallower sites, which is arguably inconsistent with preferential down-canyon transport of pollutant lead. Presumably, the gravity flow deposit also incorporates older pre-industrial sediments, masking the isotopic signature of pollutant lead.

The long-term sediment accumulation rate of 0.8 g m^{-2} d^{-1} recorded in the lower Setúbal Canyon (core 225-07, 4451 m WD) is comparable to mass fluxes observed in the trap at the same location (0.4 – 1.4 g m^{-2} d^{-1} - Chapter 6 on pg. 150) confirms that sediment gravity flows do not significantly contribute to recent sedimentation. The distinctly higher $^{206}Pb/^{207}Pb$ ratio in surface sediments compared to trap samples must therefore be explained as a result of biological mixing with underlying unpolluted sediments.

Part IV
Integration of data and Conclusions

8. FINAL CONSIDERATIONS

8.1. Major pathways of recent terrigenous sediment transport on the central Portuguese margin

On the central Portuguese margin three major submarine canyons connect the continental shelf with the abyssal plain: the Lisbon-Setúbal, Cascais and Nazaré canyons. Despite their geographic proximity, the composition of surface sediments from the canyons reflects different activity of these canyons in channelling sediments to their lower reaches and finally to the abyssal plain. The shelf and slope in between and neighbouring these submarine canyons also show differences in composition of surface sediments giving evidence of different processes driving sediment transport and deposition.

On the Sines margin lithogenic contents are high (70-75 %), considering that no major watercourse is discharging on this area. These high contents of lithogenic material are probably related to the progressive deposition of suspended fine-grained terrigenous material entrained by the flow of the Mediterranean Outflow Water along the upper continental slope (Grousset *et al.*, 1988). Northwards from the Sines margin and after interacting with the Lisbon-Setúbal Canyon a considerable portion of the lower-core water flows into the interior of the ocean (Bower *et al.*, 2002) and therefore the contribution of terrigenous material from this water mass to the seabed is much reduced on the Estremadura margin and further north (Figure 8.1).

Compared to the Sines margin, the middle and lower Setúbal Canyon has only slightly higher lithogenic content (72-77 %), suggesting that it is mostly accumulating sediment from the same source as is supplying sediment to the Sines slope, with minor addition of lithogenic material through the Lisbon Canyon and perhaps even less through the upper Setúbal Canyon. In comparison to the open slope, the Lisbon-Setúbal and Cascais canyons act as natural traps of organic material, specially the upper regions. Contents of organic matter above 3 % are only found in the upper canyon branches and according to García *et al.* (2010) only in these shallower areas a considerable portion of this organic matter is bioavailable. The mechanisms driving sediment dynamics in this canyon system will be further discussed in section 8.3.

The Estremadura slope has relatively low lithogenic contents (39-67 %), suggesting bypassing of terrigenous sediment entering via the shelf and through the Cascais and

Nazaré canyons. Terrigenous input to this part of the margin is low for what concerns the shelf as testified by the extensive areas of rock outcrops which appear from below a discontinous and relatively thin Holocene sediment cover (Badagola *et al.*, 2006). The Estremadura margin is, however, an area marked by important events of upwelling (Salgueiro *et al.*, 2008) which favour biological productivity in surface water, which in turn leads to deposition of carbonate-rich pelagic sediments.

The Nazaré Canyon is characterised by efficient down-canyon sediment transport and therefore contents of lithogenic material in surface sediments are higher than 80 % throughout the canyon, even in the lower canyon. Contents of organic matter are also high within the canyon, never decreasing below 3 %. However, according to García *et al.* (2007) most of this organic material is relatively degraded and of little use for living organisms. Especially in the lower canyon only a minor fraction is of biological interest. It is likely that most of the labile material is degraded on the way down. According to De Stigter *et al.* (2007b), particulate matter is mainly transported by tidal currents until the middle canyon and then by intermittent gravity flows further down to the lower canyon and to the abyssal plain. All together, it may take more than a year for particulate matter to travel from the canyon head to the mouth. Whereas the bulk of terrigenous sediments will not be much altered on such timescale and will eventually arrive at the abyssal plain, degradable organic material may never come that far.

The slope off Mondego shows variable contents of lithogenic material (49-80 %). Most of the slope area below 1000 m WD is characterised by a reduced supply of terrigenous sediment and predominance of pelagic sediment supply. The upper slope seems to receive a relatively abundant supply of fresh terrigenous sediment, characterised by high contents of feldspars, coming from the nearby Mondego River or possibly other rivers debouching north from this area (Douro, Minho, Cávado, Lima). Most of this terrigenous material seems not to spread to the slope area below 1000 m WD, probably as a result of blocking by slope currents.

Overall, just by considering the distribution of terrigenous material it becomes evident that sediment distribution on the central Portuguese margin is partitioned by the submarine canyons. As already suggested by other authors (e.g. Van Weering *et al.*, 2002; Oliveira *et al.*, 2007), export of shelf sediments towards the deeper continental margin is restricted by slope currents, except where canyons provide corridors for down-slope transport. Partitioning of sediment distribution on the central Portuguese margin

may to some extent also be attributed to modifications of along-slope circulation where submarine canyons cross the path of slope currents.

8.2. Pathways of recent terrigenous sediment transport in the Lisbon-Setúbal Canyon and adjacent continental shelf and slope

8.2.1. Continental shelf and sediment sources from the hinterland

The sedimentary deposits on the Lisbon-Setúbal-Sines shelf range from coarse sand with less than 10 % of fine-grained material (< 63 μm) to mud deposits with more than 90 % of fine-grained material. On the Setúbal-Sines shelf, sandy deposits prevail and muddy sediments are restricted to the northern coast of the Setúbal bay near the entrance of the Sado Estuary and to the upper reaches of the Setúbal Canyon. On the other hand, the Lisbon shelf is covered by a large expanse of mud deposit which occupies almost the entire shelf area, and which is largely fed by sediment supplied by the Tagus River.

Since at the present sea-level stand most of the sediment added to the shelf by continental runoff consists of fine-grained material (e.g. Ferreira *et al.*, 2008), one may deduce from the location of the fine-grained sediment deposits where on the shelf the main foci of recent sediment deposition are located. The mineralogical data presented in Chapter 4, specifically with regard to contents of plagioclase and kaolinite, and the crystallinity index of illite show that indeed sediments from the Tagus and Sado mud patches are fresher in a mineralogical sense than the fine fractions contained in coarser sediment deposits. According to Jouanneau *et al.* (1998) the surface nepheloid layers associated with the Tagus and Sado river discharge do not extend far onto the shelf, implying that most of the fine-grained riverine sediment input settles on the shelf and accumulates in the mud patches close to the river mouths. The distribution of plagioclase in shelf sediments, as a tracer of relatively unaltered riverine sediment input, and enrichment of trace metals (especially Zn and Cu) associated with industrial activities on land, point to the Tagus and Sado rivers as the main contributors of fine-grained sediments to the Tagus and Sado mud patches (Figure 8.1).

In the case of the Tagus mud patch, the erosion of sea-cliffs from the adjacent coastal arc between the Fonte da Telha beach and Cape Espichel seems to be an

important additional source of fine-grained sediments. As described in Chapter 4, detritus produced by sea-cliff erosion first nourishes the adjacent beach system and then reaches the adjacent shelf after high-energy storms. Contributions of sediments from the Albufeira Lagoon to the shelf certainly exist, but the mineralogical and geochemical signatures of the lagoon were not assessed and surface sediments from the shelf did not show a distinct signature which could be related to contributions from the lagoon.

Contributions from sea-cliffs and coastal lagoons are more easily tracked in the Tróia-Sines coastal arc since terrigenous sediment contributions from other sources are less important here and therefore dilution effects are less strong. Sea-cliffs in this coastal stretch are an important source of sediments to the beach system (e.g. Quevauviller, 1987; Freitas *et al.*, 1999) and subsequently to the adjacent shelf after storm waves wash the sediment offshore (Figure 8.1). Fine-grained sediment adsorbed to the beach sands is transported southward as sediment is carried along with the longshore drift. On the inner shelf adjacent to the sea-cliffs the proportion of lithogenic minerals to carbonates is markedly enhanced. This ratio reaches the highest values on the inner shelf close to the St. André and Melides lagoons. During the few weeks of the year that these lagoons are artificially opened to the sea, sediments are exported offshore, imprinting their mineralogical and geochemical signatures in the sedimentary deposits of the inner shelf (Chapters 4 and 5). Contributions of detritus resulting from the erosion of the Sines sub-volcanic massif to shelf deposits north of Cape Sines appear to be limited, which is explained by the prevailing southward transport along the coastal arc. Substantial northward longshore drift occurs only during infrequent southwesterly storms, which typically blow no more than 2 days per year (Quevauviller, 1988).

8.2.2. Continental shelf and adjacent slope

In the present study the Sines continental margin is well represented by surface sediment samples collected from water depths between 15 and 4000 m. The mineralogical and geochemical data presented in Chapters 4, 5, 6 and 7 show that on the Sines margin four different bathymetric zones can be distinguished: inner + middle shelf (< 100 m WD); outer shelf + upper slope (100 – 500 m WD); upper slope between 500 and 2000 m WD and middle to lower slope below 2000 m WD.

The Sines inner+middle shelf is characterised by the highest contents of terrigenous minerals, reflected by L/C ratios > 2.0. Despite the vigorous hydrodynamics of this area, contents of phyllosilicates and plagioclase may reach high values of 27 and 25 %, respectively, especially close to the source areas of these minerals: sea-cliffs and coastal lagoons, respectively.

On the outer shelf/upper slope reworked shelf sediments predominate, and fresh input of terrigenous material from the hinterland is lower compared to the inner+middle shelf. This is reflected by lower contents of plagioclase and phyllosilicates in the fine sediment fraction, 4 - 7 % and 9 - 17 %, respectively, whereas calcite contents reach the highest values of > 50 % and L/C ratios are generally below 1.5.

The upper slope between 500 and 2000 m WD seems to represent a transition zone where terrigenous input increases again (1.5 < L/C < 2.0). As discussed in Chapter 6 (section 6.7.3, pg. 182), modal grain size as well as carbonate content of surface sediments decrease from 500 to 1500-2000 m WD. The present study, as well as some previous studies (e.g. Schönfeld, 1997), show that fine-grained sediments are removed by winnowing from the shallower part of the upper slope which is under the influence of the upper Mediterranean Outflow Water (MOW), and are deposited near the lower MOW limit together with suspended material entrained by the MOW from the Alboran Sea (Figure 8.1). Material from the latter source is characterised by relatively high contents of smectite and degraded kaolinite.

On the middle and lower slope, below 2000 m WD, surface sediments have modal grain sizes typical for hemipelagic sedimentation (< 8 µm). In this same depth zone, contents of phyllosilicates in the fine sediment fraction increase to 38 %. Part of the sediments settling in this area may well derive from the MOW, as implied by the relatively high contents of kaolinite and smectite in sediments found even as deep as 3900 m WD. As observed in the south-western part of the Gulf of Cadiz, input from the MOW may be found in areas where the MOW flows detached from the seafloor, as the particles settle out from the MOW and accumulate as hemipelagites on the seabed (Bower *et al.*, 2002).

8.2.3. The Lisbon-Setúbal and Cascais canyons and adjacent shelf

Present-day activity of the Lisbon-Setúbal and Cascais canyons

The widespread occurrence of bottom and intermediate nepheloid layers in the upper reaches of the Lisbon-Setúbal and Cascais Canyon and high sediment fluxes recorded in sediment traps and in seabed deposits, are clear evidence of the dynamic sedimentary environment present within these canyons. SPM concentrations (De Stigter *et al.*, in press) and sediment accumulation rates in the upper canyons are an order of magnitude higher than the ones measured at comparable depths on adjacent slope areas, and values reported from other parts of the western Iberian margin (Faugères *et al.*, 1984; McCave & Hall, 2002; Oliveira *et al.*, 2002; Van Weering *et al.*, 2002). The active sedimentary regime of the upper Lisbon-Setúbal Canyon is undoubtedly related in the first place to its position, deeply entrenched in the continental shelf with the two canyon heads in the proximity of the coast, and thus forming a natural trap for sediments carried along by shelf currents. Shallow intermediate nepheloid layers observed in the upper canyon at depths corresponding to that of the adjacent shelf, are indications that suspended sediment enters the canyon via bottom nepheloid layers detached from the shelf edge (De Stigter *et al.*, in press). When crossing the canyon, the nepheloid layers will lose part of their suspended sediment load by settling. Resuspension of shelf sediments is likely to occur under influence of storm waves, particularly those incident from southwesterly direction (Figure 8.1). The Lisbon and Setúbal shelves are sheltered from northwesterly storms by the prominent Cape Roca and Cape Espichel, respectively. Internal tidal waves generated on the edges of the canyon and propagating over the adjacent shelf may be an additional mechanism resuspending shelf sediments around the canyon, analogous to what has been observed for the Nazaré Canyon area (Quaresma *et al.*, 2007). Direct sediment input from the Tagus and Sado river plumes is probably limited, as indicated by previous observations by Jouanneau *et al.* (1998). These authors observed that surface nepheloid layers issuing from the river mouths do not extend far onto the shelf but are predominantly deflected to the west following the coast. Sediment transport from the rivers to the canyons appears to be mostly indirectly via bottom nepheloid layers formed by resuspension of prodelta deposits (Tagus and Sado mud patches). However, the dispersal of suspended particulate matter over the shelf off the Tagus and Sado estuaries is still basically unknown for typical winter conditions since the study done by Jouanneau

et al. (1998) refer to particularly dry years (1993-1995), during which the strong increase in water discharge normally observed during winter did not occur. Trapped in the upper canyon, fine-grained sediments are subject to frequent resuspension and transport by the internal tide, as inferred from relatively high loads of SPM in bottom and intermediate waters. A depocentre of fine-grained sediments was identified in both the Lisbon and upper Setúbal canyon branches between 1100 and 1400 m WD (Figure 8.1). These sediment depocentres are marked by a maximum in SAR values in this depth interval and by high contents of organic matter in the surface sediment. Discharge of dredged estuarine sediments in the Lisbon Canyon has been confirmed to have occurred in 2005 and 2007 and may help to explain surface sediments characteristics in the upper reaches of the canyon, namely, the high contents of organic and lithogenic contents.

Much lower SPM concentrations (De Stigter *et al.*, in press) and sediment accumulation rates observed in the middle and lower canyon, comparable to those of the adjacent open slope, suggest that this part of the canyon has a much less active sedimentary regime than the upper canyon, and does not receive major input of sediment from either the upper canyon or from the adjacent open slope, besides the background pelagic input. Lack of down-canyon sediment transport seems to be confirmed by trends in particle size and bulk composition of surface sediments of the canyon and adjacent slope. A clear enrichment of lithogenic material, on the order of ~10 % above the background lithogenic content found further down-canyon and on the adjacent slope, was only observed in the upper reaches of the Lisbon and Cascais Canyon. A general lack of down-canyon sediment transport was confirmed also by the seaward logarithmic decrease of Pb and Zn enrichment. Both elements are mainly associated with terrigenous sediment input to this area (Chapter 7).

This is clearly different from the pattern observed in the Nazaré Canyon, where sediment with strong predominance of lithogenic material is observed all along the axis of the canyon, contrasting with finer-grained sediment with lower lithogenic content on the adjacent slope.

Sediment transport by the internal tide

The close match between semi-diurnal peaks in current speed and peaks in bottom water turbidity, as recorded in the upper Lisbon and Setúbal canyon by the BOBO landers, demonstrate the prominent role of tidal currents in resuspending and transporting fine-grained sediments. The BOBO lander records consistently show resuspension occurring

when currents exceed a threshold of 15-25 cm s^{-1}. Critical erosion velocity u* for resuspending particles from the seabed, determined experimentally for surface sediments from the Lisbon-Setúbal Canyon, are reported by García *et al.* (2010). The experimentally determined threshold values from the latter authors are in agreement with those derived from the BOBO lander records.

Internal tides, such as observed in the Lisbon-Setúbal Canyon, are clearly an important mechanism of sediment transport in many submarine canyons (Shepard *et al.*, 1979; Gardner, 1989; Petruncio *et al.*, 1998; Durrieu de Madron *et al.*, 1999), resuspending sediments especially in narrow upper canyon sections where tidal energy is focused, and driving the flow of sediment-laden waters up and down the canyon axis. A particular characteristic of tidal currents in the Lisbon-Setúbal Canyon is the prevalence of net up-canyon directed flow, observed in four of the seven sites where currents were recorded. Since the strongest currents in all these cases were also directed up-canyon, it can be assumed that the prevalent direction of suspended sediment transport was up-canyon as well. This is in apparent contrast with the Nazaré Canyon, where a net down-canyon water and sediment transport was observed in a similar observational setup (De Stigter *et al.*, 2007b). As a cautionary remark it must be added here that some of the records obtained from the upper Lisbon-Setúbal Canyon were only of short duration of 3-7 days, and thus are not necessarily representative for the longer term current regime. In the Nazaré Canyon, reversals in net flow direction were observed in the canyon down to depths of 300 m, in response to changes in wind direction and shelf circulation (Tyler *et al.*, 2009). Currents in the upper Lisbon-Setúbal Canyon may in a similar manner be coupled to variable surface water circulation.

In the upper canyons mass deposition fluxes estimated using sediment traps are consistently higher than SARs determined in the seabed through ^{210}Pb profiles in sediment cores. This indicates resuspension of seabed sediments, most certainly as a reflection of strong near-bottom current dynamics, and oversampling in the trap after repeated cycles of resuspension and deposition.

Low values of bottom water turbidity observed in BOBO lander deployments in the middle and lower canyon, combined with the observation that mass deposition fluxes measured in sediment traps and seabed SARs are well comparable, indicate that sediment resuspension from the seabed is not as important as in the upper reaches of the canyon, and that sedimentation prevails. This seems in agreement with the overall slower bottom currents and relatively infrequent resuspension recorded in the middle part of the canyon,

but the combination of intermittent high current speeds in the lower canyon with low turbidity and low deposition flux is puzzling. Possibly the sediment in the lower canyon is locally more cohesive or coarser grained, although this is not evident from the one core which was collected from that area.

Sediment transport by sediment gravity flows

Low frequency and high-energy processes like gravity flows are processes capable of transporting considerable amounts of sediment further down-canyon. Presently, they seem however very rare in the Lisbon-Setúbal Canyon. During the total time of five years and six months of BOBO deployments (2002 - 2007) no gravity flows were recorded in the Lisbon-Setúbal Canyon while for a similar period of time in the Nazaré Canyon at least three important mass flux events were recorded (De Stigter *et al.*, 2007b). These mass sediment transport processes seem to be also common in other active canyons systems like the Monterey Canyon (Xu *et al.*, 2002), the Congo Canyon (Khripounoff *et al.*, 2003) and the Palamós Canyon (Palanques *et al.*, 2005).

That sediment mass transport events reaching the lower canyon are rare is confirmed by the overall scarcity of turbidite layers in sediments of late Holocene age recovered in cores from the lower canyon (Arzola *et al.*, 2008). The most recent turbidite layer encountered in a core from the lower canyon (225-07) was tentatively attributed to the Lisbon earthquake of 1755, based on ^{210}Pb geochronology (De Stigter *et al.*, in press). The latter turbidite layer contained abundant quartz and micas (De Stigter *et al.*, unpublished data), indicating that the sediment was transported from the upper canyon reaches, and did not originate from reworking of hemipelagic sediments by a local slope failure. It represents the most recent major event, indicating that only powerful events like such an earthquake are capable of remobilising and transporting sediment down-canyon to such water depths. Even though such events may appear rare on the time-scale represented by short sediment cores and in-situ observation with landers, on geological timescales submarine canyons are primarily shaped by the action of mass sediment transport processes. The Lisbon-Setúbal Canyon is no exception to this as shown by data presented by Lastras *et al.* (2009). Slump scars, giant landslides blocks, large scours and sediment waves were observed especially in the canyon mouth area, testifying of high energy events occurring in the geologically recent past of the canyon.

The Lisbon-Setúbal Canyon as sediment trap

The data presented in Chapters 6 and 7 and summarised above seem to indicate that the upper reaches of the Lisbon-Setúbal and Cascais Canyon presently act as traps for fine-grained sediments entrained in suspension from the adjacent shelf and slope, without substantial down-canyon dispersal to the middle and lower reaches. From the results here presented one may identify two important factors which contribute to the trapping effect of the canyon. First an overall up-canyon direction of net water transport, which drives particles settling in the upper canyon toward the canyon head rather than disperse them down-canyon. The cause of the up-canyon flow probably has to be sought in the interaction of canyon morphology and present-day circulation patterns along the margin. The second factor is the apparent rareness of sediment gravity flows, which in other canyon systems are the dominant mechanism of down-canyon dispersal. Canyons known for active sediment gravity flows have in common that they head very near-shore, thus receiving massive input of sand and silt from longshore transport or riverine input. The fast accumulation of incohesive sediment on steep sides of the canyon head leads to frequent sediment slides, which may evolve into energetic high-density turbidity currents running out towards deeper water. Large scale sediment waves typically encountered in the head of active canyons appear indicative of deposition from high energy turbidity currents (Smith *et al.*, 2005). Whereas such structures are present in the head of Nazaré Canyon (Duarte *et al.*, 2000) they were not noticed in the detailed morphological study of the Lisbon-Setúbal and Cascais canyons by Lastras *et al.* (2009). Probably the heads of these canyons, located at 5, 6 and 22 km, respectively, from the nearest shoreline, are too far off the coast to intercept longshore sediment transport. Thus sediment input is largely restricted to fine-grained material settling from nepheloid layers passing over the upper canyon. In addition, the shelter against northwesterly storms provided by prominent coastal capes may limit sediment resuspension on the shelf and hence also limit suspended sediment supply to the canyons. This geomorphological setting is in clear contrast to the more exposed Nazaré Canyon. The rareness of sediment gravity flows flushing the canyon may give fine-grained sediment accumulating in the canyon time to compact into cohesive stable deposits, thus further reducing the chance of remobilisation. The presence of a sediment-filled thalweg of several hundred meters wide in the upper Lisbon-Setúbal Canyon, compared to the strongly incised narrow thalweg in the active Nazaré Canyon, may thus reflect the infrequent flushing of the canyon since the last glacial sea level lowstand.

In addition to sediment input from the shelf, a substantial part of sediment trapped in the canyon may also be derived from the adjacent slope, and notably from the interval between 500 and 1500 m occupied by the northward flowing Mediterranean Outflow Water (MOW). The strong density gradients at the boundaries of the MOW are thought to favour internal wave activity and sediment resuspension (McCave & Hall, 2002), whereas suspended sediment would be carried along-slope by the poleward flow of the water mass. From Cape São Vicente, the southernmost point of the Portuguese mainland where the MOW turns northward, the MOW flows practically unobstructed along the smooth and gently sloping Alentejo margin until the abrupt intersection with the Setúbal Canyon. Indications from sedimentology and benthic foraminifera for enhanced hydrodynamic energy and lateral sediment transport coinciding with the path of the MOW on the southern Portuguese slope have been reported by Schönfeld (1997) and, for what concerns sedimentology, were confirmed by the data here presented (Chapter 6, section 6.7.3, pg. 182). As reported by De Stigter *et al.* (in press), enhanced SPM concentrations noticed within the Lisbon-Setúbal Canyon at 500 and 1500 m depth may primarily be due to resuspension by focusing of internal tides along the canyon axis, but may conceivably also include suspended sediment entering via the MOW from the slope south of the canyon. The similarity in bulk sediment characteristics on the open slope and within the canyon (especially SPM caught in sediment traps) at this depth seems to be consistent with this interpretation (Chapter 6). Sediment accumulation rates in the upper Setúbal Canyon, the area potentially affected by lateral sediment input via the MOW, are well above the background hemipelagic sedimentation as can be assessed from mass fluxes in sediment traps and surface sediments in the lower canyon. However, since sediment accumulation on the canyon walls and edges is not constrained by the present data, the enhanced rates may also be explained as the result of focusing of sedimentation on the canyon thalweg.

In their function as traps for suspended particulate matter, supplied laterally from the adjacent shelf and slope and vertically from the overlying water column, the Lisbon-Setúbal and Cascais canyons constitute not only depocentres for inert sediment but also for biologically active organic material. Accumulation of relatively fresh organic material especially in the upper canyon, confirmed by studies of Pusceddu *et al.* (2010) and García *et al.* (2010), explains the enhanced abundance of benthic foraminifera (Koho *et al.*, 2008), and macrofauna (Cunha *et al.*, in press) observed in these canyons. Whereas the latter studies concerned fauna on soft substrates of the sediment thalweg, abundant

suspension feeding fauna observed with underwater cameras on steep canyon walls is likely to be favoured by the continuous flow of particle-rich water driven by the internal tide in the canyon.

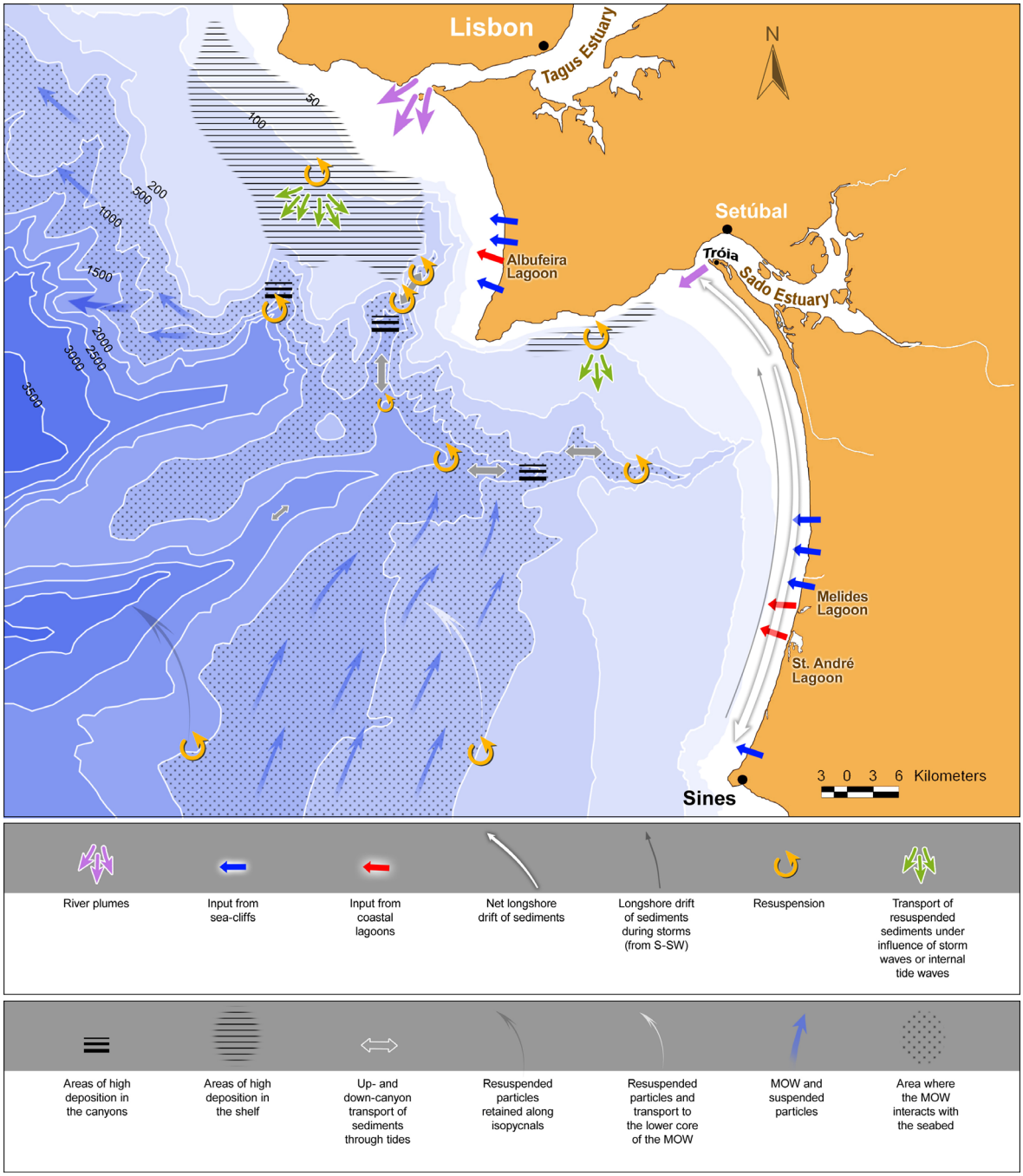

Figure 8.1. Scheme showing the main pathways of fine-grained sediment dispersal on the continental margin between Cape Raso and Cape Sines.

8.3. Trace metal enrichment in sediments from the central Portuguese continental margin

Contents of major elements Ca, Al and Fe and some trace metals like Cr and Ni in surface sediments of central Portuguese canyons and open slopes appear mostly equal to contents of these elements in pre-industrial sediments, meaning that in terms of bulk composition the sediment has not changed over the last 150 years. Pre-industrial contents of trace metals, Fe and Al are largely similar for the Lisbon-Setúbal and Nazaré Canyon systems, whereas recent surface sediments and suspended particulate matter usually show higher concentrations of trace metals, with somewhat diverging values between both areas. Surface sediments and suspended particulate matter in the Lisbon-Setúbal Canyon have higher mean concentrations of Mn, Zn, Pb, Cr, Cu and Ni compared to the Nazaré Canyon. Regarding only surface sediments, the highest mean concentrations for all trace metals are found in the Cascais canyon. The assessment of trace metal enrichment in present-day sediments on the basis of calculated enrichment factors supports the above observations. In both canyon systems, the anthropogenic contribution to total inventories of Pb and Zn generally decreases with increasing water depth. Different from Pb and Zn, present-day Cu enrichment appears to increase towards deeper water where pelagic sedimentation is predominant, suggesting that dispersal of this trace metal is at least partially linked with surface water plankton production.

The assessment of Pb enrichment on the basis of lead stable isotope ratios indicates that lead in present-day surface sediments and SPM represents a mixture between anthropogenic contaminant lead and an unpolluted "crustal" end member. Pollutant lead appears to be mostly derived from industrial sources, whereas the current contribution of remnant gasoline lead additives is of minor importance. In accordance with the observed stronger enrichment of trace metals in the Lisbon-Setúbal and Cascais canyons, as compared to the Nazaré Canyon, the anthropogenic signature in Pb isotopes appears also more pronounced in the southern canyons. Percentages of excess trace metal in the sediment column deposited over the last 150 years are also higher for the southern canyons, especially the Lisbon and Cascais canyons. The Lisbon Canyon has around 10 to 15 % more anthropogenic Pb than the Nazaré Canyon for comparable water depths. This difference between both areas refers both to present-day sediments (determined through Pb stable isotopes) and to sediments deposited over the last 150 years (determined through inventories of excess Pb).

The consistently higher loading of anthropogenic trace metals in the southern canyons is consistent with the proximity of the Lisbon and Cascais canyons to heavily populated and industrialised areas, and with sediment input from the Tagus Estuary, a potential major source of pollutants particles. The degree of trace metal enrichment found in the Lisbon and Cascais canyons is comparable to what has been previously published from other canyon and slope areas, such as the Foix Canyon in the NW Mediterranean (Palanques *et al.*, 2008), the Gulf of Lions continental slope in the NW Mediterranean (Miralles *et al.*, 2006), and the Kaoping Canyon off Taiwan (Hung & Hsu, 2004).

Focusing on the shelf area adjacent to the southern canyons, trace metal enrichment is widespread to the entire studied area of the Lisbon shelf while the Setúbal and Sines shelves have areas enriched in trace metals (Sado mud patch and the inner shelf) which contrast with others where pre-industrial concentrations where found on surface sediments. As mentioned above, the Tagus Estuary is one of the main sources of anthropogenic trace metals to the adjacent shelf, but some additional sources of anthropogenic input were detected in sediments, in particular the Sado Estuary, the St. André and Melides coastal lagoons, atmospheric input and possibly the Sines submarine outfalls. As a cautionary remark it must be said that the signal from this last source was tentatively identified in sediment samples collected between 1980 and 1988. Nowadays, after considerable improvement of wastewater treatment it is unlikely that contributions from this source can still be detected. In more recent studies by Cardoso & Palma (2007) and Maretec (2008), no trace metal enrichment was detected in sediments surrounding the submarine outfall.

In general, along the last three decades the decrease of contamination in marine sediments is expected, given the improvement of new procedures for treatment of industrial and domestic effluents and the shutdown of some industries known to discharge contaminants into both Tagus and Sado estuaries. The reduction of input of contaminants into hydrographic basins and the marine environment should decrease further in the future after the implementations required by the EU-Directive 2000/60/EC (of 23 October 2000), which establishes a framework for the protection of inland surface water, transitional water, coastal water and groundwater.

8.4. Conclusions

Pathways of terrigenous sediment transport on the Lisbon-Setúbal-Sines shelf

- On the basis of the study of the fine fractions of different sedimentary deposits of the continental shelf it is safe to say that sand deposits on the shelf comprise mature fine fractions enriched in clay-sized particles while mud deposits have fresher fine fractions enriched in particles within the "sortable silt" range (10-63 μm).
- Relatively high contents of terrigenous material are present at the shelfbreak of the Lisbon shelf. The transport of this sediment to the shelfbreak may occur not directly from river plumes issuing from the Tagus estuary but rather by cycles of resuspension and deposition from the Tagus mud patch.
- The general southward increase of biogenic carbonate content in sediments of the Lisbon-Setúbal-Sines shelf indicates a southward decrease of terrigenous input from the area off the Tagus Estuary towards Cape Sines.
- On the Lisbon shelf two important sources nourish the shelf with lithogenic fine sediments: the Tagus estuary and the sea-cliffs between Fonte da Telha beach and Cape Espichel. The Albufeira coastal lagoon most likely contributes also with lithogenic sediments to the shelf, but its contribution could not be detected in the mineralogy and geochemistry of surface sediments from the shelf.
- On the Setúbal shelf contents of lithogenic material are lower than on the Lisbon shelf. Enhanced concentrations of mineral indicators of riverine sediment input, however, highlight the Sado mud patch and the upper Setúbal Canyon as depocentres of terrigenous sediment. Suspended particulate matter coming from the Sado Estuary seems to bypass the sandy deposits of the inner shelf.
- On the Sines shelf, lithogenic sediment input appears generally low, and as a consequence the relative content of biogenic carbonate reaches maximum values in this area. Several local sources of lithogenic input can be traced, however, on the inner shelf: i) the Plio-Pleistocene sea-cliffs present in the southern half of the Troía-Sines coastal arc; ii) the Santo André and Melides coastal lagoons; iii) the Sines sub-volcanic complex.

- Dispersal patterns of mineralogical and geochemical tracers on the inner shelf between Tróia and Sines support a net northward longshore drift of sediments in the Tróia Peninsula and southward drift in the rest of the coastal arc.

Recent sediment transport and deposition in the Lisbon-Setúbal Canyon and comparisons to other environments of the central Portuguese margin

- Sediment distribution on the central Portuguese margin is partitioned by submarine canyons and export of shelf sediments towards the deeper continental margin is restricted by slope currents, except where canyons provide corridors for down-slope transport.
- The Nazaré Canyon is efficient in transporting sediments down to the lower canyon while in the Lisbon-Setúbal Canyon and probably in the Cascais Canyon the down-canyon transport to the lower canyon is very limited, conceivably only triggered by high energy events like high-magnitude earthquakes.
- Sediment accumulation rates in the upper reaches of the Lisbon, Setúbal and Cascais Canyon are an order of magnitude higher than rates measured at comparable depths on adjacent slope areas and other parts of the western Iberian margin, indicating that these submarine canyons act as sediment depocentres.
- Sediment input to the upper canyon reaches may result from: i) resuspension of shelf sediments under influence of storm waves or as a result of internal tidal waves generated on the edges of the canyons and propagating over the adjacent shelf, and subsequent advection of suspended matter to the canyon in bottom nepheloid layers; ii) direct input from turbid plumes issuing from nearby estuaries; iii) in the case of the Setúbal upper canyon: resuspension of sediments from the slope south of the canyon and entrainment with the Mediterranean Outflow Water flowing across the canyon.
- In middle and lower Setúbal Canyon sediment accumulation rates are comparable to those of the adjacent open slope, suggesting that this part of the canyon has a much less active sedimentary regime than the upper canyon, and does not receive major input of sediment from either the upper canyon or from the adjacent open slope, apart from the background pelagic input.
- In the upper Lisbon and Setúbal canyon, tidal currents have a prominent role in resuspending and transporting fine-grained sediments especially when currents (measured at one meter above the seabed) exceed the threshold speed of 15-

25 cm s^{-1}. In the middle and lower canyon, on the other hand, there is only limited resuspension from the seabed and sedimentation processes prevail. During the period covered by this study, a particular characteristic of tidal currents in the Lisbon-Setúbal Canyon is the prevalence of net up-canyon directed flow. Since the strongest currents seem to be also directed up-canyon, it can be assumed that the prevalent direction of suspended sediment transport was up-canyon as well.

- Unlike what is observed in other active canyon systems like the Nazaré Canyon, the Monterey Canyon, the Congo Canyon and the Palamós Canyon, low frequency and high-energy processes like gravity flows seem to be very rare in the Lisbon-Setúbal Canyon. The most recent sediment mass transport event detected in the lower canyon corresponds to the 1755 earthquake which means that only powerful events like such an earthquake are capable of remobilising and transporting sediment down-canyon to such water depths.
- The previous two conclusions explain why the upper reaches of the Lisbon-Setúbal Canyon (and possibly the Cascais Canyon) presently act as traps for fine-grained sediments entrained in suspension from the adjacent shelf, without substantial down-canyon dispersal to the middle and lower reaches.

Trace metal enrichment in the central Portuguese margin

- Bulk composition and trace metal composition of pre-industrial sediments is largely similar for the Lisbon-Setúbal and Nazaré canyons systems.
- Whereas bulk composition of the sediment has not changed over the last 150 years, present-day surface sediments and suspended particulate matter are significantly enriched in Pb, Zn and Cu compared to pre-industrial sediments.
- Sediments in the Lisbon-Setúbal and Cascais canyons appear more enriched in trace metals than sediments in the Nazaré Canyon, both with regard to trace metal concentrations in core top samples as well as to inventories of excess trace metals accumulated over the last 150 years. The highest levels of enrichment in Pb, Zn and Cu are found in sediment deposits in the upper reaches of the Lisbon and Cascais canyons, consistent with their proximity to heavily populated and industrialised areas of central Portugal as well as to the Tagus River, a major source of pollutant particles. Discharge of dredged contaminated sediments in the Lisbon Canyon appears also as a potentially important source of anthropogenic trace metals.

- In accordance with the overall higher contents of trace metals in the Lisbon-Setúbal and Cascais canyons, the anthropogenic signature in lead isotopes appears also more pronounced in the southern area.
- The role of submarine canyons as trap for particulate material and attached pollutants is confirmed by stronger influence of anthropogenic Pb and Zn compared to the adjacent open shelf and slope.
- The dispersal of anthropogenic Pb over the southern area (Lisbon-Setúbal Canyon and adjacent continental shelf) seems to comprise important contributions from atmospheric transport. This is not only evident from the isotopic signature of the pollutant lead in surface sediments which resembles the signature of incinerator fly ashes from industries, but also from the wide spread of Pb enrichment affecting the entire study area, even in areas where other trace metals, also enriched in the estuaries, show no enrichment.
- In the Lisbon-Setúbal Canyon system considerably high levels of anthropogenic Pb and Zn enrichment appear restricted to the upper canyon reaches, decreasing exponentially further down-canyon. This indicates inefficient down-canyon transport of sediments in this canyon.
- Trace metal enrichment in general appears widespread on the Lisbon shelf, whereas on the Setúbal and Sines shelves the areas enriched in trace metals appear more limited in extent, and are bounded by areas where pre-industrial concentrations prevail in surface sediments.
- Considering the spatial distribution of trace metal enrichment on the shelf and upper slope from the Tagus estuary to Cape Sines, Pb enrichment is detected in the largest area, whereas successively smaller areas are affected by enrichment of, respectively, Zn, Cu, Cr, and Ni. Generally, enrichment of trace metals tends to decrease with increasing water depth suggesting that the excess of trace metals is mostly derived from land.

8.5. Proposals for future investigations

Whereas the present thesis integrates a large amount of pre-existing and newly-generated data on sediment and trace metal dispersal on the central Portuguese margin, new perspectives have emerged that call for further study of particular aspects that cannot be resolved with the present data. Suggestions for further studies include the following:

- Assessment of the temporal evolution of trace metal contamination through analysis of sediment cores with high temporal resolution from areas where fresh sediment accumulates, such as the Tagus mud patch or certain areas within the Tagus estuary not affected by dredging activities. Such analysis is very relevant to assess if new procedures for treatment of industrial and domestic effluents implemented during the past 30 years have been effective in reducing trace metal contamination in estuarine and shelf environments. Application of the EU-Directive 2000/60/EC (of 23 October 2000) is expected to lead to new implementations in the near future which should affect hydrographic basins in an integrated approach to improve water quality. The objective of this Directive is to establish a framework for the protection of inland surface water, transitional water, coastal water and groundwater. On the longer run the effects of these measures are expected to affect not only the quality of water but also the quality of sediments which are known to reflect the overall contamination level of a given ecosystem.

- Study of the seasonal and interanual variability of nepheloid layers issuing from the Tagus and Sado estuaries and associated dispersal of fine-grained particulate matter on the shelf. Six cruises conducted between 1993 and 1995 in the framework of the EU projects OMEX (Ocean Margin Exchange) I and II specifically addressed the behaviour of nepheloid layers in this area during winter and summer conditions. Results concerning the dispersal and deposition of suspended particulate matter issuing from the above estuaries were treated in Garcia (1997) and resumed and published in Jouanneau *et al.* (1998). According to these authors, however, the reported results refer to particularly dry years (1993-1995), during which the strong increase in water discharge normally observed during winter did not occur. No other studies comparing winter and summer conditions have since then been carried out,

and the composition and dispersal of suspended particulate matter over the shelf off the Tagus and Sado estuaries is still basically unknown for typical winter conditions. Therefore, the true extent of the influence of these rivers over the adjacent margin for what concerns input of particulate matter may have been underestimated so far.

- Exploration of the interaction of the Mediterranean Outflow Water with the Lisbon-Setúbal Canyon and adjacent slope, and its effect on the sedimentary dynamics of the canyon. Many studies have demonstrated the important modifications of open slope circulation where along-slope currents encounter a canyon on their path (e.g. Durrieu de Madron, 1994; Puig *et al.*, 2000; Petrenko, 2003). The up-canyon flow observed at several locations within the Lisbon-Setúbal Canyon, which drives particle transport toward the canyon head rather than down-canyon, may be related to local diversions of the along-slope flow of the Mediterranean Outflow Water as it encounters the canyon. Better understanding of this interaction would be crucial to comprehend the functioning of the Lisbon-Setúbal Canyon and its poorly-known ecosystems.

- Assessment of the extent and environmental impacts of discharge of contaminated sediments in the Lisbon Canyon. Information on discharge of contaminated sediments in the Lisbon Canyon was obtained only during the final stage of writing of this thesis, so that additional information concerning the type and level of contamination in the discharged sediments and the frequency and location of these discharges by other entities than the APL (Administração do Porto de Lisboa) could not be accessed nor further evaluated. This subject is not only important to refine some of the conclusions of the present thesis, but the potential impact of discharges on canyon ecosystems should also be taken into consideration in view of the role that these canyons may play in fostering economically important biological resources.

References:

A

Abouchami, W. & Zabel, M. (2003). Climate forcing of the Pb isotope record of terrigenous input into the Equatorial Atlantic. Earth and Planetary Science Letters, 213, 221–234.

Abrantes, M.I. (2005). Os sedimentos superficiais da margem continental, sector Espinho – Cabo Mondego: a utilização das fracções finas como traçadores de dinâmica sedimentar actual. Tese de Doutoramento, Universidade de Aveiro, 239 p.

Alt-Epping, U.; Mil-Homens, M.; Hebbeln, D.; Abrantes, F.; Schneider, R.R. (2007). Provenance of organic matter and nutrient conditions on a river- and upwelling influenced shelf: A case study from the Portuguese Margin. Marine Geology, 243, 169–179.

Alves, T.M.; Gawthorpe, R.L.; Hunt, D.W.; Monteiro, J.H. (2003). Cenozoic tectono-sedimentary evolution of the western Iberian margin. Marine Geology, 195, 75–108.

Anderson, R.F.; Rowe, G.T.; Kemp, P.; Trumbore, S.; Biscaye, P.E. (1994). Carbon budget for the mid slope depocenter of the Middle Atlantic Bight. Deep-Sea Research II, 41, 669-703.

Andrade, C.; Freitas, M.C.; Cachado, C.; Cardoso, A.C.; Monteiro, J.H.; Brito, P. Rebelo, L. (2006). Zonas Costeiras (Capítulo 6) *in* Santos, F.D. & Miranda P. (ed.). "Alterações Climáticas em Portugal. Cenários, Impactos e Medidas de Adaptação - Projecto SIAM II". Gradiva. Lisboa.

Appleby, P.G. & Oldfield, F. (1992). Application of lead-210 to sedimentation studies. In: Ivanovich, M., Harmon, R.S. (Eds.), Uranium Series Disequilibrium, Applications to Earth, Marine and Environmental Sciences. Clarendon Press, Oxford, 731–778.

Arribas, J. & Tortosa, A. (2003). Detrital modes in sedimenticlastic sand from low-order streams in the Iberian Range, Spain: the potential for sand generation by different sedimentary rocks. Sediment. Geol., 159, 275–303.

Arzola, R.G.; Wynn, R.B.; Lastras, G. Masson, D.G.; Weaver, P.P.E. (2008). Sedimentary features and processes in the Nazaré and Setúbal

submarine canyons, west Iberian margin. Marine Geology, 250, 64–88.

Asper, V.L. (1996). Particle flux in the ocean: Oceanographic tools. *In*: Ittekkot, V., Schäfer, P., Honjo, S. and Depetris, P.J. (Eds.), Particle Flux in the Ocean, SCOPE Report 57. John Wiley & Sons, Chichester, 71-84.

B

Bacon, M.P.; Belastock, R.A.; Bothner, M.H. (1994). ^{210}Pb Balance and implications for particle transport on the continental shelf, U.S: Middle Atlantic Bight. Deep-Sea Research II, 41, 511-535.

Badagola, A.; Rodrigues, A.; Rosa, L. (2006). High-resolution seismic stratigraphy of the Nazaré submarine canyon adjacent shelf (West Iberian Margin). 5th Symposium on the Iberian Atlantic Margin, 23-24.

Baker, E.T.; Milburn, H.B.; Tennant, D.A. (1988). Field assessment of sediment trap efficiency under varying flow conditions. Journal of Marine Research, 46, 573-592.

Balsinha, M.J. (2008). Estudo da dinâmica sedimentar da plataforma continental portuguesa entre o canhão submarino da Nazaré e a Ericeira. Tese de Mestrado. Universidade de Lisboa, Faculdade de Ciências, 174 p.

Baptista, M.S.; Vasconcelos, M.T.; Cabral, J.P.; Carmo Freitas, M.; Pacheco, A. (2008). Copper, nickel and lead in lichen and tree bark transplants over different periods of time. Environmental Pollution, 151, 408–413.

Benito, G.; Sopeña-Moya, Y.; Machado, M.J.; Pérez-González, A. (2003). Palaeoflood record of the Tagus River (Central Spain) during the Late Pleistocene and Holocene. Quaternary Science Reviews, 22, 1737-1756.

Berner H. & Wefer G. (1994). Clay-mineral flux in the Fram Strait and Norwegian Sea. Marine Geology, 116, 327-345.

Bettencourt, A.; Mello Franco, F.; Coelho, D.; Dias, C.G. (1980). Estuário do Tejo, tomo I, II-4-1 Meios receptores, Estudos de base de engenharia RESBAL, Drena-Hidroprojecto.

Bettencourt A. & Ramos L. (2003). Estuários Portugueses. INAG. 326 p.

Biscaye, P.E. & Anderson, R.F. (1994). Fluxes of particulate matter on the slope of the southern Middle Atlantic Bight: SEEP-II. Deep-Sea Research II 41, 459–509.

Biscaye, P.E. (1965). Mineralogy and sedimentation of recent deep-sea clay in

the Atlantic Ocean and adjacent seas and oceans: Geological Society of America, Bulletin, v. 76, 803-832.

Biscaye, P.E.; Anderson, R.F.; Deck, B.L. (1988). Fluxes of particles and constituents to the eastern United States continental slope and rise: SEEP-I. Continental Shelf Research, 8, 855-904.

Biscaye, P.E.; Flagg, C.N.; Falkowsky, P.G. (1994). The Shelf Edge Exchange Processes experiment: SEEP-II: an introduction to hypotheses, results and conclusions. Deep-Sea Research II, 41, 231-252.

Boer, W.; Van den Bergh, G.D.; De Haas, H.; De Stigter, H.C.; Gieles R.; Van Weering, T.C.E. (2006). Validation of accumulation rates in Teluk Banten (Indonesia) from commonly applied ^{210}Pb models, using the 1883 Krakatau tephra as time marker. Marine Geology, 227, 263-277.

Bollhöfer, A. & Rosman, K.J.R. (2001). Isotopic source signatures for atmospheric lead: the Northern Hemisphere. Geochimica Cosmochimica Acta 65, 1727–1740.

Boström, K.; Burman, J.O.; Ponter, C.; Ingri, J. (1981). Selective removal of trace elements from the Baltic Sea by suspended matter. Marine Chemistry, 10, 335–354.

Boust, D. (1981). Les méteaux-traces dans l'Estuaire de la Seine. Thèse (3ème Cycle), Université de Caen, 207 p.

Bower, A.S.; Serra, N.; Ambar, I. (2002). Structure of the Mediterranean Undercurrent and Mediterranean Water spreading around the southwestern Iberian Peninsula. Journal of Geophysical Research, 107, 25, 1–19.

Brindley, G.W. & Brown, G. (1980). Crystal Structures of Clay Minerals and their X-ray Identification. Mineralogical Society. London.

Brito, R. S. (1994). Portugal: Perfil Geográfico. Editorial Estampa, Lisboa.

Bruland, K.W. (1983). Trace elements in seawater. *In*: Riley, J.P., Chester, R. (Eds.), Chemical Oceanography, Vol. 8. Academic Press, London, 157–221.

Bruland, K.W.; Donat, J.R.; Hutchins, D.A. (1991). Interactive influences of bioactive trace metals on biological production in oceanic waters. Limnology and Oceanography, 36 (8), 1555–1577.

Byrd, J.T.; Lee, K.W.; Lee, D.S.; Smith, R.G.; Windom, H.L. (1990). The behaviour of trace metals in the Geum estuary, Korea. Estuaries, 13 (1),

8-13.

C

Cabeçadas, L. (1993). Ecologia do Fitoplâncton do Estuário do Sado: para uma estratégia de conservação. Estudos de Conservação da Natureza, 10. SNPRCN, Lisboa.

Caeiro, S.; Costa, M.H.; Ramos, T.B.; Fernandes F.; Silveira, N.; Coimbra, A.; Medeiros, G.; Painho, M. (2005). Assessing heavy metal contamination in Sado Estuary sediment: an índex analysis approach. Ecological Indicators, 5, 151-169.

Caetano, M. & Vale, C. (2003). Trace-element Al composition of seston and plankton along the Portuguese coast. Acta Oecologica, 24, 341–349.

Câmara, A.S.; Silva, M.C.; Ramos, L.; Ferreira, J.G. (1986). Estudo ambiental do estuário do Tejo. Divisão do estuário do Tejo em zonas homogéneas. Secretario do Estado do Ambiente e Recursos Naturais. RPT5.

Cardoso, A. & Palma, C. (2007). Monitorização da Área Envolvente a Sete Emissários da Costa Portuguesa: a Qualidade dos Sedimentos. Anais do Instituto Hidrográfico, 18, 127–134.

Carpenter, R.; Peterson, M.L.; Bennett, J.T. (1982). ^{210}Pb derived sediment accumulation and mixing rates for the Washington continental slope. Marine Geology, 48, 135-164.

Carson, B.; Baker, E.T.; Hickey, B.M.; Nittrouer, C.A.; DeMaster, D.J.; Thorbjarnarson, K.W.; Snyder, G.W. (1986). Modern sediment dispersal and accumulation in Quinault submarine canyon – a summary. Marine Geology, 71, 1-13.

Cartes, J.E.; Grémare, A.; Maynou, F.; Villora-Moreno, S.; Dinet, A. (2002). Bathymetric changes in the distributions of particulate organic matter and associated fauna along a deep-sea transect down the catalan sea slope (Northwestern Mediterranean). Progress in Oceanography, 53, 29-56.

Cearreta, A.; Alday, M.; Conceição Freitas, M.; Andrade, C.; Cruces, A. (2002). Modern foraminiferal record of alternating open and restricted environmental conditions in the Santo André lagoon, SW Portugal. Orive, E.; Elliot, M. and de Jonge V.N. (eds). Nutrients and Eutrophication in Estuaries and Coastal Waters. Kluwer Academic

Publishers. 21-27.

Chamley, H. (1989). Clay sedimentology, Springer-Verlag, Heidelberg, 623p.

Cochran, U. & Neil H. (2010). Diatom (< 63 μm) distribution offshore of eastern New Zealand: Surface sediment record and temperature transfer function. Marine Geology, 270 (1-4), 257-271.

Coppier, G. & Mougenot, D. (1982). Stratigraphie sismique et évolution géologique des formations néogènes et quaternaires de la plate-forme continentale portugaise au Sud de Lisbonne. B. Soc. Geol. Fr. 24, 421–431.

Cortesão, C. & Vale, C. (1995). Metals in sediments of the Sado Estuary, Portugal. Marine Pollution Bulletin, 30, 34-37.

Cortesão, C. (2002). Distribuição e reactividade do cádmio, cobre, crómio, níquel e cobalto no Estuário do Sado. Tese de Doutoramento. Faculdade de Ciências da Universidade de Lisboa. 340 p.

Costa, A; Mil-Homens, M.; Lebreiro, S.M.; De Stigter, H.; Richter, T.; Boer, W.; Trancoso, M.A.; Melo, Z.; Mouro, F. Mateus, M. (2011). Origin and transport of trace metals deposited in the last centuary in the canyons off Lisboa and adjacent slopes (Portuguese margin). Marine Geology, 282 (3-4), 169-177.

Costa, M.; Silva, R.; Vitorino, J. (2001). Contribuição para o estudo do clima de agitação marítima na costa portuguesa. 2as Jornadas Portuguesas de Engenharia Costeira e Portuária. Associação Internacional de Navegação. Sines.

Cotté-Krief, M.H.; Guieu, C.; Thomas, A.J.; Martin, J.M. (2000). Sources of Cd, Cu, Ni and Zn in Portuguese coastal waters. Marine Chemistry, 71, 199-214.

Cunha, M.R.; Paterson, G.L.J.; Alves, D.; Amaro, T.; Blackbird, S.; De Stigter, H.C.; Ferreira, C.; Glover, A.; Hilário, A.; Kiriakoulakis, K.; Nealova, L.; Ravara, A.; Rodrigues, C.F.; Tiago, A.; Billett, D.S.M. (in press). Biodiversity of macrofauna assemblages from three Portuguese submarine canyons (NE Atlantic). Deep-Sea Research I.

D

Darnley, A.G.; Björklund, A.; Bølviken, B.; Gustavsson, N.; Koval, P.V.; Plant, J.A.; Steenfelt, A.; Tauchid, M.; Xie X. (1995). A global geochemical

database for environmental and resource management. Recommendations for international geochemical. Final report of IGCP project 259. UNESCO Publishing.

De Haas, H.; Van Weering, T.C.E.; de Stigter, H. (2002). Organic carbon in shelf seas: sinks or sources, processes and products. Continental Shelf Research, 22, 691-717.

De Stigter, H.C. and shipboard scientific party (2004). Report of cruise 64PE225 with RV Pelagia. The sedimentary environment of submarine canyons of the Portuguese continental margin and Gulf of Lions. 59 p.

De Stigter, H.C. and shipboard scientific party (2007a). Report of cruise 64PE252 with RV Pelagia. Anthropogenic lead on the Portuguese continental margin. 57 p.

De Stigter, H.C.; Boer, W.; Mendes, P.A.J.; Jesus, C.C.; Thomsen, L.; Van den Berg, G.; Van Weering, T.C.E. (2007b). Recent sediment transport and deposition in the Nazaré Canyon, Portuguese continental margin. Marine Geology, 247, 144-164.

De Stigter, H.C.; Jesus, C.C.; Boer, W.; Richter, T.O.; Costa, A.; Van Weering, T.C.E. (in press). Recent sediment and deposition in the Lisbon-Setúbal and Cascais Canyon, Portuguese continental margin. Deep-Sea Research.

Deboudt, K.; Flament, P.; Weiss, D.; Mennessier, J.-P.; Maquinghen, P. (1999). Assessment of pollution aerosols sources above the Straits of Dover using lead isotope geochemistry. Science of the Total Environment, 236, 57–74.

Dias, J. (1990). A Evolução do Litoral Actual Português. Geonovas, 11, 15-29.

Dias, J.M.A. (1987). Dinâmica sedimentar e evolução recente da plataforma continental portuguesa setentrional. Tese de Doutoramento, Universidade de Lisboa.

Dias, J.M.A.; Gonzalez, R.; Garcia, C.; Diaz-del-Rio, V. (2002b). Sediment distribution patterns on the Galicia-Minho continental shelf. Progress in Oceanography, 52, 215–231.

Dias, J.M.A.; Jouanneau, J.M.; Gonzalez R.; Araújo, M.F.; Drago, T.; Garcia C.; Oliveira A.; Rodrigues A.; Vitorino J.; Weber O. (2002a). Present day sedimentary processes on the northern Iberian shelf. Progress in Oceanography, 52, 249–259.

Dickin, A.P. (1995). Radiogenic isotope geology. Cambridge University Press, Cambridge. doi:10.1016/j.coastaleng.2008.10.006.

Dinis, J.L. (2006). Nazaré: do Canhão à "falha", da Hipótese ao Mito. VII Congresso Nacional de Geologia. 385-388.

Döring, T.; Schwikowski, M.; Gäggeler, H.W. (1997). Determination of lead concentrations and isotope ratios in recent snow samples from high alpine sites with a double focusing ICP-MS. Fresenius' Journal of Analytical Chemistry, 359, 382–384.

Druffel, E.R.M. & Robinson, B.H. (1999). Is the Deep Sea on a Diet? Science, 284, 1139-1140.

Duarte, J.F. (2002). Distribução espacial dos sedimentos no Canhão da Nazaré e plataforma adjacente. Proc. 3° Assemblea Hispano-Portuguesa de Geodesia y Geofísica,Valencia, Spain, 1162–1166.

Duarte, J.F.; Dias, J.M.A.; Taborda, R. (2000). Cabeceira do Canhão da Nazaré: erosão versus sedimentação. Proc. 3rd Symp. Iberian Atlantic Margin, Faro, Portugal, 227-228.

Durrieu de Madron, X. (1994). Hydrography and nepheloid structures in the Grand-Rhône canyon. Continental Shelf Research, 14, 457-477.

Durrieu de Madron, X.; Castaing, P.; Nyffeler, F.; Courp, T. (1999). Slope transport of suspended particulate matter on the Aquitanian margin of the Bay of Biscay. Deep-Sea Res. II, 46, 2003-2027.

E

Ehrmann, W.U.; Melles, M.; Kuhn, G.; Grobe, H. (1992). Significance of clay assemblages in Antartic Ocean. Marine Geolgy, 107, 249-273.

Emery, K.O. (1968). Relict sediments on continental shelves of the world. Bull. Am. Assoc. Petrol. Geologists, 52, 445-464.

Epping, E.; Van der Zee, C.; Soetaert, K.; Helder, W. (2002). On the oxidation and burial of organic carbon in sediments of the Iberian margin and Nazaré Canyon (NE Atlantic). Progress in Oceanography, 52, 399-431.

Esquevin, J. (1969). Influence de la composition chimique des argiles sur le cristallinité. Bulletin Centre Recherche Pau, S.N.P.A., 3, 147-154.

Estrada, M.; Varela, R.A.; Salat, J.; Cruzado, A.; Arias, E. (1999). Spatio-temporal variability of the winter phytoplankton distribution across the Catalan and North Balearic Basin fronts (NW Mediterranean). Journal of

Plankton Research, 21(1), 1-20.

Evans, D.; Stoker, M.S.; Cramp, A. (1998). Geological processes on continental margins: sedimentation mass-wasting and stability: an introduction. *In*: Stokerm M.S., Evans, D. & Cramp, A. (eds.) Geological Processes on Continental Margins: Sedimentation, Mass-Wasting and Stability. Geological Society, London, Special Publications, 129, 1-4.

F

Farre, J.A.; McGregor, B.A.; Ryan, W.B.F.; Robb, J.M. (1983). Breaching the shelfbreak: passage from youthful to mature phase in submarine canyon evolution. In: Stanley, D.J., Moore, G.T. (Eds.), The Shelfbreak: Critical Interface on Continental Margins, The Society of Economic Paleontologists and Mineralogists, vol. 33, 25–39.

Faugères, J.C.; Gonthier, E.; Pujol, C.; Devaux,M.; Philipps, I. (1984). La mission Faegas IV: Premiers résultats sur les sédiments profonds de la marge ouest-ibérique, du Golfe de Cadix et de la Mer d'Alboran. Bull. Inst. Géol. Bassin d'Aquitaine, Bordeaux 36, 67–83.

Ferentinos, G.; Collins, M.B.; Pattiaratchi, C.B.; Taylor, P.G. (1985). Mechanisms of sediment transport and dispersion in a tectonically active submarine valley/canyon system: Zakynthos Straits, NW Hellenic Trench. Marine Geology, 65, 243-269.

Ferreira, Ó.; Dias, J.A.; Taborda, R. (2008). Implications of Sea-Level Rise for Continental Portugal. Journal of Coastal Research, 24(2), 317-324.

Figuères, G.; Martin, J.; Meybeck, M.; Seyler, P. (1985). A comparative study of mercury contamination in the Tagus estuary (Portugal) and major French estuaries (Gironde, Loire, Rhone). Estuarine, Coastal and Shelf Science, 20 (2), 183–203.

Findlay, C.S. & Flores, J.A. (2000). Subtropical Front fluctuations south of Australia (45°09'S, 146°17'E) for the last 130 ka years based on calcareous nannoplankton. Marine Micropaleontology, 40 (4), 403-416.

Fisher, N. & Reinfelder, J. (1995). The trophic transfer of metals in marine systems. *In*: Tessier, A., Turner, D.R. (Eds.), Metal Speciation and Bioavalability, 3. Willey and Sons. 679 p.

Fiúza, A.F.G. (1984). Hidrologia e Dinâmica das Águas Costeiras de Portugal. Faculdade de Ciências da Universidade de Lisboa, Lisboa. 294 p.

Fiúza, A.F.G.; Hamann, M.; Ambar, I.; Diaz del Rio, G.; Gonzalez, N.; Cabanas, J.M. (1998). Water masses and their circulation off western Iberia during May 1993. Deep-Sea Research I, 145, 1127 – 1160.

Flegal, A.R. & Smith, D.R. (1995). Measurements of environmental lead contamination and human exposure. Rev. Environ. Contam. Toxicol., 143, 1 – 45.

Förstner, U. & Wittmann G.T.W. (1979). Metal Pollution in the aquatic Environment. Berlin, Heidelberg, New York, Springer-Verlag, 486 p.

França, S.; Vinagre, C.; Caçador, I.; Cabral, H.N. (2005). Heavy metal concentrations in sediment, benthic invertebrates and fish in three salt march areas subjected to different pollution loads in the Tagus Estuary (Portugal). Marine Pollution Bulletin, 50, 993-1018.

Freire, M.E. (1986). A Planície litoral entre Trafaria e a Lagoa de Albufeira: um estudo de geomorfologia litoral. Tese de Mestrado. Faculdade de Letras de Lisboa. 204 p.

Freire, P.M.S. (1993). Caracterização e dinâmica de sedimentos em sistemas de canais do Estuário do Tejo – Cala do Norte (Portugal). Tese de Mestrado, Universidade de Lisboa, Departamento de Geologia da Faculdade de Ciências. Lisboa, 164 p.

Freitas, M.C.; Andrade, C.; Cruces, A. (1999). Lagoa de Santo André – Dinâmica do Sistema Lagunar Actual. Comportamento da barra, dinâmica hidrológica e sedimentar da laguna. Evolução holocénica do sistema lagunar. Seminário "A Zona Costeira do Alentejo". Eurocoast – Portugal. 5-11.

Freitas, M.C.; Andrade, C.; Cruces, A. (2000). A importância do conhecimento geológico no ordenamento de ambiente lagunares: exemplos do litoral SW de Portugal. Seminário "Perspectivas de gestão integrada de ambientes costeiros". Eurocoast – Portugal. 127-142.

Freitas, M.C.; Andrade, C.; Cruces, A. (2002). The geological record of environmental changes in the southwestern Portuguese coastal lagoons since the Lateglacial. Quaternary International, 93-94, 161-170.

Fütterer, D.K. (2006). The solid phase of marine sediments. In Marine Geochemistry (eds.) H.D. Schulz and M. Zabel. Springer. 574 p.

G

Galgani, F.; Souplet, A.; Cadiou, Y. (1996). Accumulation of debris on the deep sea floor off the French Mediterranean coast. Marine Ecology Progress Series, 142, 225-234.

Gama, C. M. P. (2004). Dinâmica de sistemas sedimentares do litoral ocidental Português a sul do Cabo Espichel. Tese de Doutoramento, Universidade de Évora, 359 p.

Garcia, C. (1997). Dispersão e deposição da matéria particulada transportada em suspensão para a plataforma continental adjacente aos rios Tejo e Sado. Tese de Mestrado. Faculdade de Ciências de Lisboa. 170 p.

Garcia, C.; Coelho, H.; Neves, R. (2003). Some hydrological and nephelometric aspects over Nazaré and Setúbal submarine canyons (Portugal). In: Fourth Symposium on the Iberian Atlantic margin, Thalassas, 19 (2b), 51-52.

García, R.; Koho, K. A.; de Stigter, H. C.; Epping, E.; Koning, E.; Thomsen, L. (2007). Distribution of meiobenthos in the Nazaré canyon and adjacent slope (western Iberian Margin) in relation to sedimentary composition. Marine Ecology Progress Series, 340, 207-220.

García, R.; Thomsen, L.; de Stigter, H.C.; Epping, E.; Soetaert, K.; Koning, E.; de Jesus Mendes, P.A. (2010). Sediment bioavailable organic matter, deposition rates and mixing intensity in the Setúbal-Lisbon canyon and adjacent slope (Western Iberian Margin). Deep-Sea Research I, 57 (8), 1012-1026.

Gardner, W.D. (1980a). Sediment trap dynamics and calibration: a laboratory evaluation. Journal of Marine Research, 38, 17-39.

Gardner, W.D. (1980b). Field assessment of sediment traps. Journal of Marine Research, 38, 41-52.

Gardner, W.D. (1989). Baltimore Canyon as a modern conduit of sediment to the deep sea. Deep-Sea Research, 36, 323-358.

Gardner, W.D. (1995). Report on the JGOFS Symposium in Villefranche sur Mer in May, 1995. Edited by Wilford E. Gardner.

Gardner, W.D.; Biscaye, P.E.; Richardson, M.J. (1997). A sediment trap experiment in the Vema Channel to evaluate the effect of horizontal particle fluxes on measured vertical fluxes. Journal of Marine Research, 55, 995-1028.

Gibbs, R.J. (1973). Mechanisms of trace metals transport in rivers. Science,

180, 71–72.

Gibbs, R.J. (1986). Segregation of metals by coagulation in estuaries. Marine Chemistry, 18, 149–159.

Gil, O. & Vale, C. (2001). Evidence of polychlorinated biphenyls dechlorination in the sediments of Sado estuary, Portugal. Marine Pollution Bulletin, 42 (6), 453–461.

Gomes, C. (1988). Argilas, o que são e para que servem. Fundação Calouste Gulbenkian. Lisboa. 457 p.

Gomes, N. (1992). Dinâmica dunar no arco litoral Tróia-Sines (Portugal). Tese de Mestrado. Universidade de Lisboa. 121 p.

Goudie, A.S. (1995). The Changing Earth: Rates of Geomorphological Processes. Blackwell, Oxford. 302 p.

Grant, A. & Middleton, R. (1990). An assessment of metal contamination of sediments in the Humber estuary, UK. Estuarine, Coastal and Shelf Science, 31, 71-85.

Griffin, J.J.; Windom, H.; Goldberg, E.D. (1968). The distribution of clay minerals in the World Ocean. Deep-Sea Research, 15, 433-459.

Grousset, F.E.; Joron, J.L.; Biscaye, P.E.; Latouche, C.; Treuil, M.; Maillet, N.; Faugères, J.C.; Gonthier, E. (1988). Mediterranean outflow through the Strait of Gibraltar since 18,000 years B.P.: mineralogical and geochemical arguments. Geo Mar. Lett., 8, 25–34.

Grousset, F.E.; Quétel, C.R.; Thomas, B.; Buat-Ménard, P.; Donard, O.F.X.; Bucher, A. (1994). Transient Pb isotopic signatures in the Western European atmosphere. Environmental Science and Technology, 28, 1605–1608.

Grousset, F.E.; Quétel, C.R.; Thomas, B.; Donard, O.F.X.; Lambert, C.E.; Guillard, F.; Monaco, A. (1995). Anthropogenic vs. lithogenic origins of trace elements (As, Cd, Pb, Rb, Sb, Sc, Sn, Zn) in water column particles: northwestern Mediterranean Sea. Marine Chemistry, 48, 291–310.

H

Hall, I. R.; Schmidt, S.; McCave, I. N.; Reyss, J. L. (2000). Particulate matter distribution and 234Th/238U disequilibrium along the Northern Iberian Margin: implications for particulate organic carbon export. Deep-Sea

Research I, 47 (4), 557-582.

Hansmann, W. & Köppel, V. (2000). Lead-isotopes as tracers of pollutants in soils. Chemical Geology 171, 123–144.

Hickey, B.; Baker, E. T.; Kachel, M. (1986). Suspended particle movement in and around Quinault submarine canyon. Marine Geology, 71, 35-83.

Hidroprojecto; Coba; Hidrotécnica Portuguesa; Atkins; Consulgal; Gibb-Portugal (1999). Plano de Bacia Hidrográfica do Sado.

Honjo, S.; Manganini, S.J.; Poppe, L. (1982). Sedimentation of lithogenic particles in the deep ocean. Marine Geology, 50, 199-220.

Horowitz, A.J. (1991). A primer on sediment trace element chemistry. 2nd edition. CRC Press. 144 p.

Huber, L. (1998). LC-GC Int. 11, 96.

Huertos, G. & de los Monteros, E. (1974). Les caolinos en España: características, identificación y ensayos cerámicos. Ed. Soc. Esp. de Ceramica, Madrid.

Hung, J.-J. & Hsu, C.-L. (2004). Present state and historical changes of trace metal pollution in Kaoping coastal sediments, southwestern Taiwan. Marine Pollution Bulletin, 49, 986–998.

Hung, J.-J., Lin, C.-S., Chung, Y.-C., Hung, G.-W and Liu, W.-S. (2003). Lateral fluxes of biogenic particles through the Min-Hua canyon in the southern East China Sea slope. Continental Shelf Research, 23, 935-955.

Huthnance, J.M.; Van Aken, H.M.; White, M.; Barton, E.D.; Cann, B.L.; Coelho, E.F.; Fanjul, E.A.; Miller, P.; Vitorino, J. (2002). Ocean margin exchange-water flux esimates. Journal of Marine Systems, 32, 107-137.

I

Inverno, C.; Manuppella, G.; Zbyszewski, G.; Pais, J.; Ribeiro, M. (1993). Carta Geológica de Portugal, escala 1:50000, Folha 42C (Santiago do Cacém) e respectiva notícia explicativa. Serviços Geológicos de Portugal, Lisboa. 75 p.

J

Jenne, E. A. (1976). Trace element sorption by sediments and soils - sites and processes. In: Symposium on Molybdenum, ed. by W. Chappel & K. Petersen, vol. 2, 425-553. Marcel Dekker, New York.

Jesus, C.C.; de Stigter, H.C.; Richter, T.O.; Boer, W.; Mil-Homens, M.; Oliveira,

A.; Rocha F. (2010). Trace metal enrichments in Portuguese submarine canyons and open slope: anthropogenic impact and links to sedimentary dynamics. Marine Geology, 271, 72-83.

Jesus, C.C.; Inácio, M.; Ferreira da Silva, E.; Oliveira, A.; Rocha, F. (2005). Enriquecimento de metais em sedimentos de praia (SW Portugal). X Congresso Brasileiro de Geoquímica dos Países do Mercosul. CD do Congresso.

Jesus, C.C.; Miranda, P.; Rocha, F.; Oliveira, A. (2007). Mineralogy and geochemistry of fine-fraction beach sediments as markers of sedimentary dynamics (SW Portugal). Journal of Coastal Research, 50, 990-994.

Jesus, C.C.; Miranda, P.; Rocha, F. (2006). Mineralogy and metals of fine-grained beach sediments (SW Portugal). Proceedings of the Joint Meeting Groupe Français des Argiles & The Clay Minerals Society, France.

Jouanneau, J.M.; Garcia, C.; Oliveira, A.; Rodrigues, A.; Dias, J., Weber, O. (1998). Dispersal and deposition of suspended sediment on the shelf off Tagus and Sado estuaries, SW Portugal. Progress in Oceanography, 42, 233-257.

K

Kahle, M.; Kleber, M.; Jahn, R. (2002). Review of XRD-based quantitative analyses of clay minerals in soils: the suitability of mineral intensity factors. Geoderma, 109, 191-205.

Kairyte M.; Stevens, R.; Trimonis, E. (2005). Provenance of silt and clay within sandy deposits of the Lithuanian coastal zone (Baltic Sea). Marine Geology, 218, 97-112.

Karlin, R. (1980). Sediment sources and clay mineral distributions off the Oregon coast. Journal of Sedimentary Petrology, 50 (2), 543-560.

Khripounoff, A.; Vangriesheim, A.; Babonneau, N.; Crassous, P.; Dennielou, B.; Savoye, B. (2003). Direct observation of intense turbidity current activity in the Zaire submarine valley at 4000 m water depth. Marine Geology, 194, 151-158.

Knauer, G.A. & Asper, V.L. (eds). (1989). U.S. GOFS Planning Report Number 10: Sediment Trap Technology and Sampling. U.S. Joint Global Ocean

Flux Study (JGOFS) Planning Office, WoodsHole, 94 p.

Koho, K.A.; García, R.; de Stigter, H.C.; Epping, E.; Koning, E.; Kouwenhoven, T.J.; Van der Zwaan, G.J. (2008). Sedimentary labile organic carbon and pore water redox control on species distribution of benthic foraminifera: A case study from Lisbon-Setúbal Canyon. Progress in Oceanography, 79, 55-82.

Komar, P.D. (1976). Beach processes and sedimentation. Prentice-Hall, Inc., New Jersey, 429 p.

Kubler, B. (1964). Les argiles, indicateurs de métamorphisme. Revue Institute Français Pétrole, 19, 1093-1112.

Kylander, M.E.; Weiss, D.J.; Martínez Cortízas, A.; Spiro, B.; Garcia-Sanchez, R.; Coles, B.J. (2005). Refining the pre-industrial atmospheric Pb isotope evolution curve in Europe using an 8000 year old peat core from NW Spain. Earth and Planetary Science Letters, 240, 467–485.

L

Lasaga, A. (1984). Chemical Kinetics of Water-Rock Interactions. Journal of Geophysical Research, 89, B6, 4009-4025.

Lastras, G.; Arzola, R.G.; Masson, D.G.; Wynn, R.B.; Huvenne, V.A.I.; Hühnerbach, V.; Canals M. (2009). Geomorphology and sedimentary features in the Central Portuguese submarine canyons, Western Iberian margin. Geomorphology, 103 (3), 310–329.

Lee, G.; Nicholls,R.J.; Birkemeier, W.A. (1998). Storm-induced profile variability of the beach-nearshore profile at Duck, North Carolina, USA, 1981-1991. Marine Geology, 148, 163-177.

Lewis, K.B. & Barnes, P.M. (1999). Kaikoura Canyon, New Zealand: active conduit from near-shore sediment zones to trench-axis channel. Marine Geology, 162, 39-69.

Lohse, L.; Helder, W.; Epping, E.H.G.; Balzer, W. (1998). Recycling of organic matter along a shelf-slope transect across the NW European Continental Margin (Goban Spur). Progress in Oceanography, 42, 77-110.

Lohse, L.; Kloosterhuis, R.T.; de Stigter, H.C.; Helder, W.; Van Raaphorst, W.; Van Weering, T.C.E. (2000). Carbonate removal by acidification causes loss of nitrogenous compounds in continental margin sediments. Marine Chemistry, 69, 193-201.

Long, E.; MacDonald, D.; Smith, S.; Calder, F. (1995). Incidence of adverse biological effects within ranges of chemical concentrations in marine and estuarine sediments. Environmental Management, 19, 81-97.

Loring D. & Rantala, R. (1992). Manual for the geochemical analyses of marine sediments and suspended particulate matter. Earth-Science Reviews, 32, 235-283.

Löscher, B.M. (1999). Relationships among Ni, Cu, Zn, and the major nutrients in the Southern Ocean. Marine Chemistry, 67, 67–102.

Loureiro, J.M. & Macedo, M.E. (1986). Bacia hidrográfica do rio Tejo. In Monografias hidrológicas dos principais cursos de água de Portugal continental. Direcção Geral dos Recursos e Aproveitamentos Hidráulicos. 281–337.

Loureiro, J.M. (1979). Curvas de duração dos caudais médios diários no rio Tejo. Technical report, Servico Hidraulico (DGRAH), Lisbon.

M

Magalhães, F. (2001). Os sedimentos da Plataforma Continental Portuguesa: contrastes espaciais, perspectiva temporal, potencialidades económicas. Tese de Doutoramento, Univ. de Lisboa, Documentos Técnicos, Inst. Hidrográfico, 287 p.

Maretec (2008). Plano de Monitorização na envolvente do emissário submarino de Sines. Relatório de Síntese do 1º ano. Maretec-IST. 93 p.

Marques, F.M.S.F. (1999). Evolução das arribas e da linha de costa no arco litoral Tróia-Sines (Portugal) *in* Soares de Carvalho, G.; Veloso Gomes, F.; Pinto, F.T. (Eds.). A Zona Costeira do Alentejo. Associação Eurocoast – Portugal. 69-80.

Martín, J. (2005). Sedimentary dynamics in the Palamós Submarine Canyon. PhD thesis. Universidad Politécnica de Cataluña. 196 p.

Martín, J.; Palanques, A.; Vitorino, J. (2004). Particulate matter fluxes and composition in the Nazaré submarine canyon. Joint Eurodelta-Eurostrataform meeting. Venice, 20-23rd October 2004.

Masó, M. & Duarte, C.M. (1989). The spatial and temporal structure of hydrographic and phytoplankton biomass heterogeneity along the Catalan coast (NW Mediterranean). Journal of Marine Research, 47(4), 813-827.

Mastbergen, D.R. & Van den Berg, J.H. (2003). Breaching in fine sands and the generation of sustained turbidity currents in submarine canyons. Sedimentology, 50, 625–637.

May, J.A.; Warme, J.E.; Slater, R.A. (1983). Role of submarine canyons on shelfbreak erosion and sedimentation: modern and ancient examples. SEPM special publication, 33, 315-332.

McCave, I.N. & Hall, I.R. (2002). Turbidity of waters over the Northwest Iberian continental margin. Progress in Oceanography, 52, 299-313.

McCave, I.N.; Hall, I.R.; Antia, A.N.; Chou, L.; Dehairs, F.; Lampitt, R.S.; Thomsen, L.; Van Weering, T.C.E.; Wollast, R. (2001). Distribution, composition and flux of particulate material over the European margin at 47º-50º N. Deep-Sea Research II, 48, 3107-3139.

Mélières, F. (1974). Recherches sur la dynamique sédimentaire du Golfe de Cadix, Espagne. These Doctorat d'Etat, Univ. Paris VI, 224 p.

Meunier, A. (2005). Clays. Springer, Berlin, 472 p.

Mil-Homens, M.; Branco, V.; Vale, C.; Boer, W.; Alt-Epping, U.; Abrantes, F.; Vicente, M. (2009). Sedimentary record of anthropogenic metal inputs in the Tagus prodelta (Portugal). Continental Shelf Research, 29 (2), 381–392.

Mil-Homens, M.; Stevens, R.L.; Abrantes, F.; Cato, I. (2006). Heavy metal assessment for surface sediments from three areas of the Portuguese continental shelf. Continental shelf Research, 26, 1184-1205.

Miller, J.R. & Orbock, S.M. (2007). Contaminated rivers: a geomorphological-geochemical approach to site assessment and remediation. Spring Verlag, Berlin, Heidelberg, New York, 418 p.

Milliman, J.D. & Summerhays, C.P. (1975). Upper continental margin sedimentation of Brasil. Contribution to Sedimentology, 4, Schweizerbart, Stuttgart, 175 p.

Milliman, J.D.; Pilkey, O.H.; Ross, D.A. (1972). Sediments of the continental margins off the eastern United States. Geological Society of America Bulletin, 83, 1315-1334.

Millot, G. (1964). Géologie des Argiles. Masson.

Millot, R.; Allègre, C.-J.; Gaillardet, J.; Roy, S. (2004). Lead isotopic systematics of major river sediments: a new estimate of the Pb isotopic composition of the Upper Continental Crust. Chemical Geology, 203, 75–90.

Miralles, J.; Véron, A.J.; Radakovitch, O.; Deschamps, P.; Tremblay, T.; Hamelin, B. (2006). Atmospheric lead fallout over the last century recorded in Gulf of Lions sediments (Mediterranean Sea). Marine Pollution Bulletin, 52, 1364-1371.

Miranda, P. (2006). Estudo das fracções arenosas dos sedimentos do litoral Tróia – Sines. Tese de Mestrado, Universidade de Aveiro. 150 p.

Miranda, P.; Jesus, C.C.; Cascalho, J.; Bernardes, C.; Rocha, F. (2007). Interpreting beach sedimentary dynamics between Tróia and Sines (SW Portugal) using heavy minerals and textural analyses. Journal of Coastal Research, 50, 599-603.

Moita, I. & Quevauviller, P. (1986). Les differents faciès sédimentaires de la plateforme continentale nord alentejanaise. comparaison avec l'ensemble continental. Boletin Informação Sociedade Geológica Portugal, 13, 30.

Mol, J.W. (2003). Sedimentation Estimation from ADCP Measurements. Hydro International. 7 (6). Online article.

Monaco, A.; Biscaye, P.; Soyer, J.; Pocklington, R.; Heussner, S. (1990a). Particle fluxes and ecosystem response on a continental margin: the 1985-1988 Mediterranean ECOMARGE experiment. Continental Shelf Research, 10, 809-839.

Monaco, A.; Courp, T.; Heussner, S.; Carbonne, J.; Fowler, S.W.; Deniaux, B. (1990b). Seasonality and composition of particulate fluxes during ECOMARGE-I, western Gulf of Lions. Continental Shelf Research, 10, 959-987.

Monna, F.; Lancelot, J.; Croudace, I.W.; Cundy, A.B.; Lewis, J.T. (1997). Pb isotopic composition of airborne particulate material from France and the southern United Kingdom: implications for Pb pollution sources in urban areas. Environmental Science and Technology, 31, 2277–2286.

Monteiro, J.H. & Moita, I. (1971). Morfologia e sedimentos da plataforma continental e vertente continental superior ao largo da península de Setúbal. Direcção Geral Minerais e Serviços Geológico. 301–330.

Morais, J.O.; Tintelnot, M.; Irion, G.; Souza Pinheiro, L. (2006). Pathways of clay mineral transport in the coastal zone of the Brazilian continental shelf from Ceará to the mouth of the Amazon River. Geo-Marine Letters, 26, 16-22.

Mulder, T.; Weber, O.; Anschutz, P.; Jorissen, F.J.; Jouanneau, J.M. (2001). A few months-old storm generated turbidite deposited in the Capbreton Canyon (Bay of Biscay, SW France). Geo-Marine Letters, 21, 149-156.

N

Naya, A. (1984). Meteorología superior. Espasa-Calpe, S. A., Madrid, 546 pp.

Nelson, C.H. (1976). Late Pleistocene and Holocene depositional trends, processes, and history of Astoria deep-sea fan. Northeast Pacific. Marine Geology, 20, 129-173.

Nemecz, E. (1981). Clay minerals. Budapeste: Ak. Kiado.

Nemus (2011). Estudo de Impacte Ambiental da Relocalização do Cais de Acesso de Navios ao Terminal de Líquidos da Tanquipor, Barreiro.

Nisbet, E.G. & Piper, D.J.W. (1998). Giant submarine landslides. Nature, 392, 329-330.

Nittrouer, C. A. & Wright, L.D. (1994). Transport of particles across continental shelves. Reviews of Geophysics, 32, 1, 85-113.

Nittrouer, C.A.; Sternberg, R.W; Carpenter, R.; Bennett, J.T. (1979). The use of Pb-210 geochronology as a sedimentological tool: Application to the Washington continental shelf. Marine Geology, 31, 297-316.

O

O'Connor, P. & Paul, J. (2000). Misfit between sediment toxicity and chemistry. Marine Pollution Bulletin, 40 (1), 59-64.

Olivar, M.P.; Sabatés, A.; Abelló, P.; Garcia, M. (1988). Transitory hydrographic structures and distribution of fish larvae and neustonic crustaceans in the north-western Mediterranean. Oceanologica Acta, 21(1), 95-104.

Oliveira, A. (2001). Dinâmica da Matéria Particulada em Suspensão na Plataforma Continental Minhota e sua Relação com a Cobertura Sedimentar. Tese de Doutoramento. Universidade do Algarve. 278 p.

Oliveira, A.; Rocha, F.; Rodrigues, A.; Jouanneau, J.; Dias, A.; Weber, O.; Gomes, C. (2002). Clay minerals from the sedimentary cover from the Northwest Iberian shelf. Progress in Oceanography, 52, 233-247.

Oliveira, A.; Santos, A.I.; Rodrigues, A.; Vitorino, J. (2007). Sedimentary particle distribution and Dynamics on the Nazaré canyon system and adjacent shelf (Portugal). Marine Geology, 246 (2-4), 105-122.

Oliveira, I.; Valle, C.; Miranda, F. (1982). Littoral problems in the Portuguese

West Coast. Proceedings Coastal Engineering, 3, 1959-1969.

Ortiz, J.D. & Mix, A.C. (1992). The spatial distribution and seasonal succession of planktonic foraminifera in the California Current off Oregon, September 1987–September 1988. In: Summerhayes, C.P., Prell,W.L., Emeis,K.C. (Eds.), Upwelling Systems: Evolution Since the Early Miocene. Geological Society Special Publication, London, 197–213.

P

Palanques, A.; Garcia-Ladona, E.; Gomis, D.; Martín, J.; Marcos, M.; Pascual, A.; Puig, P.; Ermelianov, M.; Guillén, J.; *et al.* (2005). General patterns of circulation, sediment fluxes and ecology of the Palamós (La Fonera) submarine canyon, northwestern Mediterranean. Progress in Oceanography, 66, 89-119.

Palanques, A.; Masqué, P.; Puig, P.; Sánchez-Cabeza, J.A.; Frignani M.; Alvisi, F. (2008). Anthropogenic trace metals in the sedimentary record of the Llobregat continental shelf and adjacent Foix submarine canyon (northwestern Mediterranean). Marine Geology, 248, 213-227.

Paull, C.K.; Greene, H.; Ussler, W.; Mitts, P. (2002). Pesticides as tracers of sediment transport through Monterey Canyon. Geo-Marine Letters, 22, 3, 121-126.

Paull, C.K.; Ussler, W.; Greene, H.G.; Keaten, R.; Mitts, P.; Barry, J. (2003). Caught in the act: the 20 December 2001 gravity flow event in Monterey Canyon. Geo-Marine Letters, 22, 227-232.

Pera, E.L. & Arribas, J. (2004). Sand composition in an Iberian passive-margin fluvial course: the Tajo River. Sedimentary Geology, 171, 261–281.

Petrenko, A.A. (2003). Variability of circulation features in the Gulf of Lion NW Mediterranean Sea. Importance of inertial currents. Oceanologica Acta, 26, 323-338.

Petruncio, E.T.; Rosenfeld, L.K.; Paduan, J.D. (1998). Observations of the Internal Tide in Monterey Canyon. J. Phys. Oceanogr., 28, 1873-1903.

Petschick, R. (2000). MacDiff 4.2.2.

Petschick R.; Kuhn G.; Gingele F. (1996). Clay mineral distribution in surface sediments of the South Atlantic: sources, transport and relation to oceanography. Marine Geology, 130, 203-229.

Pfannkuche, O. (1993). Benthic response to the sedimentation of particulate

organic matter at the BIOTRANS station, 47 N, 20 W. Deep-Sea Research II, 40, 135-149.

Pickering, K.T.; Hiscott, R.H.; Hein, F.J. (1989). Deep marine environments: clastic sedimentation and tectonics. Unwin Hyman, London, 416 p.

Piedade, M.; Freitas, M.C.; Araújo, M.F.; Cruces, A.; Andrade, C. (2004). Caracterização geoambiental da Lagoa de Santo André e seus afluentes. Resumos do 1º Seminário sobre Sistemas Lagunares Costeiros, 48-49.

Pierce, J.W. & Stanley, D.J. (1975). Suspended-sediment concentration and mineralogy in the central and western Mediterranean and mineralogic comparison with bottom sediment. Marine Geology, 19, 15–25.

Pimentel, N. (1997). O Terciário da Bacia do Sado: Sedimentologia e Análise Tectono-sedimentar. Tese de Doutoramento, Universidade de Lisboa. 381 p.

Pombo, J. (2004). Sedimentos superficiais da plataforma continental portuguesa entre o Cabo Mondego e S. Martinho do Porto. Tese de Mestrado, Faculdade de Ciências da Univ. de Coimbra, 185 p.

Procesl; Gibb-Portugal; HidroRumo; Hidrotécnica Portuguesa (1999). Plano de Bacia Hidrográfica do Tejo.

Puig, P. & Palanques, A. (1998a). Temporal Variability and composition of settling particle fluxes on the Barcelona continental margin (Northwestern Mediterranean). Journal of Marine Research, 56, 639-654.

Puig, P. & Palanques, A. (1998b). Nepheloid structure and hydrographic control on the Barcelona continental margin, Northwestern Mediterranean. Marine Geology, 149, 39-53.

Puig, P.; Ogston, A.S.; Mullenbach, B.L.; Nittrouer, C.A.; Sternberg, R.W. (2003). Shelf-to-canyon sediment-transport processes on the Eel continental margin (northern California). Marine Geology, 193, 129-149.

Puig, P.; Ogston, A.S.; Mullenbach, C.A.; Nittrouer, C.A.; Parsons, J.D.; Sternberg, R.W. (2004). Storm-induced sediment gravity flows at the head of the Eel submarine canyon, northern California margin. Journal of Geophysical Research, 109(C3), C03019.

Puig, P.; Palanques, A.; Guillén, J.; García-Ladona, E. (2000). Deep slope currents and suspended particle fluxes in and around the Foix submarine canyon (NW Mediterranean). Deep-Sea Research I, 47, 343-

366.

Puig, P.; Palanques, A.; Sanchez-Cabeza, J.A.; Masqué, P. (1999). Heavy metals in particulate matter and sediments in the southern Barcelona sedimentation system (North-western Mediterranean). Marine Chemistry, 63(3-4), 311-329.

Pusceddu A.; Bianchelli, S.; Canals, M.; Sanchez-Vidal, A.; Durrieu de Madron, X.; Heussner, S.; Lykousis , V.; De Stigter, H.; Trincardi, F.; Danovaro, R. (2010). Organic matter in sediments of canyons and open slopes of the Portuguese, Catalan, Southern Adriatic and Cretan Sea margins. Deep-Sea Research, 57, 441–457.

Q

Quaresma, L.S.; Vitorino, J.; Oliveira, A. (2007). Evidence of sediment resuspension by nonlinear internal waves on the western Portuguese mid-shelf. Marine Geology, 246, 123-143.

Quevauviller, P. (1987). Evolution and stabilization of headland-bay beaches. Journal of Shoreline Management, 269-284.

Quevauviller, P. (1988). Ètude geomorphologique, sedimentologique et geochimique du litoral de Galé et de l'estuaire du Sado (Portugal). Thèse, Université de Bordeaux, 255 p.

R

Ramos, C. & Reis, E. (2001). As Cheias no Sul de Portugal em Diferentes Tipos de Bacias Hidrográficas, Finisterra, Revista Portuguesa de Geografia, XXXVI, 71, Centro de Estudos Geográficos, U.L., 61-82.

Rateev, M. A.; Gorbunova, Z. N.; Lisitzyn, A. P.; Nosov, G. L. (1969). The distribution of clay minerals in the oceans. Sedimentology, 13, 21–43.

Ribani, M.; Bottoli, C.; Collins, C.; Jardim I. (2004). Validação em métodos cromatográficos e electroforéticos. Quim. Nova, 27 (5), 771-780.

Ribeiro, A.; Antunes, M.T.; Ferreira, M.P.; Rocha, R.B.; Soares, A.F.; Zbyszewski, G.; Almeida, F.M.; Carvalho, D.; Monteiro, J.H. (1979). Introduction à la géologie générale du Portugal. Serviços Geológicos de Portugal, Lisboa, 114 p.

Richter, T.O.; De Stigter, H.C.; Boer, W.; Jesus, C.C.; Van Weering, T. (2009). Dispersal of natural and anthropogenic lead through submarine canyons at the Portuguese margin. Deep-Sea Research Part I, 56 (2), 267–282.

Ríos, A.F.; Pérez, F.F.; Fraga, F. (1992). Water masses in the upper and middle North-Atlantic Ocean east of the Azores. Deep-Sea Research Part A — Oceanographic Research Papers, 39 (3–4), 645–658.

Rocha, F. (1993). Argilas aplicadas a estudos litoestratigráficos e paleoambientais na bacia sedimentar de Aveiro. Tese de Doutoramento, Universidade de Aveiro, 399 p.

Roma-Torres, J.; Silva, S.; Costa, C.; Coelho, P.; Henriques, M.A.; Teixeira, J.P.; Mayan, O. (2007). Lead exposure of children and newborns in Porto, Portugal. International Journal of Hygiene and Environmental Health, 210, 411–414.

Rothwell, R.G. (1989). Minerals and mineraloids in marine sediments: an optical identification guide. Elsevier Applied Science. 279 p.

S

Sabatés, A. & Masó, M. (1990). Effect of a shelf-slope front on the spatial distribution of mesopelagic fish larvae in the western Mediterranean. Deep-Sea Research, 37, 1085-1098.

Sabatés, A.; Gili, J.M.; Pagès, F. (1989). Relationship between zooplankton distribution, geographic characteristics and hydrographic patterns off the Catalan coast (Western Mediterranean). Marine Biology, 03, 153-159.

Silva, A.P.G. (1999). Mineralogia e geoquímica das fracções finas do Miocénico da Península de Setúbal. Litoestratigrafia e reconstruções paleoambientais. Tese de Mestrado. Universidade de Aveiro, 126 p.

Savidge, D.K. & Bane Jr., J.M. (2001). Wind and Gulf Stream influences on along-shelf transport and off-shore export at Cape Hatteras, North Carolina. Journal of Geophysical Research, 106, 11, 505-527.

Salgueiro, E.; Voelker A.; Abrantes F.; Meggers H.; Pflaumann, U.; Lončarić, N.; González-Álvarez, R.; Oliveira, P.; Bartels-Jónsdóttir, H.; Moreno, J.; Wefer, G. (2008). Planktonic foraminifera from modern sediments reflect upwelling patterns off Iberia: Insights from a regional transfer function. Marine Micropaleontology, 66, 135–164.

Salomons, W. & Förstner, U. (1984). Metals in the Hydrocycle. Spring Verlag, Berlin, Heidelberg, New York. 349 p.

Sanchez-Cabeza, J.A.; Masque, P.; Ani-Ragolta, I.; Merino, J.; Frignani, M.;

Alvisi, F.; Palanques, A.; Puig, P. (1999). Sediment accumulation rates in the southern Barcelona continental margin (NW Mediterranean Sea) derived from 210Pb and 137Cs chronology. Progress in Oceanography, 44, 313–332.

Sangster, D.F.; Outridge, P.M.; Davis, W.J. (2000). Stable lead isotopes characteristics of lead ore deposits of environmental significance. Environ. Rev., 8, 115–147.

Santos Oliveira, M.; Farinha, J.; Matos, J. X.; Ávila, P. F.; Rosa, C.; Canto Machado, M. J.; Daniel, F. S.; Martins, L.; Machado Leite, M. R. (2002). Diagnóstico Ambiental das Principais Áreas Mineiras Degradadas do País. Boletim de Minas - Vol. 39, Nº 2. 21 p.

Santos Zalduegui, J.F.; García de Madinabeitia, S.; Gil Ibarguchi, J.I.; Palero, F. (2004). A lead isotope database: the Los Pedroches–Alcudia area (Spain); implications for archaeometallurgical connections across Southwestern and Southeastern Iberia. Archaeometry, 46, 625–634.

Schmidt, S.; de Stigter, H.C.; Van Weering, T.C.E. (2001). Enhanced short term sediment deposition within the Nazaré Canyon, North East Atlantic. Marine Geology, 173, 55–67.

Schönfeld, J. (1997). The impact of the Mediterranean Outflow Water (MOW) on benthic foraminiferal assemblages and surface sediments at the southern Portuguese continental margin. Marine Micropaleontology, 29, 211-236.

Segonzac, G. D. (1969). Les mineraux argileux dans la diagenèse. Passage au métamorphisme. Service Carte Geólogy Alsace-Lorraine, Mémoire, 29, 320.

Shepard, F.P. (1979). Currents in submarine canyons and other types of seavalleys. SEPM Spec. Publ. 27, 85-94.

Shotyk, W.; Weiss, D.; Appleby, P.G.; Cheburkin, A.K.; Frei, R.; Gloor, M.; Kramers, J.D.; Reese, S.; Van Der Knaap, W.O. (1998). History of atmospheric lead deposition since 12,370 ^{14}C yr BP from a peat bog, Jura Mountains, Switzerland. Science, 281, 1635–1640.

Silva, A.; Taborda, R.; Rodrigues, A.; Duarte, J.; Cascalho, J. (2007). Longshore drift estimation using fluorescent tracers: new insights from an experiment at Comporta Beach, Portugal. Marine Geology, 240, 137-150.

Smith, D.P. ; Ruiz, G. ; Kvitek, R. ; Iampietro, P.J. (2005). Semiannual patterns of erosion and deposition in upper Monterey Canyon from serial multibeam bathymetry. Geol. Soc. Am. Bul., 117, 1123-1133.

Soto-Jiménez, M.F. & Páez-Osuna, F. (2001). Distribution and normalization of heavy metal concentrations in mangrove and lagoonal sediments from Mazatlán Harbor (SE Gulf of California). Estuarine, Coastal and Shelf Science, 53, 259-274.

Stow, D.A.V. (1986). Deep clastic seas. In: Reading, H.G. (ed.). Sedimentary Environments and Facies. Blackwell Scientific Publications, Oxford, 399-444.

T

Teixeira, S. (1990). Dinâmica das praias da Península de Setúbal (Portugal). Tese de Mestrado. Universidade de Lisboa. 189 p.

Thomsen, L. (1999). Processes in the benthic boundary layer at continental margins and their implication for the benthic carbon cycle. Journal of Sea Research, 41, 73-86.

Thorbjarnarson, K.W.; Nittrouer, C.A.; DeMaster, D.J. (1986). Accumulation of modern sediment in Quinault submarine canyon. Marine Geology, 71, 107-124.

Thunell, R. & Sautter, L.R. (1992). Planktonic foraminiferal faunal and stable isotopic indices of upwelling: a sediment trap study in the San Pedro Basin, Southern California Bight. In: Summerhayes, C.P., Prell, W.L., Emeis, K.C. (Eds.), Upwelling Systems: Evolution Since the Early Miocene. Geological Society Special Publication, 77–91.

Trigo, R.M.; Pozo-Vásquez, D.; Osborn, T.J.; Castro-Díez, Y.; Gámiz-Fortis, S.; Esteban-Parra, M. (2004). North Atlantic Oscillation influence on precipitation, river flow and water resources in the Iberian Península. International Journal of Climatology, 24, 925–944.

Turchetto, M.; Boldrin, A.; Langone L.; Miserocchi, S.; Tesi, T.; Foglini F. (2007). Particle transport in the Bari Canyon (southern Adriatic Sea). Marine Geology, 246, 231–247.

Twichell, D.C. & Roberts, D.G. (1982). Morphology, distribution, and development of submarine canyons on the United States Atlantic continental slope between Hudson and Baltimore Canyons. Geology, 10,

408–412.

Tyler, P.; Amaro, T.; Arzola, R.; Cunha, M.R.; de Stigter, H.; Gooday, A.; Huvenne, V.; Ingels, J.; Kiriakoulakis, K.; Lastras, G.; Masson, D.; Oliveira, A.; Pattenden, A.; Vanreusel, A.; Van Weering, T.; Vitorino, J.; Witte, U.; Wolff, G. (2009). Europe's Grand Canyon: Nazaré Submarine Canyon. Oceanography, 22, 46-57.

V

Vale, C. (1981). Input of suspended particulate matter in the Tagus estuary during the flood of February 1979. Recursos Hídricos, 2, 37–45.

Vale, C. (1990). Temporal variations of particulate metals in the Tagus River Estuary. Science of the Total Environment, 97/98, 137-154.

Vale, C., & Sundby, B. (1987). Suspended sediment fluctuations in the Tagus estuary on semi-diurnal and fortnightly time scales. Estuarine Coastal and Shelf Science, 25, 495–508.

Vale, C.; Canário, J.; Caetano, M.; Lavrado, J.; Brito, P. (2008). Estimation of the anthropogenic fraction of elements in surface sediments of the Tagus estuary (Portugal). Marine Pollution Bulletin, 56 (7), 1364–1367.

Vale, C.; Cortesão, C.; Castro, O.; Ferreira, A.M. (1993). Suspended-sediment response to pulses in river flow and semidiurnal and fortnightly tidal variations in a mesotidal estuary. Marine Chemistry, 43, 21-31.

Vale, C.; Ferreira, A.M.; Guerra, M.; Gaudêncio, M.J.; Caetano, M.; Fernandes, F.; Pereira, A.; Luz, D.; Gomes, I.; Granja, R. (1994). Estudo de impacte ambiental das operações de dragagem no estuário do Mondego. Relatório de Progresso, IPIMAR, 13 p.

Valente, A.S. & da Silva, J.C.B. (2009). On the observability of the fortnightly cycle of the Tagus estuary turbid plume using MODIS ocean colour images. Journal of Marine Systems, 75, 131-137.

Van Aken, H.M. (2000a). The hydrography of the mid-latitude northeast Atlantic Ocean I: the deep water masses. Deep-sea Research I, 47, 789 – 798.

Van Aken, H. M. (2000b) - The hydrography of the mid-latitude North-East Atlantic Ocean - Part II: the intermediate water masses. Deep-Sea Research I, vol. 47, 789-824.

Van de Meent, D.; De Leeuw, J.W.; Schenck, P.A.; Salomons, W. (1985). Geochemistry of suspended particulate matter in two natural

sedimentation basins of the river Rhine. Water Res., 19, 1333-1340.

Van der Zee, C.; Slomp, C.P.; Van Raaphorst, W. (2002). Authigenic P formation and reactive P burial in sediments of the Nazaré canyon on the Iberian margin (NE Atlantic). Marine Geology, 185, 379-392.

Van Rijn, L.C. (2009). Prediction of dune erosion due to storms. Coastal Engineering, 56 (4), 441-457.

Van Weering, T.C.E. & Weaver, P.P.E. (2007). Canyons processes, an introduction. Marine Geology, 246, 65-67.

Van Weering, T.C.E.; de Stigter, H.C.; Boer, W.; de Haas, H. (2002). Recent sediment transport and accumulation on the NW Iberian margin. Prog. Oceanogr., 52, 349-371.

Van Weering, T.C.E.; Thomsen, L.; Heerwaarden, J.; Koster, B.; Viergutz, T. (2000). A seabed lander and new techniques for long term in situ study of deep-sea near bed dynamics. Sea Technol., 41, 17-27.

Vanney, J.R. & Mougenot, D. (1981). La plateforme continentale du Portugal et les provinces adjacentes: analyse géomorphologique. Mem. Serv. Geol. Port., 28, 1–86.

Vanney, J.R. & Mougenot, D. (1990). Un canyon sous-marin du type ≪gouf≫: le Canhão da Nazaré (Portugal). Oceanol. Acta, 13, 1–14.

Verardo, D.J.; Froelich, P.N.; McIntyre, A. (1990). Determination of organic carbon and nitrogen in marine sediments using the Carlo Erba NA-1500 analyser. Deep-Sea Research, 37 (1), 157-165.

Véron, A.J.; Church, T.M.; Patterson, C.C.; Flegal, A.R. (1994). Use of stable isotopes to characterize the source of anthropogenic lead in North Atlantic surface waters. Geochimica Cosmochimica Acta, 58, 3199–3206.

Vitorino, J.; Oliveira, A.; Jouanneau, J.M.; Drago, T. (2002a). Winter dynamics on the northern Portuguese shelf. Part 1: physical processes. Prog. Oceanogr., 52, 129-153.

Vitorino, J.; Oliveira, A.; Jouanneau, J.M.; Drago, T. (2002b). Winter dynamics on the northern Portuguese shelf. Part 2: bottom boundary layers and sediment dispersal. Prog. Oceanogr., 52, 155–170.

W

Walsh, J.J.; Rowe, G.T.; Iverson, R.L.; McRoy, C.P. (1981). Biological export of shelf carbon: a neglected sink of the global CO_2 cycle. Nature, 291, 196-

201.

Weaver, P.P.E. & Canals, M. (2003). The Iberian and Canaries Margin including NW Africa. In: Mienert, J., Weaver, P.P.E. (Eds.), European Margin Sediment Dynamics. Springer-Verlag, Berlin, 251–260.

Weaver, P.P.E.; Billett, D.; Boetius, A.; Danovaro, R.; Freiwald, A.; Sibuet, M. (2004). Hotspot ecosystem research on Europe's deep-ocean margin. Oceanography, 17 (4), 132–143.

Wedepohl, K.H. (1995). The composition of the continental crust. Geochimica Cosmochimica Acta, 59, 1217–1232.

Weiss, D.; Boyle, E.A.; Wu, J.; Chavagnac, V.; Michel, A.; Reuer, M.K. (2003). Spatial and temporal evolution of lead isotope ratios in the North Atlantic between 1981 and 1989. Journal of Geophysical Research, 108 (C10), 3306.

Windom, H.L. (1976). Lithogeneous material in marine sediments. *In*: Riley, J.P. and Chester, R. (eds), Chemical Oceanography. Academic Press, London, New York, 103-135.

Wollast, R. & Chou, L. (2001). The carbon cycle at the ocean margin in the northern Gulf of Biscay. Deep-Sea Research II, 48, 3265-3293.

Wright, L.D. & Short, A.D. (1984). Morphodynamic variability of surf zones and beaches: a synthesis. Marine Geology, 56, 93-118.

X

Xu, J.P.; Noble, M.; Eittreim, S.L.; Rosenfeld, L.K.; Schwing, F.B.; Pilskaln, C.H. (2002). Distribution and transport of suspended particulate matter in Monterey Canyon, California. Marine Geology, 181, 215-234.

Z

Zhang, J. (1995). Geochemistry of trace metals from Chinese river/estuary systems: an overview. Estuarine, Coastal and Shelf Science, 41 (6), 631-658.

Zöllmer, V. & Irion, G. (1993). Clay mineral and heavy metal distribution in the northeastern North Sea. Marine Geology, 111, 223-230.

Zwolsman, J.J.G. & Van Eck, G.T.M. (1999). Geochemistry of major elements and trace metals in suspended matter of the Scheldt estuary, southwest Netherlands. Marine Chemistry, 66, 91-111.

Appendixes

Appendix A1

Table A1.1. Location and water depth of grab samples collected on the Lisbon-Setúbal-Sines shelf.

Station	x	y	Water depth (m)
		Lisbon shelf	
2035	101896.11	170564.82	280
2063	98603.82	163203.53	265
4175	89931.76	167758.7	33
4190	88116.79	162787.06	305
4233	105108.31	171636.61	37
4269	100624.05	173541.31	226
4282	93666.41	175110.93	102
4342	83132.56	180439.33	110
4346	91701.69	180318.93	50
4349	100273.06	180392.76	23
2069	100011.18	159299.8	165
2061	101803.6	162978.88	73
2053	96320.41	166748.64	395
2042	98089.65	168576.57	535
2026	98427.32	172273.41	135
2049	103885.44	166654.76	50
4185	93679.67	165117.52	520
4348	97223.13	180431.34	26
4233	105108.31	171636.61	37
4310	102263.56	176852.19	61
4242	89686.53	171093.23	123
4246	82268.02	171013.37	235
4285	87998.40	175187.98	110
4202	84107.68	167470.37	572
		Setúbal shelf	
2116	115777.2	148942.8	527
2139	122327.7	162940	78
2182	139168.8	157244.5	24
2215	138981.3	151695.1	35
4108	137608.2	162622.2	7
4994	133607.7	171720.8	8
4995	132436.9	170805.3	14
5000	130239.9	168973.8	35
5012	127466.7	167888	2
5014	127592.2	165666.5	8
5069	124654.2	145487.7	503
5071	121036.5	146965.4	450
5072	114309.5	148032.9	395
5074	110955.3	148032.1	450
4984	134142.4	165980.3	3
4985	132980	166175	1
2067	103942.8	159252.1	125
2074	103733.2	153888.2	328
2083	107230.4	153847.3	173
2089	109623.9	159371.5	110
2094	111225.6	159353.7	112
2104	113116.5	159148.1	114
2109	114865.9	159314.5	115
2118	116847.3	153742.6	203
2121	116902.5	159108.2	112
2137	120579.4	162772	86
2141	122290.2	159054.5	101
2144	122384.3	153687.6	120

2159	126110.1	162719.3	66
2162	131788	162854.4	37
2175	127825.2	159188.1	73
2178	132921.6	159144.2	51
2187	135308.2	148023	97
2204	133312.6	153590.1	73
2206	129815.6	153619.7	94
2225	125976.4	148102.9	225
2227	129913.3	148068	125
2232	138953.4	147994.8	39
2243	129897.2	146217.8	225
4109	139339.5	160573.7	10
4114	140483.7	157789.8	13
4120	141341.4	155563.2	12
4126	142041.9	151672.6	16
4131	142753.7	149262.2	9
2097	111140.3	153803.3	158
	Sines shelf		
2234	140982.7	146314.6	28
2289	140793.6	140395.2	35
2313	140753.2	134844.9	34
2364	138814.3	129493.6	43
2366	140553.2	127445.6	24
4036	135075.5	118791.4	49
4063	138764.4	122833.4	27
4105	138338.1	124501.7	33
4134	143030.9	147225.1	11
4144	142697.5	141306.6	20
4154	142053.1	132800.3	18
2305	127187.5	136805.2	135
2309	135218.2	136737.3	106
2310	136967.5	136353.5	82
2344	133276	131387.3	118
2346	129621.7	131233	130
3969	109950.3	109777.9	377
3971	115662	109532.2	278
3973	119465.7	108939	192
3976	124750.4	109998.8	135
3979	130462.2	109763.4	87
3980	131927.2	109751.2	52
4007	134899.7	115092.5	35
4014	123189.3	115378.9	150
4019	111619.7	115125.7	372
4049	114020.6	120651	365
4053	123095.1	120930.5	145
4058	132458.3	120847.8	105
4091	115545	126556	440
4097	126802.4	126447.3	132
4100	132356.5	126214.3	118
4102	135865.3	126185.9	70
4545	110455	142338.4	480
4549	109044.4	133657.3	435
5067	118082.7	146217.5	278
2244	129735.3	144368.9	265
2246	133528.1	144336.9	110
2254	137159.3	142272.7	105
2261	123882.9	142571.4	168
2265	118792.7	144286.1	180

2300	116968.4	137088.2	222
4137	143163.7	145373.9	11
4152	142653.1	135016.2	14
2365	140712.9	129294.6	28
4106	139654.2	124491.8	23
4034	137855.9	118769.8	21
4033	137256.3	116924.2	17
4148	142975.1	139269.5	15

Coordinates presented in Datum Lisboa

Table A1.2. Information about the lander deployments: station number, latitude and longitude, water depth (m), start and end date.

Station	Latitude/ Longitude	Depth (m)	Start date/ End date	Nº samples	Sampling intervals per sample (days)
64PE269-02	38°30.0'N 009°16.0'W	497	21-May-07 28-May-07	7	~1
64PE252-34	38°26.4'N 009°20.4'W	1070	1-Aug-06 19-Sep-06	11	~1
64PE225-03	38°19.9'N 009°19.6'W	1858	6-May-04 30-Apr-05	12	30
64PE204-23	38°17.0'N 009°06.0'W	972	11-Nov-02 14-Nov-02	3	~1
64PE218-36	38°16.4'N 009°09.0'W	1324	26-Oct-03 1-May-04	12	14
64PE204-35	38°12.0'N 009°31.4'W	2716	14-Nov-02 23-Oct-03	12	~30
64PE252-62	38°06.5'N 009°58.1'W	4402	18-Sep-06 29-May-07	12	21
64PE218-01	38°15.0'N 009°32.0'W	1213	15-Oct-03 23-Oct-03	1	~8

Table A1.3. Location and water depth of cores used in this study; pc – piston-core; mc – multi-core.

Station	Latitude	Longitude	Water depth (m)
Mondego transect			
64PE252-12	40º10.0′N	009º00.0′W	48
64PE252-11	40º10.0′N	009º10.0′W	103
64PE252-09	40º10.0′N	009º30.0′W	156
64PE252-08	40º10.0′N	009º40.0′W	416
64PE252-07	40º10.0′N	009º50.0′W	959
64PE252-06	40º10.0′N	009º56.0′W	1463
64PE252-04	40º10.0′N	009º60.0′W	3475
64PE252-03	40º10.0′N	010º10.0′W	3981
64PE252-02	40º10.0′N	010º30.0′W	4445
64PE252-01	40º10.0′N	010º60.0′W	4902
Nazaré Canyon			
64PE225-41	39º34.7′N	009º09.2′W	301
64PE218-05	39º38.8′N	009º15.0′W	321
64PE204-56	39º38.9′N	009º14.7′W	336
64PE236-21	39º34.5′N	009º24.3′W	532
64PE236-13mc	39º35.9′N	009º24.2′W	927
64PE236-13pc	39º35.8′N	009º24.3′W	941
64PE225-26	39º36.0′N	009º24.0′W	1118
64PE236-07	39º36.0′N	009º24.3′W	1160
64PE236-16	39º31.2′N	009º50.7′W	2990
64PE236-14	39º30.7′N	009º51.0′W	3097
64PE236-24	39º29.5′N	009º51.0′W	3200
64PE225-22	39º53.9′N	011º09.4′W	4969
Open slope and shelf adjacent to the Nazaré Canyon			
64PE218-57	39º38.5′N	009º17.0′W	151
64PE225-27	39º33.9′N	009º41.0′W	1009
64PE204-49	39º34.0′N	009º50.0′W	1881
64PE236-20	39º34.0′N	009º50.0′W	1884
64PE204-60	39º33.0′N	009º49.0′W	2323
64PE204-61	39º28.0′N	009º49.0′W	2467
64PE225-25	39º46.5′N	011º00.0′W	4798
Estremadura transect			
64PE252-27	39º10.4′N	010º15.2′W	1034
64PE252-17	39º08.9′N	010º30.0′W	1590
64PE252-16	39º10.6′N	010º40.0′W	2084
64PE252-13	39º17.3′N	011º20.0′W	4847
Cascais Canyon			
64PE252-35	38º29.6′N	009º28.7′W	445
64PE252-36pc	38º27.9′N	009º28.5′W	953
64PE252-32	38º21.8′N	009º30.4′W	2100
64PE252-31	38º18.7′N	009º42.2′W	2957
64PE252-30	38º20.0′N	009º51.5′W	3914
Lisbon Canyon			
64PE225-01	38º31.1′N	009º16.4′W	365
64PE269-02pc	38º30.0′N	009º16.0′W	497
64PE252-34pc	38º25.8′N	009º20.9′W	1112
64PE204-31pc	38º22.0′N	009º20.5′W	1710
64PE225-03	38º20.0′N	009º19.6′W	1856
Setúbal Canyon			
64PE204-18	38º17.5′N	008º54.0′W	315
64PE204-19	38º16.5′N	008º60.0′W	595
64PE236-55	38º16.5′N	008º60.0′W	644
64PE204-23	38º17.1′N	009º06.0′W	971

64PE218-36	38º16.4′N	009º09.0′W	1321
64PE236-52	38º15.0′N	009º23.1′W	2118
64PE225-07	38º06.4′N	010º00.2′W	4445
	Open slope adjacent to the Lisbon-Setúbal Canyon		
64PE225-02	38º12.5′N	009º19.9′W	301
64PE225-20	38°12.5′N	009°19.9′W	1004
64PE225-45	38º14.5′N	009º35.0′W	1266
64PE236-10	38º05.1′N	009º29.8′W	1364
64PE225-21	38º05.0′N	009º35.0′W	1760
	Sines transect		
64PE252-58	37°50.0′N	009°05.0′W	282
64PE252-57	37º50.0′N	009º15.0′W	490
64PE252-56	37º50.0′N	009º28.5′W	1002
64PE252-55	37º50.0′N	009º35.0′W	1374
64PE252-52	37º50.0′N	010º05.0′W	2908
64PE252-51	37º50.0′N	010º30.0′W	3908

Appendix A2

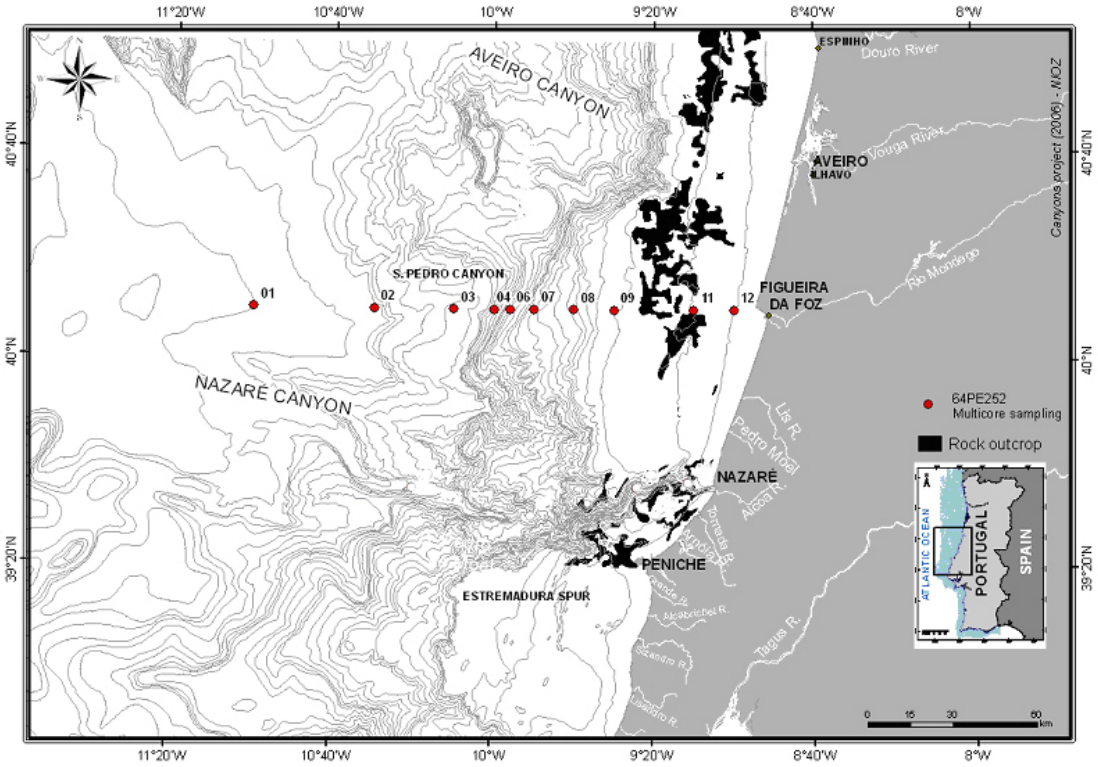

Figure A2.1 Location of samples of the Mondego transect.

Appendix A3

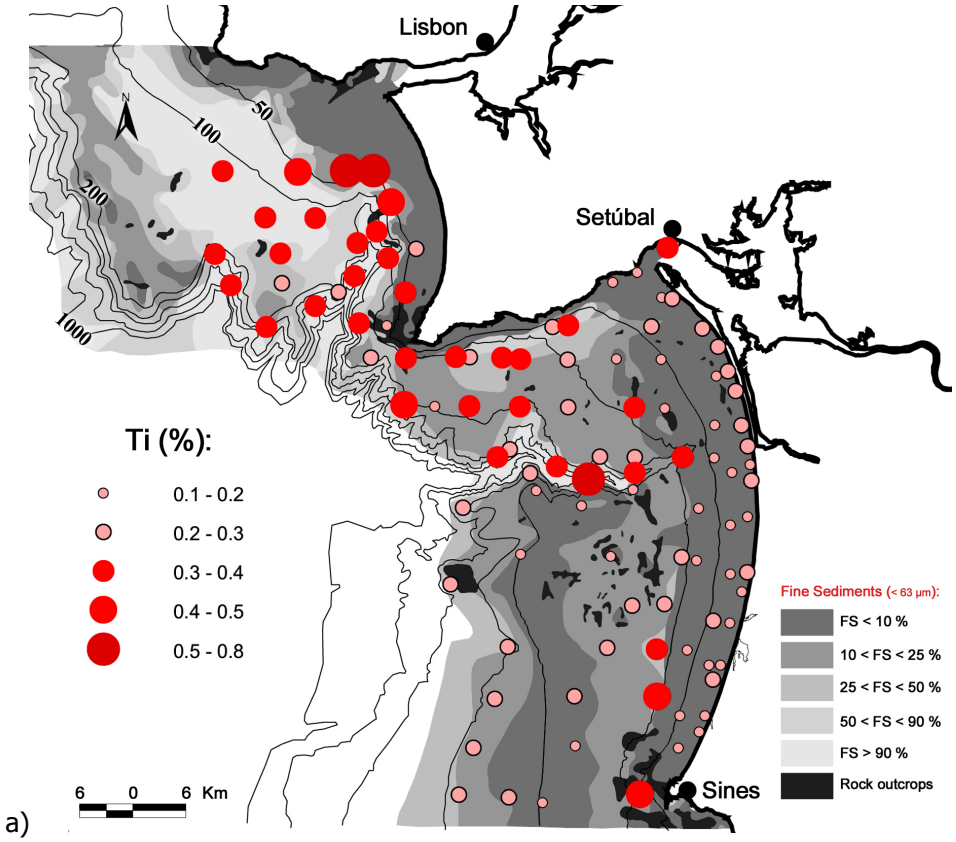
Lisbon
Setúbal
Sines
50
100
200
1000
Ti (%):
0.1 - 0.2
0.2 - 0.3
0.3 - 0.4
0.4 - 0.5
0.5 - 0.8
6 0 6 Km
Fine Sediments (< 63 µm):
FS < 10 %
10 < FS < 25 %
25 < FS < 50 %
50 < FS < 90 %
FS > 90 %
Rock outcrops

a)

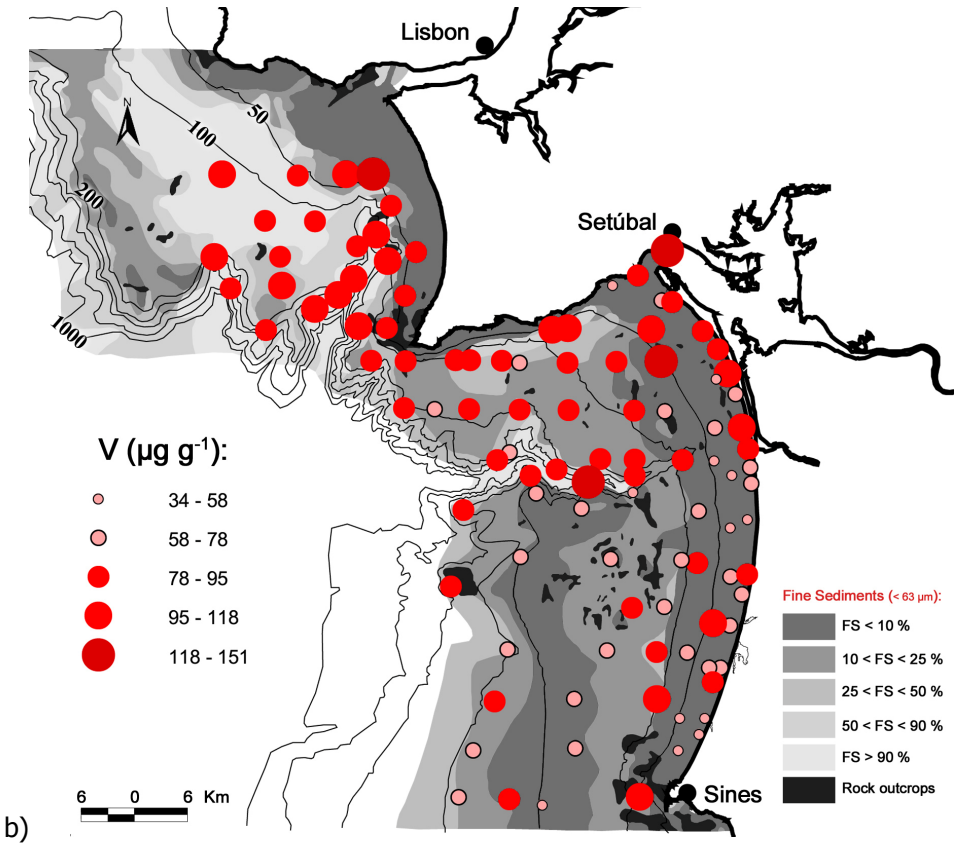
Lisbon
Setúbal
Sines
50
100
200
1000
V (µg g-1):
34 - 58
58 - 78
78 - 95
95 - 118
118 - 151
6 0 6 Km
Fine Sediments (< 63 µm):
FS < 10 %
10 < FS < 25 %
25 < FS < 50 %
50 < FS < 90 %
FS > 90 %
Rock outcrops

b)

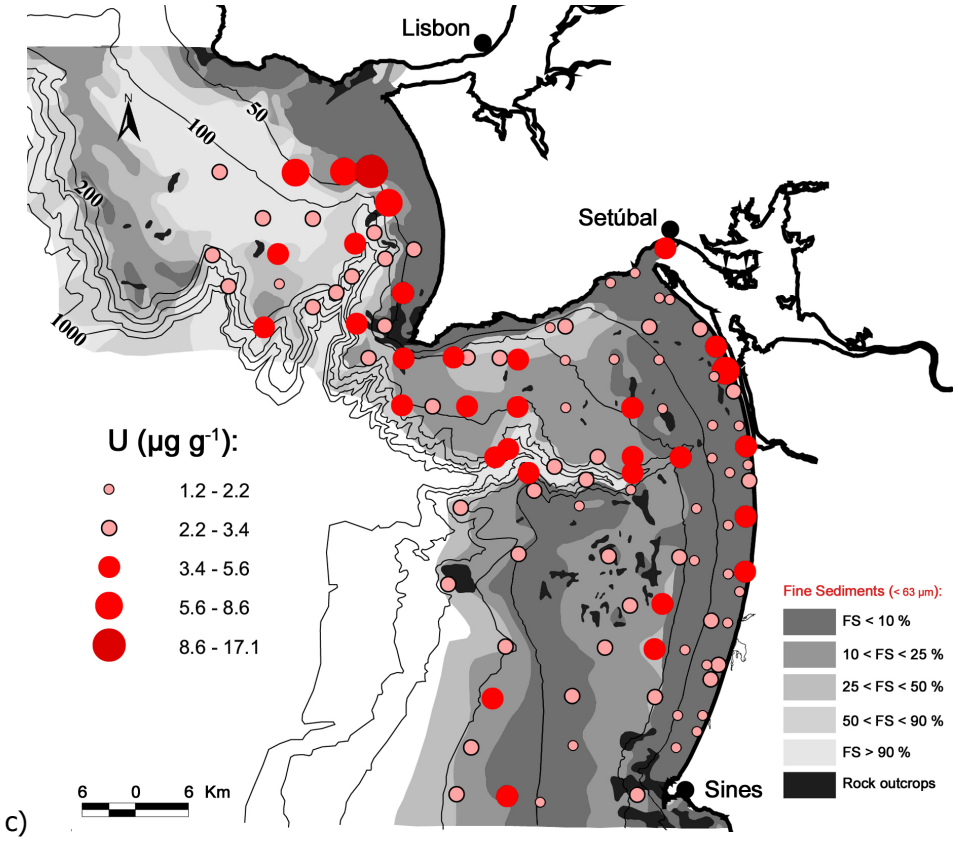
Lisbon
Setúbal
Sines
50
100
200
1000
U (µg g-1):
1.2 - 2.2
2.2 - 3.4
3.4 - 5.6
5.6 - 8.6
8.6 - 17.1
6 0 6 Km
Fine Sediments (< 63 µm):
FS < 10 %
10 < FS < 25 %
25 < FS < 50 %
50 < FS < 90 %
FS > 90 %
Rock outcrops

c)

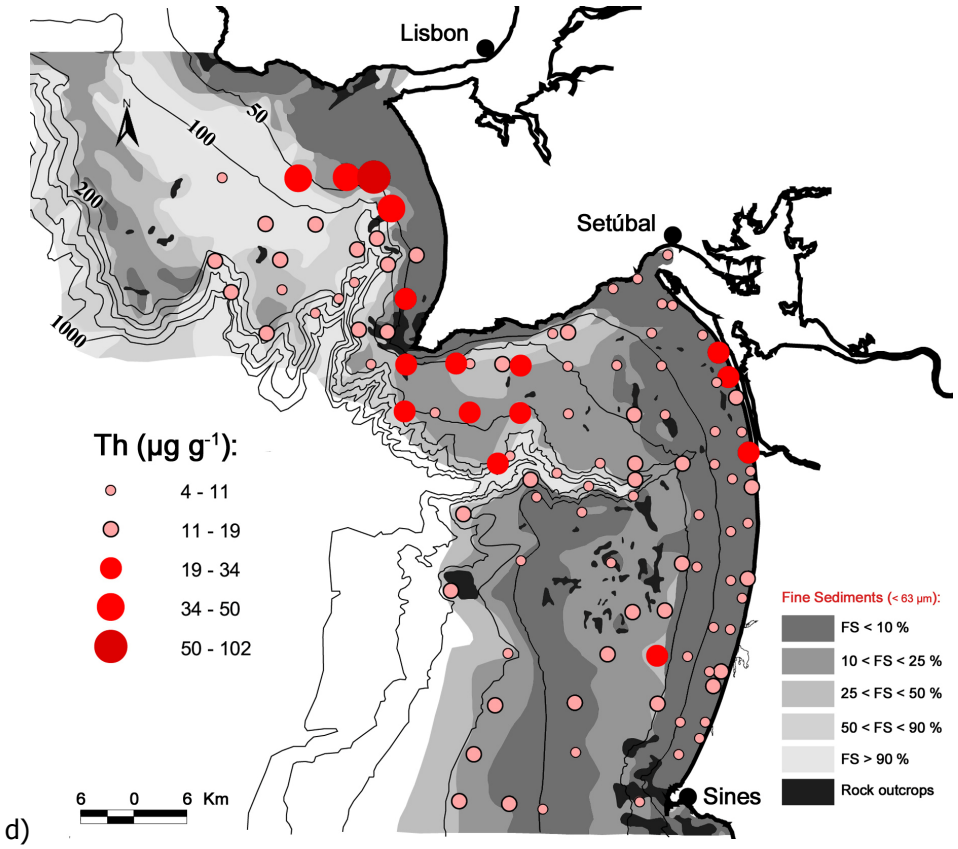
Lisbon
Setúbal
Sines
50
100
200
1000
Th (µg g-1):
4 - 11
11 - 19
19 - 34
34 - 50
50 - 102
6 0 6 Km
Fine Sediments (< 63 µm):
FS < 10 %
10 < FS < 25 %
25 < FS < 50 %
50 < FS < 90 %
FS > 90 %
Rock outcrops

d)

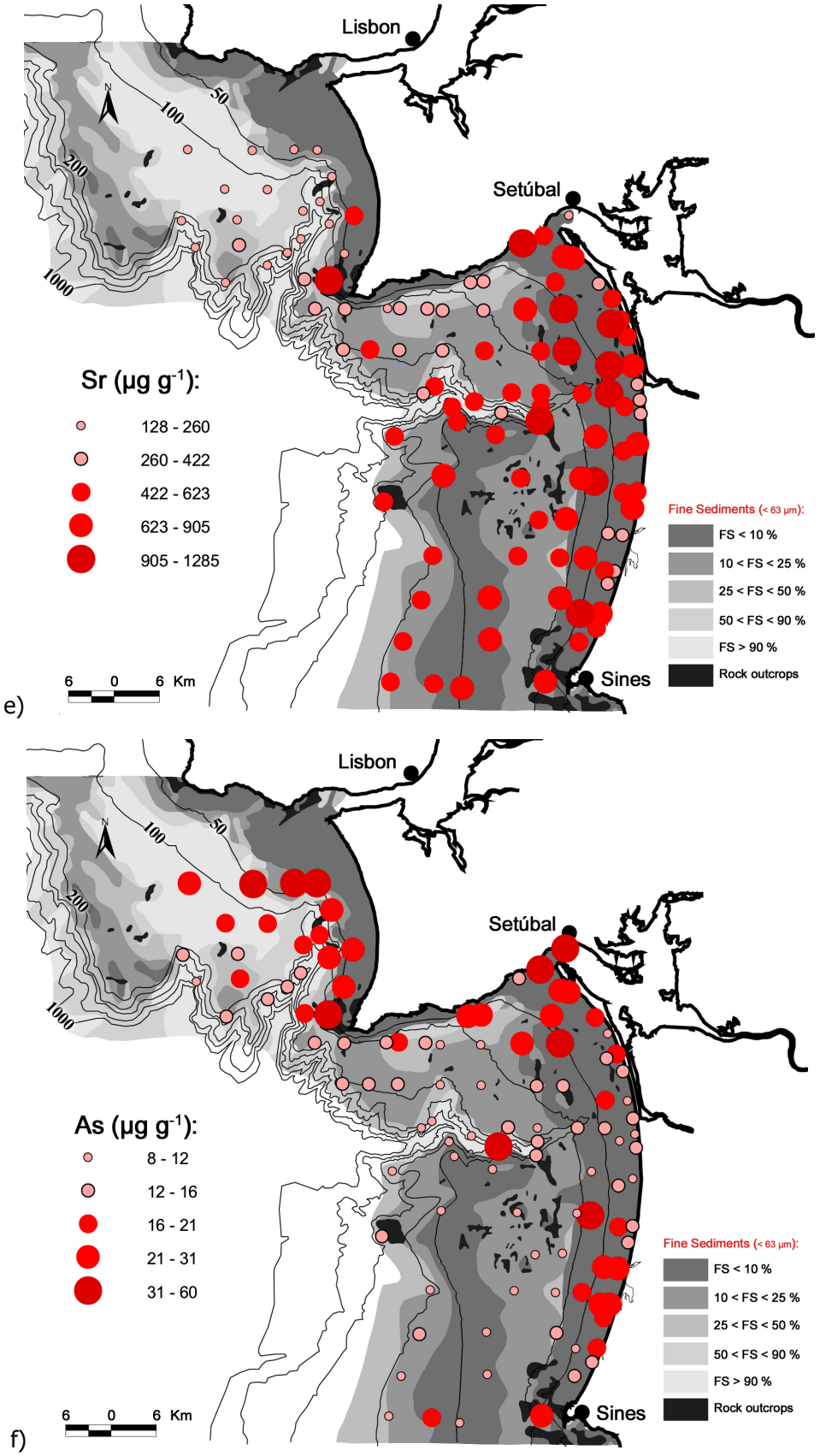

Figure A3.1 Spatial distribution of elements Ti (**a**), V (**b**), U (**c**), Th (**d**), Sr (**e**) and As (**f**) in surface sediments from the Lisbon-Setúbal-Sines shelf and upper slope.

Appendix A4

Table A4.1. Mean elemental values of surface sediments collected in the Lisbon-Setúbal-Sines continental shelf and upper slope per different sectors of the shelf/slope. Ca, Al, Fe, Mg and Ti are expressed as % while the other elements are expressed as μg g^{-1}.

		Ca	Al	Fe	Mg	Ti	Mn	Zn	Cr	Pb	Ni	Cu	As	Th	U
Lisbon	Inner (n = 6)	5.2	6.5	3.4	1.3	0.5	632	236	169	146	98	33	36	40	7
	Middle (n =2)	11.7	5.5	3.2	1.2	0.4	526	174	52	97	26	23	39	31	6
	Outer (n = 6)	3.6	8.3	3.7	1.2	0.4	299	177	55	72	31	27	18	14	3
	Upper slope (n = 9)	4.2	8.9	3.9	1.3	0.4	303	172	60	66	36	29	16	12	3
Setúbal	Inner (n = 13)	11.5	5.4	2.8	1.1	0.3	659	201	149	122	89	33	21	13	3
	Middle (n = 9)	13.3	5.4	3.4	1.1	0.3	295	137	146	57	89	25	20	9	2
	Outer (n = 10)	8.1	7.1	3.4	1.2	0.3	284	143	53	51	31	24	14	16	3
	Upper slope (n = 8)	8.9	7.4	3.7	1.2	0.4	310	108	55	48	38	22	14	17	4
Sines	Inner (n = 17)	8.5	4.2	1.9	0.9	0.2	272	148	234	70	166	23	310	9	2
	Middle (n = 3)	16.0	4.3	3.4	1.3	0.3	533	85	273	57	169	26	28	7	2
	Outer (n = 13)	12.0	6.0	3.3	1.0	0.3	282	94	48	37	30	19	11	11	3
	Upper slope (n = 10)	12.0	6.1	3.2	1.1	0.3	282	89	55	54	36	20	12	12	3

Appendix A5

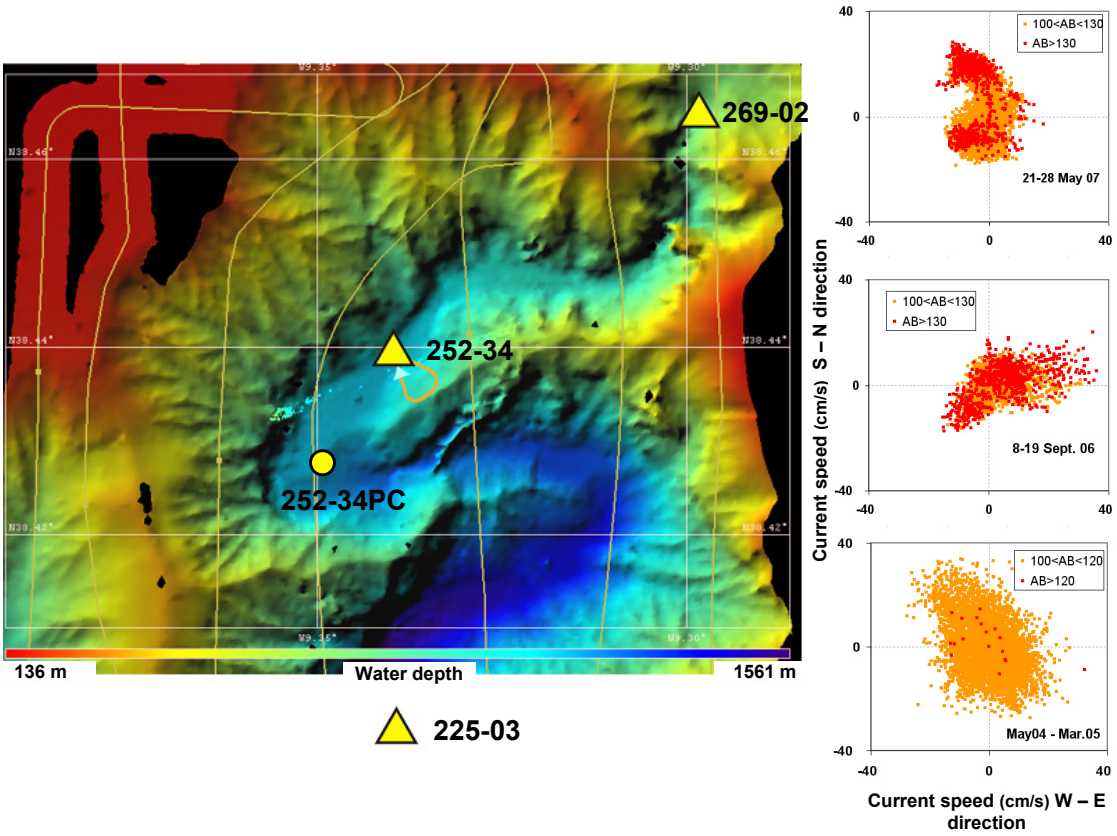

Figure A5.1 A sharp meander bend in the Lisbon Canyon as mapped with the EM300 multibeam echosounder of RV Pelagia. Depicted area is about 9.5 X 7 km. Yellow triangles and circle indicate positions of, respectively, BOBO lander deployments and piston core 252-34. On the right, diagrams represent current speed, direction and related turbidity (AB - acoustic backscatter) measured in each deployment of the BOBO lander.

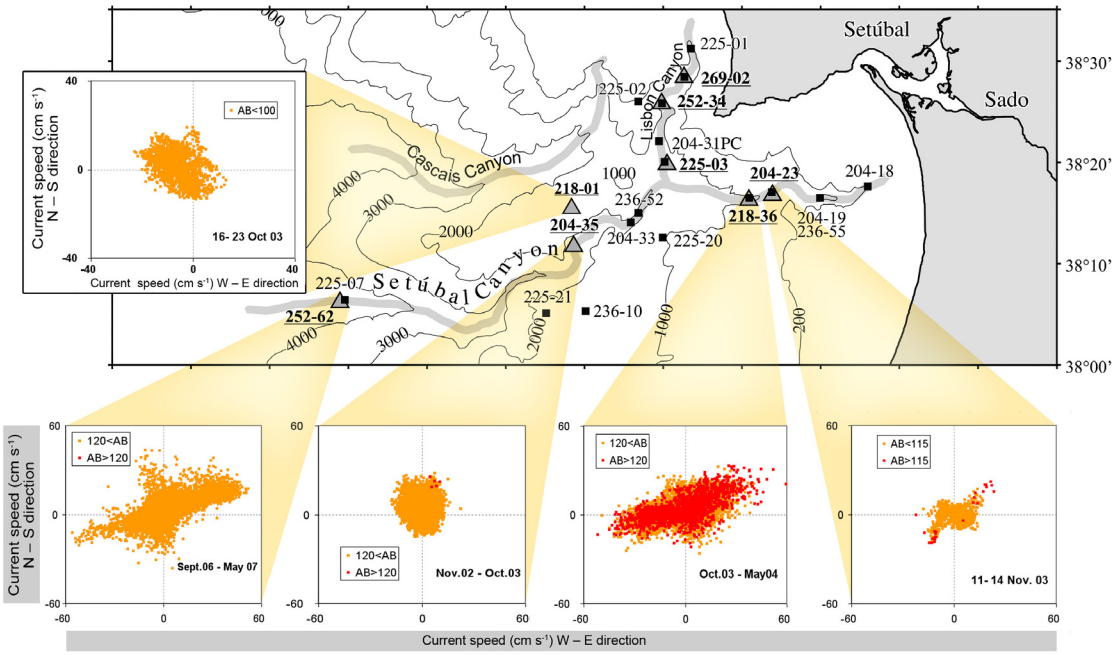

Figure A5.2 Plots represent current speed, direction and related turbidity (AB - acoustic backscatter) measured in each deployment done in the Setúbal Canyon.